THERMO-TECTONIC HISTORY OF THE KISSEYNEW DOMAIN NEAR SANDY NARROWS, SASKATCHEWAN

A Thesis

Submitted to the Faculty of Graduate Studies and Research

in Partial Fulfillment of the Requirements for the Degree

of

Master of Sciences

in the

Department of Geological Sciences

University of Saskatchewan

Saskatoon

by

Shannon Balzer

Spring, 2001

PERMISSION TO USE

In presenting this thesis in partial fulfillment of the requirements for a Master of Sciences degree from the University of Saskatchewan, I agree that the libraries of this University may make it freely available for inspection. I further agree that permission for copying of this thesis in any manner, in whole or in part, for scholarly purposes may be granted by my supervisor Dr. Y. Pan, or in his absence, by the Head of the Department of Geological Sciences or Dean of the College of Graduate Studies. It is understood that any copying or publication or use of this thesis or parts thereof for the purpose of financial gain shall not be allowed without my written permission. It is also understood that due recognition shall be given to me and the University of Saskatchewan in any scholarly use which may be made of any material in this thesis.

Requests for permission to copy or make other use of material in this thesis, in whole or in part, should be addressed to:

Head of the Department of Geological Sciences
114 Science Place, University of Saskatchewan
Saskatoon, Saskatchewan, S7N 5E2.

ABSTRACT

The Sandy Narrows study area is comprised of mainly 1.86-1.84 Ga Kisseynew Domain marine metaturbidite rocks which represent the uppermost stratigraphic level in the Reindeer Zone. Based on mineralogical changes from west to east, isograds delineating metamorphic and compositional zones are recognized. Zone 1 consists of andalusite-cordierite-staurolite bearing gneisses. Zone 2, on the eastern side of Zone 1, consists of sillimanite-garnet-cordierite-muscovite-biotite gneisses. Zone 3 rocks consist of intercalated garnet-biotite and sillimanite-garnet-cordierite-biotite gneisses. Zone 4 is mineralogically similar to Zone 3, but contains an additional late cross-cutting cordierite-garnet bearing leucosome.

Fabric development and collisional tectonics were accompanied by the first metamorphic event (M1), which began pre-D_2 but waned before the end of deformation at ~1825 Ma. Growth of andalusite and staurolite is documented in the lower grade area (Zone 1), along with sllimanite, garnet, cordierite, K-feldspar, and melt development in the higher grade zones (Zones 2,3,4). Peak metamorphism is deduced to have occurred prior to 1830 Ma and reached conditions of 720-730 °C at pressures less than 6.5 kbars. Timing is recorded in numerous 1833-1830 Ma zircon ages. A period of retrogression followed, prior to the end of D_2, evident by the D_2 deformation of replacement minerals.

A second metamorphic event (M2) is recognized, broadly coeval with a third deformational event (D_3). Metamorphism resulted in growth of andalusite in Zone 1, and garnet, cordierite, sillimanite, and K-feldspar in Zones 2,3, and 4. A second generation of melt also developed; evident cross-cutting the S_2 fabric, but is present only within Zone 4. M2 mineral growth texturally overprints the S_2 fabric, and is observed oriented parallel to the axial plane of F_3 folds. Peak temperatures exceeded that of M1, upwards 741-758 °C with pressures less than 6 kbars. Peak conditions were achieved by 1805 Ma, and were followed by rapid uplift and cooling.

M1 metamorphism is attributed to a remnant thermal anomaly associated with back arc basin crust, along with magmatism above southwards subducting Kisseynew oceanic/back arc crust, which resulted from collision of the Sask Craton and the Flin Flon-Glennie Complex.

The second metamorphic event may have resulted from subsequent foundering of a Sask Craton detached slab after subduction reversal, which would have allowed influx of hot asthenosphere beneath the Kisseynew, creating a thermal anomaly.

ACKOWLEDGEMENTS

I am indebted to Dr. Yuamming. Pan who not only provided financial support through an NSERC grant and supervisory guidance, but whose constant and persistent inquiries into how far along the project was, ultimately lead to a finished manuscript. I also wish to acknowledge and thank Dr. Kevin Ansdell, for genuinely reviewing the Thesis and providing many helpful ideas. I wish to thank Dr. Ken Ashton, who showed me how to map in high-grade terrains, and along with Saskatchewan Energy and Mines, Saskatchewan Geological Survey, provided me with the knowledge and equipment to complete the field work required.

I also thank the Department of Geological Sciences, University of Saskatchewan, for providing facilities throughout my studies. In particular I wish to acknowledge Blain Novakowski from the thin section lab, and Tom Bonli from the microprobe lab, both of whom provided invaluable assistance. I also thank my fellow graduate students at the University, and in particular Craig Therens, for always providing interesting and intellectual conversation at our many social gatherings.

Finally I give special thanks to my wife, who has undergone many sacrifices and hardships, and my parents who provided me with financial support and patient understanding throughout my scholarly endeavors. Without their encouragement and support, my work would not have been possible.

TABLE OF CONTENTS

LIST OF TABLES

LIST OF FIGURES

CHAPTER 1:

INTRODUCTION AND SCOPE

1.0. Problems and objectives

In the past few years there has been a large amount of scientific work done in the Trans-Hudson, the largest Proterozoic Terrane in the world, as part of the Canada-Saskatchewan and Canada-Manitoba mineral development agreements. NATMAP and the LITHOPROBE seismic reflection survey have been instrumental in the development of new ideas and the confirmation of older theories including the existence of Archean crust beneath the Proterozoic.

However, even with the influx of geoscientists into the Trans-Hudson Orogen there are large areas that need to be evaluated to better understand the Proterozoic evolution of the Orogen. This study investigates an area that may be instrumental in the interpretation of the relationship between Proterozoic and Archean crust including the metamorphic and deformational history. The study area is located 85 km northwest of Flin Flon and approximately 15 km southwest of the community of Pelican Narrows (Figure 1.1). To the east, the Sahli

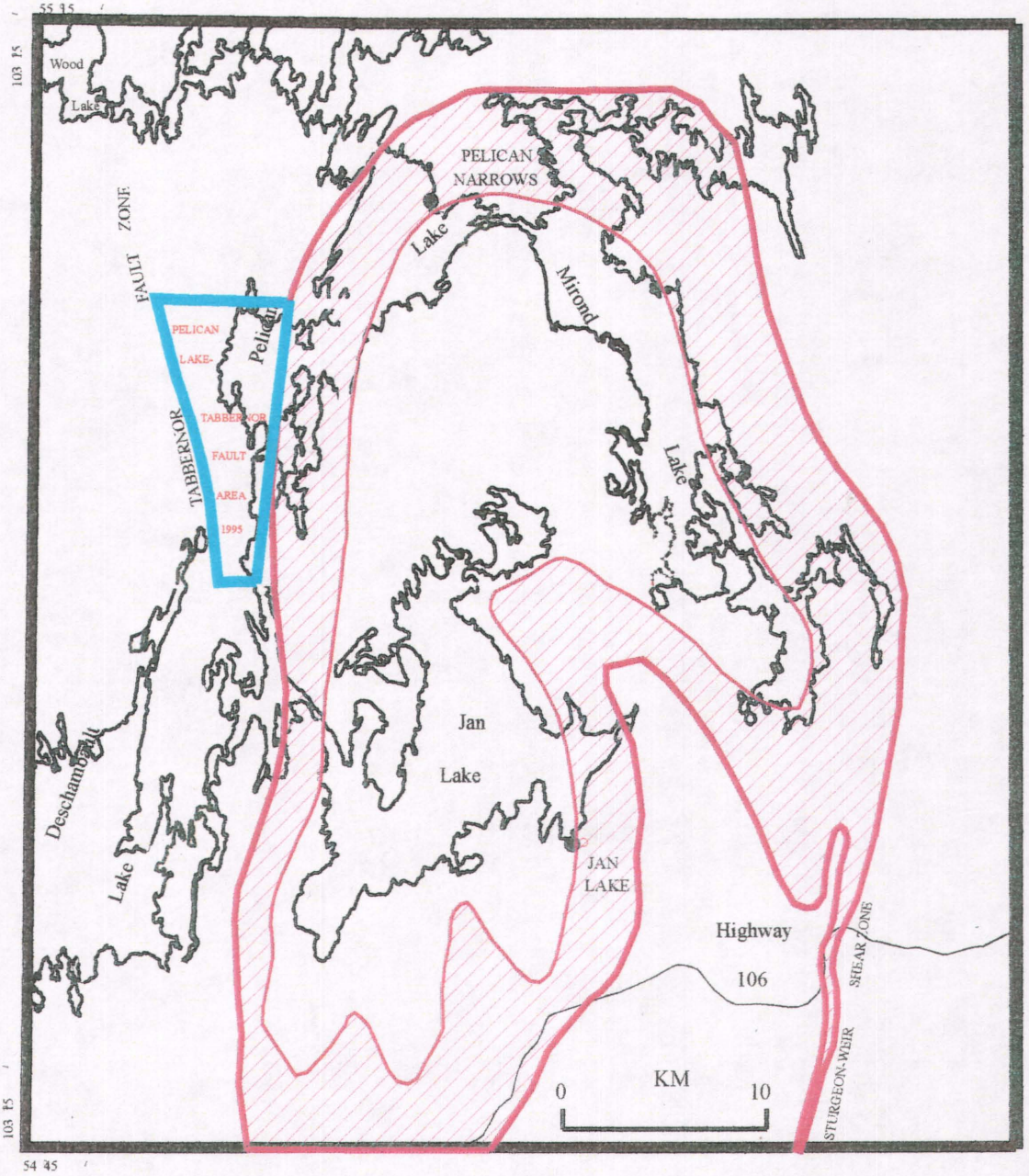

Figure 1.1 Location of the area mapped in 1995 and the area of investigation for this Thesis (outlined in blue) in relation to the Pelican Window (outlined in magenta). Modified after Ashton and Balzer (1995; original in color).

Granite represents a window through the Proterozoic Trans-Hudson Orogen into the Archean basement which is mantled by the structurally complex Pelican Décollement.

Historically regional metamorphism has been attributed to a single prolonged event (Sibbald, 1978; Gordon 1989 Zwanzig, 1990) which peaked in the core of the Kisseynew Domain at about 1815 Ma. Closer to the study area, within the adjacent Attiti Complex, metamorphic zircon has been dated at 1807-1805 Ma (Ashton *et al.*, 1992; Heaman *et al.*, 1992). More recently (Ansdell *et al.*, 1995; Ansdell and Norman, 1995; Heaman *et al.*, 1995; Norman *et al.*, 1995; and Ashton, 1999) documentation of overprinting relationships has lead to the understanding that metamorphism may have begun prior to or coeval with the main fabric developing event, the Pelican Thrust (Lewery *et al.*, 1996; Sun *et al.*, 1996) at about 1835 Ma. This is supported by a monazite grain dated at 1831 Ma (Hartlaub *et al.*, 1997), and by a secondary population of zircons within an 1848 Ma granodiorite that date at 1833 Ma (Elliot 1995a). Numerous studies focusing on determining metamorphic conditions and relating these conditions to time have been undertaken (e.g., Froese and Gasparrini, 1975; Bailes and McRitchie 1978; Lewry *et al.*, 1978; Gordon 1981,1984; Gordon and Gall 1982; Gordon *et al.*, 1994; Jackson and Gordon 1985, 1986; Ashton and Wheatley 1986; Digel *et al.*, 1991; Perkins 1988, 1991a, 1991b; and Ansdell and Norman 1995) however, with the exception of Kraus and Menard, (1997), Menard and Gordon, (1997), and Tran, (1997) examining the possibility of two separate

metamorphic events has not been exploited. From these few accounts it is clear that documentation of mineral fabric relationships within the Kisseynew Domain Metasedimentary rocks pertaining to metamorphic mineral growth is lacking, and further investigation into this area is needed to reconcile the interpreted metamorphic dates to metamorphic conditions. By careful study of the mineralogical and textural features of the rocks, it is possible to build an understanding of the interrelationships between mineral phases, deformational events, and metamorphism. Textural analysis and determination of growth positions for selected porphyroblasts may help delineate pre-, syn-, and post-tectonic relationships. Some porphyroblasts, such as garnet, may show textural and/or chemical zonation resulting from multiple growth episodes. As well, inclusions within porphyroblasts, or coronas can lead to an understanding of metamorphic conditions during growth, and precursor mineral assemblages.

The focus of this study is to (1) relate metamorphic mineral growth to deformational events in this portion of the Kisseynew Domain by documenting textures, establishing the existence of two separate metamorphic events in the Proterozoic past; and (2) investigate the nature of the metamorphic conditions.

1.1. Thesis Outline

This thesis discusses observations and interpretations previously reported in part within Ashton and Balzer (1995), and Balzer and Pan (1997). The

geological setting of the study area, within the regional framework of the Reindeer Zone of the Trans-Hudson Orogen, including rock type descriptions, and a structural synthesis, are the subject of Chapter 2. Analytical methods are outlined in Chapter 3. Chapter 4 discusses textural interpretations and deformation of key minerals as they relate to growth generations, and mineral chemistry as determined by electron microprobe. Chapter 5 investigates metamorphism, and Chapter 6 deals with timing and tectonic mechanism of metamorphism. The last chapter (Chapter 7) summarizes the geological history of the area with reference to the conclusions derived from within this thesis.

CHAPTER 2:

GEOLOGICAL SETTING

2.0. Regional Tectonic Framework

The Proterozoic Trans-Hudson Orogen extends in subsurface from South Dakota to the edge of the Canadian Shield; flanked in the northwest and southeast by Archean cratons. Type sections in northern Saskatchewan and Manitoba show that the south and central areas are underlain by east-west trending metasedimentary and volcanic belts, which comprise the juvenile Reindeer Zone (Stauffer, 1984), (Figure 2.1). The Reindeer Zone consists mainly of rocks derived from an oceanic, subduction related arc setting (Lewry *et al.*, 1987; Van Schumas *et al.*, 1987; Gordon *et al.*, 1990), separated into distinctive lithostructural domains based on lithological, metamorphic, and structural differences. The Flin Flon, La Ronge, and Lynn Lake Domains consist of relatively low-grade, mafic to felsic metavolcanic rocks, metasedimentary rocks, and granitoid intrusions. High grade metasedimentary rocks dominate the Rottenstone-Southern Indian, and Kisseynew Domains; derived as basin infill from surrounding volcanic arcs. The Glennie Domain is a

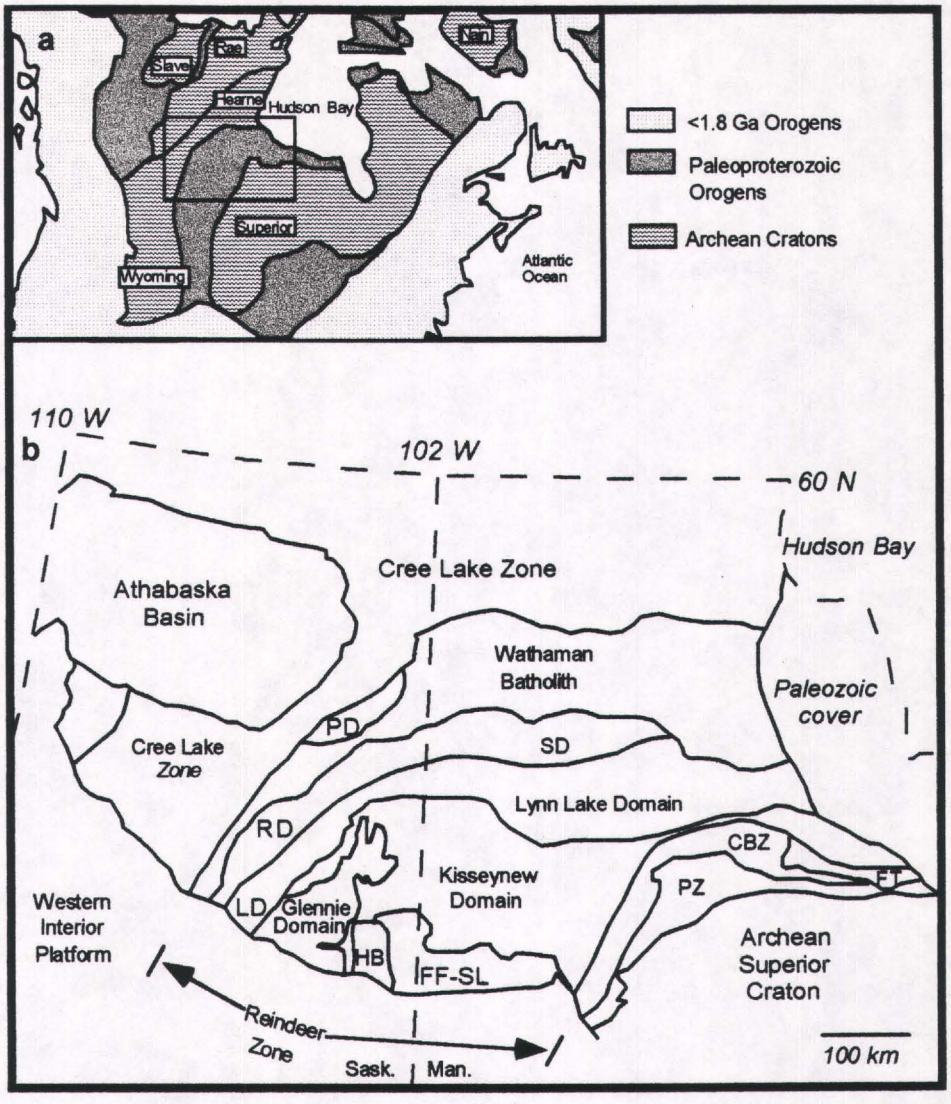

Figure 2.1 (a) The Trans-Hudson Orogen within the context of the Precambrian classification of North America. (modified after Lucus *et al.*, 1993; Ashton, 1999). The rectangle indicates the area displayed in Figure (b). (b) The zonal classification of the Trans-Hudson Orogen in Northern Saskatchewan and Manitoba. Abbreviations: PD=Peter Lake Domain, RD=Rottenstone Domain, LD=La Ronge Domain, HB=Hanson Lake Block, FF-SL=Flin Flon-Snow Lake Belt, SD=South Indian Domain, Pz=Pikwitonei Zone, FT= Fox Terrane, CBZ=Churchill-Superior boundary Zone.

volcano-granitoid terrain. Further to the east, is the Hanson Lake Block, comprised of Paleoproterozoic superacrustal and plutonic rocks, interpreted as part of the Flin Flon Domain (Ashton, 1999). Both the Glennie Domain, and the Hanson Lake Block contain Archean inliers which represent the underlying Sask Craton (Lewry *et al*, 1990, 1994; Ansdell *et al.*, 1995). To the north the Wathaman-Chipewan batholiths intrude the Trans-Hudson Orogen representative of a continental magmatic arc above a north dipping subduction zone (Lewry, 1981; Meyer *et al.*, 1992).

Subsurface data suggest that Archean basement is generally continuous beneath the Proterozoic Juvenile terranes of the Reindeer Zone (Lewry *et al.*, 1994). Paleoproterozoic rocks of the Hanson Lake Block structurally overlie the Archean basement. Near the Pelican Window these rocks comprise the proximal hanging wall which makes up the external suite of the highly strained Pelican Décollement Zone, mantling the Archean rocks of the internal zone of the Pelican Window. These Paleoproterozoic rocks are believed to correlate with those of the Attitti Complex, which is considered to be a high grade equivalent of the Flin Flon Domain (Ashton *et al.*, 1987; Ashton and Leclair, 1991; Ashton, 1999). To the north, rocks of the Scimitar Complex have recently been re-interpreted as an eastern extension of the Glennie Domain (Ashton *et al.*, 1997; Ashton, 1999). These volcano-plutonic rocks are also believed to be continuous with the Attitti Complex rocks beneath the Kisseynew metasediments (Ashton *et al.*, 1996; Ashton, 1999), all part of the volcano-

plutonic assemblage now termed the Flin Flon-Glennie Complex (Lucas *et al.*, 1999).

2.1. Tectonic Environment and Timing of the Assembly of the Reindeer Zone

Age constraints on the development of the Trans-Hudson Orogen were summarized by Ansdell and Norman (1995) and Lucas *et al.*, (1997). Extension and rifting of Archean continental crust of the Superior margin as well as in the Hearne province began at about 2100 Ma (Heaman and LeCheminant, 1993; Bleeker, 1996; Heaman and Corkery, 1996; Lucas et al., 1997). Passive margins developed on the Manikewan Ocean (Stauffer, 1984), likely beginning at 2100 Ma. The Reindeer Zone began to develop as oceanic arc magmatism and associated marginal basin volcanoclastic assemblages throughout the Manikewan Ocean from about 1920 Ma to 1870 Ma (Lucas et al., 1997). The juvenile Flin Flon-Glennie protocontinent developed as an accretion of arcs, associated sediments, oceanic crust and Archean inliers around 1870 Ma (Lucas et al., 1997). At about 1865 Ma the Flin Flon-Glennie protocontinent and the La Ronge-Lynn Lake arc were well separated by the Manikewan Ocean; postulated to be up to 5000 km wide at this point (Symons *et al.*, 1995, Lucas et al., 1997). The continental margin of the Hearne province and the La ronge-Lynn Lake arc collide some time (~1860 Ma) prior to the emplacement of the Wathaman Batholith at 1855 Ma. The latter intruded above a west dipping

subduction zone following the arc-continent collision (Bickford *et al.*, 1990). At this stage, back arc extension may have initiated, developing the Kisseynew Basin (Ansdell *et al.*, 1995). 1850 Ma to 1835 Ma was a period of widespread plutonism and basin sedimentation, including back arc sedimentation in the Kisseynew Basin. Arrival of the Sask Craton at about 1835 Ma initiated oceanic closure with generation of southwest-vergent crustal imbrication and tectonic thickening; which lead to emplacement of juvenile nappe sheets across the Craton (Ashton and Lewry, 1994; Heaman *et al.*, 1995). Southwest vergent tectonic transport across the Sask Craton continued until 1805 Ma (Lucas et al., 1997). Terminal closure at 1800 Ma to 1700 Ma resulted north-south and northeast-southwest fold phases through the transpression and indentation of the Superior Craton, refolding previously generated thrust stacking associated with the Sask Craton-Reindeer Zone collision (Lucas et al., 1997). Late to post-tectonic leucogranites and pegmatites intruded at approximately 1780 Ma, followed by uplift and cooling (Lucas et al., 1997). Deformation along oblique-slip reverse high strain zones continued until approximately 1690 Ma (Fedorowich *et al.*, 1993).

The study area is located in the south central part of the Reindeer Zone. The area itself is comprised mainly of Burntwood Group rocks from the Kisseynew Domain (Figure 2.2). This area adjoins the Glennie Domain to the west, and the Attitti Complex rocks of the Flin Flon-Glennie Complex to the east. The Kisseynew Domain within the study area is separated from the rocks of the

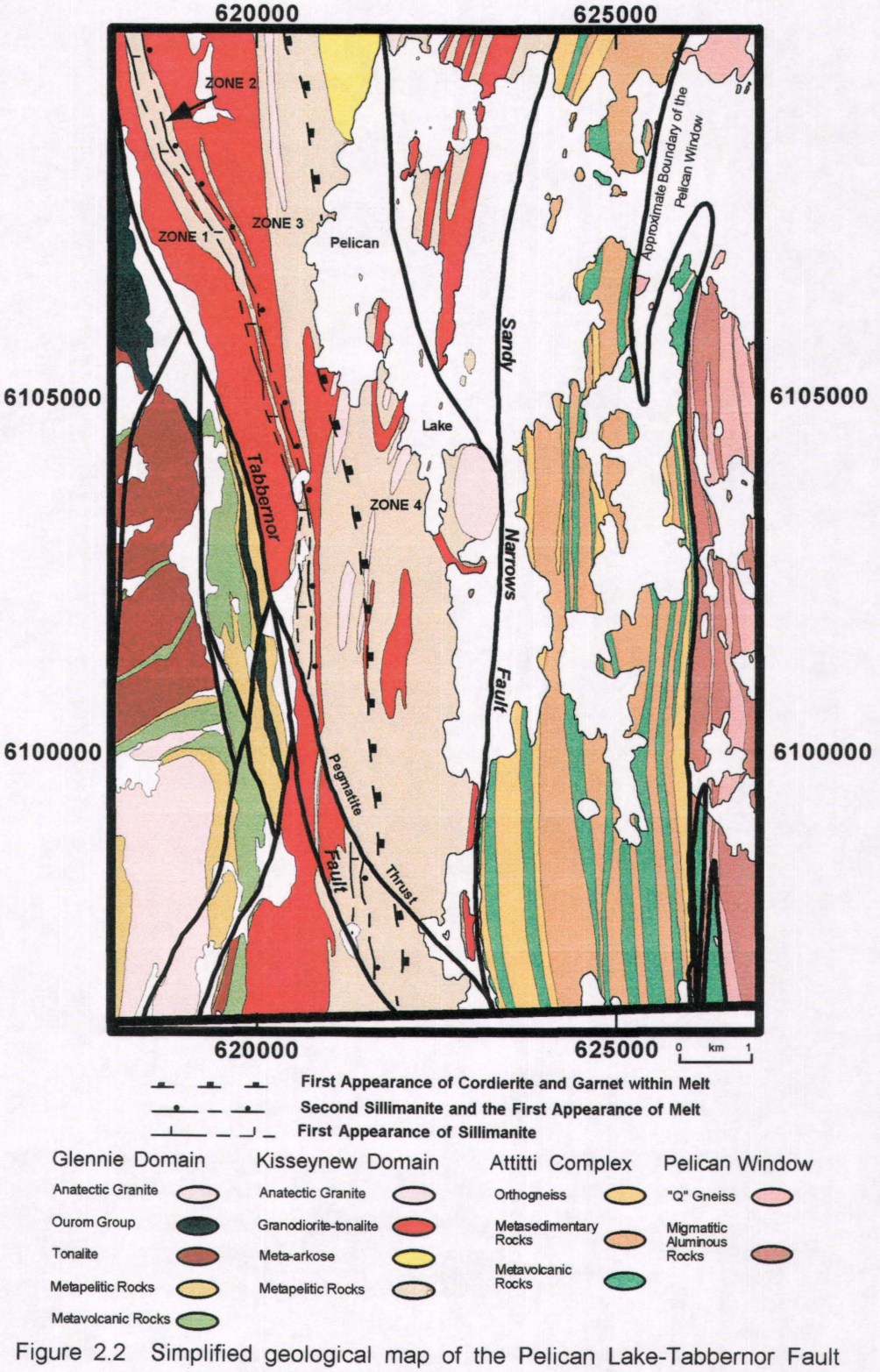

Figure 2.2 Simplified geological map of the Pelican Lake-Tabbernor Fault area (modified after Ashton and Balzer, 1995; original in color).

Glennie Domain by the narrow, north trending, ductile/brittle Tabbernor Fault Zone. Rocks of the Attitti Complex are separated from the Kisseynew rocks on the eastern side of the study area by the brittle/ductile Sandy Narrows Fault.

2.2. Lithology of the Pelican Window

The eastern map area (Figure 2.2) encompasses a portion of the Pelican Window, and rocks of the ≥ 2960 Ma Jan Lake Complex (Ashton *et al.*, 1999). These are typically highly strained and attenuated migmatitic aluminous wackes, and rocks of the "Q" Gniess suite (Macdonald, 1974; Macdonald and MacQuarrie, 1978). Further to the east (not on the map) is the charnockitic Sahli Granite. The highly strained rocks comprise the footwall of the Pelican Thrust, and the internal zone of the Pelican Décollement.

2.2.1. Migmatitic Aluminous Rocks

These are variably mylonitized and migmatitic to diatexitic rocks containing up to 80 percent white leucosomal layers. The paleosome consists of 50-60 percent quartz and feldspar, 20-25 percent biotite, 10-15 percent garnet, with minor sillimanite and trace graphite. Sillimanite is present within the leucosome, of which there is an associated well developed garnet-biotite-sillimanite melanosome. The areanaceous component locally grades into fine grained

variably boudinaged feldspathic-quartzite (30 percent feldspar and 70 percent quartz) layers up to a few centimeters thick.

2.2.2. The "Q" Gneiss Suite

The "Q" Gneisses consist of leucocratic granitoid rocks with a color index of less than 10 (Ashton and Shi, 1994). Outcrops are commonly complex with abundant mafic and granitiod dykes, and up to 30 percent partial melt. Five varieties have been distingushed (Ashton and Shi, 1994), based on the relative percentages of K-feldspar, quartz, biotite, and hornblende. These include: Leucogranodiorite-tonalite; Leucogranite-granodiorite; Hornblende-magnetite leucogranite-granodiorite; Biotite-magnetite leucogranodiorite; and a Heterogeneous leucogranite-tonalite. All units are typically very highly strained to form banded to laminated quartzofeldspathic mylonites. Based on $^{207}Pb/^{206}Pb$ single zircon analysis, Sun *et al.*, (1996) determined these rocks are as old as ca. 2900 Ma.

2.3. Lithology of the Attitti Complex

Rocks of the Attitti Complex are believed to be a western extension and high grade equivalent of the Proterozoic volcano-plutonic supracrustral rocks of the Flin Flon Domain (Ashton *et al.*, 1987; Ashton and Leclair, 1991; and Ashton *et al.*, 1993). They completely mantle the Archean gneisses of the Pelican

Window, and have been demonstrated to occur in the Scimitar Complex to the north (Ashton *et al.*, 1996; Ashton *et al.*, 1997).

Attitti Complex within the map area is comprised of a series of interlayered mafic to felsic metavolcanic rocks with intercalated metasedimentary rocks. They are highly deformed, with up to four deformational phases recognized. Metamorphism has reached upper amphibolite facies, which coupled with intense deformation makes protolith identification and interpretation difficult. All phases of volcanic rocks are present within the Attitti Complex, however only samples of the mafic to intermediate metavolcanic rocks and migmatitic granodiorite-tonalite rocks were collected.

2.3.1. Mafic to Intermediate Metavolcanic Rocks

The mafic rocks are composed of intensely foliated fine grained hornblende-plagioclase±clinopyroxene±garnet gneisses with approximately 0-20 % quartz. Locally they may exhibit intercalations of centimeter to decimeter wide clinopyroxene-pyrrhotite rich layers. Intermediate volcanic rocks are fine grained, containing 20-40 % hornblende, 25-35 % quartz, 25-30 % feldspar and trace pyrrhotite.

2.3.2. Metasedimentary Rocks of the Attitti Complex

Metasedimentary rocks of the Attitti Complex consist of hornblende-bearing wackes and aluminous wackes. No samples were collected, however field relations indicate the hornblende-bearing wackes are interlayered with the volcanics and compositionally consist of quartzo-feldspathic gneisses with major biotite-hornblende, and minor graphite and garnet. They also contain hornblende-bearing leucosomes and hornblendite pods.

The aluminous wackes are gradational from the hornblende-bearing wackes and typically consist of quartz, feldspar, 20 to 30 percent biotite, garnet, and minor graphite and sillimanite. Both the hornblende-bearing and aluminous wackes are considered correlative with the Welsh Lake Assemblage of the Flin Flon Domain (Ashton *et al.*, 1993).

2.3.3. Intrusive rocks of the Attitti Complex

Ashton and Balzer (1995) distinguish four intrusive phases with one of questionable affinity. These are as follows: a unit of medium to fine grained layered dioritic to gabbroic intrusive rocks found within the Attitti Complex metasedimentary rocks; an ca. 1850 Ma (Ansdell and Kyser, 1991; Heaman *et al.*, 1993), migmatitic granodioritic-tonalititc orthogneiss consisting of 30-90 % quartzo-feldspathic, biotite, and hornblende leucosome which may contain hornblendite pods; an undifferentiated unit of mylonitic tonalite-granodiorite which is derived from the inability to separate the Archean orthogneisses of the

Pelican Window and the Proterozoic granodiorite-tonalite; and an early pegmatitic white granite, exhibiting an internal foliation parallel to the main regional foliation (S_2).

2.4. Lithology of the Glennie Domain within the Map Area

The Glennie Domian is dominantly comprised of plutonic, and volcanic to volcaniclastic rocks with a tholeiitic geochemical signature (Slimmon, 1994); believed to have originated from an island-arc setting. Rocks consistent with the Glennie Domain are encompassed within the western most portion of the map area (Figure 2.2). Five basic rock groups were delineated based on previous work by Sibbald (1978), Wilcox (1990), and Elliott (1993). These are: The Ourom Group metasedimentary and volcanic rocks; an anatectic granite consisting of a peraluminous pegmatite; a tonalite; metasedimentary rocks; and metavolcanic rocks.

2.4.1. Ourom Group

The Ourom Group is primarily a sedimentary sequence (Tran *et al.*, 1996) of psammitic to psammopelitic arkose, conglomerate, and interlayered mafic to felsic volcanic rocks (Delaney, 1987). McNicoll (*et al.*, 1992) determined that deposition of the Ourom Group occurred between 1848 and 1838 Ma,

consistent with the interpretation that they unconformably overlie the volcano-plutonic rocks (Wilcox, 1991; Elliott, 1993; Tran *et al.*, 1996).

The conglomerates are comprised of polymictic layers with clasts consisting of fine-grained arkose, granitic-granodioritic rocks, fine grained mafic rocks, and quartz. Some rare units contain clasts with up to 50 percent magnetite and hematite, consistent with a high areomagnetitc signature (Tran *et al.*, 1996).

The arkosic portion of the Ourom Group is comprised mainly of a fine to medium grained arkosic arenite consisting of feldspar, quartz, and biotite with minor muscovite, and sillimanite. Interlayered with the fine to medium grained arkose is a pebbly/gritty unit which is laterally gradational to the conglomerates. These rocks are composed mainly of quartz and feldspar grains from <1 to 4mm in diameter (Tran *et al.*, 1996). Locally occurring pebbly horizons contain clasts of polycrystalline quartz, granodiorite-tonalite, mafic to felsic volcanics, and highly flattened dark "fiamme" (Sibbald, 1978) clasts of uncertain origin (Tran *et al.*, 1996).

2.4.2. Anatectic Granite

The anatectic granite consists of white to pink pegmatitic masses, concordant sheets, and discordant dykes, all of which exhibit a variable weak to moderate foliation. This rock unit is present intruding the Glennie Domain as well as the

Burntwood Metasedimentary rocks in the Kisseynew Domain. The granite contains major quartz, plagioclase, and microcline, with minor amounts garnet, biotite, muscovite, and sillimanite; as both faserkiesel and individual fibrolite grains. Ashton and Balzer (1995) suggest that the granite is an anatectic melt derived from aluminous sediments at depth.

2.4.3. Tonalite-Granodiorite

A generally weakly foliated granodiorite tonalite, is comprised 50-60 percent plagioclase, 20-25 percent quartz, less than 15 percent K-feldspar, biotite and hornblende, and trace magnetite. Within the map area these rocks are locally affected by heterogeneous brittle/ductile deformation related to the Tabbernor Fault.

2.4.4. Metasedimentary Rocks

The assemblage labeled metasediments (Figure 2.2) within the Glennie Domain comprises mainly of andalusite bearing schists which exhibit local variations in strain related to the Tabbernor Fault. Mineralogically the schists contain quartz-feldspar-biotite±andalusite±staurolite with trace magnetite.

2.4.5. Metavolcanic Rocks

Within the map area metamorphosed volcanic rocks are represented by dark green to black/brown fine grained hornblende schists. These mafic metavolcanics are highly deformed and locally mylonitic. Wilcox (1990) interpreted the protoliths to be sub-volcanic intrusive rocks to basaltic flows and pillow lavas. Based on two rhyolite packages in the Gee Lake area, Heaman *et al.*, (1991, 1992) report volcanism to have occurred at approximately 1875-1866 Ma.

2.5. General Geology of the Kisseynew Domain

The Kisseynew Domain is a 150 x 300 km gneissic belt situated in northern Saskatchewan and Manitoba. It is located in the Reindeer Zone (Stauffer, 1984), a composite terrane formed through the collision of the Superior and Hearne Provinces and the Saskatchewan Craton (Ansdell *et al.*, 1995). Rocks within the Kisseynew Domain consist of metasediments and migmatites (Perkins, 1991a). It is a remnant of the largest arc-related basin in the Reindeer Zone (Zwanzig, 1990).

Five supracrustal suites have been recognized: (1) fine-grained amphibolites and felsic gneisses, the equivalents to Amisk Group metavolcanics and volcaniclastics of the Flin Flon belt; (2) siliceous, pelitic and calc-silicate gneisses termed the Sherridon gneisses; (3) Burntwood Suite metasediments, interpreted to be metamorphosed greywackes and mudstone turbidites; (4) quartzofeldspathic gneisses of the Sickle Suite; and (5) quartz-rich sedimentary

and volcanic rocks of the Missi Suite, interpreted to be equivalent to those in the Flin Flon Domain. Intrusive bodies within the Kisseynew range from diorite to leuocogranite, and have various ages ranging from ~ 1860-1810 Ma (Zwanzig, 1990).

Burntwood metasediments are interpreted to be marine sediments deposited in an island arc setting (Zwanzig, 1990). Sickle and Missi sediments represent the two tectonic stages of a continental-arc setting that evolved into a crustal setting, at which time basin sedimentation ceased (Zwanzig, 1990).

2.6. Lithology and Metamorphic Zonation Within the Thesis Area

Previous studies of the thesis area include Sibbald (1978), Wilcox (1990), Elliot (1993, 1994), and Ashton and Balzer (1995). Lithologically there are four main Kisseynew rock types within the study area. These are the Burntwood Group metasedimentary rocks; an intrusive granodiorite-tonalite; a peraluminous anatectic granite; and the late stage Jan Lake Intrusive Suite (Ashton and Balzer, 1995).

Burntwood Group rocks within the study area consist of metamorphosed turbidites composed of intercalated shale and psammitic layers (Ashton and Balzer, 1995). Layering of the sandy and shaly beds vary in scale from decimeters to metres, grain size ranges from fine to medium. The mineralogy of

the metaturbidites changes from west to east with an interpreted increase in metamorphic conditions. Directly adjacent to the Tabbernor Fault are andalusite-cordierite-staurolite gneisses, the low grade end members of the Burntwood Suite within the area. These rocks are fine grained and consist of approximately 40-60% quartz, 10-15% biotite, 5-15% plagioclase, 5-10% chlorite, 5-10% muscovite, ±5-10% andalusite, ±5% staurolite, ±1-2%cordierite, 2% apatite, 2% opaques (mainly ilmenite) and trace graphite. Towards the east the mineralogy changes in accordance with metamorphic grade to include the disappearance of andalusite; appearance of garnet and sillimanite; disappearance of primary muscovite; and the appearance of variably concordant early melt, and cross-cutting late melt. In the highest grade area to the east, the metapelitic layers are medium to fine grained and consist of 30-40% subhedral quartz, 20-25% biotite, 20% plagioclase (An 25-50), 1-2% potassium feldspar, 5% sillimanite, 1-5% cordierite, 1-5% garnet, with minor muscovite (0-2%) and albite, with trace amounts of ilmenite, graphite, apatite, titanite, and zircon. The psammitic layers are fine grained and are comprised of 30% quartz, 20-25% biotite, 30% plagioclase (An 25-50), 0-5% sillimanite, 0-2% muscovite, 0-1% garnet, with trace ilmenite, apatite, titanite, graphite, and zircon. Based on the mineralogical changes, isograds delineating metamorphic and compositional zones have been placed on a map of the area (Figure 2.2). Zone 1 is termed the Andalusite Zone, and consists of andalusite-cordierite-staurolite bearing gneisses. Zone 2, on the eastern side of Zone 1, consists of sillimanite-garnet-cordierite-muscovite-biotite gneisses. Within Zone 3 the rocks consist of

intercalated garnet-biotite and sillimanite-garnet-cordierite-biotite gneisses. Zone 4 is mineralogically similar to Zone 3, however within this Zone an additional late cordierite-garnet bearing melt is present. Two generations of leucosomes are recognized, and are present within the last two zones only. Both leucosomes are comprised of quartz, feldspar, ±cordierite, ±garnet, however the earlier generation is variably concordant with the main fabric of the rock (S_2), showing evidence of isoclinal folding. The later generation of leucosome is present only within Zone 4. It is coarse grained and comprised of 60% quartz, 0-20% garnet, 5-10% plagioclase (An 25-30), 5-10% cordierite, and 2-4% biotite. Observations based on cross-cutting relationships and kinematic features suggest that development of this melt began prior to D_3, and lasted throughout. These leucosomes are observed in positions gradational between the two end member positions, cross-cutting the S_2 fabric, and dextrally rotated into axial planar position to F_3 folds; and as a crosscutting patch melt (Figure 2.3a and b). Myrmeketic textures are common, and the cordierite porphyroblasts within the late leucosomes are euhedral to subhedral in shape. The majority of the garnet grains are, however, anhedral and contain numerous mineral inclusions (e.g., quartz, biotite, and feldspar). These garnet grains are interpreted to be partially resorbed grains from the matrix. Table 2.1 indicates the general mineralogy of the metapelitic rocks.

A small unit of meta-arkose crops-out within Zone 4 at the northwest end of Shaw Bay. The rocks are well foliated and weakly layered, with a significant

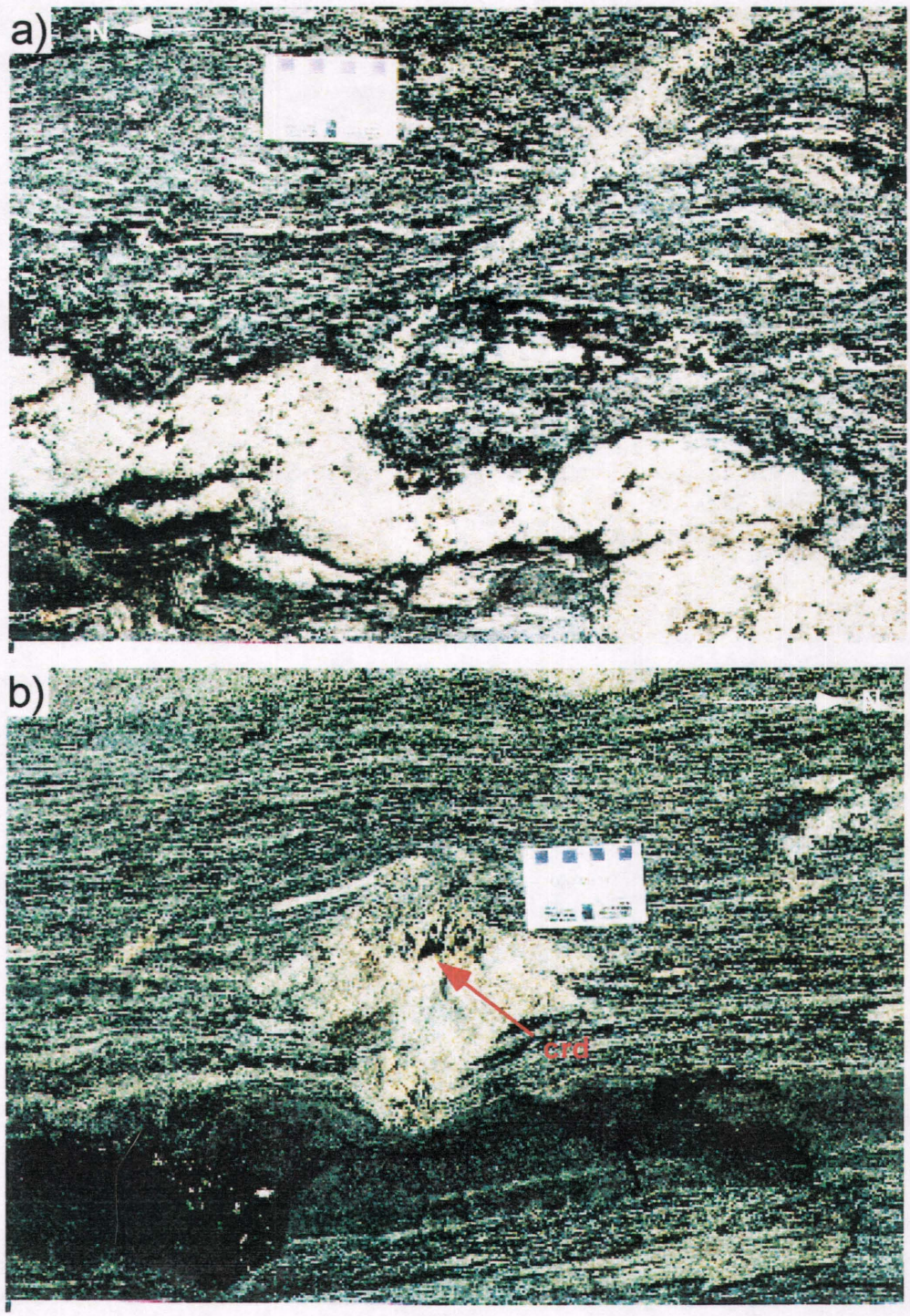

Figure 2.3 Outcrop photographs of the two types of leucosome within Zone 4. (a) Photograph of outcrop 5068 showing the relationships between the two types of melt. An early concordant leucosome and a later crosscutting leucosome that has been rotated into axial planar position to F3 folds. (b) Photograph of outcrop 0011 showing the crosscutting patch melt leucosome, indicating that conditions were hot enough to cause leucosome development late syn- to post D3. crd = cordierite

TABLE 2.1 General mineralogy of the Kisseynew Domain Metaturbidite rocks in the Pelican Lake, Tabbernor Fault area.

METAMORPHIC ZONES	1	2	3	4
MINERALS	ANDALUSITE	SILLIMANITE	SECOND SILLIMANITE	MELT WITH CORDIERITE-GARNET
QUARTZ	X	X	X	X
PLAGIOCLASE	X	X	X	X
BIOTITE	X	X	X	X
CHLORITE	X			
STAUROLITE	X			
ANDALUSITE	X	X		
MUSCOVITE	X	X	RETROGRADE	RETROGRADE
K-FELDSPAR			X	X
ALBITE		RETROGRADE	RETROGRADE	RETROGRADE
SILLIMANITE		X	X	X
GARNET		X	X	X
CORDIERITE	X	X	X	X
APATITE	X	X	X	X
GRAPHITE	x	X	X	X

partial melt component. No samples were collected, however mineralogical examination within the field indicates these rocks consist of 80-85% quartz and feldspar, 5-10% biotite, with minor amounts of garnet and hornblende.

2.6.1. Intrusive Rocks

Three intrusive rock types are found regionally throughout the Thesis Area. These include a granodioritic-tonalitic pluton which intrudes the Burntwood Group throughout all four zones. These rocks are well foliated orthogneisses which in Zones 3 and 4 exhibit garnet growth at the contact margins with the Burntwood metasediments. Mineralogically the granodiorite contains 30-40% quartz, 30-40% feldspar, 10-20% biotite, and 0-10% hornblende with trace titanite. The grain size is a function of proximity to the many small scale D_2 ductile, sinistral shears that run through the intrusive body, and ranges from fine to mylonitic.

Also intruding the Metaturbidites as pink to pale pegmatitic masses, variably concordant and discordant masses is a peraluminous anatectic granite. This granite contains major quartz, plagioclase, and microcline, with minor amounts garnet, biotite, muscovite, and sillimanite; as both faserkiesel and individual fibrolite grains. Ashton and Balzer (1995) suggest that the granite is an anatectic melt derived from the aluminous Burntwood metasediments. The mineralogy of this rock body indicates that it intruded the upper Burntwood

Metaturbidites while the metamorphic conditions were within the sillimanite stability field, but lower than the second sillimanite isograd. This pegmatite exhibits a foliation consistent with emplacement prior to the main phases of deformation.

The Jan Lake Suite of intrusive rocks are granitic in composition and range in grain size from medium to pegmatitic. They were emplaced at approximately ca. 1770 Ma (Bickford *et al.*, 1987; Ashton *et al*, 1992) and represent the last intrusive phase in the area.

2.7. Recent Structural Interpretations

The two most recent structural interpretations of the region have been formulated by Ashton and Balzer (1995) and Tran et al., (1996). Ashton and Balzer (1995) recognized five phases of regional scale deformation, Tran et al., (1996) condensed them into three ductile phases, and one later faulting stage. Within the study area, this investigation identifies four phases of deformation, including late brittle/ductile faulting associated with the Tabbernor Fault system. Table 2.2 relates the main features of the deformational events as reported by Ashton and Balzer (1995), Tran et al., (1996), and this study. The main pervasive fabric is layer parallel and generally steeply east dipping to vertical with some segments exhibiting a steep westwards dip. This foliation is a result of the combination of deformation episodes D_1 and D_2. S_1/S_2 was then altered

Table 2.2. Features of the deformational events from the most recent interpretations.

Deformational Episodes	Ashton and Balzer (1995)	Tran et al., (1996)	This Study
D1	- not clearly present, but believed to be a foliation that resulted from D1 as the same deformational event within the Flin Flon Domain	-weak to intense foliation (S1) defined by mineral orientation - isoclinal folds - possibly a result of the Pelican Thrust	- early foliation (S1) defined by mineral orientation
D2	- existent as an early foliation, that resulted from a combination of the deformational events D1 and D2 as the same events within the Flin Flon Domain	- large scale south plunging antiforms and synforms - S2 foliation is predominantly a strain slip schistosity oblique to S1	- resulting from the Pelican Thrust - refolding of the So/S1 foliation into tight isoclinal folds which transposed the early foliation into S2, axial planar to F2 folds - protomylonitic to mylonitic shears termed the Pegmatite thrusts
D3	- tight to isoclinal folding as a result of the Pelican Décollement, and the development of S3 axial planar to F3 - development of the Pegmatite Thrust	- two sets of gentle open folds which refold D2 structures	- Sandy Narrows brittle-ductile Fault - gentle to tight crenulating folding of the S2 foliation - development of an S3 foliation parallel to the axial plane of F3 folds - rotation of leucosomal
D4	- open folding of the F3 folds - development of an S4 fabric parallel to the axial plane of F4 folds	- steeply dipping north- to northeast-striking late faults - part of the Tabbernor Fault system	- late steeply dipping north striking brittle faults, which cross-cutt and offset the Pegmatite Thrusts -Tabbernor Fault system
D5	- steeply dipping north- to northeast-striking late faults - part of the Tabbernor Fault system	non existent	non existent

by a third ductile event to produce open to tight folds, and a late S_3 fabric aligned parallel to the F_3 axial plane. Brittle to ductile deformation post-dating D_3 resulted in the present positions of both the Tabbernor and Sandy Narrows Faults.

2.7.1. D_1 and development of S_1

The earliest deformation event D_1 is exhibited as an early foliation (S_1) delineated by the preferred orientation of elongated minerals. This fabric is not easily identified by itself as later deformational episodes have overprinted and transposed this early alignment. This fabric forms the original gneissic banding within the rocks. Tran et al., (1996) defined an early schistosity subparallel to sedimentary layering (S_0) as well as development of coeval isoclinal folding. Within the current study area, however, the S_1 fabric is distinguishable only within tight folds interpreted to be the result of D_2. Isoclinal folds recognized as F_1 in the Wood Lake area (Tran, 1996) are not recognizably expressed in this more southerly extension of the Kisseynew. This is likely the result of more intense shortening from later deformational episodes, and the proximity to the Pelican Window. This original foliation has also been associated with deformational episodes parallel to the D_1 and D_2 events within the Flin Flon Domain (Ashton and Balzer, 1995). This is an assumption based on the fact that the deformational episodes within the Flin Flon Domain affect the local sedimentary rock packages, such as the Missi Group, which was believed to be

somewhat younger (minimum age of 1847 to 1842 Ma; Syme et al., 1993) than the Kisseynew Metaturbidites (1875 Ma; Gordon, 1989). More recent dating (Ansdell and Norman, 1995) has shown, however, that the Burntwood was deposited relatively coeval with the Missi Group. No major structures are obviously evident as a result of D_1 within the thesis area.

2.7.2. D_2 and the development of the S_2 fabric

The early S_1 fabric was then modified by southwest-northeast compression during D_2 with collision of the Sask Craton at ~1835 Ma. This second period of deformation gave rise to a straight zone termed the Pelican Décollement (Thrust) (Lewry et al., 1996; Sun et al., 1996), covering the margins of the Kisseynew Domain and the Pelican Window, as well as the Attitti Complex. This deformational event involved intense shearing which was long lived and resulted in tight to isoclinal folding transposing S_1 parallel the axial plane of F_2 folds. The resultant position of the fabric (S_2) is the most pervasive throughout the study area. Isoclinal folding related to D_1 (Tran *et al.*, 1996), if present has been transposed into the axial plane of F_2, making separation difficult.

A major structure interpreted to be a component of the D_2 event is the "Pegmatite Thrust" (Wilcox, 1990; Ashton and Balzer, 1995) (Figure 2.2); a one kilometer wide ductile shear system. This ductile shear exhibits heterogeneous strain in the form of protomylonitic to mylonitic zones each in the order of 1-10m

wide. These areas of strain are most evident within the granodioritic plutonic rock which intrudes the Burntwood Group metatubidites. The entire system of ductile shear is crosscut and offset by the Tabbernor Fault. The former exhibits an east dipping shear foliation; a south to southeast plunging stretching lineation; and shear band kinematic indicators that suggest sinistral-reverse shear (Ashton and Balzer, 1995). The apparent direction of movement, along with the presence of later F_3 overprinting crenulations indicates that this ductile shear is presumably part of the D_2 episode and may be a splay from the Pelican Décollement.

Within the peraluminous anatectic granite, S_2 is locally defined by sillimanite. Within the Burntwood Metasedimentary rocks the D_2 event is associated with a pre- to syn- metamorphic event (M_1) by the growth of biotite, andalusite, sillimanite, cordierite, garnet, K-feldspar, and a concordant garnet/cordierite-bearing leucosome.

2.7.3. D_3 and the development of the S_3 fabric

The D_3 event is exhibited in the rocks by tight to open folds and crenulation of S_2, with steeply dipping north to northeast striking axial planes, and the development of an axial planar fabric (Ashton and Balzer, 1995). Within the Pelican Window D_3 is typically expressed as tight folding with steeply east to rarely west dipping axial planes, and a locally developed axial planar fabric

delineated by quartz flattening. F_3 crenulations and kink folding are a common expression of the D_3 event throughout the region. It is believed that this deformation is the result of collision with the Superior Craton, which may have begun at about ~1820-1810 Ma (Lucas *et al.*, 1997).

F_2/F_3 fold interference structures show a "type III" pattern (Ramsay, 1962, 1967; Ramsay and Huber, 1987). It is within these structures that F_2 is most easily recognized. The development of "type III" patterns results from refolding tight to isoclinal folds about folds with steeply dipping axial planes and hinges subparallel to parallel the early structures; accompanied by movement at a high angle to the earlier folding phase axial surface (Ramsay and Huber, 1987).

Direction of movement and shear during this deformational episode is indicated by several equivocal kinematic structures. Pinch and swell structures with asymmetric F_3 z-folding show dextrally rotated porphyroclasts. Other important features believed to have developed during D_3 include decimeter-scale cordierite-garnet leucosome filled tension gashes or boudin necks (Figure 2.4a and b), that were rotated into the D_3 flattening plane. These late leucosomes crosscut the S_2 fabric and show dextral rotation into approximately the same northerly position at 345° parallel F_3 axial planes. Leucosome generation continued throughout D_3 as patch melt crosscutting the S_2 fabric, but not oriented within the D_3 flattening plane (Figure 2.3a and b) indicating that melt conditions persisted post-D_3.

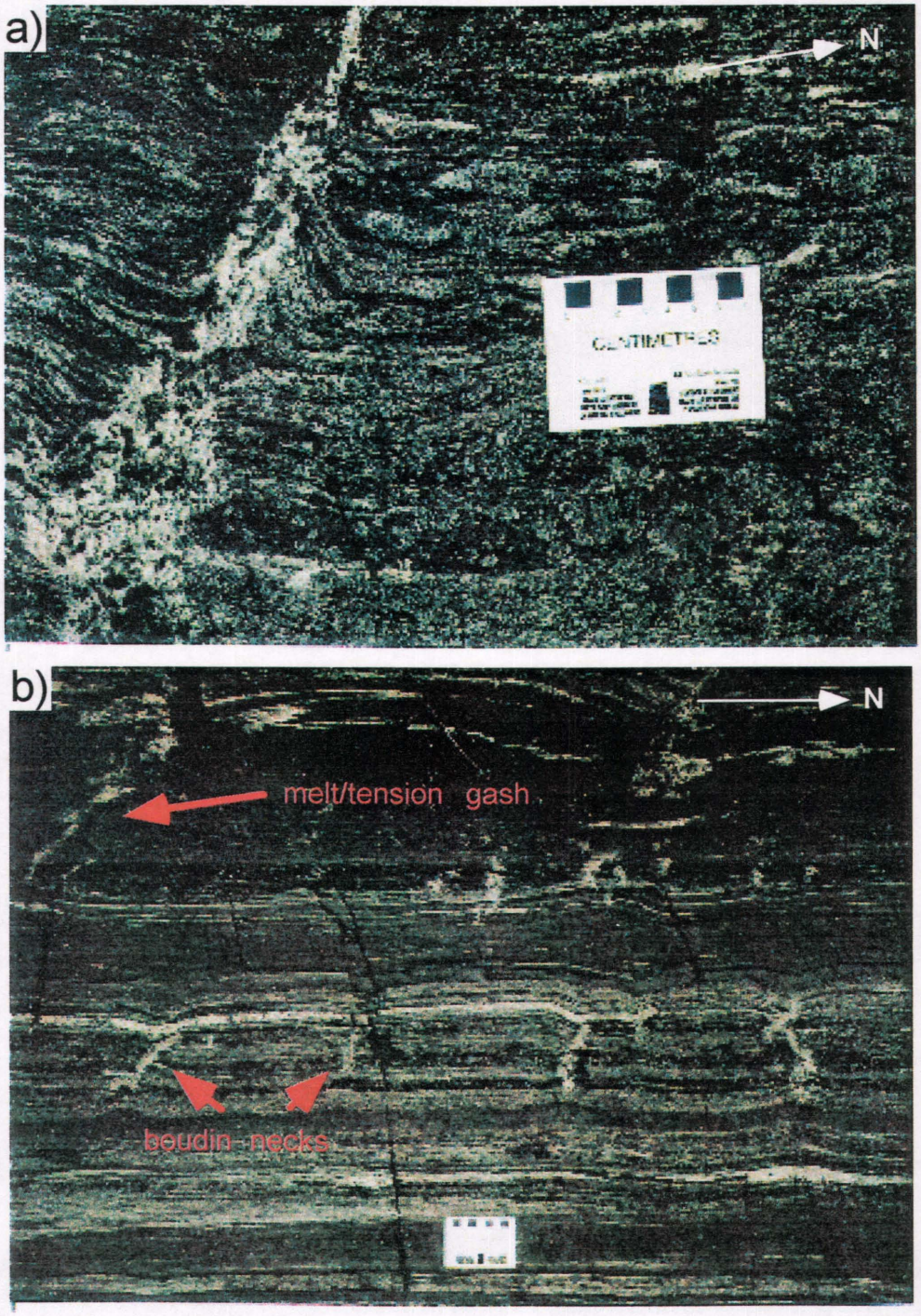

Figure 2.4 a) Tension gash rotated into the D3 flattening plane.
b) Boudin necks showing orientation parallel a tension gash at 345 °.

A foliation coeval with D_3 is displayed as both a crenulation cleavage and as new mineral growth in the Kisseynew Domain, oriented within the flattening plane parallel to the axial trace of F_3 folds (Figure 2.5a and b). A second metamorphic episode occurred syn-D_3 with mineral development of sillimanite, cordierite, biotite, garnet, and k-feldspar. These minerals overprint earlier fabrics, and have consistent textural differences from minerals associated with the early metamorphic event (Chapter 4).

2.7.4. Sandy Narrows Fault

A major feature on the eastern side of the Thesis area is the Sandy Narrows Fault (Ashton and Balzer, 1995) (Figure 2.2); a brittle-ductile fault separating the Attitti Block from the Kisseynew Domain. A southeast plunging stretching lineation combined with kinematic examination of the brittle faulting indicate sinistral-reverse movement. However, movement along this Fault is somewhat enigmatic. To the north, the Sandy Narrows Fault merges with the Guilloux Fault (Kirkland, 1976; Macdonald, 1981); which has a dextral component of movement documented by apparent displacement of rock units, quartz rodding, and slickensides, all consistent with east-side-up (Tran, Thesis, 1997). The apparent sinistral-reverse direction of movement in the Thesis area suggests that there was more than one period of activation. In the Woody Lake area Tran (Thesis, 1997) suggested that there were several reactivations along the faults, and that dextral movement post-dated sinistral shear.

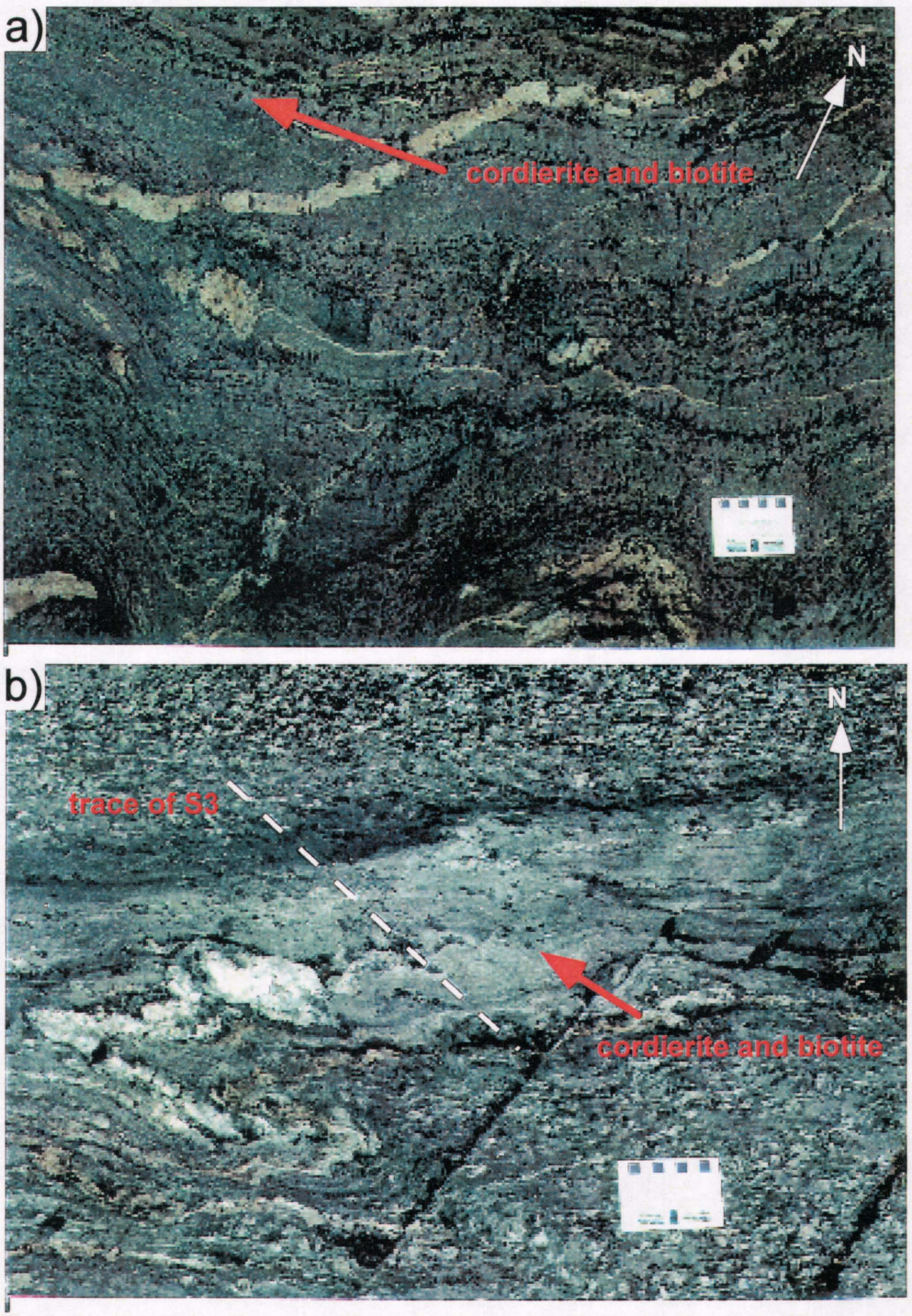

Figure 2.5 a) S3 foliation showing development as both a crenulation cleavage and growth of cordierite and biotite. b) Foliation exhibited by growth of cordierite and biotite.

2.7.5. Tabbernor Fault System

The Tabbernor Fault system (Figure 2.2) has also had a complex series of multiple activations. This brittle fault cross-cuts and offsets splays, part of the D_2 Pelican Décollement, which leads to confusion about the age of this north-south lineament. This zone of movement is also parallel to the Sandy Narrows Fault and may have been active during this event (Ashton and Balzer, 1995). Southeast plunging slickenslides along with the observed offset of the D_2 splays (Pegmatite Thrust, Wilcox, 1990) indicates a sinistral movement with displacement on the order of hundreds of metres (Ashton and Balzer, 1995). This is consistent with northwest-southeast shortening and collision of the Superior Province (Ashton and Balzer, 1995). However, late brittle dextral kinematic indicators have been documented as late as 1.737 Ga (Elliot, 1994, 1995b). Tran (Thesis, 1997) suggested that late dextral fault displacement may be attributed to late- to post-orogenic southwestward escape wedging of the western part of the Kisseynew Domain due to changes in terrain displacement during terminal collision (Lewry, 1981; Hoffman, 1989; Stauffer and Lewry, 1993).

It has also been suggested that the Tabbernor Fault structure may have acted as a buttress to the west verging D_3 movement, trapping material and resulting in the intense deformation and development of the steeply dipping straight zone (Ashton and Balzer, 1995). This would account for the difference in deformation

intensities between the eastern and western side of the Pelican Window. If the Pelican Window and the early version of the Tabbernor Fault acted as competent masses, the rocks existing between the two competent blocks would have been more intensely deformed then the rocks on the eastern side of the Pelican Window. Indeed the deformation styles on the western side of the Pelican Window are more intense, as there is a greater amount of D_3 overprinting then on the eastern side.

CHAPTER 3:

ANALYTICAL TECHNIQUES

3.0. Mapping and Sampling

The thesis area was mapped in detail during the 1995 summer season with the Geological Survey of Saskatchewan under the supervision of Dr. Ken Ashton. Lithologies have been traced and structural relationships recorded. Samples were collected from traverses through the Attitti Complex and Kisseynew Domain.

3.1 Whole Rock Geochemistry

Whole rock geochemistry was carried out on selected samples of metasedimentary rocks from each metamorphic zone, and two granodiorite samples, all from within the Kisseynew Domain. Major element concentrations were determined by X-ray Fluorescence analysis, while trace elements including rare earth elements analyzed by the inductively coupled plasma-mass spectrometer at the University of Saskatchewan following the procedures of Jenner *et al.* (1990). Samples for major element analysis were crushed in an

agate grinder and further crushed using an agate mortar and pestle, before being sent to McGill University, Montreal for X-ray fluorescence analysis using a Philips 2400 XRF. Crushed material exceeded 100 grams to ensure a representative sample for each analysis. Detection limits for major element analysis were 0.01 weight%. Repeat analysis produced errors of less than 1% for all major element oxides.

Trace elements were analyzed by inductively coupled plasma mass spectrometry (ICP-MS) at the University of Saskatchewan using a Perkin Elmer Elan 5000. About 200mg of agate crushed powder was digested using the sodium peroxide sinter technique (Robinson et al., 1986) to determine REE concentrations. Detection limits for this data are La (0.1 ppm), Ce (0.1 ppm), Pr (0.2 ppm), Nd (0.1 ppm), Sm (0.1 ppm), Eu (0.05 ppm), Gd (0.1 ppm), Tb (0.1 ppm), Dy (0.1 ppm), Ho (0.05 ppm), Er (0.1 ppm), Tm (0.1 ppm), Yb (0.1 ppm), Lu (0.05 ppm), Y (1 ppm), Th (0.1 ppm), and U (0.1 ppm). Duplicate samples produced errors of less than 1% for all trace elements analyzed. Procedural blanks were all less than detection limits.

3.2. Petrographic Analysis

Thin sections were cut of the representative rock types and examined for minerals present as well as for textural relationships after Vernon, (1976), Vernon, (1978), Bell and Rubernach, (1983), Spear *et al.*, (1984), Bell, (1985),

Vernon, (1987a, 1987b, 1988, 1989), Barker, (1990), and Vernon, (1999), in order to establish structural relationships between mineral growth and deformation, as well as the mineral reactions that took place.

3.3. Mineral Chemistry

Mineral compositional analysis on selected polished thin sections were analyzed after microscopic examination by the JEOL JXA-8600 microprobe in the Department of Geological Sciences at the University of Saskatchewan. Compositions of texturally distinct minerals of the same phase are here examined, and used to obtain pressure-temperature conditions of growth. Textural information was supplemented through back-scattered imagery. Quantitative analysis was carried out using wavelength dispersive spectrometry (WDS). Operating conditions include an accelerating voltage of 15 kV, a beam current of 10 nA, and a beam diameter of 5 to 10 μm. Calibration standards used for specific minerals include:

1) Garnet – Cordierite – Si, Mg (pyrope), Al, Fe (Harvard almandine), Ti (rutile), Cr (chromite), Mn (bustamite), Ca (diopside), Na (jadeite), K (sanidine);
2) Biotite – Si, Al, K (Harvard muscovite), Ti (rutile), Cr (chromite), Fe (Harvard biotite), Mg (chlorite), Mn, Ca (bustamite) Na (jadeite), Cl (tugtupite), F (flourite), Zn (willemite);

3) Plagioclase – Si, Al, Ca (plagioclase), Ti (rutile), Fe (kaersutite), Na (jadeite), K (sanidine), Ba (benitoite), Sr (celestite);
4) Hornblende – Si, Ca, Mg (diopside), Al (Smithsonian kaersutite), Ti (rutile), Cr (chromite), Fe (fayalite), Mn (bustamite), Na (jadeite), K (sanidine), Cl (tugtupite), F (flourite), Zn (willemite);

All mineral standards are distributed from SPI (Standard Probe Inclined). Data were corrected using the ZAF calibration program. Errors for major element oxides are within ± 1%, but can be significantly higher for minor constituents.

Metamorphic conditions are primarily calculated using TWEEQ with the calibrations of Berman (1988, 1991), and the least squares method following the techniques of and Gordon *et al.*, (1994; http://ichor.geo.ucalgary.ca/Webinveq). Temperatures were also calculated using the garnet-biotite thermometer of Ferry and Spear (1978).

CHAPTER 4:

METAMORPHIC MINERAL GROWTH, AND CHEMISTRY

4.0. Mineral Growth and Chemistry: Introduction

Section 2.7 discussed the polyphase deformational character of the region. Examined in this chapter are the textural and chemical properties of select minerals from the Kisseynew Metasedimentary rocks that support the suggestion that two periods of metamorphism have affected the region. The history of mineral growth is documented based on overprinting relationships and kinematic features as seen in thin section and outcrop (after: Vernon, 1976; Vernon, 1978; Bell and Rubernach, 1983; Spear *et al.*, 1984; Bell, 1985; Vernon, 1987a, 1987b, 1988, 1989; Barker, 1990; Vernon, 1999).

4.1. Garnet

Garnet is ubiquitously present in Zones 2,3 and 4 of the Burntwood metaturbidites. Garnet is also present in the granodiorite, but typically occurs within a few meters of the sediment/intrusive contact. These grains are usually larger then those in the metasediments, up to 7cm across, and exhibit distinct

depletion rings of quartz and feldspar (Figure 4.1). Commonly restite material is locally found near the contacts consisting of biotite and garnet. It too is mantled in most cases by a depletion ring of quartz and feldspar.

Garnet within the metaturbidites shows two possible generations of growth. The early garnet occurs mainly within the psammitic layers as inclusion-rich rotated porphyroblasts up to >1cm across. This early garnet clearly overgrew an earlier relict fabric consisting of quartz, feldspar, and biotite (Figure 4.2). The quartz and feldspar inclusions are typically round in shape. Spherical feldspar inclusions are indicative of overgrowth by another mineral where interfacial energy among host and inclusion are minimized (Vernon, 1999). These planes of inclusions are for the most part oriented oblique to the main external fabric (S_2); and between different grains show variable orientations. Some grains show a slight "s" development of the (Si) internal fabric (Figure 4.3) indicating that the garnet grew post-D_1 but possibly early syn-D_2. Quartz pressure shadows are present (Figure 4.4), indicating that the garnet grains have experienced strain after growth. This in conjunction with a D_3 crenulation of the S_2 fabric within the thin section (sample 0278) indicates these garnet grains must have grown prior to and early syn- development of the S_2 fabric. Garnet grains of similar type are also located within the early concordant quartz and feldspar leucosomal melts. First generation garnet porphyroblasts along F_2 fold limbs show extensive flattening and elongation concordant with the S_2 fabric

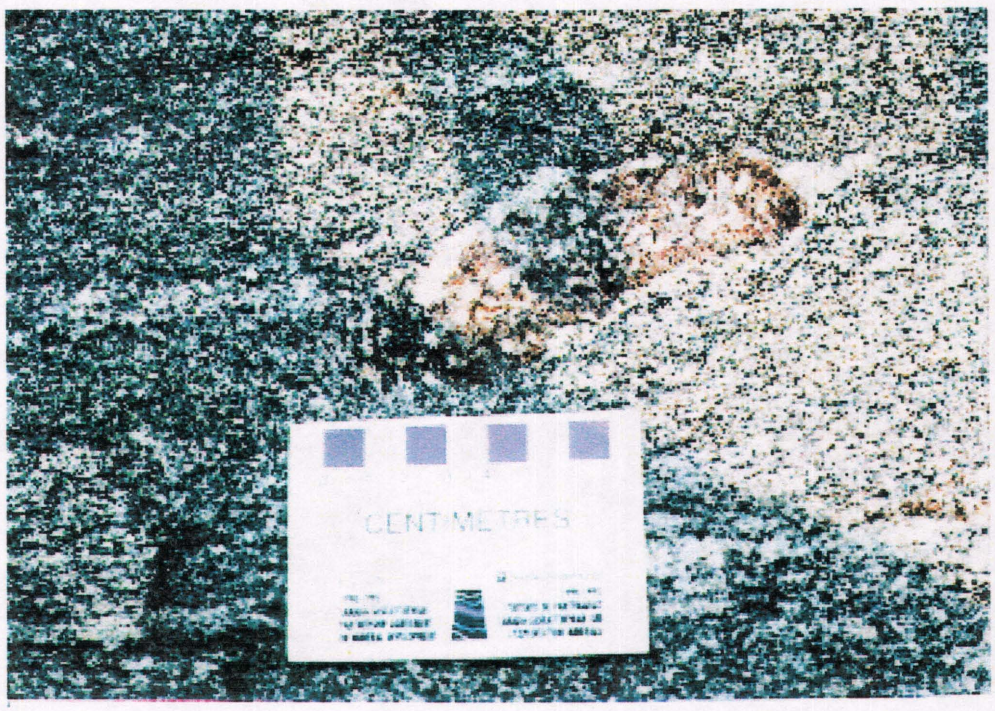

Figure 4.1. Garnet in the granodiorite intrusive rock, close to the sediment /intrusive contact.

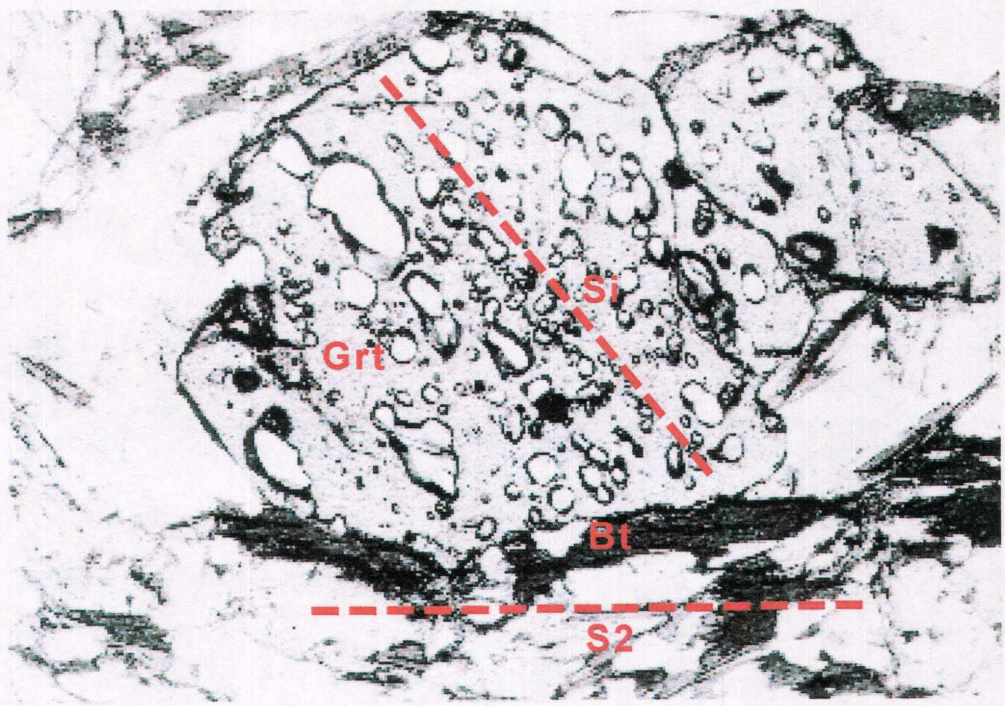

Figure 4.2. Early first generation garnet showing an internal fabric (Si) discordant to the external S2 fabric. (Field of view 2mm.) Grt = garnet; Bt = biotite (Sample 0278b)

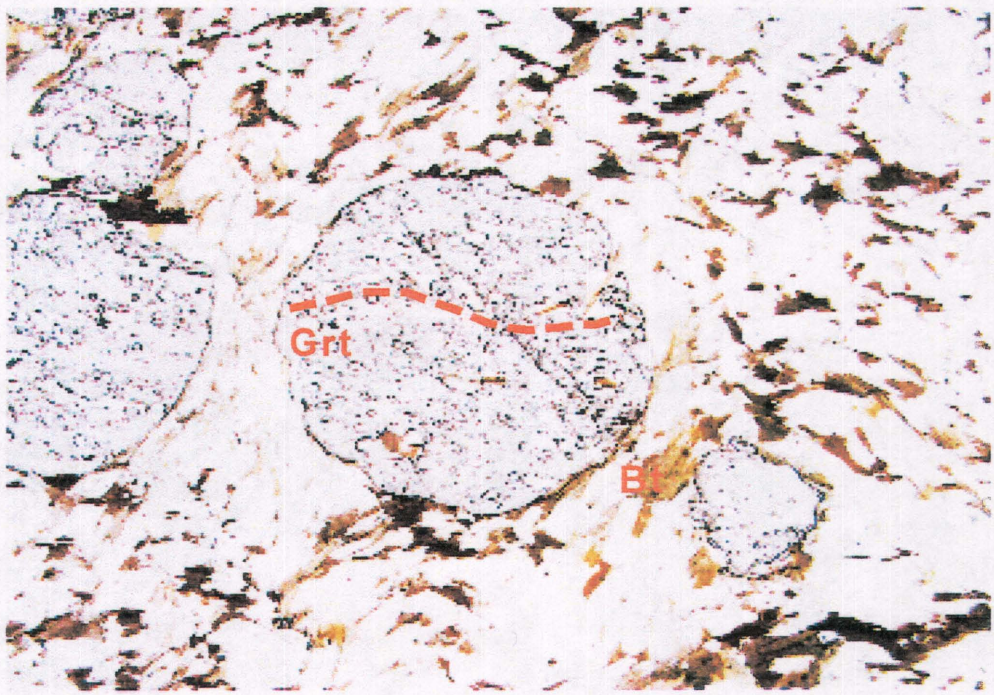

Figure 4.3. First generation garnet demonstrating a slight "s" development of the internal fabric. (Field of view 7mm.) Grt = garnet; Bt = biotite (Sample 0278b)

Figure 4.4. Quartz pressure shadows adjacent to first generation garnet rims. (Photograph with x-polars; Field of view 2mm.) Grt = garnet; Bt = biotite; Qtz = quartz (Sample 0278b)

(Figure 4.5). In some cases a slight rotation consistent with D_3 crenulation is observed.

A second generation of garnet is present within the ground mass of the metapelitic portion of the Metaturbidites within Zones 3 and 4. It ranges up to , 1cm across, helicitic, and generally associated with biotite, quartz, plagioclase, K-feldpar and sillimanite. Some grains show a sigmoidal inclusion trail (Figure 4.6), consisting of biotite and quartz previously aligned within S_2. Typically the second generation garnet grains show a post- D_2 overgrowth of the S_2 fabric (Figure 4.7). Late replacement by cordierite (Figure 4.8) is evident in some samples, typical during decompression.

Garnet is also present within the late cross-cutting leucosomal veins and patch melts of Zone 4, interpreted to have been emplaced post D_2, but syn- to post-D_3. These grains are typically anhedral and in some cases exhibit inclusion planes similar to those of the first garnet generation, and are for the most part, likely partially resorbed first generation grains.

4.2. Biotite

Two generations of biotite are recognized. Biotite grains aligned parallel to the S_2 foliation and outlining isoclinal S_2 folds which define the main fabric in the metaturbidites; are interpreted to be early. This biotite generation was deformed

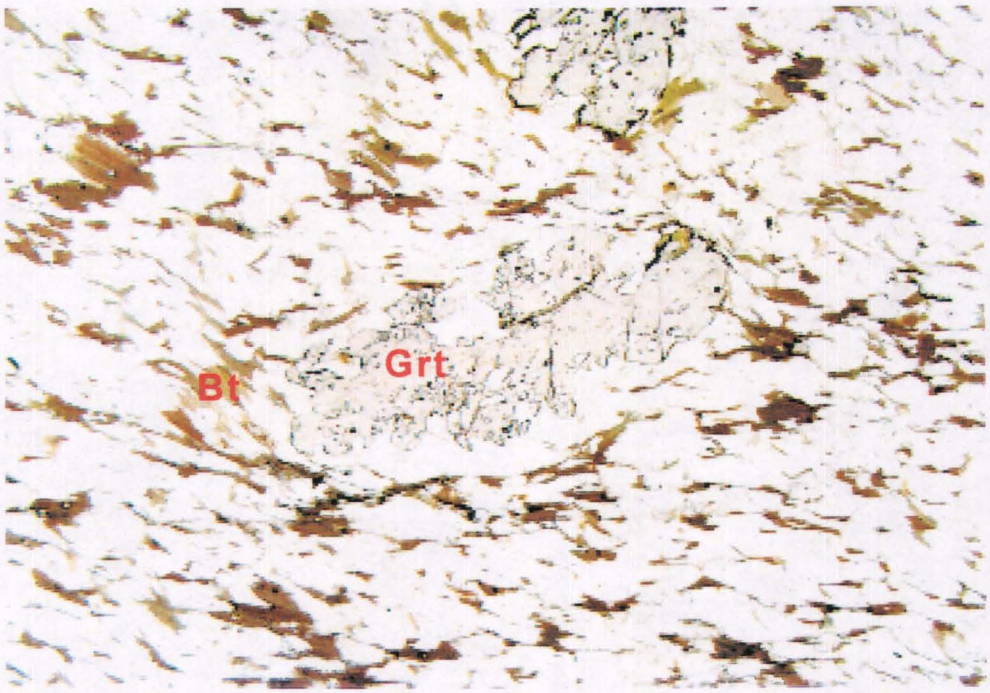

Figure 4.5. First generation garnet exhibiting extensive flattening within S2. (Field of view 7mm.) Grt = garnet; Bt = biotite (Sample 5011)

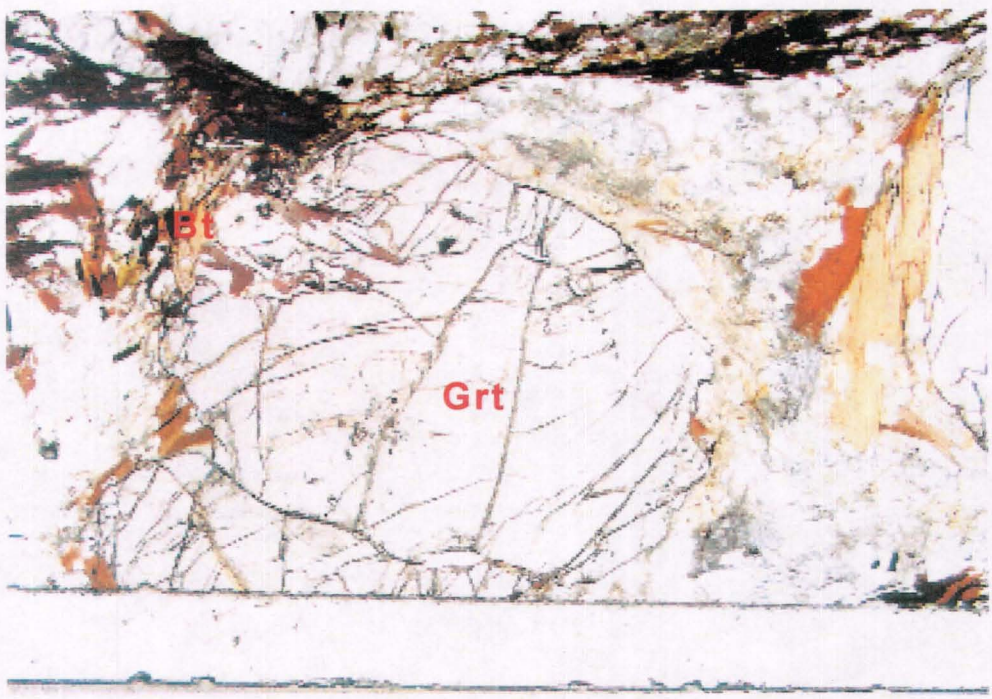

Figure 4.6. A second generation garnet in a metapelitic layer, showing overprinting of an earlier S2 fabric, and a slight sigmoidal inclusion trail. (Field of view 7mm.) Grt = garnet; Bt = biotite (Sample 5000)

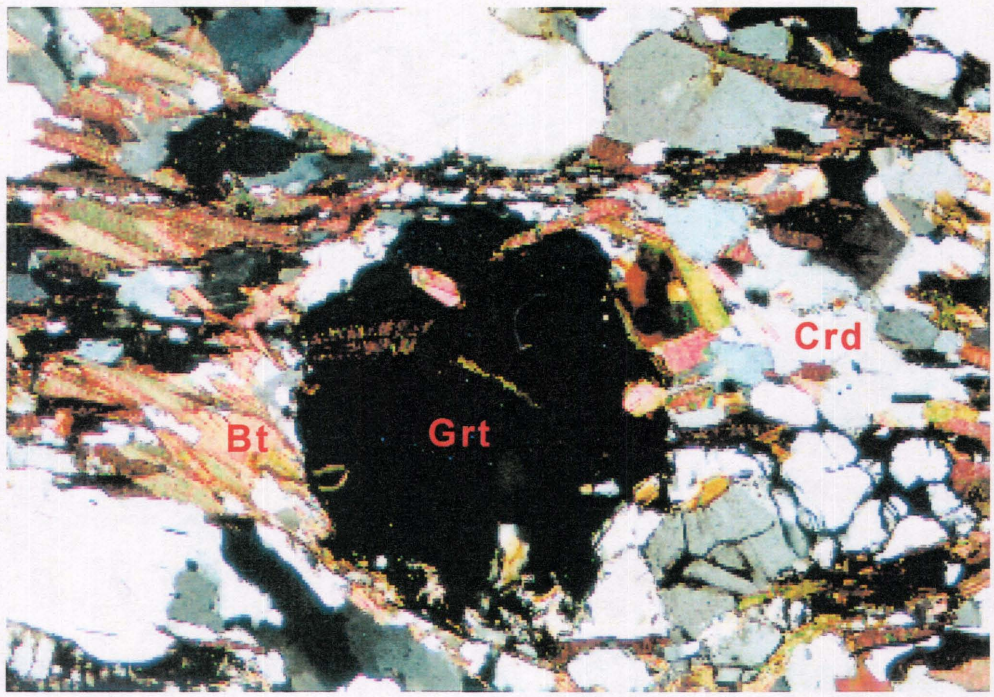

Figure 4.7. Crossed polar photomicrograph of a second generation garnet porphyroblast, demonstrating that it overgrew on the existing S2 fabric. (Field of view 2mm.) Grt = garnet; Bt = biotite; Crd = cordierite (Sample S9)

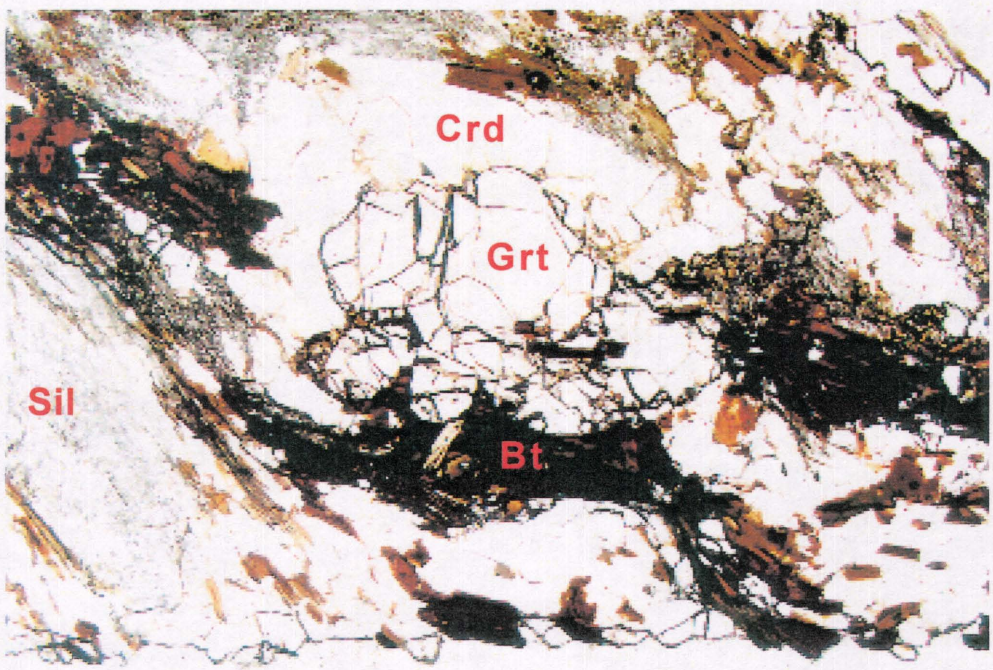

Figure 4.8. Second generation garnet rimmed by cordierite. (Field of view 7mm.) Grt = garnet; Bt = biotite; Crd = cordierite; Sil = sillimanite (Sample 10a)

during D_2 and D_3 often resulting in undulose extinction, and curved and kinked cleavages (Figure 4.9a and b). Inclusions of biotite within the first generation garnets are also interpreted to have developed early. A second generation of biotite is believed to have developed syn-D_3 as it is oriented with the long axis parallel to the axial plane of F_3 folds (Figure 4.10). Both generations are clearly identified within Zone 4 rocks as inclusions within late cordierite porphyroblasts, oriented in two positions (Figure 4.11).

4.3. Feldspar

Plagioclase is the main feldpsar (An 17-43), and is ubiquitous throughout the four Zones. Potassium feldspar is present within the groundmass of the metaturbidites mainly in Zones 3 and 4, as part of the reaction producing sillimanite of the second sillimanite isograd. Albite is present, locally as retrograde reaction product (Figure 4.12). Textural analysis of thin sections shows poikiloblastic plagioclase overprinting an early generation of cordierite as a replacement mineral. These grains show D_2 deformation and therefore must have grown either prior to or early syn-deformation (Figure 4.13). This evidence along with abundant symplectic intergrowths and myrmekitic quartz-feldspar textures within Zones 3 and 4 indicate that there may have been a period of cooling and uplift prior to D_3. Replacement of cordierite with plagioclase and symplectic intergrowths are indicative of decompression (Spear, 1993).

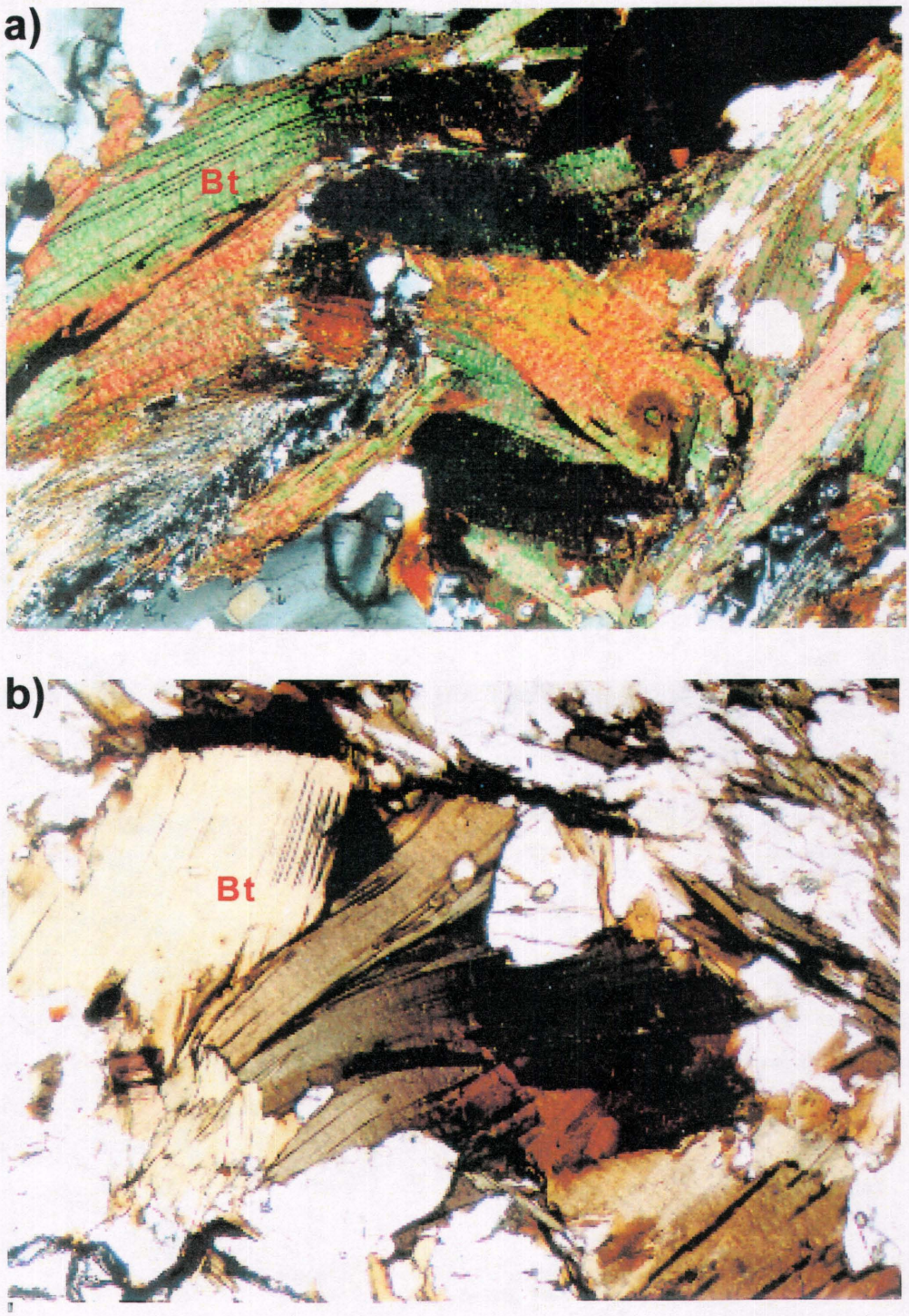

Figure 4.9. a) Early generation biotite showing undulose extinction under crossed polars; a result of deformation. (Field of view 2mm.) (Sample 5024) b) Early generation of biotite clearly showing curved cleavage, resulting from deformation. (Field of view 2mm.) Bt = biotite (Sample 5130)

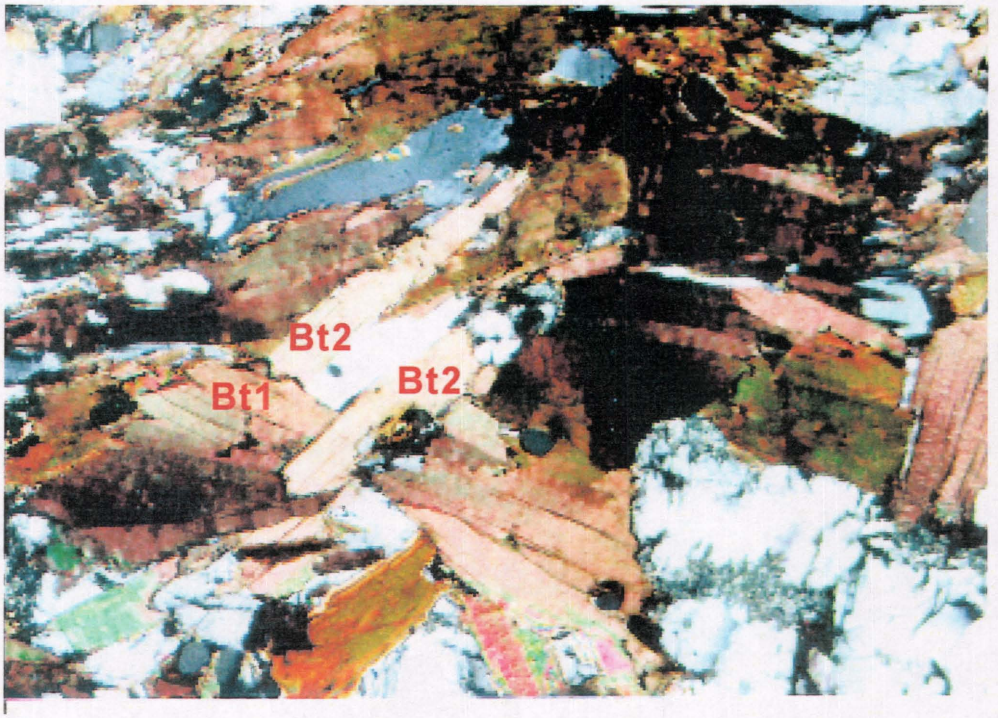

Figure 4.10. Photomicrograph taken under crossed polars, showing two generations of biotite; a deformed earlier generation cross-cut by a later generation parallel to the axial plane of F3 folds. (Field of view 2mm)
Bt1 = first generation biotite; Bt2 = second generation biotite (Sample 5003)

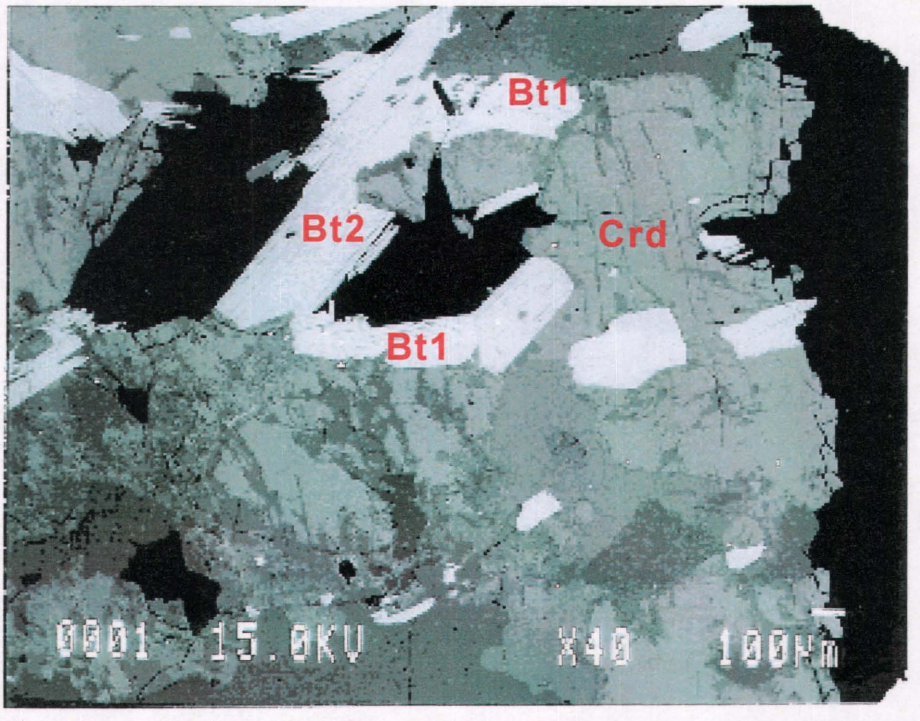

Figure 4.11. Secondary backscatter image showing a cordierite porphroblast overprinting two generations of biotite. Note the second generation cross-cuts the earlier generation oriented within S2. Bt1 = first generation biotite; Bt2 = second generation biotite; Crd = cordierite (Sample SBP12)

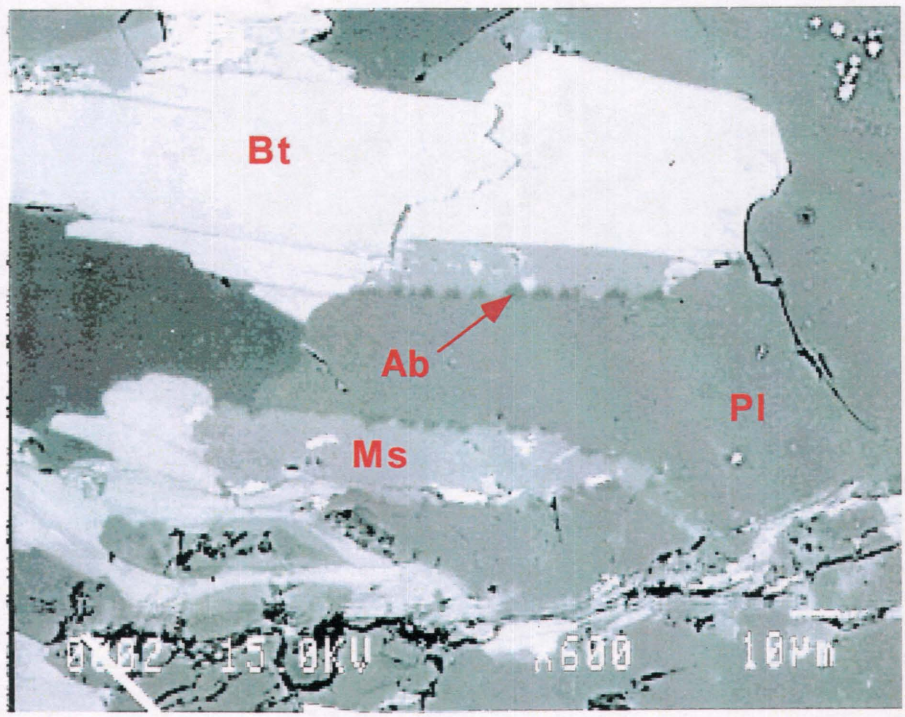

Figure 4.12. Electron backscattered image showing albite at contact between plagioclase and retrograde muscovite. Bt = biotite; Pl = plagioclase; Ms =muscovite; Ab = albite (Sample 5038a)

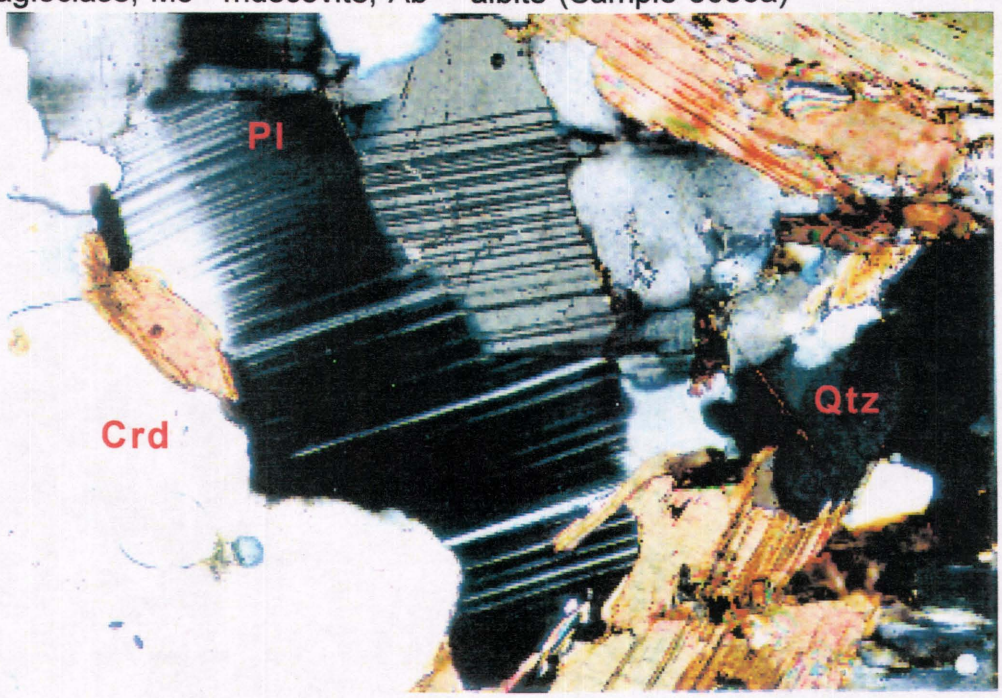

Figure 4.13. Photomicrograph under crossed polars showing a cordierite porphyroblast being replaced by plagioclase and quartz. The undulose extinction of the plagioclase indicates that it has undergone deformation. (Field of view 7mm.) Pl = plagioclase; Qtz = quartz; Crd = cordierite (Sample 5003)

4.4. Cordierite

Cordierite shows at least two different generations within the Kisseynew Metaturbidite rocks. These are identified by their mineralogical association as well as their apparent textural relationships to the matrix. The first generation of cordierite is recognizable within Zones 3 and 4 in the metaturbidites, present within the matrix and aligned parallel to the S_2 fabric. It has a fibrous appearance in hand sample and is brownish in color. Petrography reveals that the fibrous appearance is due to a close association with sillimanite. These cordierite porphyroblasts enclose inclusions of fibrolitic sillimanite (Figure 4.14) and are presumably derived from a reaction involving the breakdown of sillimanite and biotite to form the porphyroblast. Crystals with these textural associations often grow laterally along the foliation after deformation mineral partitioning relaxes (Vernon, 1987). Sibbald (1978) also attributed the growth of these porphyroblasts to mimic growth after deformation, therefore suggesting they did not develop prior to D_2. However, porphyroblast interfolial alignment with S_2 and evidence of deformation indicate that this mineral generation was not mimetic, but grew pre- to early syn- development of the S_2 fabric (Figure 4.15). The second generation of cordierite overgrows the S_2 fabric (Figure 4.16), enclosing sllimanite, biotite, and quartz. In outcrop, this porphyroblast generation is observed oriented within the axial plane of F_3 folds (see Chapter 2, Figure 2.5). Locally two generations of cordierite are evident as late overgrowth of cordierite enclosing an earlier generation distinguished by clearly different

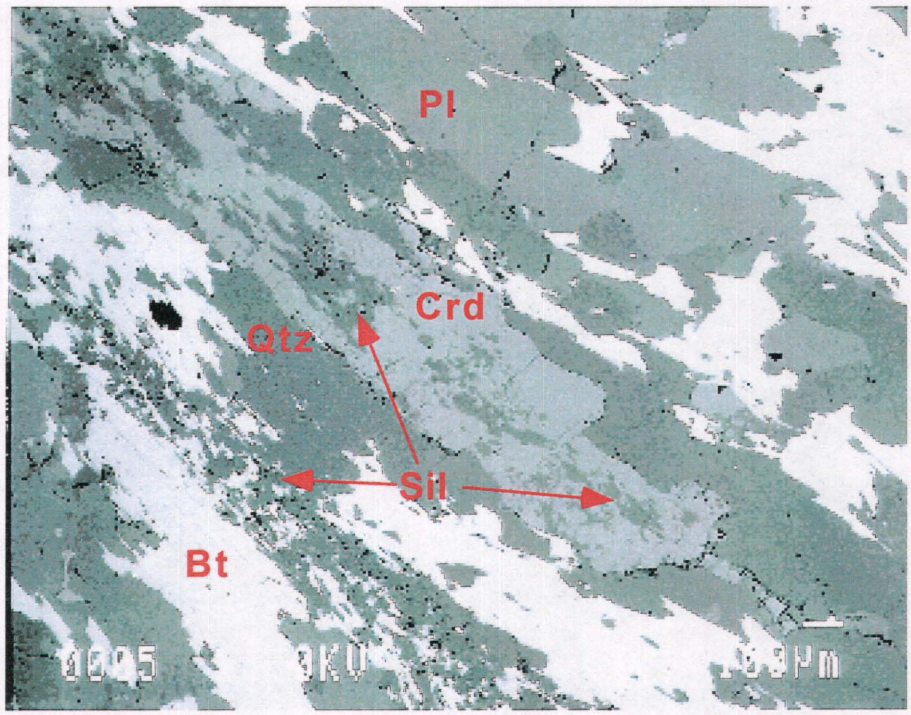

Figure 4.14. Electron backscattered image showing a first generation cordierite porphyroblast with sillimanite inclusions, aligned within S2. Crd = cordierite; Bt = biotite; Pl = plagioclase; Qtz = quartz; Sil = sillimanite (Sample 10a)

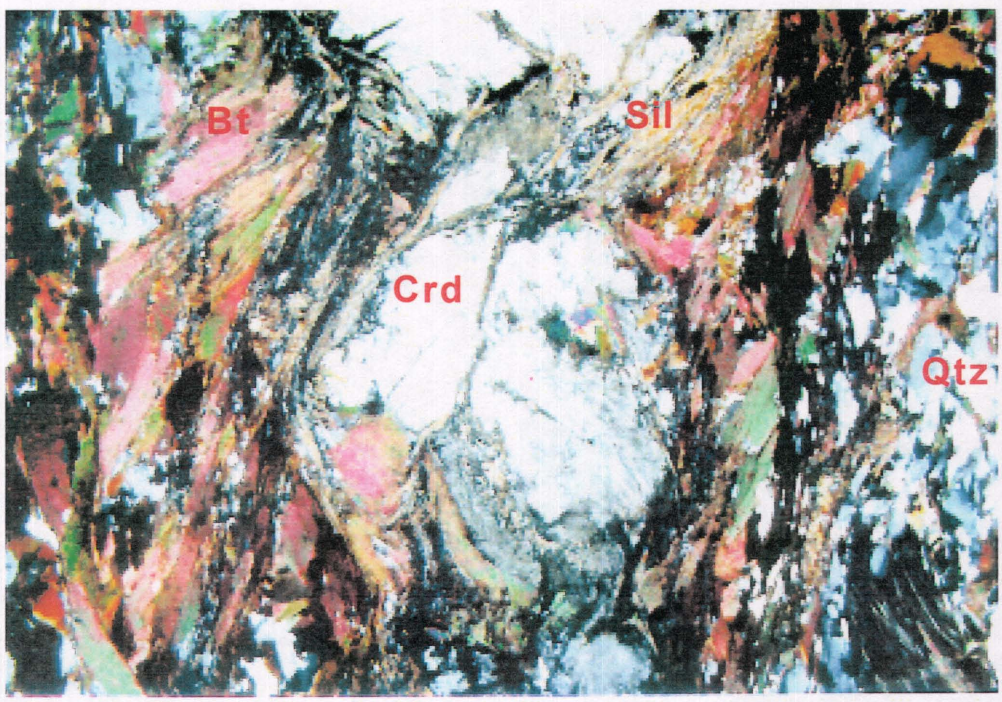

Figure 4.15. Photomicrograph under crossed polars showing a deformed first generation cordierite porphyroblast. (Field of view 7mm.) Bt = biotite; Crd = cordierite; Qtz = quartz; Sil = sillimanite (Sample 0325)

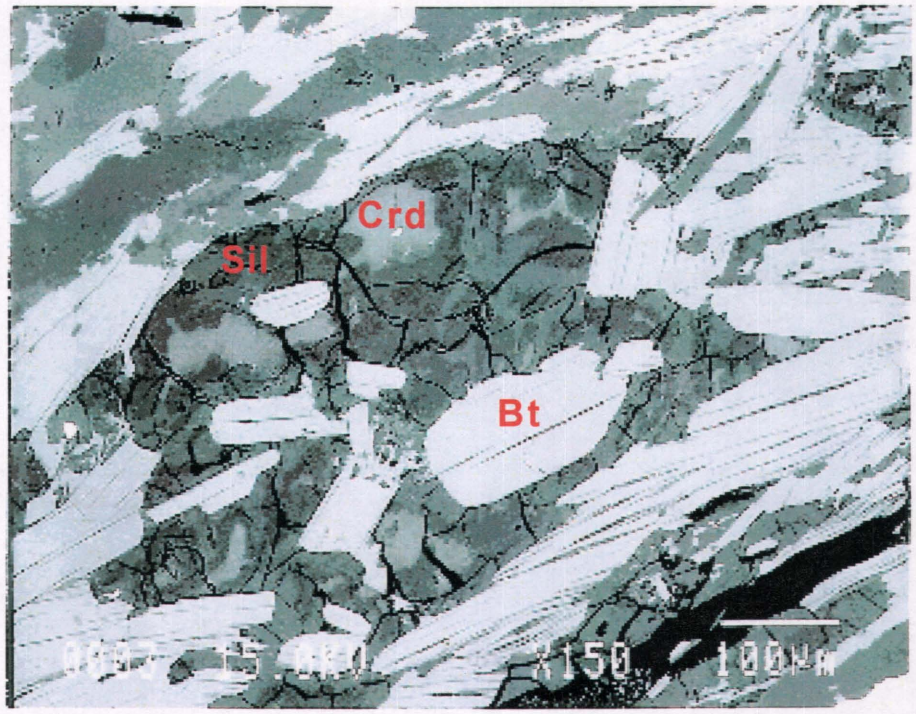

Figure 4.16. Electron backscatter image of a second-generation cordierite porphyroblast that overprinted the S2 fabric. The grain has subsequently been partially replaced by sillimanite. Crd = cordierite; Bt = biotite; Sil = sillimanite (Sample 5004a)

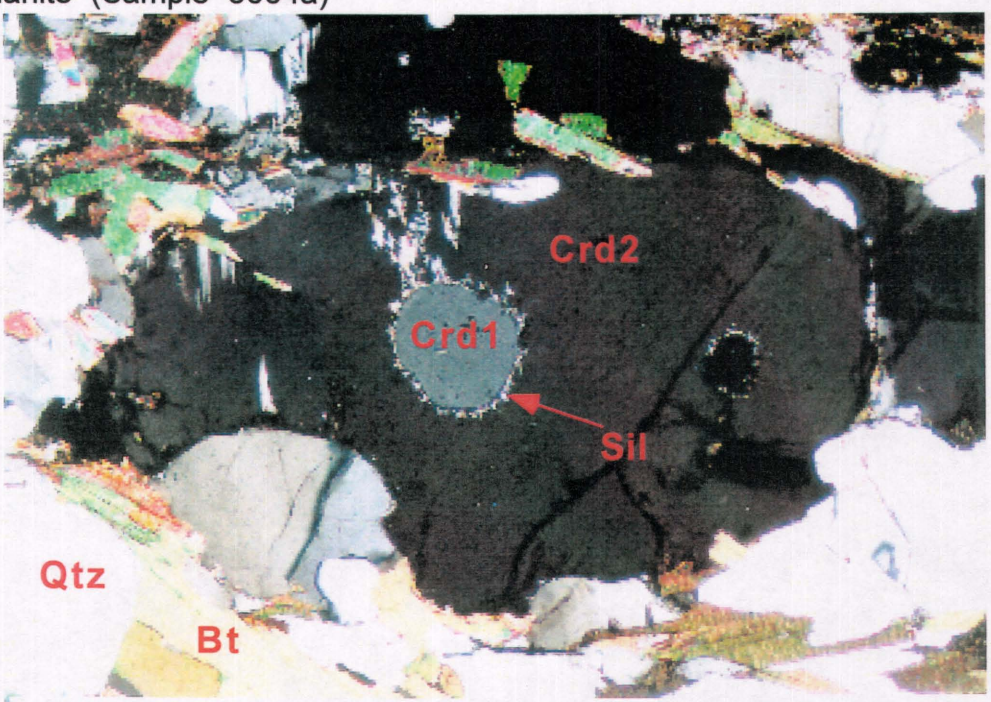

Figure 4.17. Photomicrograph taken with polars crossed, showing two generations of cordierite. The earlier generation (Crd1) is separated from the later generation (Crd2) by a different extinction pattern, and by a rim of sillimanite. (Field of view 7mm.) Bt = biotite; Qtz = quartz; Sil = sillimanite (Sample S9)

extinction patterns (Figure 4.17), and the presence of sillimanite around each rim; indicating a possible decompression reaction after each period of growth. Cordierite is also observed rimming and totally enclosing garnet (Figure 4.18), possibly also the result of decompression. Cordierite within Zone 1 is likely a result of the later metamorphic episode, because it is closely associated with late andalusite mineral growth. The interpretation of mimetic cordierite growth (Sibbald, 1978) may be attributed the mimetic growth of the mineral over D_2 microstructures during the second metamorphic episode, as it is difficult to separate early cordierite from these mimic crystals.

Late crosscutting leucosomes of Zone 4, also comprise cordierite. These grains are subhedral to euhedral in hand sample and dark blue to black in color (Figure 4.19). The crosscutting nature and patchy shape of the of the leucosomes along with the well formed nature of the porphyroblasts indicates that the cordierite grew during and slightly post D_3.

4.5. Sillimanite

Zones 2 and 3 delineate the sillimanite isograds. There are at least two generations of sillimanite. It is observed both as inclusions within cordierite, garnet, plagioclase, K-feldspar, and biotite, and as rims around both generations of cordierite. It is present as fine grained fibrolitic and idioblastic masses, euhedral lath-like, and prismatic crystals. The first generation is identified as

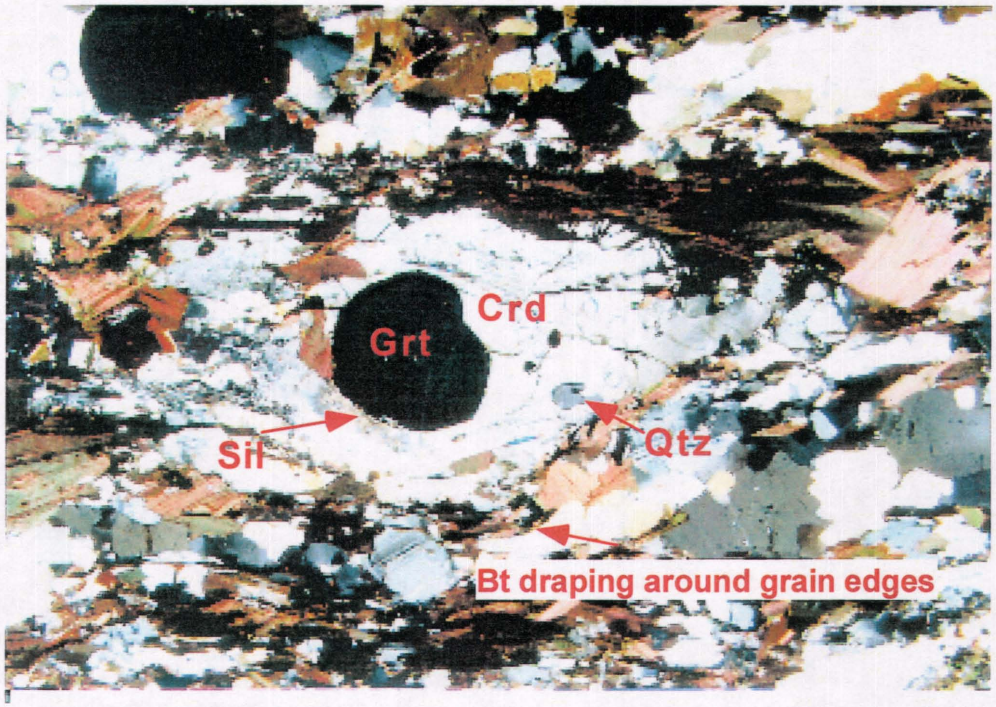

Figure 4.18. Photomicrograph taken under crossed polars, showing cordierite (Crd) enclosing garnet (Grt). The draping of biotite around the margins of cordierite may indicate that the porphyroblast was present prior to fabric development. (Field of view 7mm.) Sil = sillimanite; Qtz = quartz; Bt = biotite (Sample S9)

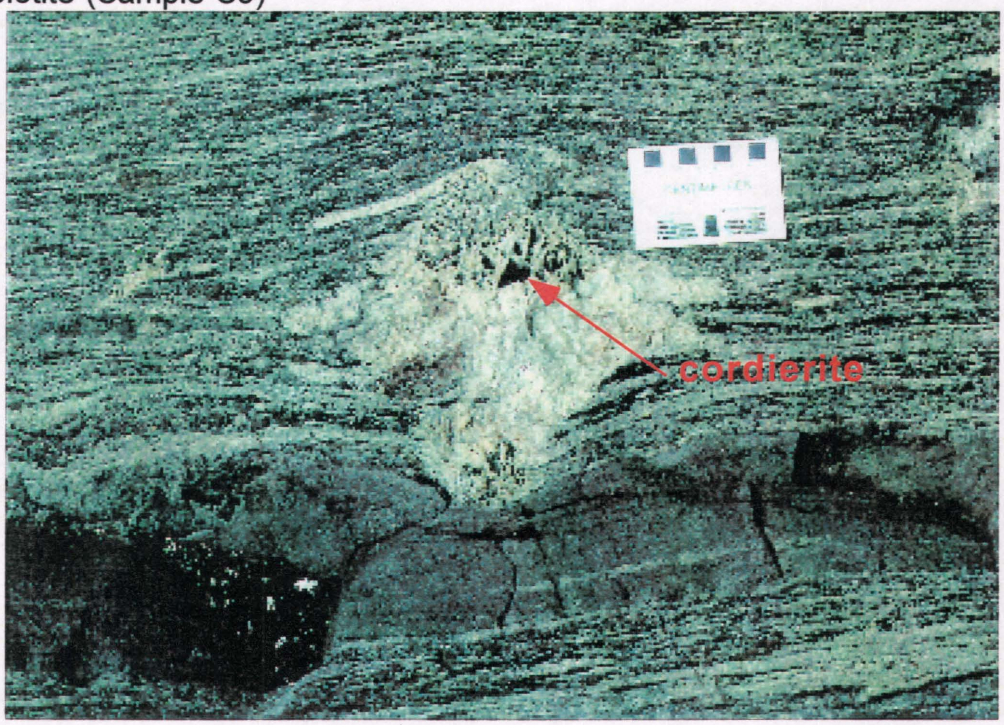

Figure 4.19. Photograph showing dark blue cordierite porphyroblasts within the late cross-cutting leucosome.

fine grained, lensoid fibrolitic masses, typically aligned intrafolial with S_2. These sillimanite aggregates show F_2 isoclinal folding (Figure 4.20), and sometimes exhibit F_3 overprinting (Figure 4.21). The deformation along with replacement minerals suggests that it grew from a prograde reaction pre- to syn- D_2. First generation sillimanite is commonly replaced by cordierite, plagioclase, K-feldspar and lath-like coarser grained sillimanite, a product of post D_2 annealing.

The second generation of sillimanite overgrows both the lensoid fibrolitic masses, as well as the lath-like crystals. This generation developed as coarse grained laths and prismatic crystals, replacing and overprinting both biotite and early sillimanite (Figure 4.22). Outcrop relationships show that it is also oriented parallel to F_3 axial planes.

4.6. Andalusite

Andalusite is present within Zones 1 and 2; its disappearance coinciding with the disappearance of muscovite. Two distinct generations of andalusite are recognized. The first generation exhibits textural characteristics that suggest andalusite developed prior to and during the development of S_2. This is evident as the internal fabrics of the porphyroblast show discordant relationships with external S_2 fabrics (Figure 4.23). These grains show the external foliation draped and deformed around grain edges suggesting that the porphyroblasts was more competent during foliation development. In other cases it is evident

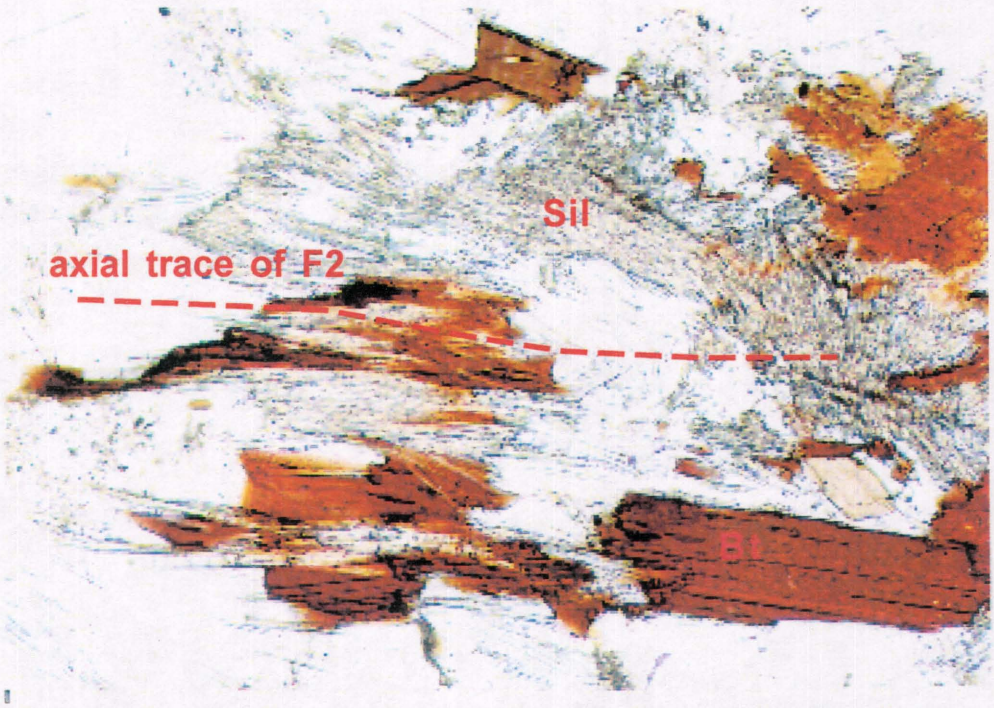

Figure 4.20. Photomicrograph taken under plain light showing first generation sillimanite isoclinally folded into F2/S2.(Field of view 1mm) Sil = sillimanite; Bt = biotite (Sample 5000)

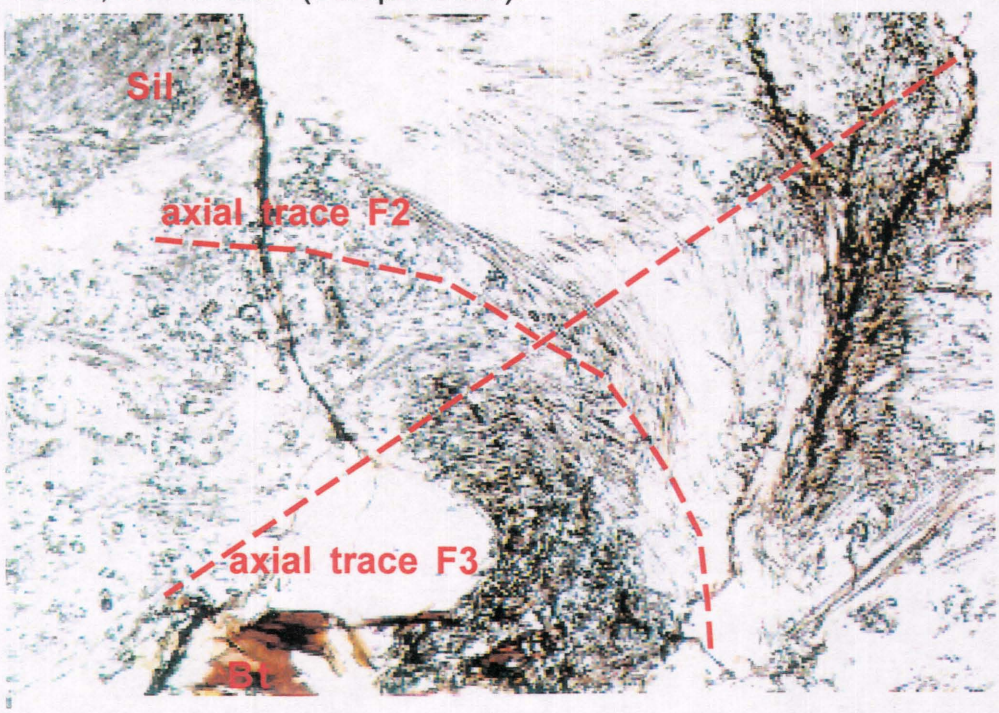

Figure 4.21. Photomicrograph taken in plain light showing first generation sillmanite folded about both F2 and F3. (Field of view 2mm) Sil = sillimanite; Bt = biotite (Sample 10a)

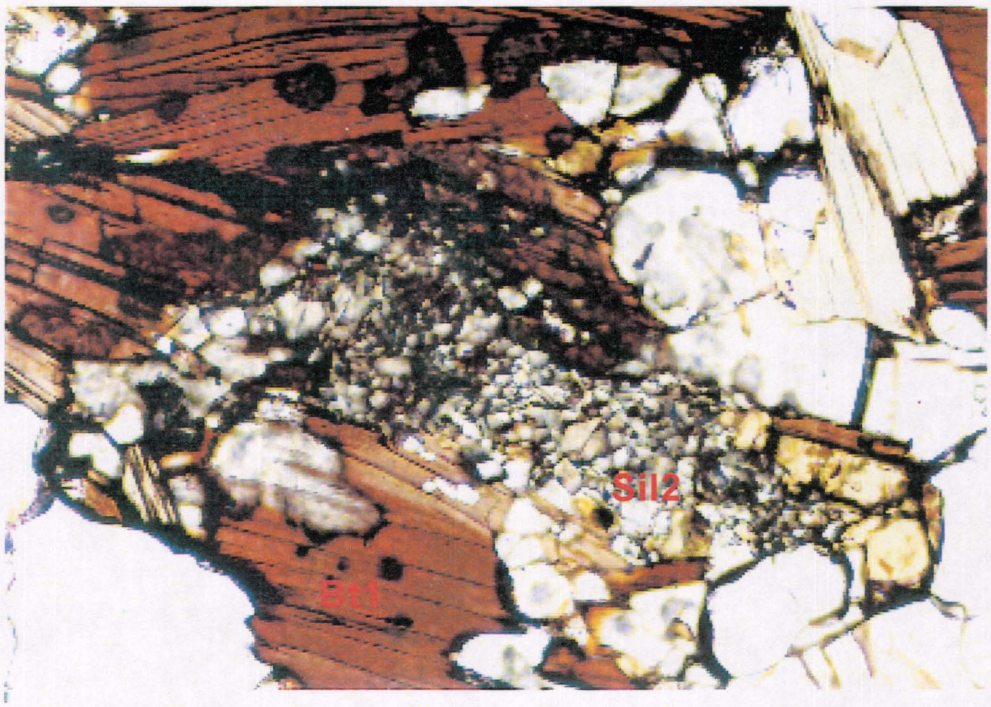

Figure 4.22. Photomicrograph taken in plane light showing second generation sillimanite (Sil2) replacing deformed first generation biotite (Bt1). (Field of view 1mm.) (Sample 10a)

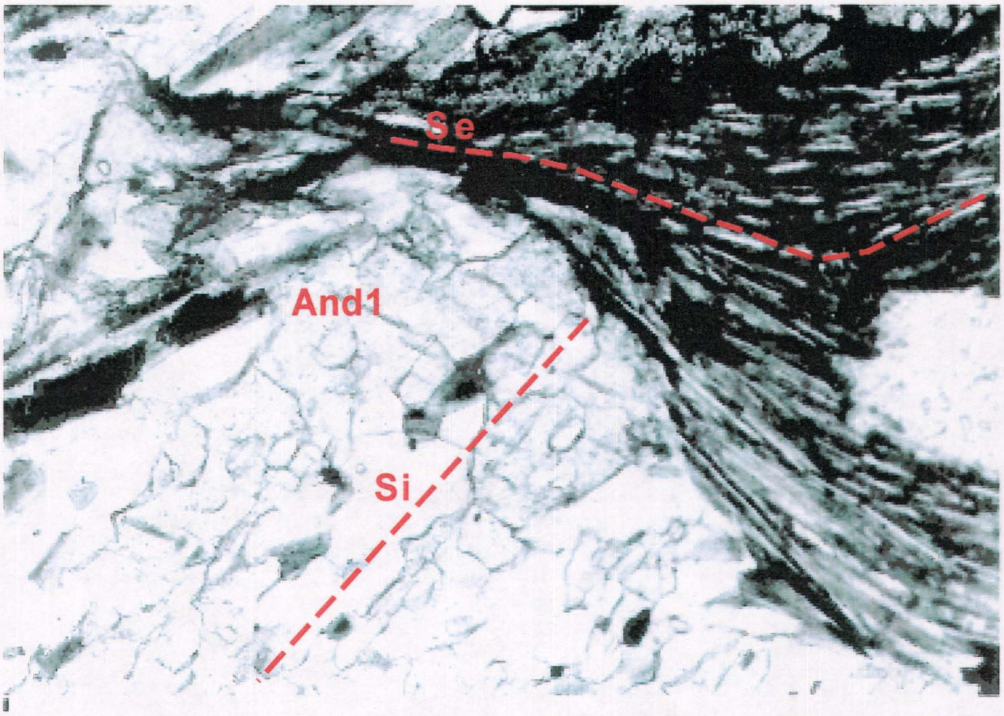

Figure 4.23. Photomicrograph of first generation andalusite (And1) with an internal fabric (Si) discordant to the external fabric (Se). Note how Se drapes around the grain edges. (Sample 5055)

that the andalusite grain grew while rotating during S_2 fabric development. In these cases the internal fabric is relatively continuous with the matrix but shows sigmoidal deflection near grain edges (Figure 4.24). These andalusite grains show replacement by muscovite, quartz, and biotite.

The second generation of andalusite is closely associated with staurolite as it is present typically riming staurolite grains as a replacement product (Figure 4.25). The xenoblastic staurolite within the grains exhibits an early fabric evident as aligned quartz and biotite inclusions. These andalusite porphyroblasts show relatively little ductile deformation and therefore are interpreted to have grown post D_2. Later brittle deformation attributed to the Tabbernor Fault is evident however, as brittle shear bands showing dextral movement (Figure 4.26).

4.7. Staurolite

Staurolite shows growth as one generation and is seen only within Zone 1. Associated with quartz and biotite it is observed rimmed and replaced by andalusite, and aligned within the main S_2 fabric. It is interpreted to have grown pre- D_2, but post D_1 due to the presence of an internal fabric (Figure 4.27) consisting mainly of quartz and biotite.

4.8. Muscovite

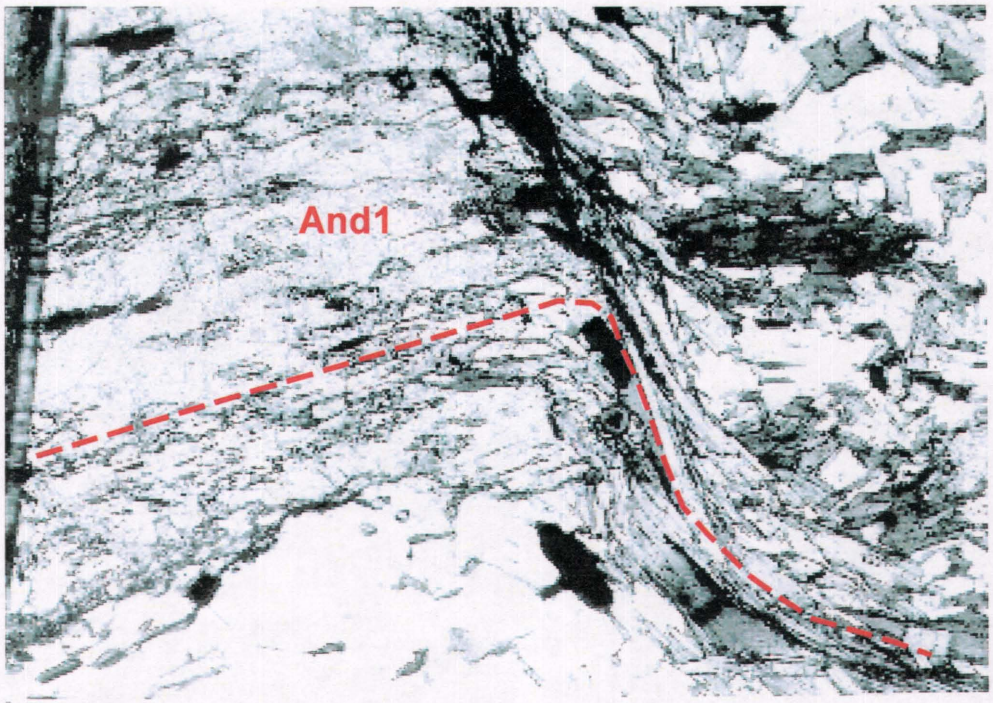

Figure 4.24. First generation andalusite (And1) exhibiting an internal fabric relatively continous with the matrix, but showing a degree of of rotation after growth. (Field of view 1mm.) (Sample 5055)

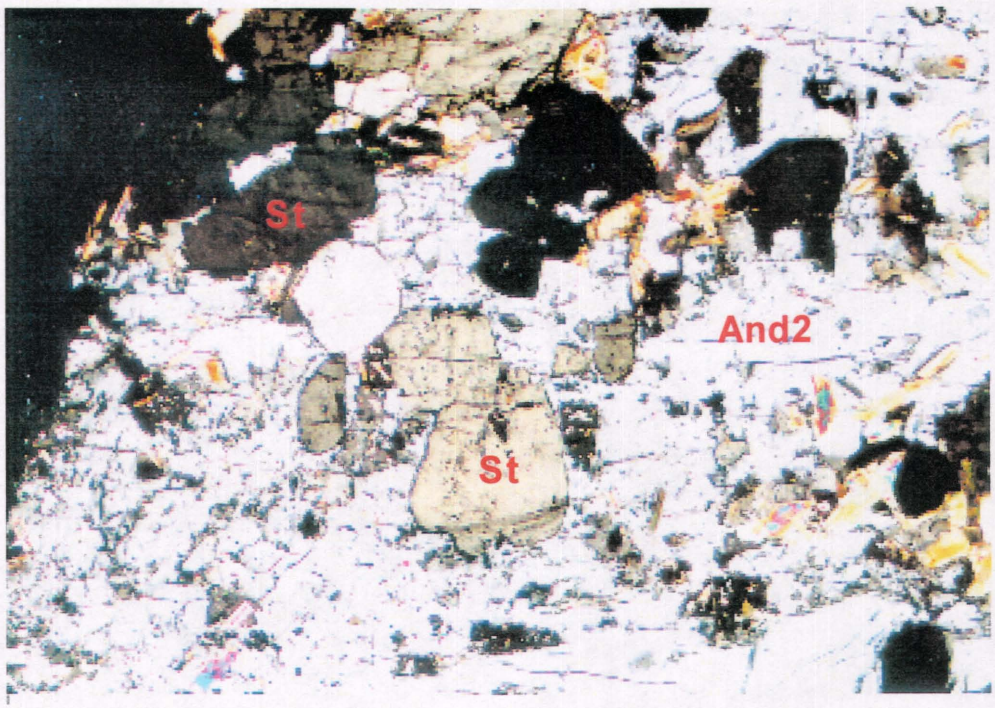

Figure 4.25. Photomicrograph taken under crossed polars showing second generation andalusite (And2) replacing staurolite (St). (Field of view 2mm.) (Sample N130)

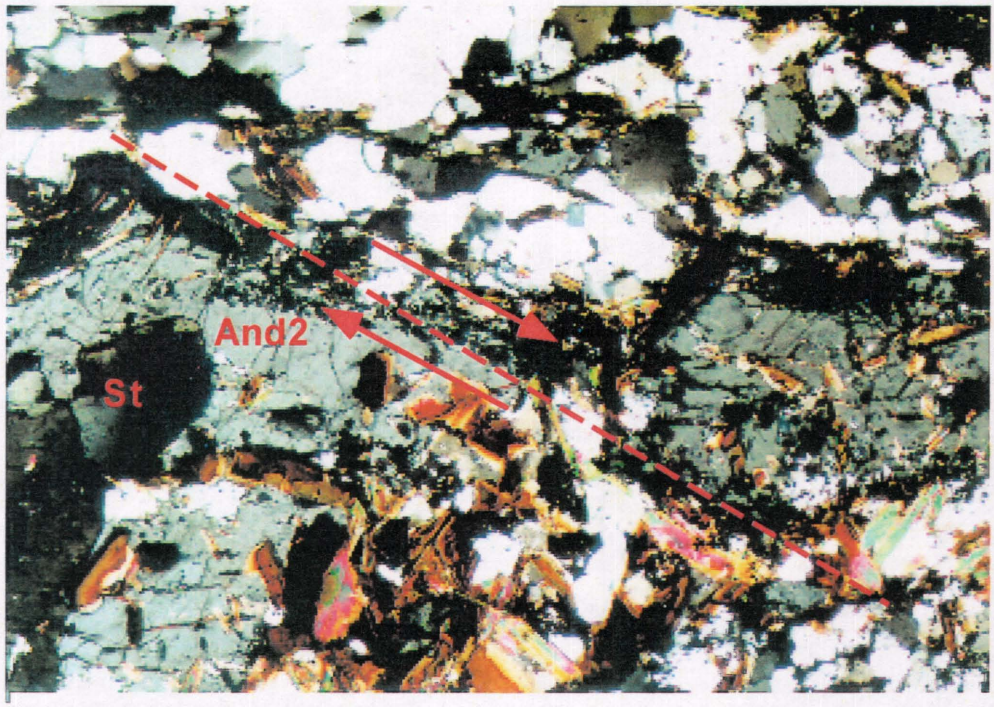

Figure 4.26. Photomicrograph taken under crossed polars showing second generation andalusite (And2) with a brittle dextral shear band. Sample was collected near the Tabbernor Fault. (Field of view 1mm.) St = staurolite (Sample N130)

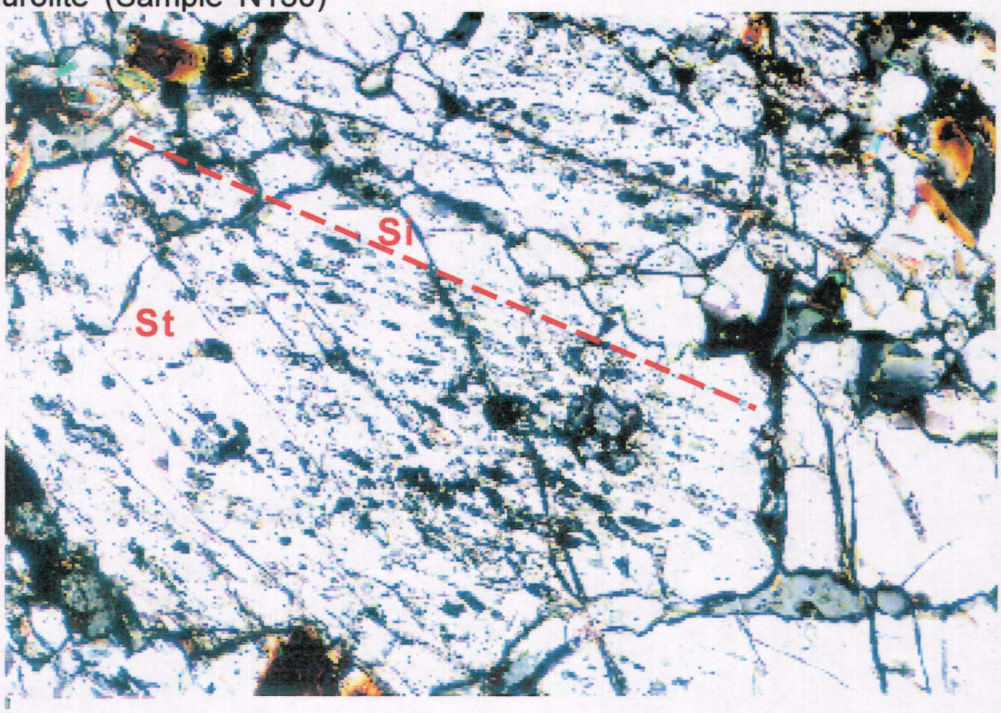

Figure 4.27. Photomicrograph taken under plain light showing the internal fabric (Si) within staurolite (St). (Field of view 1mm.) (Sample N130)

Muscovite is common in Zones 1 and 2, and is present as a retrograde phase in Zones 3 and 4. Muscovite has been found locally as inclusions in cordierite in Zone 4 (Figure 4.28). Within Zones 1 and 2 first generation muscovite along with biotite delineates the foliation and is commonly deflected around and incorporated within first generation andalusite. A second generation is seen replacing andalusite. Adjacent to the Tabbernor Fault, aggregates of muscovite are common; interpreted to be late, resulting from movement along the Fault (Figure 4.29).

Muscovite along with andalusite disappears at the isograd marking the onset of anatexis and Zone 3, indicating that this mineral was no longer stable under those conditions.

4.9. Cummingtonite

On the western shore of Pelican Lake in Zone 4, a unit of quartz-biotite-plagioclase-cordierite-garnet and amphibole is present. The amphibole porphyroblasts are mainly cummingtonite in composition and show textural characteristics that suggest porphyroblast growth during M1. The porphyroblasts show an equivocal internal fabric delineated by biotite and quartz, that is discordant and oblique to the external S_2 fabric (Figure 4.30). The external fabric also appears to have been draped around the

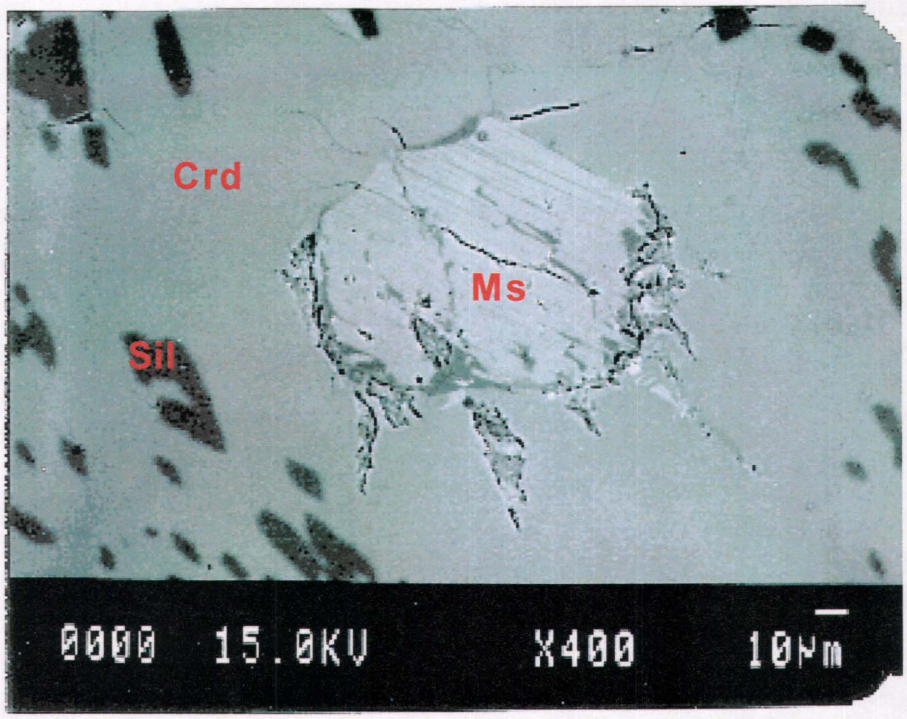

Figure 4.28. Electron backscattered image showing a muscovite (Ms) inclusion in cordierite (Crd). Sil = sillimanite (Sample 10a)

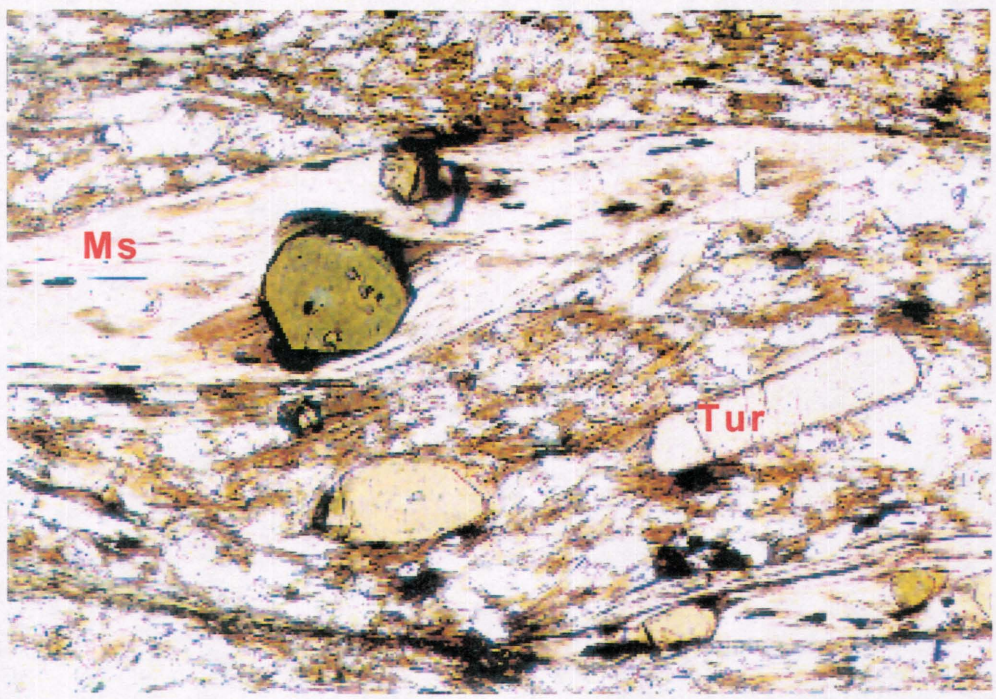

Figure 4.29. Photomicrograph taken in plain light showing muscovite (Ms) fish and late tourmaline (Tur). (Field of view 7mm.) (Sample 0254a)

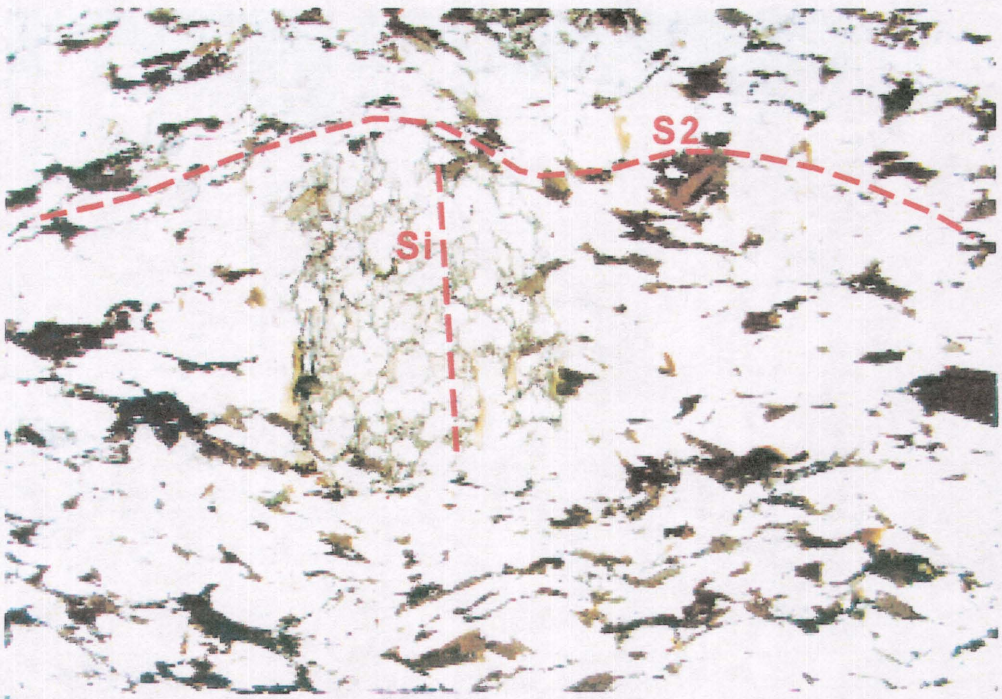

Figure 4.30. Photomicrograph taken in plain light showing a cummingtonite porphyroblast with an internal fabric (Si) delineated by biotite, that is discordant with the external S2 fabric which appears to drape around the amphibole grain. (Field of view 7mm.) (Sample 0291)

porphyroblasts, consistent with S_2 fabric development post dating mineral growth.

4.10. Mineral Chemistry of Garnet, Biotite, and Plagioclase

A main objective of this microprobe analysis is to determine if the texturally distinct generations of minerals are compositionally distinguishable. If so, this may provide further evidence for two metamorphic events, and aid in the selection of minerals for quantitative calculations of metamorphic conditions (Chapter 5). Determined mineral compositions are presented in Appendix B.

4.10.1. Mineral Chemistry of Garnet

Garnet from all three garnet-bearing zones exhibits very minor zonation; the percentage of almandine increases towards the rim in most cases but typically by less than 2 mol.%. Of note is the chemical difference between the first and second generations of garnet (Table 4.1a and b). Typically the early garnet shows an almandine content of less than 0.75 (Table 4.1a). Garnet of Zone 4 identified as having grown during the second metamorphic event is relatively more Fe-rich with Xalm of 77-83 % (Table 4.1b). However, garnet identified as most likely to have grown early is more easily recognized within the psammitic portion of the metaturbidites, where the bulk composition of Fe_2O_3 is slightly lower than in the pelitic layers. Garnet grains interpreted as resorbed first

TABLE 4.1. Garnet compositions.

a) First generation garnet

	Sample 0278b	
Wt.% oxides	core	rim
SiO2	37.44	37.69
TiO2	0.02	0.03
Al2O3	21.99	22.10
Cr2O3	0.01	0.07
FeO	32.50	32.76
MgO	5.13	4.90
MnO	0.76	0.69
CaO	2.05	1.89
Na2O	0.01	0.01
K2O	0.00	0.00
Total	99.92	100.14
Molar Proportions		
Grossular	0.06	0.05
Pyrope	0.20	0.20
Almandine	0.72	0.73
Spessartine	0.02	0.02
Fe/(Fe+Mg)	0.78	0.79

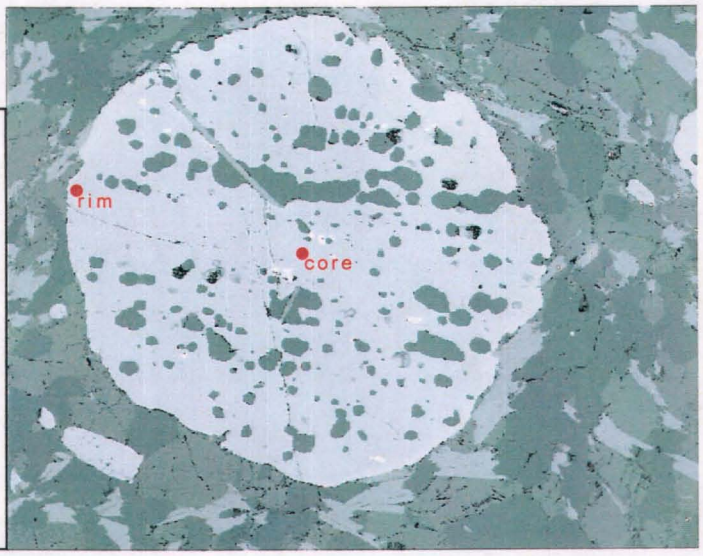

b) Second generation garnet

	Sample 5000	
Wt.% oxides	core	rim
SiO2	37.00	37.04
TiO2	0.01	0.00
Al2O3	21.74	21.73
Cr2O3	0.01	0.00
FeO	34.86	35.82
MgO	3.29	3.17
MnO	1.25	1.55
CaO	1.47	0.86
Na2O	0.01	0.03
K2O	0.00	0.00
Total	99.63	100.21
Molar Proportions		
Grossular	0.04	0.02
Pyrope	0.13	0.13
Almandine	0.79	0.81
Spessartine	0.03	0.04
Fe/(Fe+Mg)	0.86	0.86

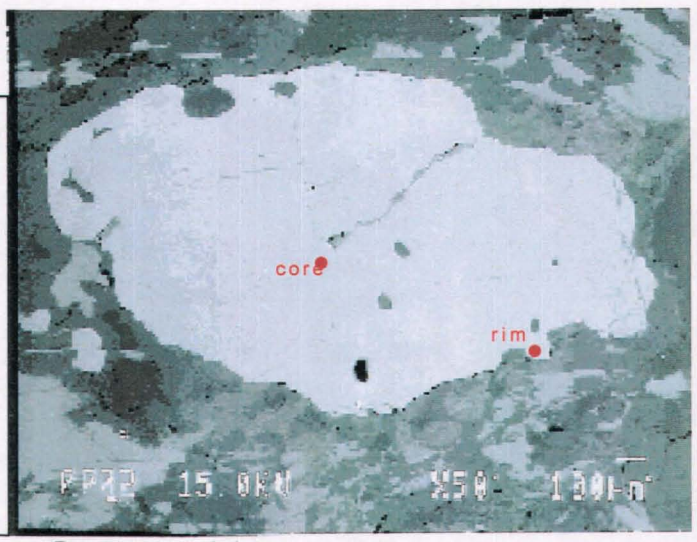

● Denotes spot analysis

c)

Typical second generation garnets								
	Zone 4				Zone 3		Zone 2	
Sample	7005B		5000		5011		5100	
	core	rim	core	rim	core	rim	core	rim
SiO2 (wt. %)	35.64	36.85	37.53	37.56	37.03	37.02	37.33	37.27
TiO2	0.00	0.00	0.00	0.01	0.00	0.01	0.00	0.01
Al2O3	22.07	21.64	21.71	22.23	22.33	22.20	21.59	21.91
Cr2O3	0.01	0.00	0.01	0.01	0.00	0.04	0.00	0.01
FeO	34.77	34.74	34.66	33.58	34.22	34.56	33.25	33.41
MgO	3.23	3.14	3.54	3.64	3.74	3.50	3.12	2.83
MnO	2.61	2.41	1.07	1.38	0.93	1.22	2.27	2.48
CaO	0.88	0.83	1.54	0.91	1.75	1.72	1.70	1.70
Na2O	0.03	0.02	0.00	0.05	0.00	0.00	0.00	0.01
K2O	0.00	0.00	0.00	0.00	0.00	0.00	0.00	0.00
Total	99.24	99.64	100.08	99.36	100.00	100.28	99.26	99.63
Molar Proportions								
Grossular	0.03	0.02	0.04	0.03	0.05	0.05	0.05	0.05
Pyrope	0.13	0.13	0.14	0.15	0.15	0.14	0.13	0.12
Almandine	0.79	0.79	0.79	0.79	0.78	0.78	0.77	0.77
Spessartine	0.06	0.06	0.02	0.03	0.02	0.03	0.05	0.06
Fe/(Fe+Mg)	0.86	0.86	0.85	0.84	0.84	0.85	0.85	0.86

generation grains located within the late cordierite-garnet-bearing melts within the pelitic layers of the metaturbidites, however, yield average Xalm values of up to 78%; giving credence to the argument that early garnets in the pelitic layers of the metaturbidites also comprised of lower almandine/pyrope ratios. Garnets of Zone 3 which exhibit resorbtion, yield slighty lower Xalm contents up to 77% than the interpreted second generation grains. These grains, however, show the most marked zonation with core almandine percentages of 75%, to 80% near the rims. Another typical chemical difference between the two garnet generations is the Xgr component. The early garnets generally contain up to 0.05 Xgr, where as the later garnets have decreased values of up to 0.03 Xgr. This corresponds with higher An contents in the core of early plagioclase. Growth of the second generation garnet occurred in an environment somewhat more depleted in Ca than the early generation.

Stated earlier, the pelitic layers of the metaturbidites generally have higher Fe contents than the psammitic layers. However, this does not preclude the fact that Fe in lithological layers travels relatively freely along grain boundaries and structural tracks between the layers during metamorphism. Element mobility within these rocks is not restricted to individual layers; evident in the growth of garnet up to 3-5 m away from granodiorite / sediment contacts. This along with the evidence of lower Xalm content of resorbed garnet within the metapelitic layers suggests that the interpreted early garnet with relatively lower Xalm than

the interpreted second generation garnets are not necessarily the result of lower bulk Fe contents within the rocks.

Sample 5011 of Zone 3 contains garnet of the type shown in Figure 4.5. One hundred and sixty spot analyses were performed on this garnet grain to contour the compositional zoning to determine if the elongate nature of the grain is coeval with mineral growth or consistent with the apparent textural interpretation that deformation post-dated mineral growth. The determined chemical pattern (Figure 4.31) shows apparent truncations of the contours, which is consistent with the interpretation that this garnet grew prior to deformation. Wang and Ji (1999) concluded that silicate garnet behaves mostly rigid and brittle in the crust, and ductile in high temperatures and low strain rates. This garnet shows brittle fracturing and core separation consistent with moderate to low temperatures (Wang and Ji, 1999). Several areas within the grain show core fragments that exhibit a concentric limited and nearly homogeneous growth zonation pattern affected by later diffusion zoning (Spear, 1993). Fe diffusion permeated the rim; however it did not penetrate deep enough to completely alter the composition of the core fragments. The chemistry along with the texture of the garnet is consistent with the interpretation that this grain is an early generation that has undergone D_2 deformation, and then further Fe diffusion zoning post deformation.

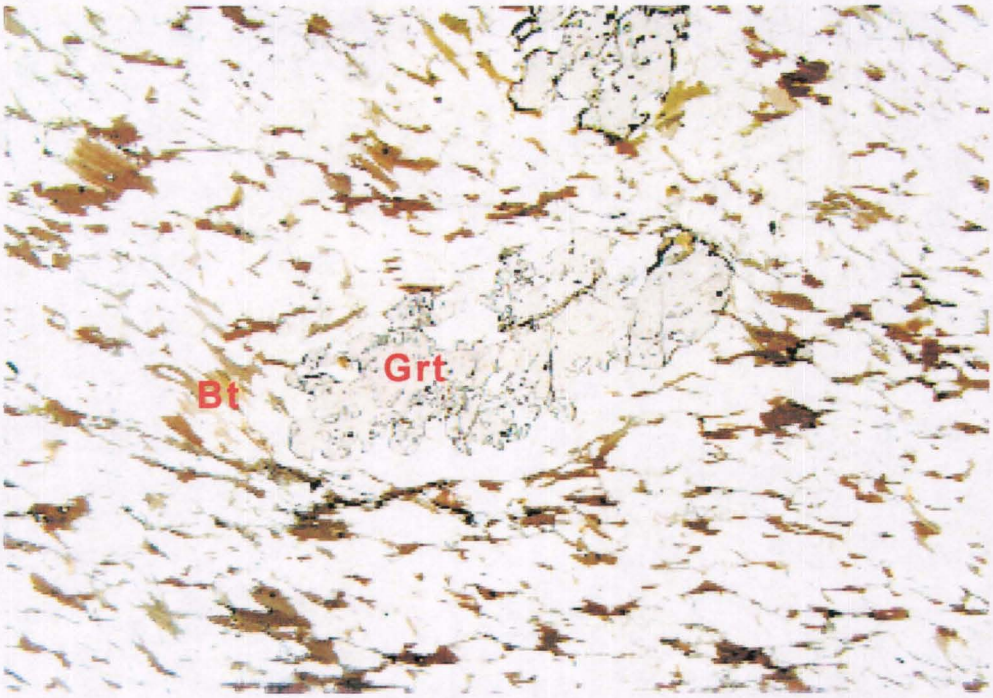

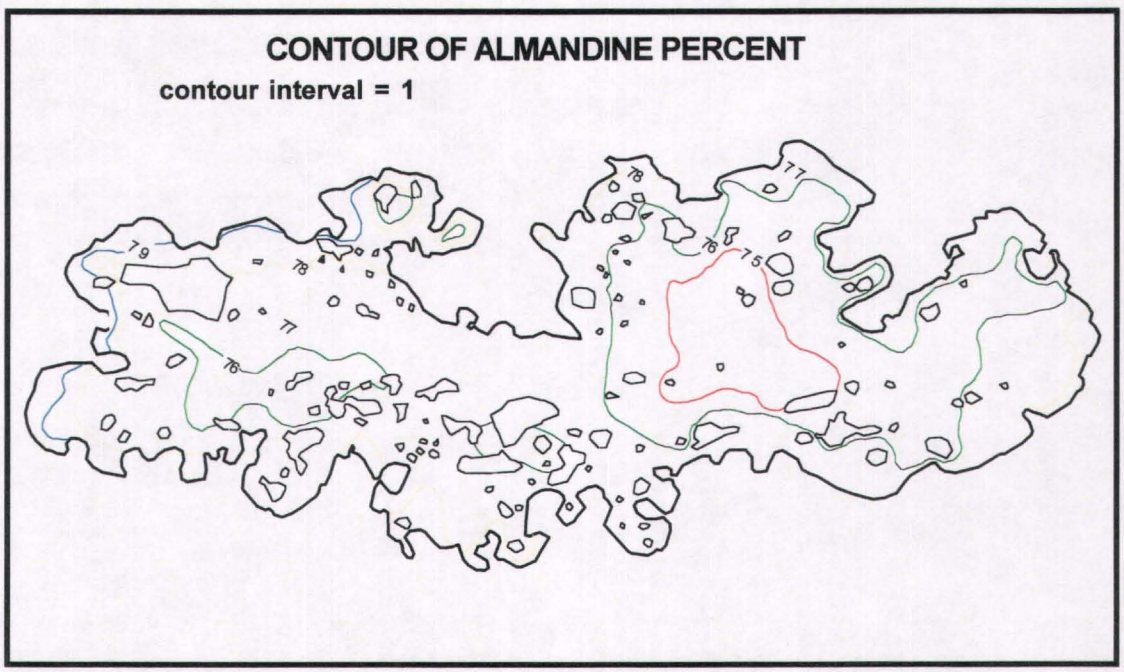

Figure 5.31. Almandine content of a first generation garnet from sample 5011. The contour patterns indicate that after initial growth, the garnet grain experienced a period of deformation, resorbtion and Fe diffusion. Bt = biotite; Grt = garnet

As discussed above, second generation garnets show higher Fe contents then the earlier generation. Profiles of almandine, pyrope, spessartine, and grossular in the second generation garnet from Zone 4 are illustrated on Figure 4.32a and b. These grains are interpreted to have grown post-D_2. Most notable is the lack of a significant increase in almandine content towards the rim typically associated with the earlier garnet generation. Fe/Fe+Mg values also show a flat line, except where the rim is in direct contact with biotite (points 13-14 on grain 0810a, and 23-29 on garnet grain 0810e). Mg contents of the second generation garnets are typically lower then the earlier generation as well (Table 4.1). This along with the higher Fe content is consistent with the interpretation that these grains may have grown during a higher temperature, lower pressure environment than the earlier garnet generation (Spear, 1993).

4.10.2. Mineral Chemistry of Biotite

There are slight variations in biotite compositions across the metamorphic zones (Table 4.2). For example, the Ti content of biotite shows a general increase from Zone 1 to Zone 4. The general increase in Ti composition is consistent with an increase in temperature from west to east (Guidotti, 1984). Magnesium values in biotite of Zone 3 are slightly higher than biotite from the other zones. Iron contents show the opposite trends, likely indicating that re-equilibration of Fe was more prevalent in Zone 4. Chemically the two texturally distinct generations of biotite are in most cases indistinguishable, and seem to have

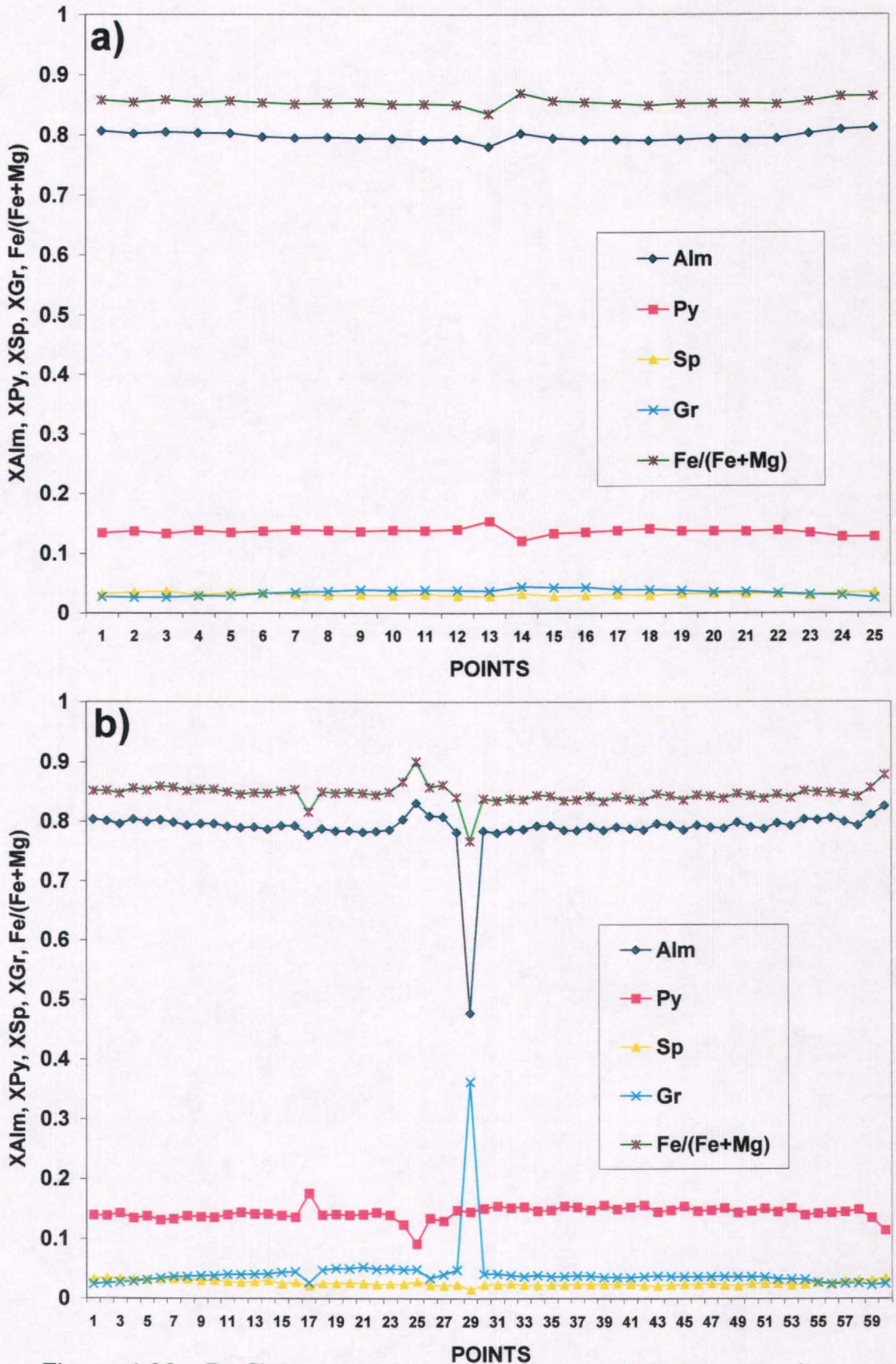

Figure 4.32. Profiles across two second generation garnet grains from sample 5000, collected within Zone 4. a) Scan 0810a (Appendix B2). b) Scan 0810e (Appendix B2).

TABLE 4.2. Average biotite compositions.

Label	Incl. 1st Gen. Garnet (6 analysis sample 9278b)	Adj. 1st Gen. Garnet (6 analysis sample 9278b)	Av. Zone 1(19 analysis)	Av. Zone 2 (13 analysis)	Av. Zone 3 (22 analysis)	Av. Zone 4 (67 analysis)
SiO2 (wt. %)	37.10	36.59	35.97	36.00	36.19	35.64
TiO2	2.74	2.69	1.81	2.05	2.66	2.56
Al2O3	18.12	18.34	19.67	19.65	18.58	19.27
Cr2O3	0.04	0.08	0.04	0.08	0.04	0.06
FeO	15.79	18.15	20.00	19.66	19.77	19.58
MgO	13.26	11.52	9.27	8.97	9.74	9.64
MnO	0.03	0.02	0.10	0.13	0.12	0.05
CaO	0.01	0.01	0.01	0.01	0.02	0.01
SrO						
BaO	0.17	0.16	0.17	0.40	0.13	0.13
Na2O	0.27	0.12	0.29	0.14	0.15	0.15
K2O	9.05	8.98	8.37	8.50	8.84	9.15
Cl	0.01	0.01	0.01	0.01	0.03	0.02
F	0.00	0.00	0.00	0.00	0.00	0.00
Total	96.60	96.67	95.80	96.02	96.34	96.32
Mg/(Fe+Mg)	0.60	0.53	0.45	0.44	0.47	0.47
Standard Deviation						
FeO	1.76	0.20	0.57	0.84	0.86	1.19
MgO	1.23	0.40	0.53	0.88	1.24	1.24
Mg/(Fe+Mg)	0.05	0.01	0.02	0.03	0.03	0.04

equilibrated during the last period of metamorphism. This is not uncommon since biotite has a relatively fast rate of diffusion (Spear, 1993). However biotite inclusions within early first generation garnet grains in sample 0278b from Zone 4 are compositionally distinct; exhibiting Mg/(Mg+Fe) values higher than those from biotite in the matrix. These inclusions have been isolated from the matrix and may have equilibrated with the first generation garnet.

Inclusions of biotite within early formed garnet grains contain Ti contents similar to, but generally lower than grains within the matrix, but adjacent to the garnet rims. Ti versus Mg/(Mg+Fe) comparisons (Figures 4.33-4.35) show the relationship between Ti and Fe-Mg. Interpreted early generation biotite (inclusions within early garnet: Figure 4.33b) show a decreased content of Ti in response to an increase in Mg, consistent with lower temperature development. Zone 1 biotites (Figure 4.34a) show a relatively low amount of Ti accompanied with a lower Mg/(Mg+Fe) ratio. This is consistent with the mineral assemblages, indicating the lowest metamorphic grade in the study area. However, the relatively low Mg/(Mg+Fe) values indicate Fe-Mg exchange after mineral growth. The presence of ilmenite within the rocks ensures Ti saturation. The Fe, Mg, and Ti contents of biotite and its textural relationships are consistent with an interpretation of an early low-temperature metamorphism and corresponding mineral growth, followed by a high-temperature metamorphic event resulting in mineral growth and re-equilibration of the early generation biotite grains.

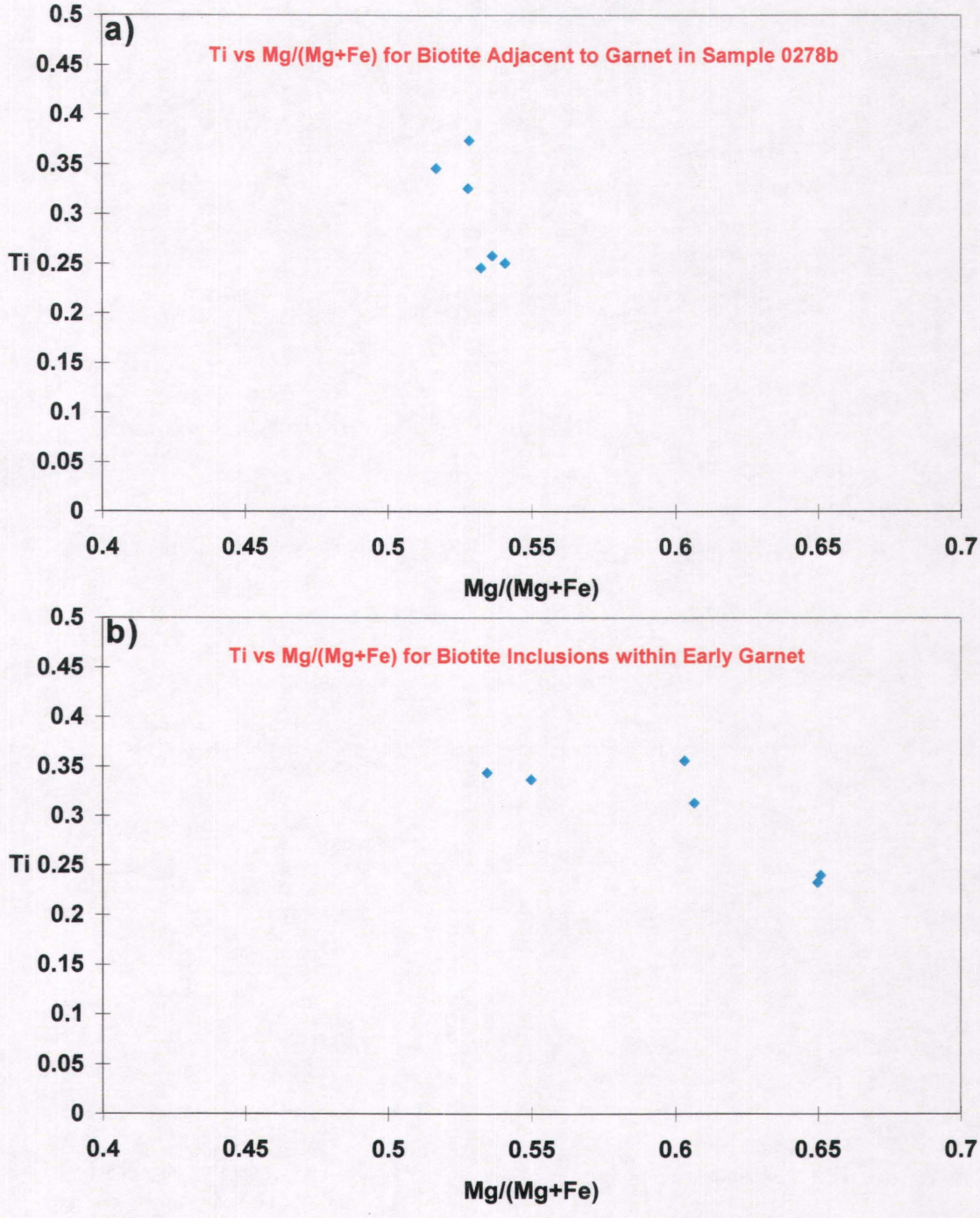

Figure 4.33. a) Ti vs Mg/(Mg+Fe) diagram displaying values from biotites within sample 0278b that are adjacent to the early first generation garnet. b) Ti vs Mg/(Mg+Fe) diagram displaying values from biotite inclusions within first generation garnets of sample 0278b.

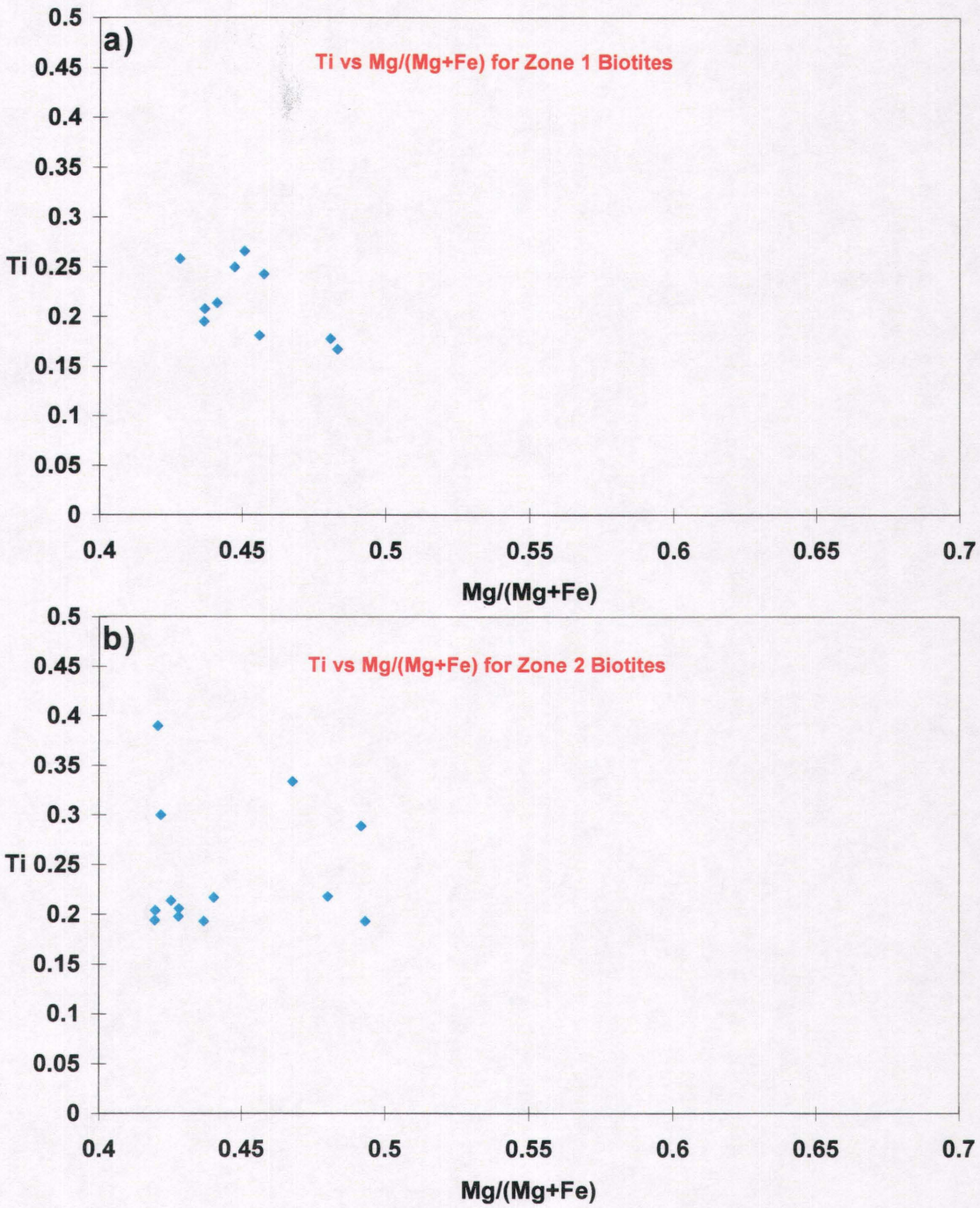

Figure 4.34. Ti vs Mg/(Mg+Fe) diagrams: a) displaying values from biotites within Zone 1; and b) displaying values from biotites within Zone 2.

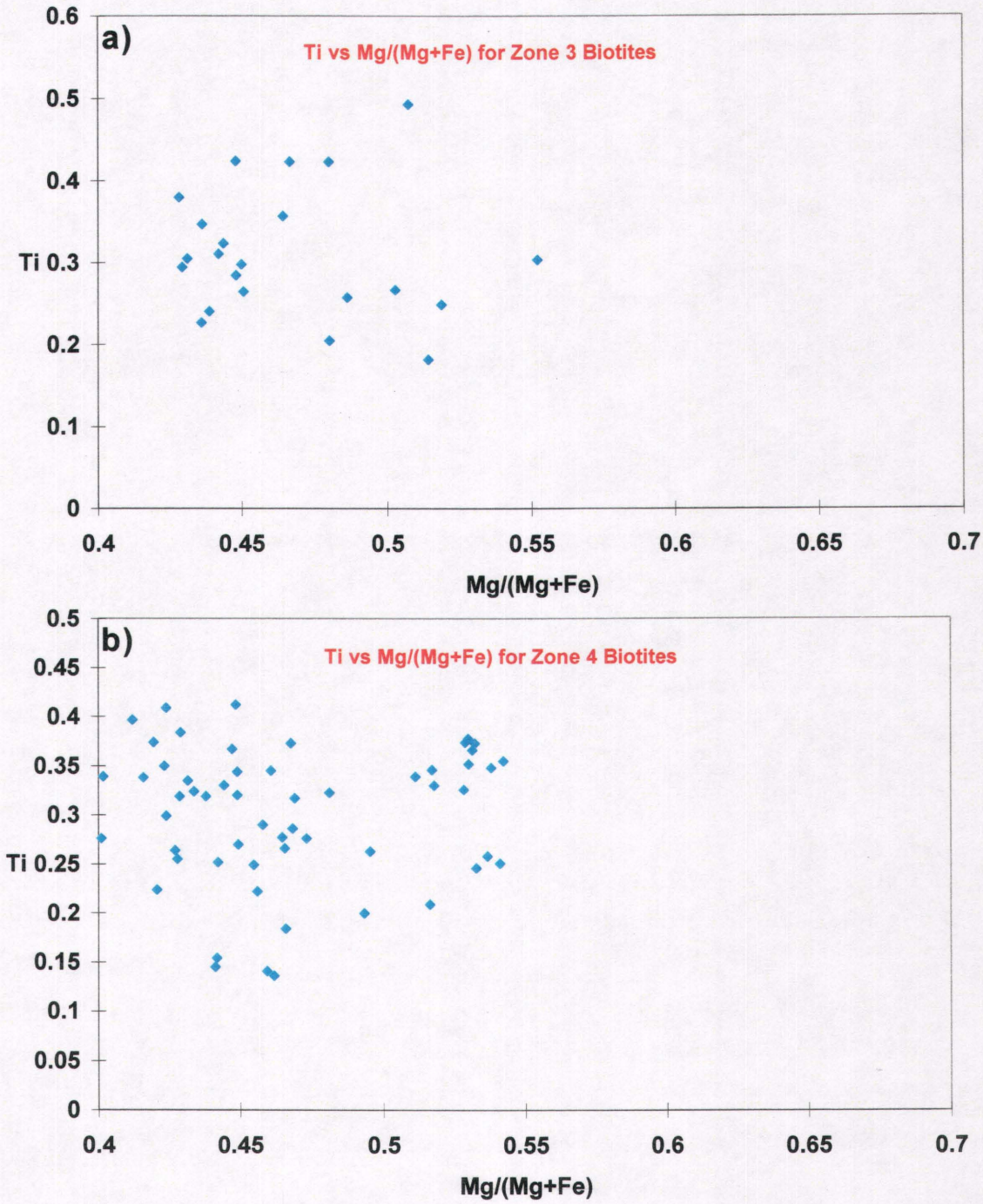

Figure 4.35. Ti vs Mg/(Mg+Fe) diagrams: a) displaying values from biotites within Zone 3; and b) displaying values from biotites within Zone 4, without the values from biotite inclusions within early garnet (Figure 4.33b).

4.10.3. Mineral Chemistry of Plagioclase

The chemistry of plagioclase and its zoning, especially when considered coexisting with other minerals such as garnet, have important implications in geobarometry. In calcic rocks, it is expected that plagioclase becomes increasingly more calcic with increasing grade of metamorphism; whereas in pelites and low calcic rocks, plagioclase may become more albite rich with increasing grade (Spear, 1993). However, due to slow cation diffusion (Grove et al., 1984), once plagioclase forms it does not change composition except through dissolution and reprecipitation. It is with this premise in mind that it becomes necessary to examine the compositions of plagioclase to be able to properly employ them in quantitative geothermobarometry (Chapter 5).

The typical plagioclase composition from the metasedimentary rocks of all four metamorphic zones is illustrated in Table 4.3b. The Ca content is somewhat variable. Albite is the dominant constituent in plagioclase in most cases. Interpreted early garnet in sample 0278b contains plagioclase, in addition to quartz and biotite inclusions. The high An content (Table 4.3a) of the inclusions are generally different from their counterparts in the matrix. The inclusions along with rare zoned plagioclase crystals in the matrix are interpreted to have formed pre- to syn-D_2. Zoned plagioclase crystals within the matrix have undergone relatively monotonic development through changing metamorphic conditions, however, the An content appears to decrease from core to rim

TABLE 4.3. Plagioclase compositions.

a) Inclusion in first generation garnet vs. Matrix

	Sample 0278b	
Wt % Oxides	Inclusion	Adjacent
SiO2	58.01	59.36
TiO2	0.01	0.01
Al2O3	26.47	25.66
Fe2O3	0.04	0.13
CaO	8.67	7.68
BaO	0.07	0.00
SrO	0.33	0.38
Na2O	6.40	6.92
K2O	0.07	0.08
Total	100.07	100.22
An	0.42	0.37
Ab	0.56	0.61
Or	0.00	0.00

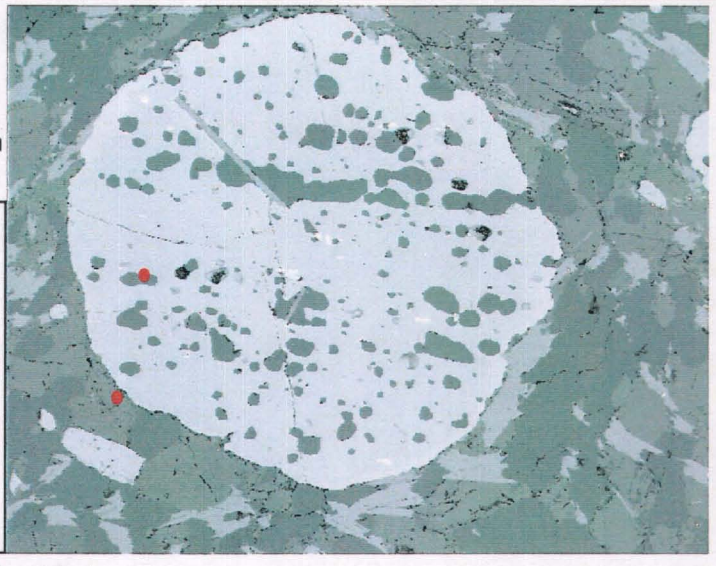

●Denotes spot analysis

b)

Typical Plagioclase Compositions								
Sample	Zone 4 5023		Zone 3 5024		Zone 2 5100		Zone 1 5055	
	core	rim	core	rim	core	rim	core	rim
SiO2 (wt. %)	61.97	62.82	61.37	60.95	60.80	61.36	62.85	61.84
TiO2	0.00	0.00	0.01	0.02	0.00	0.01	0.00	0.02
Al2O3	23.73	23.34	24.12	23.82	24.34	24.82	23.82	23.56
Fe2O3	0.02	0.55	0.03	0.06	0.04	0.12	0.00	0.03
CaO	5.54	5.24	5.49	5.28	5.92	6.02	5.04	4.91
BaO	0.00	0.21	0.04	0.00	0.05	0.02	0.00	0.00
SrO	0.21	0.24	0.31	0.29	0.30	0.28	0.26	0.22
Na2O	8.21	8.48	8.27	8.57	8.07	8.23	8.19	8.40
K2O	0.12	0.10	0.28	0.18	0.07	0.04	0.07	0.09
Total	99.80	100.99	99.91	99.17	99.60	100.91	100.23	99.07
An	0.27	0.25	0.26	0.25	0.29	0.28	0.25	0.24
Ab	0.72	0.73	0.71	0.73	0.70	0.71	0.74	0.75
Or	0.01	0.01	0.02	0.01	0.00	0.00	0.00	0.01

(Figure 4.36). This is consistent with prograde metamorphic conditions and the uptake of calcium into the coexisting garnet. Since cation diffusivity within plagioclase is slow, the inclusions along with the zoned crystals may preserve original compositions.

4.11. Deformation and Mineral Growth

Mineralogical, textural and chemical evidence lead to the recognition of two periods of high-temperature, low to medium-pressure metamorphism. The first metamorphism (M1; Figure 4.37) likely began late to post-D_1 and lasted through early D_2. This is evident as relict internal fabrics within porphyroblasts that are for the most part discordant to the S_2 external fabric. Further evidence is present as deformed mineral grains and chemical compositions relatively higher in Mg than the relatively Fe rich compositions of minerals interpreted to have overprinted the S_2 fabric. The second metamorphism (M2) and associated mineral growth show a general trend of overprinting the S_2 fabric and the earlier mineral generation. This second metamorphic episode likely began during the very late stages of D_2 broadly coeval with D_3, outlasting it; evident by late cordierite-bearing cross-cutting leucosomes in the metaturbidites rocks. The compositions of the two prograde mineral assemblages suggest that M1 occurred at a slightly lower temperature than M2, but may have took place under a slightly higher pressure. Results of quantitative constraints on these two episodes of metamorphism are presented in Chapter 5.

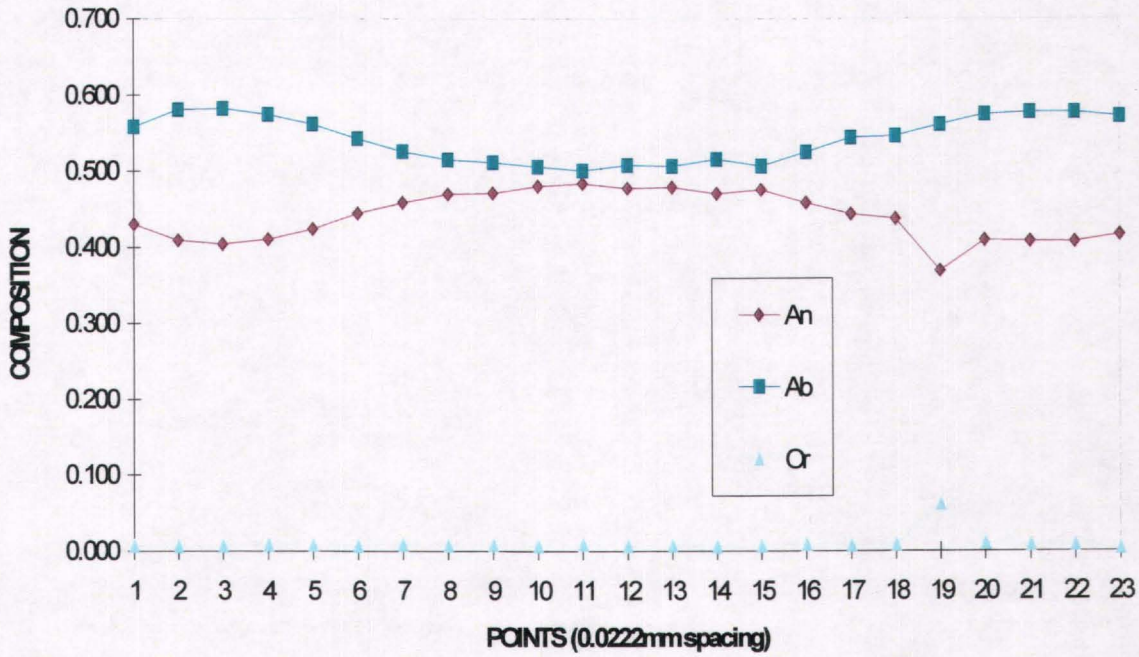

FIGURE 4.36. Profile scan of a zoned plagioclase grain from Zone 3 (Scan 1402a sample 5088)

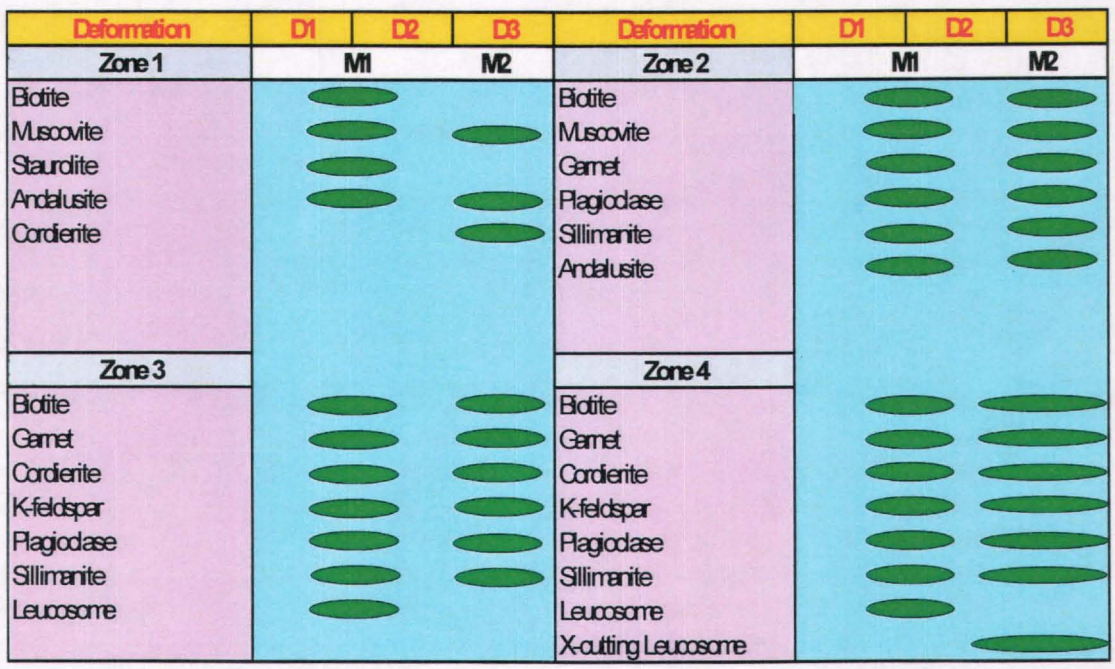

FIGURE 4.37. Chart showing the periods of mineral growth (M1 and M2; metamorphic episodes) for the prograde mineral assemblages within each Zone, in relation to the deformational events.

CHAPTER 5:

METAMORPHISM

5.0. Metamorphism: Introduction

Metamorphic investigations addressing the Kisseynew Domain, near the current study area include Sibbald (1978), Lewry and Sibbald (1980), Wilcox, (1990), Perkins (1991a, 1991b), and Tran *et al.*, (1996). Two periods of mineral growth and recrystallization have previously been recognized within the region (Sibbald, 1978). Sibbald (1978) reported the first period of mineral growth began prior to the development of the main regional foliation and lasted throughout it; coinciding with D_2 (this investigation). The second period of mineral growth began prior to D_3 and is marked by widespread recrystallization as well as the growth of garnet, cordierite and biotite in the Kisseynew Domain rocks. It was proposed that metamorphic conditions occurred during a thermal high over a prolonged period (Sibbald, 1978). This investigation also recognizes two periods of mineral growth and recrystallization within the Burntwood metatubidite rocks, but has determined the first period (M1) began post- D_1 and lasted through early D_2. The second metamorphic episode (M2) is characterized by overprinting the earlier fabrics with new mineral growth, recrystallization and partial resorbtion of earlier mineral generations. It

has been determined that M2 was relatively coeval with but outlasted D_3. Menard and Gordon (1997) and Kraus and Menard (1997) documented two periods of metamorphism within the Kisseynew Domain near Snow Lake Manitoba, where M1 is proceeded by a higher temperature M2. Here the metamorphic cycles are separated by an increase in temperature, with a decease in pressure from M1 to M2.

5.1. Petrogenetic Determination of Metamorphic Conditions

Both M1 and M2 within the Kisseynew Burntwood metapelites, resulted in developing similar mineral assemblages throughout the four zones, but are differentiated by contrasting mineral-fabric relationships (Chapter 4). All Zones, with the exception of zone 2, show both prograde and retrograde mineral assemblages associated with both recognized metamorphic episodes. Zone 1 is characterized by andalusite-staurolite-muscovite-cordierite-chlorite-biotite assemblages. Zone 2 consists of sillimanite-garnet-muscovite-biotite-chlorite metamorphic assemblages. Both Zones 3 and 4 are comprised of sillimanite-cordierite-garnet-biotite metamorphic assemblages with melt development. Zone 3, however, shows melt development variably concordant to slightly discordant with S_2, but showing D_2 deformation and commonly isoclinal folding. Within Zone 4 two generations of melt are evident; the early generation consistent with that in Zone 3, and a later generation that cross-cuts S_2 and is variably aligned sub-parallel to parallel F_3 axial planes.

The identified zones are equivalent to Schumacher *et al.*, (1990) metamorphic field gradients where the mineral isograds represent changes in metamorphic conditions and express Pressure-Temperature (P-T) histories of the rocks. Prograde assemblages most probably represent the temperature of maximum entropy (Ts_{max}), which may be lower than the true maximum temperature (T_{max}) (England and Richardson, 1977). However, a correlation between prograde mineral assemblages can be justified on the basis of reaction kinetics since reaction rates increase with temperature. Maximum temperature assemblages are preserved upon cooling. Preservation is particularly good if the assemblages developed through dehydration reactions where the volatile H_2O or CO_2 is removed from the system, making the reaction irreversible (Shumacher *et al.*, 1990). Constraints on a P-T path can be obtained through determining reaction sequences, correlating deformation and kinematic sequences with metamorphic assemblages (e.g. Chapter 3); analysis and interpretation of chemical zoning (e.g. Spear and Selverstone, 1983; Spear *et al.*, 1984); and application of geothermobarometry (numerous references: e.g. Streepey *et al.*, 1999).

5.1.1. Zone 1 Mineral Reactions

Metamorphic mineral assemblages within Zone 1 consist of andalusite-staurolite-muscovite-chlorite-biotite-cordierite and represent the lowest

conditions of metamorphism in the area. These rocks are fine grained and consist of approximately 40-60% quartz, 10-15% biotite, 5-15% plagioclase, 5-10% chlorite, 5-10% muscovite, ±5-10% andalusite, ±5% staurolite, ±1-2%cordierite, 2% apatite, 2% opaques (mainly ilmenite) and trace graphite. Two generations of andalusite were recognized. The first likely grew as a direct result of the decomposition of pyrophyllite (reaction 5-1) at conditions less than 3 kbar and 375° C. The first appearance of biotite within the zone likely formed via reaction 5-2.

pyrophyllite $\Rightarrow$ andalusite+quartz+H_2O (5-1)

chlorite+muscovite $\Rightarrow$ chloritoid+biotite+quartz+H_2O. (5-2)

Staurolite within Zone 1 contains inclusions of biotie, chlorite and quartz, and shows a textural relationship consistent with breakdown to form andalusite. The first generation andalusite porphyroblasts shows no sign of transformation into the higher grade polymorph sillimanite. This may suggest that at the time of staurolite growth conditions of stability for andalusite persisted. Second generation andalusite developed in part with the breakdown of staurolite, and obviously occurred within the andalusite stability field. M1 and M2 conditions contrast with M1 obtaining higher pressures than M2. Based on the Spear and Cheney (1989; Spear, 1993) KFMASH petrogenetic grid, the set of reactions that may have contributed to the final mineral assemblage could be as follows.

chloritoid+Al_2SiO_5 ⇒ staurolite+chlorite (5-3)

chloritoid+biotite+H_2O ⇒ garnet+chlorite (5-4)

garnet +chlorite ⇒ staurolite+biotite+H_2O (5-5)

staurolite+chlorite ⇒ andalusite+biotite+H_2O (5-6)

chlorite ⇒ cordierite+biotite+andalusite (5-7)

staurolite ⇒ garnet+biotite+andalusite (5-8)

Reaction 5-3 would have been first encountered at just above 450 °C. Once temperatures proceeded to ~ 500 °C chloritoid also began breaking down by reaction 5-5. The amount of garnet produced may have been limited by the small quantity of chloritoid left from reaction 5-3. Shortly after, with an increase of only 10-20 °C (Spear, 1993) garnet and chlorite break down to produce staurolite plus biotite (reaction 5-5). However, since conditions did not proceed above the andalusite-sillimanite join, reactions 5-4 and 5-5 must have occurred during a decompression phase (Figure 5.1). This translates into a peak pressure for M1 in Zone 1 of ~3 kbar at just above 500 °C; in accordance with the intersection of reaction 5-3 and the andalusite-sillimanite join. Peak temperature for M1 is delineated by the difference in the textural associations of the two generations of andalusite outlined in Chapter 3. The second generation of andalusite envelopes staurolite, shows no D_2 deformation, and is recognized as having grown during M2. Therefore peak temperatures for M1 must not have exceeded the temperatures applicable for the reactions that have been

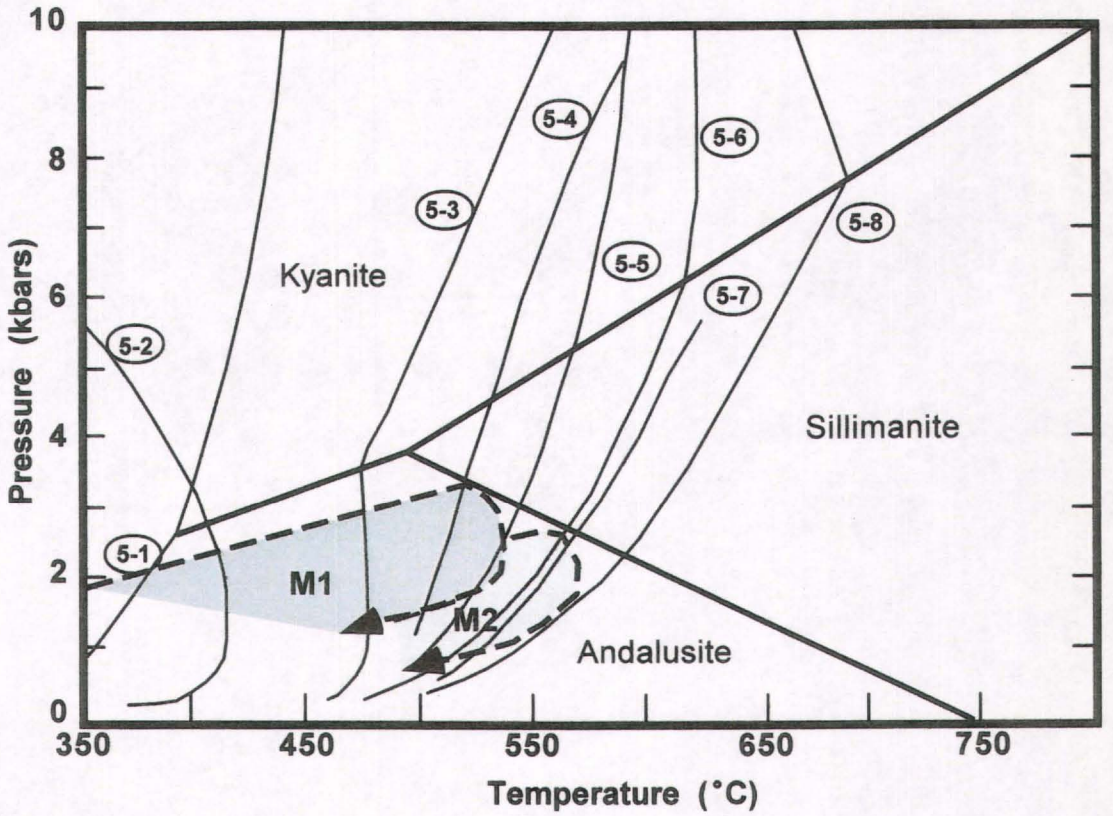

Figure 5.1. A petrogenetic grid based on Spear and Cheney (1989) showing the interpreted reactions based on mineralogy and textural information from Zone 1 rocks; along with the interpreted P-T paths for the two metamorphic events. Reactions: (5-1) pyrophyllite = andalusite +quartz+H2O; (5-2) chlorite+muscovite = chloritiod+biotite+quartz+H2O; (5-3) chloritoid+andalusite = staurolite+chlorite; (5-4) chloritoid+biotite+ H2O = garnet+chlorite; (5-5) garnet+chlorite = staurolite+biotite+H2O; (5-6) staurolite+chlorite = andalusite+biotite+H2O; (5-7) chlorite = cordierite+biotite+andalusite; (5-8) staurolite = garnet+biotite+andalusite. M1 = first metamorphic episode; M2 = second metamorphic episode. Al2SiO5 phase relations from Holdaway (1971).

deduced to have produced second generation andalusite within Zone 1 (reactions 5-6 and 5-7; Figure 5.1); at <565 °C. Reactions 5-6 and 5-7 delineate the maximum pressure that Zone 1 could have obtained during M2 at ~2.7 kbar. Peak temperatures are estimated using the limiting reaction 5-8, since no garnet is present within the rocks of this zone. Temperatures for M2 then did not exceed 600 °C.

Retrograde minerals include biotite, chlorite, and muscovite. These minerals resulted from reactions 5-5 and 5-7 from M1 and M2 respectively; proceeding towards the left during cooling and decompression following peak conditions. This is clearly evident from the extensive retrograde pseudoporphyroblasts consisting mainly of biotite, chlorite, muscovite, and quartz, and the abundance of partially retrograded biotite-chlorite crystals parallel foliation.

5.1.2. Zone 2 Mineral Reactions

Across the isograd marked by the appearance of sillimanite and garnet, within Zone 2 the metapelitic rocks consist of sillimanite-garnet-muscovite-biotite-chlorite gneisses. These rocks are fine to medium grained and consist of 40-50% subhedral quartz, 10-20% plagioclase (An~25), 20-25% biotite, ± 6-15% muscovite, 0-5% sillimanite, 2-3% garnet, ± 2-5% cordierite, 2% apatite, minor albite (<1%) ilmenite, and graphite.

The psammitic metasediments from Zone 2 consist of fine grained Biotite Gneisses with a modal mineralogy of 60-70% quartz, 20-25% biotite, 6-10% plagioclase feldspar, 0-2% muscovite, 0-5% sillimanite, 0-1% garnet, trace opaques (mainly ilmenite), graphite, and apatite. Biotite, muscovite, and sillimanite delineate the foliation (S_2) which is slightly undulating (F_3).

Within Zone 2 no staurolite has been found, and sillimanite is the main Al_2SiO_5 polymorph. The reactions governing the western boundary of the Zone are likely 5-9 and 5-10.

andalusite $\Rightarrow$ sillimanite (5-9)

staurolite $\Rightarrow$ garnet+biotite+sillimanite . (5-10)

Garnet, sillimanite, and biotite may also have developed through reaction 5-11 (Diskerson and Holdaway, 1989). Here, with isobaric heating, staurolite is also replaced by pseudomorphs of muscovite, biotite, and plagioclase, as sillimanite grows, consistent with total consumption of staurolite at 610 °C and 4 kbar (Foster, 1999). This limits the western boundary of Zone 2 to minimum conditions of 610 °C and 4 kbar.

staurolite+muscovite+quartz $\Rightarrow$ garnet+sillimanite+biotite+H_2O (5-11)

The eastern boundary of Zone 2 represents the highest metamorphic conditions in the zone. The highest P-T condition is delineated by the decomposition of muscovite in the presence of quartz. Muscovite becomes unstable in the presence of quartz along the melt absent dehydration reaction curve 5-12 (Evans, 1965).

$$\text{muscovite+quartz} \Rightarrow \text{k-feldspar+sillimanite+}H_2O \qquad (5\text{-}12)$$

No melt is present within the zone, and muscovite+quartz exist in equilibrium, therefore the intersection of reaction 5-12 with the incipient melting curve (Figure 5.2) represents the maximum P-T conditions within the zone. Pressures above this point cause the decomposition of muscovite through partial melting where the K-feldspar component dissolves into the melt; at pressures below the intersection muscovite disappears through reaction 5-12 (Bucher and Frey, 1994). The reaction curve 5-12 then represents the limits of physical conditions within Zone 2. The maximum P-T that may have been achieved is 680° C at 4 kbar (Bucher and Frey, 1994). Conditions for both M1 and M2 were similar throughout this Zone.

5.1.3. Zone 3 Mineral Reactions

The presence of potassium feldspar, sillimanite, absence of primary muscovite and the development of quartz-feldspar±cordierite±garnet melt, marks the next

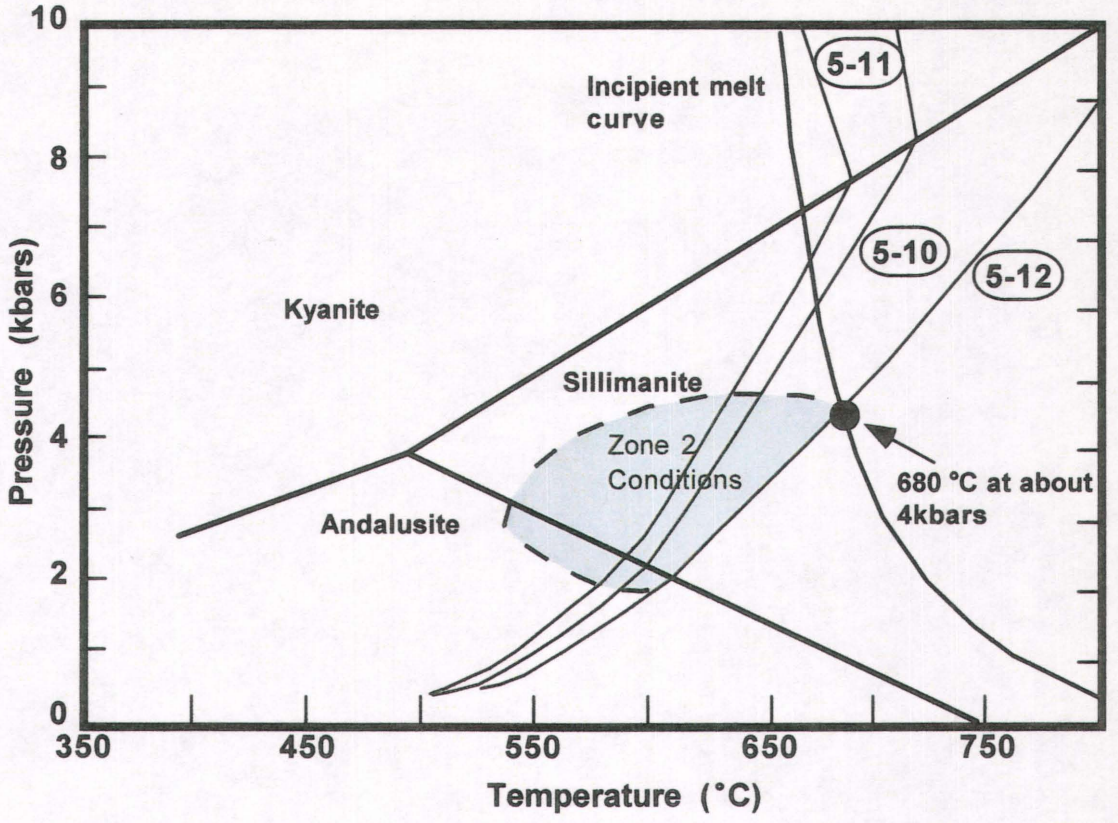

Figure 5.2. A petrogenitic grid based on Spear and Cheney (1989) showing the reaction curves discussed in the text interpreted to have defined the mineral assemblage in Zone 2. The intersection of curve 5-12 and the incipient melting curve represent the highest point of pressure and temperature that could have been achieved in the Zone. Reactions: (5-10) staurolite = garnet+biotite+sillimanite; (5-11) staurolite+muscovite +quartz = garnet+sillimanite+biotite+H2O; (5-12) muscovite+quartz = K-feldspar+sillimanite+H2O. Al2SiO5 phase relations from on Holdaway (1971).

isograd and the beginning of Zone 3. Within this zone the metaturbidites rocks are also represented by metapelites and the more quartz rich metapsammites. Metapelitic garnet-cordierite-biotite gneissic rocks are fine to medium grained and consist of 30-40% subhedral quartz, 20-25% biotite, 20% plagioclase (An~26-30), 1-2% potassium feldspar, 5% sillimanite, 1-5% cordierite, 1-5% garnet, with minor muscovite (0-2%) and trace amounts of ilmenite, graphite, apatite, titanite and zircon. All samples are well foliated, and under optical microscopy show extensive recrystallization due to deformation. Microcline (K-feldspar) is not particularly abundant, but it is present. Some samples exhibit a very close association between sillimanite and muscovite, indicating the breakdown of muscovite to form sillimanite and potassium feldspar. The sillimanite is often present adjacent to and interfingered with potassium feldspar, with symplectic textures common. The cordierite present within the rocks is aligned with quartz, feldspar and biotite along the main pervasive foliation and often exhibits replacement by feldspar, quartz, biotite, and sillimanite. The melt portions of the rock are also variably concordant with the S_2 foliation.

Biotite Gneisses are fine grained and consist of 30% quartz, 20-25% bitoite, 30% plagioclase (An 30-35), 0-5% sillimanite, 0-2% muscovite, 0-1% garnet with trace ilmentite, apatite, titanite, graphite, and zircon.

Reaction 5-12 represents the western boundary of Zone 3 with the decomposition of muscovite and the development of second sillimanite with leucosome. This melt is variably concordant with S2, indicating that temperatures during M1 achieved a minimum of 680° C at 4 kbar.

Beyond this point vapour absent reactions dominate and granitic melt is produced through the dehydration and decomposition of muscovite and biotite through reactions 5-12, 5-13, 5-14, and 5-15 (Le Breton and Thompson, 1988; Wickam, 1987; Spear, 1993; Bucher and Frey, 1994).

biotite+sillimanite+plagioclase+quartz $\Rightarrow$

$\pm$cordierite$\pm$garnet+k-feldspar+melt (5-13)

Within Zone 3 cordierite may have developed through reactions 5-14 and 5-15. Reaction 5-14 is a continuous reaction where k-feldspar and water dispersed into the melt fraction (Bucher and Frey, 1994). Cordierite develops preferentially before garnet, if albite is substituted for plagioclase in reaction 5-15. Wickam (1987) estimated that the onset of melting with cordierite development intitiates at approximately 3-4 kbar at 670-700° C. The dehydration reactions 5-12 through 5-15 produce a high volume of fluid, which may have resulted in lowering the melting temperatures of the rocks allowing for anatexis to occur at temperatures below 650° C (Thompson, 1982).

2biotite+6muscovite+15quartz $\Rightarrow$ 3cordierite+8k-feldspar+8H_2O (5-14)

biotite+plagioclase+sillimanite+quartz $\Rightarrow$ garnet+cordierite+H_2O (5-15)

The absence of orthopyroxene and reaction 5-16 delineates the maximum P-T conditions that may have been attained within the zone during M1. Intersections of reaction curves 5-15 and 5-16 (Figure 5.3) yield the upper limit of P-T conditions to be approximately 6.5 kbar at $\approx$ 730° C.

biotite+garnet $\Rightarrow$ cordierite+orthopyroxene+k-feldspar+melt (5-16)

Following M1, conditions regressed enough to cause reaction 5-15 to proceed to the left, partially replacing cordierite locally with plagioclase, sillimanite and quartz. The presence of such textures indicates that there must have been fluid present during retrogradation, or the prograde assemblage would have been intact (Schumacher *et al.*, 1990). The retrograde path is established since these reactions do no occur below 600° C and less than 2 kbar. Incipient melting ceased during D_2 as some melts are slightly discordant with S_2, but still exhibit variable amounts of D_2 isoclinal folding.

Conditions during M2 proceeding after M1 retrogression did not acquire temperatures high enough to produce another generation of melt within this zone. However, the temperatures achieved during the second metamorphism

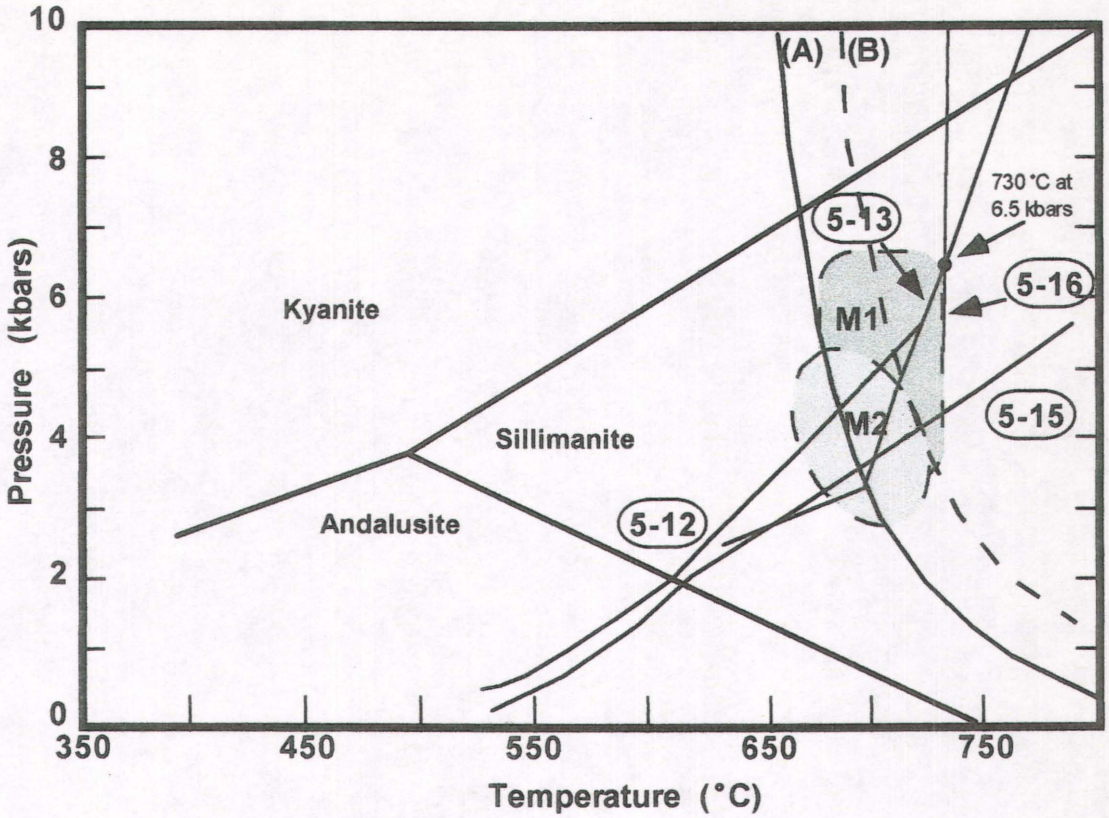

Figure 5.3. A petrogenitic grid based on Spear and Cheney (1989) showing the reaction curves discussed in the text interpreted to have defined the mineral assemblage in Zone 3. The intersection of curve 5-12 and the incipient melting curve represent the estimated peak minimum pressure and temperature of M1 in the Zone. Maximum conditions are delineated by the intersection of 5-13 and 5-16, at 730 °C and approximately 6.5 kbars. Reactions: (5-12) muscovite+quartz = K-feldspar+sillimanite+H2O; (5-13) biotite+sillimanite+plagioclase+quartz =cordierite+garnet+k-feldspar+melt; (5-15) biotite+plagioclase+sillimanite +quartz = garnet+cordierite+H2O; (5-16) biotite+garnet = cordierite+ orthopyroxene+K-feldspar+melt. A) Initial incipient melt curve; (B) illustrates a rightward shift of the melt curve resulting from the partial removal of fluid during M1 and lower PH2O. M1 = first metamorphic episode; M2 = second metamorphic episode. Al2SiO5 phase relations from Holdaway (1971).

within Zone 3 may have been similar or even exceeded that of M1, but due to reduced water activity, the incipient granitic melting curve may have been displaced to the right (Johannes and Holtz, 1990) (Figure 5.3). However, cordierite and garnet are present texturally overprinting S_2 fabrics; in some cases mimicing early generation retrogressed porphyroblasts of cordierite. This indicates conditions needed to drive reaction 5-15 to the right were achieved. Maximum temperatures during M2 then, likely achieved near melting conditions, but at a lower pressure.

5.1.4. Zone 4 Mineral Reactions

On the eastern side of the isograd indicating the development of melt containing cordierite and garnet, the Zone 4 metapelitic and psammitic rocks have similar mineralogy as those within the zone directly to the west; with the exception of an increase in the relative amount of garnet to cordierite within the early melt. The reason for delineating a separate zone is based on the mineralogical difference of the melt which reflects a compositional difference. The sillimanite-garnet-cordierite-biotite gneisses are medium grained, and consist of 26-30% quartz, 30% plagioclase (An 30-35), 20-25% biotite, 6-10% cordierite, 5% sillimanite, 2-5% garnet, minor muscovite (1%) and graphite, with trace titanite, apatite, and zircon. The psammitic portion of the metaturbidites within this zone exhibits some important textures for deciphering mineral growth (discussed in Chapter 3). Mineralogically the garnet-biotite gneisses are fine grained and

consist of 30-40% quartz, 20-30% plagioclase (An 36-40), 20% biotite, 10% garnet, 0-2% sillimanite, with trace amounts of apatite, titanite, graphite, and zircon. Symplectic recrystallization and myrmekitic quartz-feldspar textures are common. Multiple generations of garnet, sillimanite, cordierite, and biotite have been identified within Zone 4 (Chapter 3).

The reactions producing the mineral assemblage in this zone are identical to those identified for Zone 3. Early cordierite developed through reactions 5-13, 5-14, and 5-15 (Chapter 4, Figure 4.29); early garnet within the metapelites developed through reactions 5-13 and 5-15. Both k-feldspar and sillimanite are present as a result of reactions 5-12 surpassing the second sillimanite reaction. However, the relatively higher proportion of garnet within the early melt and psammitic layers of the metaturbidites (e.g. Chapter 2, Figure 2.3-2.4) is likely produced through reaction 5-17, were garnet was favored over cordierite (Le Breton and Thompson, 1988; Spear, 1993). This is consistent with the interpretation that M1 peaked at higher pressures in Zone 4 than in Zone 3. No orthopyroxene is present within these rocks however, again limiting the maximum P-T conditions for M1 to approximately 6.5 kbar and 730° C.

biotite+sillimanite+plagioclase+quartz $\Rightarrow$ garnet+k-feldspar+melt (5-17)

Reaction textures are readily identified (Chapter 4, Figures 4.17, 4.18) clearly demonstrating the existence of a decompression period following M1, possibly

coincident with late syn-D_2. Almandine garnet is enclosed as inclusions within cordierite that shows an apparent draping of the external fabric about the grain edges (e.g. Chapter 4, Figure 4.18). This is consistent with decompression and movement of the P-T path through the reaction curve 5-18 (Figure 5.4) which occurs from 650-710° C at 3.4-2.9 kbar (Holdaway and Lee, 1977).

almandine+sillimanite+quartz+$H_2O \Rightarrow$ cordierite (5-18)

Cordierite is again replaced by plagioclase, sillimanite and quartz indicating a similar retrogradation path as Zone 3. Figure 4.17 shows an early generation of cordierite rimmed by sillimanite, and enclosed as an inclusion within a later generation of cordierite. This texture is consistent with decompression after development of the early cordierite by reaction 5-13 moving towards the left. A subsequent increase in temperature followed, driving the reaction once again to the right, enclosing the two minerals as inclusions (Figure 5.4).

Within the Metaturbidites of Zone 4 a late crosscutting melt exhibiting growth of both cordierite and garnet is present. Mineralogically this melt is coarse grained and consists of 60% quartz, 0-20% garnet, 6-10% plagioclase (An 25), 6-10% cordierite, and 2-4% biotite. Observations based on outcrop suggest that the development of this melt began prior to D_3, and lasted throughout. The leucosome is observed in positions gradational between two end member positions. It is seen crosscutting the S_2 fabric, and dextrally rotated into axial

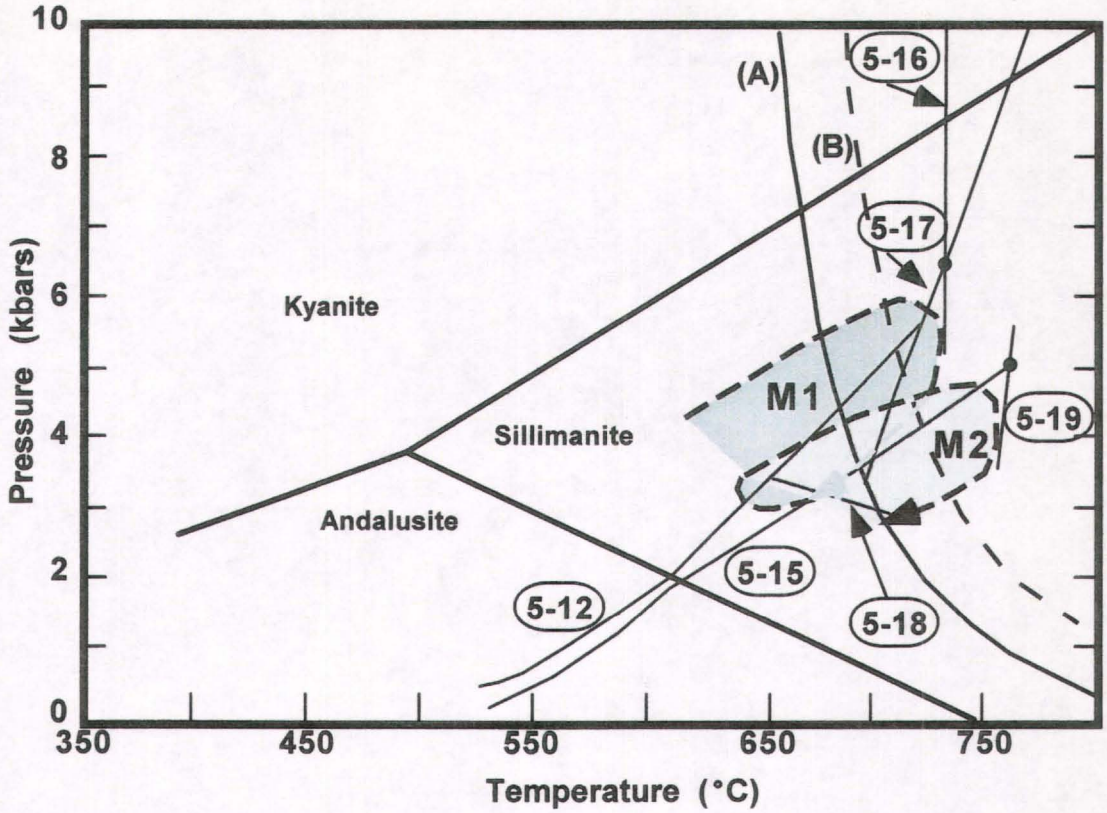

Figure 5.4. A petrogenitic grid based on Spear and Cheney (1989) showing the reaction curves discussed in the text interpreted to have defined the mineral assemblage in Zone 4. The intersection of curve 5-12 and the incipient melting curve represent the estimated minimum peak pressure and temperature of the Zone. Maximum conditions for M1 are delineated by the intersection of of 5-17 and 5-16, at 730 °C and approximately 6.5 kbars. Maximum conditions for M2 are constrained by the curves 5-15 and 5-19, at 750 °C and 5 kbars. Reactions: (5-12) muscovite+quartz = K-feldspar+sillimanite+H2O; (5-15) biotite+plagioclase +sillimanite+quartz = garnet+cordierite+H2O;(5-16) biotite+garnet = cordierite+orthopyroxene+K-feldspar+melt; (5-17) biotite+plagioclase+ sillimanite+quartz = garnet+K-feldspar+quartz; (5-18) almandine+sillimanite +quartz+H2O = cordierite; (5-19) cordierite+garnet = sillimanite+ orthopyroxene+quartz+H2O. (A) Initial incipient melt curve; (B) illustrates a rightward shift of the melt curve resulting from the partial removal of fluid during M1 and lower PH2O. M1 = first metamorphic episode; M2 = second metamorphic episode. Al2SiO5 phase relations from Holdaway (1971).

planar position to F_3 folds; and as a crosscutting patch melt. Within the melt, myrmeketic quartz-feldspar textures are common. The cordierite porphyroblasts are euhdral to subhedral in shape (Chapter4, Figure 4.19); the garnet grains however, are usually irregularly shaped, and exhibit many inclusions. The chemistry, along with the anhedral nature of the garnet grains (Chapter 4), indicate that the majority of the garnets within this melt, are an earlier resorbed generation. The abundance of well formed cordierite however, suggests that metamorphic conditions were lower than the P-T conditions involved in producing the earlier concordant garnet bearing melt. Clemens and Wall (1981) show that the presence of large cordierite crystals within melt form at a maximum pressure of 5 kbar. Likely then, this leucosome was produced through reactions 5-13 and 5-15, in a lower pressure regime than M1, conducive to the development of cordierite over garnet (Bucher and Frey, 1994). Reactions 5-15 and 5-19 intersect at an invariant point of 5 kbar and 750° C (Grant, 1985), indicating maximum conditions for M2.

cordierite+garnet $\Rightarrow$ sillimanite+orthopyroxene+quartz+H_2O (5-19)

Also within Zone 4, a small region of quartz-feldspar-biotite-cummingtonite±cordierite±garnet crops out. The orthoamphibole porphyroblasts are texturally consistent with development during M1; post- D_1 but pre- to early syn- D_2 (e.g. Chapter 4, Figure 4.30). Typically orthoamphibole develops through the decomposition of chlorite and biotite in the presence of

quartz (e.g. reaction 5-20) between 600-650° C and 3-5 kbar (Bucher and Frey, 1994).

chlorite+quartz $\Rightarrow$ orthoamphibole+cordierite+H_2O (5-20)

The assemblage containing cummingtonite+cordierite is relatively rare, and restricted to low pressures (Spear, 1993). This is consistent with the orthoamphiboles textural association indicating a relatively early growth period.

5.2. Geothermobarometry

Quantitative estimation of metamorphic conditions is used to enhance the knowledge of actual pressure and temperature values that metamorphic rocks have experienced. Mineral compositions are used to calculate equilibrium constants (K_{eq}) to determine the temperature (T), pressure (P), or both simultaneously to estimate the conditions at which the samples equilibrated. It is the dependence of the equilibrium constant on T and P that allows for the calculation of these conditions. The thermodynamic law of mass action describes the temperature and pressure dependence of the equilibrium constant (below; ΔH^o = enthalpy; ΔC_p = heat capacity of reaction; ΔV = volume change; ΔS^o = entropy; ΔG = free energy; "^{o}" = standard state), where there is a unique $\ln K_{eq}$ for every P and T.

$$0=\Delta H^{o} + T\Delta C_{p} + P\Delta V - T\Delta S^{o} + RT\ln K_{eq} = \Delta G \quad (5\text{-}21)$$

Most geothermometers are based on exchange reactions involving components such as Fe-Mg between garnet-biotite (eg. Ferry and Spear, 1978) or garnet-cordierite (eg. Holdaway and Lee, 1977). Geobarometers however are based on net transfer equilibria, and the consumption and production of mineral phases (e.g. garnet-plagioclase-quartz-aluminosilicate [GASP], Ganguly and Saxena,1984; Koziol and Newton, 1988; Koziol, 1989). When estimating equilibrium constants, it is particularly important to use mineral compositions from phases that are in textural equilibrium. Proper petrographic information must be documented (Chapter 4) to ensure that textural equilibrium between the mineral phases has been achieved. This is of particular importance in the current region of investigation, since two metamorphic episodes have been recognized. Mineral compositional data that is to be used must be chosen from phases that are assumed to be in equilibrium as a result of the same metamorphic episode. However, interpretation of textural equilibrium is usually equivocal at best.

Precision and accuracy of the results obtained through thermobarometry is based on the errors that may arise throughout the processes of obtaining data from analysis of mineral compositions, to uncertainties in mineral activity models used. The major sources of error are numerous and include the accuracy experimental calibrations used; error in the ΔV of reaction; analytical

imprecision in microprobe analysis; uncertainty of electron microprobe standard compositions; correlations between errors in temperature estimates and errors in pressure; mineral activity model uncertainty; and geological uncertainty (Spear, 1993).

Geothermometry of the Kisseynew metaturbidites is investigated using the methods described and developed by Ferry and Spear (1978). Geobarometry calculations follow that of Gordon (1992) and Gordon *et al.*, (1994) inverse equilibrium geothermobarometer (WEBINVEQ: http://ichor.geo.ucalgary.ca/~tmg/Webinveq). TEEWQ (Thermobarometry with Estimation of Equilibrium; Berman, 1988, 1991) is also employed to investigate thermobarometry.

5.2.1. First Metamorphic Episode (M1)

Figure 5.5 shows plots of the P-T estimates calculated. From these plots it is evident that an overall separation between metamorphic conditions resulting in growth of the two texturally distinct mineral generations is clear. Minerals texturally identified as having developed during the first metamorphic episode show generally higher-pressure conditions than those that developed during the second metamorphic episode. Temperature conditions however show relatively similar values. This is compatible with the petrographic estimates.

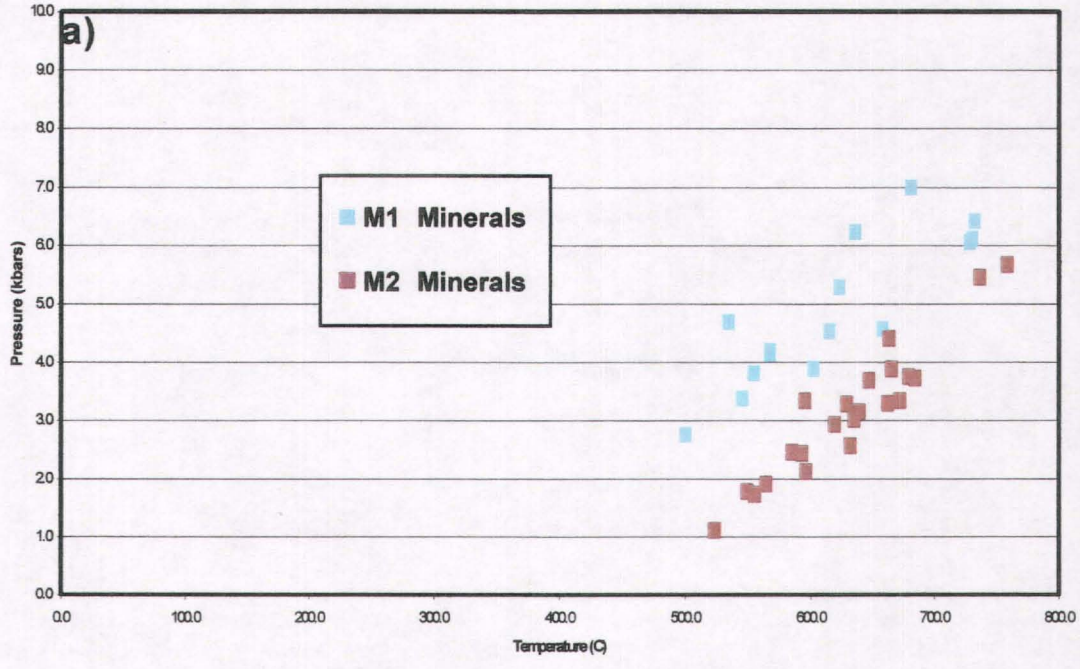

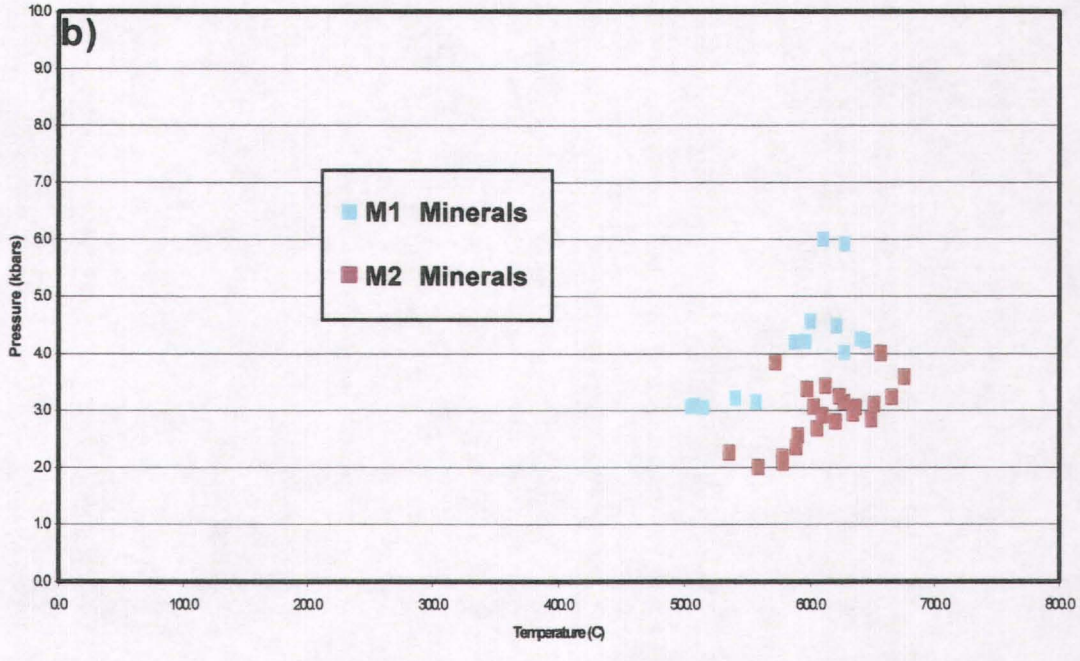

Figure 5.5. Plots of pressure-temperature estimates showing the grouping of results from the two proposed metamorphic events. Estimates are based on minerals texturally identified as having grown during either the first or second metamorphism. a) Results from WEBINVEQ (http://ichor.geo.ucalgary.ca/-tmg/Webinveq). b) Results from TWEEQ (Berman, 1988, 1991). M1= first metamorphic episode; M2 = second metamorphic episode

5.2.1.1. Ferry and Spear (1978) Geothermometry Results for M1

Table 5.1 shows the calculated P-T estimates from the various methods. Each temperature estimate calculated from Ferry and Spear (1978) has been corrected for Ca by adding 4 °C for every 0.01 xCa in the garnet (Ferry and Spear, 1978). The highest M1 temperature estimate from the Ferry and Spear calculation is derived from a garnet rim and an adjacent biotite in sample 0278b from zone 4, at 717 °C. The lowest temperature calculated is derived from sample 5011 in zone 3, at 508 °C, and is based on a garnet core and a biotite inclusion. Biotite inclusions in this instance likely equilibrated with the enclosing garnet during the growth of the particular mineral, suggesting that the temperatures obtained reflect the temperature at the time of garnet growth. This does not represent peak temperatures, but possibly the temperature for the onset of garnet growth during M1. However, a temperature of 717 °C was obtained utilizing a garnet core and a matrix biotite from sample 0278b in zone 4. This value likely represents the peak temperature achieved during M1, as calculated through the Ferry and Spear (1978) method. These calculated values show a general trend of increasing from zone 2 to 4. Estimates calculated using garnet core analysis with isolated matrix biotite yield near maximum temperatures for zone 2 of 594 °C, 646 °C for zone 3, and the 717 °C peak temperature for zone 4. All temperatures utilizing isolated matrix biotites may reflect somewhat of a lower estimate than actual temperatures due to the

TABLE 5.1. Temperature-Pressure Values for the Kisseynew Metaturbidite Rocks.

Mineral Association	Zone	Samples Minerals from M1	Ferry and Spear (1978) T ©	WEBINVEQ (Gordon *et al*., 1994; http://icho.geo.ucalgary.ca/-tmg/Webinveq) T ©	WEBINVEQ P (kbars)	TWEEQ (Berman, 1988, 1991) T ©	TWEEQ P (kbars)
	4	0278b	549	534	4.7	587	4.2
Garnet	4	0287b	595	602	3.9	557	3.2
core with Bt	4	0278b	543	554	3.8	600	4.6
inclusions	4	0278b	530	545	3.4	596	4.2
	3	5011	508	500	2.8	540	3.2
	4	0278b	717	732	6.4	621	4.5
Garnet core	3	5088	646	658	4.6	640	4.3
with isolated	3	5011	627	615	4.5	515	3.1
Bt.	2	5100	594	623	5.3	505	3.1
Garnet Rim, Adj. Bt.	4	0278b	717	728	6.1	644	4.2
	4	0278b	716	730	6.1	627	4.0
Garnet rim	3	5088	647	681	7.0	627	5.9
with isolated	3	5088	608	636	6.2	610	6.0
Bt.	2	5100	560	567	4.2	505	3.1
	2	5100	544	567	4.1	507	3.1
		Minerals from M2					
	4	10a	640	647	3.7	623	3.2
	4	10a	634	639	3.2	620	2.8
	4	5000	658	665	3.9	627	3.1
Garnet core	4	5000	732	736	5.5	657	4.0
with isolated	4	5000 grt adj Pl	581	595	3.3	597	3.4
Bt.	4	5002	590	593	2.4	589	2.4
	4	5023	674	663	4.4	612	3.4
	4	5068	673	672	3.3	666	3.2
	4	5131	649	635	3.0	636	3.1
	4	7005b	625	629	3.3	610	2.9
	4	10a	559	564	1.9	577	2.2
Garnet rim	4	10a	579	585	2.5	590	2.6
with isolated	4	5000	676	679	3.7	634	2.9
Bt.	4	5068	520	523	1.1	578	2.1
	4	5068	636	632	2.6	649	2.8
	4	5131	681	662	3.3	651	3.1
	4	7005b	615	619	2.9	605	2.7
Garnet with	4	5000	564	555	1.7	535	2.3
Bt. inclusions.	4	5000	549	549	1.8	675	3.6
	4	5000 Grt core, Bt inc.	741	758	5.7	603	3.1
Garnet rim	4	5000 Grt rim, adj Pl, adj Bt.	680	596	2.1	572	3.8
with adjacent Bt.	4	5000	674	684	3.7	558	2.0

(Bt = biotite; Pl = plagioclase; Grt = garnet; adj = adjacent; M1 = first metamorphic episode; M2 = second metamorphic episode)

low closure temperature of biotite, and continued Fe-Mg exchange post peak M1 conditions (Spear, 1993).

5.2.1.2. Web Inverse Equilibrium Results (WEBINVEQ) (http://ichor.geo.ucalgary.ca/~tmg/Webinveq) for M1

The WEBINVEQ method (Gordon *et al.*, 1994) uses the least squares method of determining P and T. A detailed description of the mathematics is presented at http://ichor.geo.ucalgary.ca/~tmg/Webinveq and Gordon *et al.*, (1994), and is briefly outlined below. At a fixed temperature and pressure the Gibbs free energy of a solution can be represented as a surface in composition. The free energy of a particular composition may be described by the tangent plane to the free energy surface at the particular composition. Partial molar free energies of the end members of the particular solution are defined by the intersection of the tangent plane with the compositions of the end members. These partial molar free energies for a fixed composition are functions of pressure and temperature. All estimates calculated here use the same compositions of garnet-biotite used for the previous method, but include plagioclase end member information to estimate for pressure.

WEBINVEQ temperature estimates for M1 are relatively consistent with the Ferry and Spear (1978) method (Table 5.1; Figure 5.6a); and the pressures calculated are consistent with the petrographic estimates of the previous

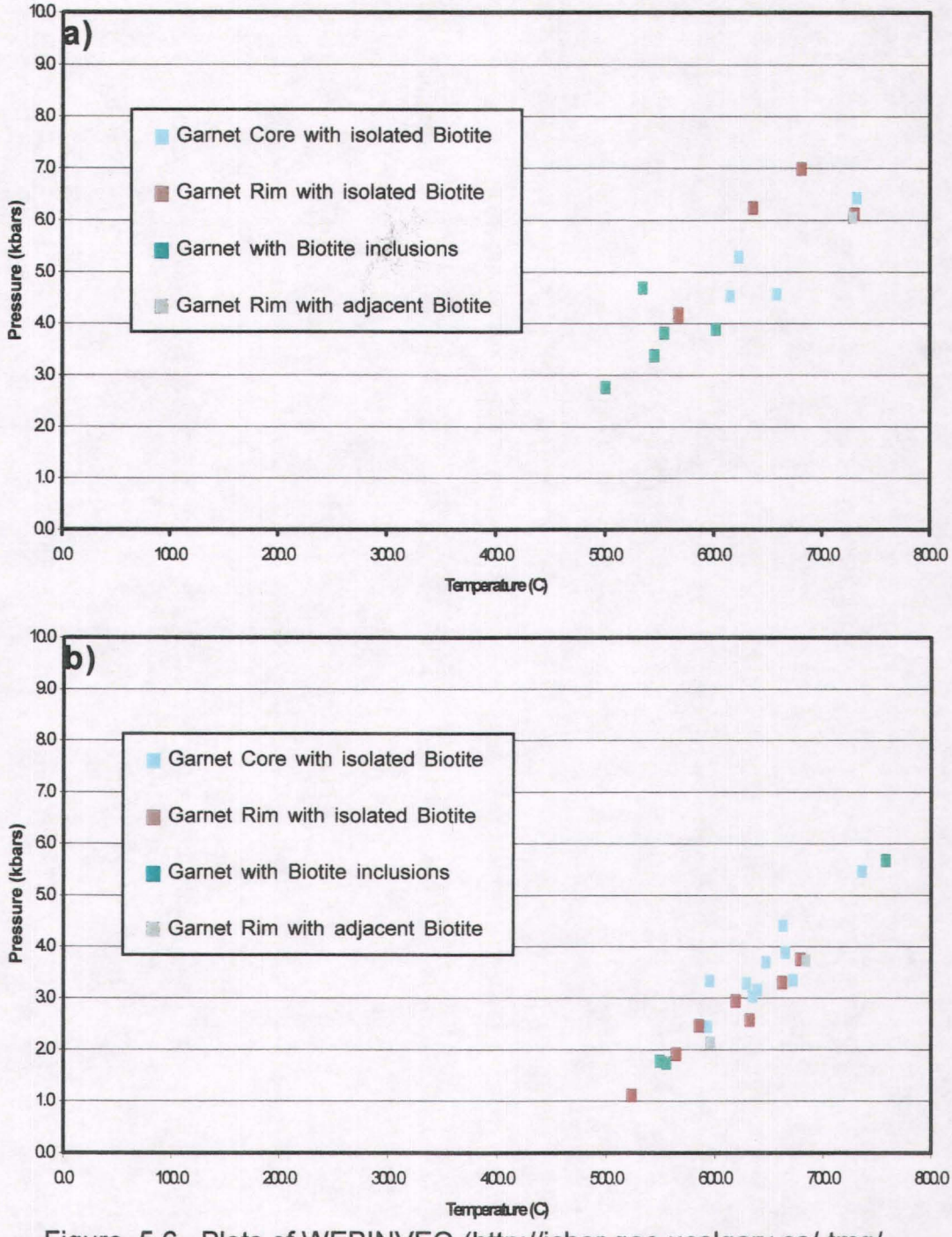

Figure 5.6. Plots of WEBINVEQ (http://ichor.geo.ucalgary.ca/-tmg/Webinveq) estimates. a) Estimates derived from minerals texturally identified as having developed during the first metamorphic episode. b) Estimates calculated from minerals believed to have grown during the second metamorphic episode.

sections. The peak temperature for M1 is estimated at 732 °C, derived once again from a garnet core and an isolated biotite from sample 0278b (Zone 4). This temperature corresponds with a pressure of 6.4 kbar, consistent with an estimated peak pressure from petrological inference of 6.5 kbar. Using analysis from garnet cores, isolated matrix biotites, and cores of plagioclase grains which exhibit early textural and chemical characteristics, are again best likely to give the most accurate P-T results. Zone 2 shows estimates at 5.3 kbar and 623 °C. Zone 3 mineral analysis yields pressures up to 4.6 kbar, and 658 °C.

5.2.1.3. Thermobarometry with Estimation of Equilibrium (TWEEQ; Berman, 1988,1991) for M1

Thermobarometric estimates based on Berman, (1988, 1991) and calculated using TWEEQ, show patterns consistent with the previous methods of thermobarometry, however the averaged values are variably lower (Table 5.1; Figure 5.7a and b). Peak conditions are derived from different analysis than the two previous methods. Estimation of peak conditions from analysis that gave peak P-T in the previous calculations for M1, here yield values of 4.5 kbar and 621 °C. The highest temperatures obtained are derived from garnet rim analysis, which may be slightly affected by the later metamorphism at 4.2 kbar and 644 °C. Garnet rim analysis also yields the highest pressures obtained at 5.9-6.0 kbar and 610-627 °C. These values do however correspond with relatively high pressures utilizing the WEBINVEQ method at 6.2-7.0 kbar and

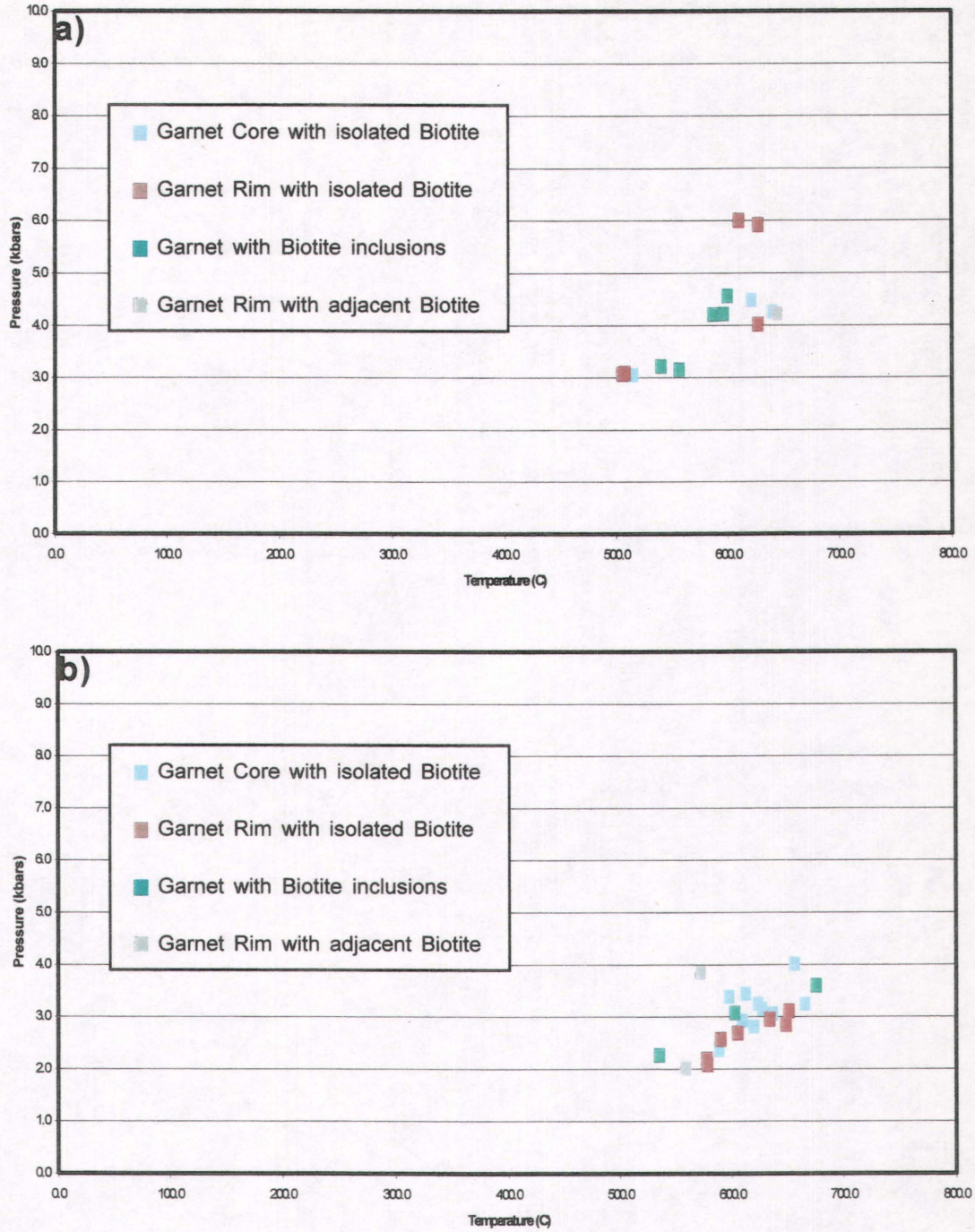

Figure 5.7. Plots of TWEEQ estimates using the Berman (1988, 1991) database. a) Estimates derived from minerals texturally identified as having developed during the first metamorphic episode. b) Estimates calculated from minerals believed to have grown during the second metamorphic episode.

636-681 °C. It is concluded however, that these values reflect a certain degree of disequilibrium and do not represent real conditions. Pressure values from garnet core analysis paired with matrix plagioclase believed to have developed early, do however show a general increase of 3.1 kbar to 4.5 kbar from zone 2 to 4.

5.2.2. The Second Metamorphic Episode (M2)

Results calculated for M2 reflect temperatures similar to M1, however the textural associations of the garnets used suggest a temporal gap from the garnets discussed above. All calculated estimates are based on zone 4 samples, since M2 is most easily recognized within that zone.

5.2.2.1. Ferry and Spear (1978) Geothermometry Results for M2

The highest estimate calculated with the Ferry and Spear (1978) method is derived from a garnet core and an adjacent biotite inclusion in sample 5000, at 741 °C (Table 5.1). This value likely reflects near peak temperature conditions for M2 (using the Ferry and Spear, 1978 method) since the growing garnet reacted and enclosed the biotite grain relatively early in the growth period of that garnet, effectively shutting off the biotite from exchange with outside minerals. It must also be noted that other garnets in sample 5000 show temperatures of 549-564 °C when analyzed with biotite inclusions. These

values reflect temperatures of the onset of garnet growth, which continued upwards 741 °C. Peak temperatures from a garnet core and a matrix isolated biotite from sample 5000, yield 732 °C, supporting the estimated higher peak temperature of M2. Temperature estimates based on garnet rims (Table 5.1) show that Fe-Mg exchange continued during the downward portion of the metamorphic loop until at least 520 °C.

5.2.2.2. Web Inverse Equilibrium Results (WEBINVEQ) (http://ichor.geo.ucalgary.ca/~tmg/Webinveq) for M2

WEBINVEQ estimates for M2 also mirror estimates from the Ferry and Spear (1978) method. Peak conditions are derived from a garnet core, biotite inclusion, and a matrix plagioclase in sample 5000; which yield a pressure of 5.7 kbar and 758 °C (Table 5.1; Figure 5.6b). Another estimate based on a garnet core, the same plagioclase, but an isolated matrix biotite yields a pressure of 5.5 kbar and 736 °C. The majority of pressures calculated however are less than 5 kbar and range mainly within 3.0 to 4.4 kbar.

5.2.2.3. Thermobarometry with Estimation of Equilibrium (TWEEQ; Berman, 1988, 1991) for M2

TWEEQ estimates obtained for M2 yield relatively low temperatures, variably consistent with the low M1 values calculated through this method. Peak

conditions calculated are based on garnet cores, isolated matrix biotites, and matrix plagioclase. Sample 5000 yields a peak pressure of 4.0 kbar at 657 °C. Estimates obtained from sample 5068 give a pressure of 3.2 kbar at 666 °C. The sample believed to give the most reasonable P-T estimate for the two previous methods however gives a low temperature of 603 °C at 3.1 kbar. All pressures obtained from TWEEQ for M2 range from 2.0 kbar to 4.0 kbar.

5.3. Summary

Two periods of metamorphism have been documented. The first metamorphic event began post D_1 and lasted through early D_2. Based on the presence of andalusite and staurolite, M1 within zone 1, was limited to approximately 3 kbar at just above 565 °C. Within zone 2, M1 conditions progressed through 610 °C and 4 kbar (Foster, 1999), but did not exceed 680 °C. This is evident by the absence of staurolite, the presence of garnet and sillimanite, and the absence of leucosome. Quantitative estimates of M1 in Zone 2 are best reflected by the Ferry and Spear (1978) thermometer and Gordon (1992) and Gordon *et al.*, (1994) WEBINVEQ (http://ichor.geo.ucalgary.ca/~tmg/Webinveq) thermobarometer at 594 °C to 623 °C and 5.3 kbar.

Zone 3 during M1 exceeded the maximum stability of muscovite and the minimum melting curve, evident by the absence of muscovite and the presence of S_2 concordant leucosome. The upper P-T conditions are constrained by the absence of orthopyroxene, indicating conditions did not surpass 6.5 kbar and

750 °C. Quantitative measurements (Table 5.2) show that zone 3 achieved at least 658 °C and 4.6 kbar, and possibly up to 6.2 kbar.

TABLE 5.2. Peak metamorphic conditions assigned to each Zone.

	M1		M2	
Zone	Pressure (kbar)	Temperature (°C)	Pressure (kbar)	Temperature (°C)
1	3.0[A]	< 565[A]	2.7[A]	600[A]
2	4.0[A]	680[A]	4.0[A]	680[A]
	5.3[B2]	594[B1]-623[B2]		
3	6.5[A]	730[A]	< 6.5[A]	730[A]
	4.6[B2]	658[B2]		
4	6.5[A]	730[A]	5.0[A]	750[A]
	6.4[B2]	717[B1]-732[B2]	5.5[B2]-5.7[B2]	732[B1]-758[B2]

A = maximum estimate based on mineralogical constraints
B1 = estimate based on geothermometry by Ferry and Spear (1978)
B2 = estimate based on geothermobarometry using WEBINVEQ

Zone 4 rocks underwent the highest metamorphic conditions, and again the peak P-T is limited by the absence of pyroxene. This suggests both zones 3 and 4 experienced similar metamorphic conditions during M1. Quantitative estimates show however that temperatures of 717-732 °C and pressures of 6.4 kbar were attained. These estimates show a 60-80 °C increase in temperatures from zone 3.

Decompression textures (see Figure 4.18) governed by reaction 5-18 demonstrate that decompression did indeed occur after peak M1 pressures were attained. Deformation of replacement minerals (see Figure 4.13)

demonstrates that thermal relaxation accompanied decompression before D_3. This period of relaxation was than followed by the second metamorphic event (M2).

The second metamorphism is expressed in zone 1 by the by the prograde replacement of staurolite by andalusite. The absence of garnet again limits the metamorphic conditions. Pressures likely went as high as 2.7 kbar with temperatures up to 600 °C.

Zone 2 experienced similar physical conditions during M2 as in M1. No distinction in mineralogical differences between metamorphic events is observed, and a maximum P-T of 4 kbar and 680 °C is assumed.

Within zone 3, M2 conditions also approach those estimated for M1. However, an important distinction is noted, with the absence of another melt generation. Maximum temperatures did not achieve that needed to produce melt. This may be the result of decreased water activity, effectively shifting the melting curve to the right. Garnet and cordierite are present however, overprinting the S_2 fabric indicating that conditions needed to push reaction 5-15 to the right were achieved. These observations suggest a lower pressure regime than M1 as maximum pressures up to 6.5 kbar would likely have resulted in melt generation (Figure 5.3).

The second metamorphic event is most pronounced within zone 4. Peak conditions are delineated by the absence of pyroxene and the presence of a cordierite bearing melt leucosome cross-cutting the S_2 foliation. Garnet and cordierite are also present texturally overprinting the fabric within the matrix of the metapelitic rocks. The presence of cordierite bearing melt indicates conditions likely did not exceed 5 kbar and 750°C (Clemens and Wall 1981; Grant, 1985). Quantitative estimates yield temperatures for M2 in zone 4 of 741-758 °C at 5.5 to 5.7 kbar (Table 5.2).

5.4. Discussion

Menard and Gordon (1997) and Kraus and Menard (1997) both documented the presence of two successive thermal events that varied in time and intensity. The first event was recognized to have reached a peak of 550 °C at 5.5 kbar, with garnet growth commencing at 500 °C and 4 kbar (Kraus and Menard, 1997). This event was recognized to have begun during the F_1 folding event, reaching a peak during F_2 folding. Cooling commenced prior to F_3 (Kraus and Menard, 1997). Within the Kisseynew rocks a thermal anomaly persisted post F_3 folding (Kraus and Menard, 1997; Menard and Gordon, 1997). The central Kisseynew Domain is believed to have been metamorphosed at uniform conditions of 750 °C ± 50 °C and 5-6 kbar.

The two metamorphic events recognized in this study area are supported by mineral-textural and quantitative pressure-temperature estimates that are relatively consistent with the findings of Kraus and Menard (1997) and Menard and Gordon (1997). However, the pressure estimates for M1 documented here show that in the study area M1 reached peak conditions of 6.4 kbar at 732 °C. This was followed by a period of decompression and thermal degradation, which was then proceeded by M2. Peak conditions during M2 reached up to 758 °C, but likely occurred under lower pressure than M1. Quantitative barometric estimates indicate maximum pressures up to 5.7 kbar.

CHAPTER 6:

METAMORPHIC TIMING and MECHANISM

6.0. Metamorphic Timing and Mechanism: Introduction

The first metamorphic cycle began pre-D_2, correlated with the introduction and collision of the Sask Craton (SC) with the Flin Flon-Glennie Complex (FFGC) at roughly 1835 Ma (Lucas *et al.*, 1999). The second metamorphic cycle occurred approximately 20-30 m. y. later, coeval with terminal closure of the Kisseynew Basin and collision with the Superior Craton. The latter metamorphic event is recorded in numerous metamorphic mineral ages between 1815-1800 Ma (Gordon, 1989; Ashton *et al.*, 1992; Heaman *et al.*, 1993; Heaman and Ashton, 1996; Ashton *et al.*, 1999). Reconciliation of the two thermal events with tectonic source is difficult and highly equivocal. Origin of high temperature (T)/low pressure (P) metamorphic regimes is hotly contested in the literature. The following interpretation pertaining to mechanism of thermal anomalies is primarily based on the proposed tectonic framework of the Trans-Hudson Orogen in Lucas *et al.*, (1997) and Lucas *et al.*, (1999).

6.1. Timing of the First Metamorphic Episode

The generally accepted age of the Kisseynew Burntwood Metaturbidites is approximately 1860-1840 Ma (Lucas *et al.*, 1997). Within the study area a granodioritic pluton intruded the Kisseynew metaturbidites at ~1848 Ma (Elliot, 1995a), indicating these sediments are at least that old. To the north in the Wintego Lake area, Ansdell and Stern (1997) determined the age of deposition to be 1844 Ma. Northwest of the study area, Slimmon (1994) obtained a minimum marine sedimentation age of 1837 Ma indicating that by this time the Kisseynew Basin had closed; consistent with collision of the Sask Craton and the Flin Flon-Glennie Complex at ~ 1835 Ma (Lucas *et al.*, 1997); and the Pelican Thrust (D_2). The first metamorphic cycle took place pre- to syn-D_2 (Chapter 3), with peak conditions occurring prior to the end of deformation.

Ashton *et al.*, (1999) suggest metamorphism began at about 1831 Ma (Hartlaub *et* al., 1997) based on a nearly concordant monazite grain from a quartzofeldspathic gneiss of the Archean (3.1-2.45 Ga) Jan Lake Complex. This mineral date is generally consistent with a secondary population of zircon grains within the 1848 Ma granodiorite in the study area, at 1833 Ma (Elliot, 1995a). However, these dates likely represent peak metamorphism, during M1 rather than metamorphic onset. The beginning of M1 is yet unclear, however the fact it began prior to D_2 suggests it began shortly after sedimentation ceased at 1837 Ma. This metamorphic episode is coeval with widespread plutonism

within the Kisseynew Domain and the FFGC from 1840-1830 Ma (Gordon *et al.*, 1990; McNicoll *et al.*, 1992; Ansdell and Norman, 1995), which may reflect the anomalous thermal conditions at the time. By ~1830 Ma, via the Pelican Thrust, rocks of the study area were thrust over the adjacent Flin Flon Domain, which lies stratigraphically over the Archean Sask Craton. Rocks from Zone 1 in the study area reached maximum pressures of about 2.7 kbars by 1830 Ma. Assuming the typical 3.3 km/kbar geobarometric gradient this correlates to a burial depth of approximately 9 km. Zone 2 was buried to a depth of approximately 13 km; and Zones 3 and 4 were buried to depths of up to 20 km. Metamorphic mineral growth ceased some time prior to the end of D_2, which based on a quartz-diorite dyke emplaced near the end of D_2 mylonitization within the Pelican Décollement Zone, ended shortly after 1826 Ma (Hartlaub *et al.*, 1997; Ashton *et al.*, 1999). The M1 metamorphic cycle likely lasted a maximum of 10 to 11 Ma from 1837-1826 Ma, with peak conditions occurring at about 1833-1830 Ma. Estimation of the timing of peak conditions is consistent with other investigations (Ansdell and Norman, 1995; Ansdell *et al.*, 1995; Heaman *et al.*, 1995; Norman *et al.*, 1995).

6.2. Timing of the Second Metamorphic Episode

The second metamorphic cycle began prior to D_3 and lasted through the main phase of deformation, reaching peak temperatures post- deformation. This is evident by the numerous melts oriented parallel the axial trace of F_3 folds; and

by the patch melts which show no preferential alignment. D_3 is correlated to collision of the Superior Craton with the SC and FFGC. Based on east-southeast vergent fold-thrusts in the Thompson Belt, collision with the Superior Craton is estimated at ~1820 Ma (Lucas *et al.*, 1997). The second metamorphic cycle likely began at this time, broadly coeval with F_3 fold development in the study area. Adjacent to the study area, D_3 created a domal structure resulting in the Pelican Window. Structures on the western side of the dome, including those in the study area are steeply overturned due to the D_3 north-south folding. Timing of peak temperatures are recorded in zircon and titanite ages taken throughout the region. Gordon *et al.*, (1990) suggested that peak metamorphism in the core of the Kisseynew occurred at ~1815 Ma. This date is consistent with 1815 Ma zircon metamorphic in the Sahli Granite of the Pelican Window (Ashton *et al.*, 1999). Ashton *et al.*, (1992) and Heaman *et al.*, (1992) record peak metamorphic ages of 1805 and 1807 Ma based on zircon from migmatitic rocks within the adjacent Attitti Complex rocks of the Flin Flon Domain.

Following peak conditions, rapid uplift and cooling had by 1804 Ma, lowered temperatures to about 550-600 °C (Ashton *et al.*, 1992). Continued retrogression through uplift and erosion brought the present erosional surface to 250 °C by 1700 Ma (Gordon, 1989).

6.3. Source of Metamorphism and Tectonic Environment

Origin of high temperature/low pressure metamorphism within metamorphic belts is somewhat enigmatic, with diverse model sets hotly contested in the literature. The metamorphic cycles must be explained within the context of primarily compressional tectonism. Both metamorphic cycles are similar to the andalusite-sillimanite facies series of Miyashiro (1961, 1973, 1994). Geothermal gradients fall between 40-60 °C/km, similar to Buchan type metamorphism. The high geothermal gradient indicates that along with compressional tectonism and crustal thickening additional heat was supplied to the region. Three possible mechanisms capable of producing a deep seated heat source that may have caused the ensuing regional metamorphisms include: 1) Thickening of the crust with simultaneous thinning of the lithosphere (Loosveld, 1989; Loosveld and Etheridge, 1990); 2) convective removal of the base of the lithosphere (Platt and England, 1993); and 3) delamination of the lithosphere (Bird, 1979; Bird and Baumgardner, 1981;Sacks and Secor, 1990; Kay and Kay, 1993). All three mechanisms lead to addition of heat through intrusion/ and or accretion of asthenospheric mantle beneath the crust.

6.3.1. Tectonic Environment During M1

Earlier it was stated that M1 is broadly coeval with 1840-1830 Ma plutonism (Gordon, 1989; Gordon *et al.*, 1990; Ansdell *et* al., 1995; Hartlaub *et al.*, 1997; Ashton *et al.*, 1999). These include abundant granodioritic-tonalitic to enderbitic

bodies, along with rare mafic dykes (Gordon, 1989; Gordon *et al.*, 1990; Hartlaub *et al.*, 1997; Ashton *et al.*, 1999). Wickam and Oxburgh (1985, 1987) suggest that high T/low P regimes may represent areas of rift zones in which mafic intrusions emplaced in the lower crust caused high thermal anomalies producing crustal melt. The mafic dykes and enderbitic plutons may be indicative of mantle derived magmatism. Ansdell and Norman (1995), Ansdell *et al.*, (1995) and Norman *et al.*, (1995) suggested that the magmatism is the result of arc development associated with southward subduction of Kisseynew Basin oceanic/back arc crust beneath the FFGC (Figure 6.1a and b). M1 was then attributed to advective heat transfer from plutonism. Since metamorphism began prior to the onset of deformation, temperatures within the sedimentary pile must have been elevated prior to D_2. Typically, back arc basins are sites of high heat flow (Powell, 1983). Sediments above extended oceanic crust experience heat transfer due to convective heat flux. Powell (1983) suggested that this heat flow anomaly would persist for some time, continuing during the early stages of deformation. Advective heat transfer from plutonism after back arc extension during compressional thrust stacking by the Pelican Thrust likely raised temperatures during burial to those documented. Continued south-southwesterly tectonic transport of the FFGC over the SC, with a subduction polarity reversal of the Kisseynew Basin crust, may explain the gradational/and or structural contact between the Kisseynew Metasedimentary rocks and the FFGC in the Southern Flank of the Kisseynew Domain (Lucas *et al.*, 1999), by creating an accretionary wedge of sediments that thrust onto underlying FFGC

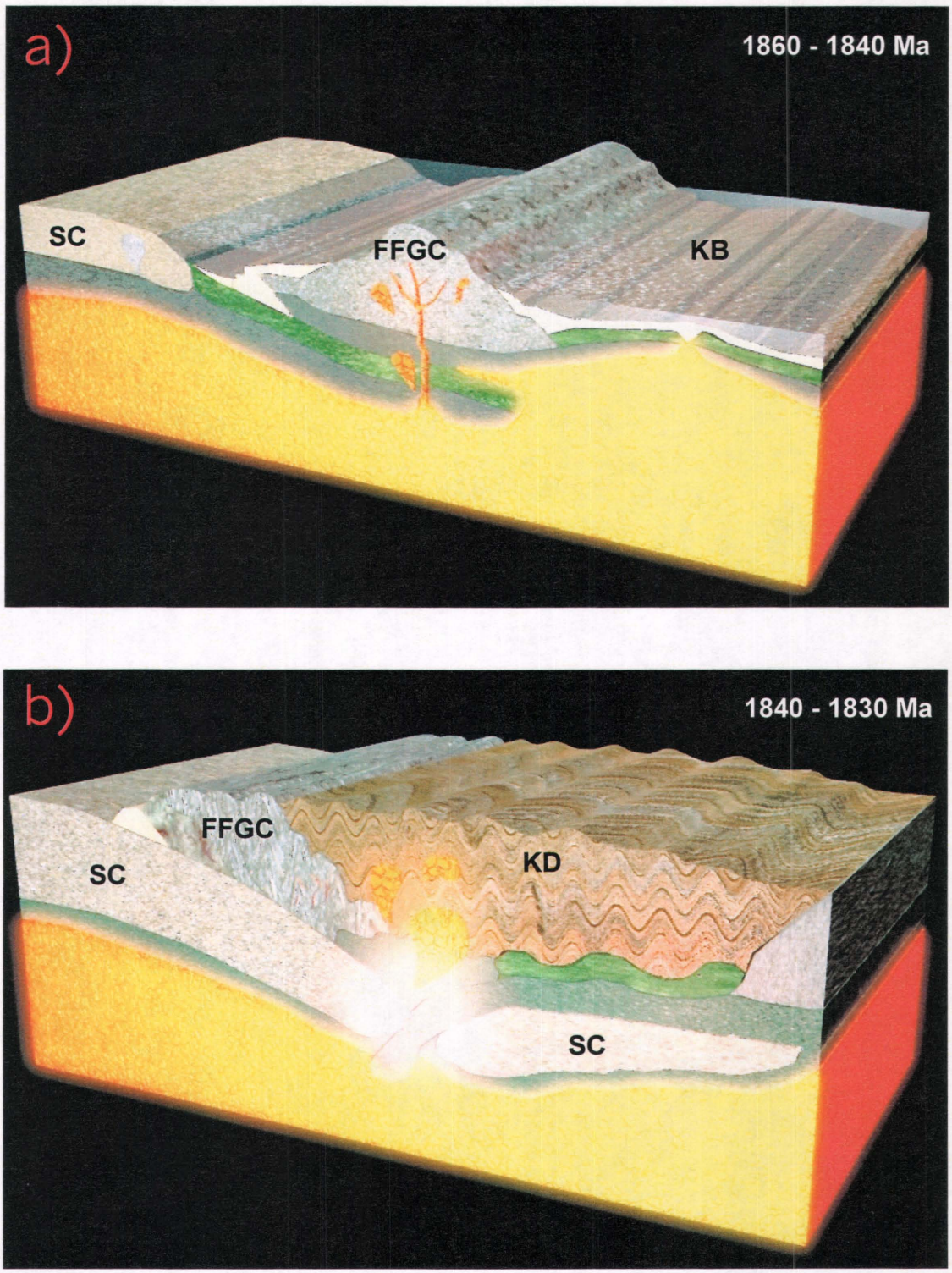

Figure 6.1. Diagrams illustrating the proposed mechanism for the first metamorphic event. a) Subhorizontal subduction of the Sask Craton oceanic lithosphere beneath the Flin Flon Glennie Complex (1860 Ma - 1840 Ma). b) Collision of the Sask Craton with the Flin Flon Glennie Complex and a subduction polarity reversal with southwards subduction of Kisseynew oceanic crust. This is accompanied by heating near the Sask Craton detachment, and plutonism (1840 Ma - 1830 Ma). SC = Sask Craton; FFGC = Flin Flon Glennie Complex; KB = Kisseynew Basin; KD = Kisseynew Domain

rocks. If this occurred around ~1835-1830 Ma then the uplift of the sediments explains the thermal and barometric relaxation of M1 post 1830Ma.

6.3.2. Tectonic Environment During M2

Determining the source of heat to explain M2 is problematic. Evidence of plutonism during the proposed time period of 1815-1805 Ma is for the most part lacking. Gordon (1989) and Gordon *et al.*, (1990) report monazite ages from ~1815 Ma granitic rocks in the Central Kisseynew Domain, of 1806±2 Ma and 1804±2 Ma which record cooling through 725±25 °C (Parrish, 1990) and near peak conditions (Kraus and Menard, 1997). Ansdell and Norman (1995) document near peak pegmatites with crystallization ages of 1801±3 Ma to 1799±3 Ma indicating melting conditions compatable with syn- to post-D_3 melt development in the study area. Kraus and Menard (1997) suggest that ~1815-1805 Ma metamorphism is consistent with conductive/advective heat transfer from the emplacement of multiple staged sheet-like bodies in the crust. They proposed that such a thermal anomaly as described originated through crustal thickening and lithospheric thining by convection. Ansdell *et al.*, (1995) contested that localization of M2 within the Kisseynew precludes a model involving convective removal of the lithosphere, and proposed that M2 was the result of advective heat transfer via 1840-1830 Ma magmatism coupled with a remnant thermal anomaly related to basin extension. This theory may represent a plausible explanation, however the advective transfer of heat is relatively short

lasting and is unlikely to cause a thermal increase in overlying rock 30 Ma post magmatism. As well, it has been documented (Chapter 3 and 4) that following M1 there was a period of metamorphic retrogression. This would be unlikely if fluids from the 1840-1830 Ma magmatism were transferring heat through the crust.

Another model which may explain a heat source for M2, involves slab detachment and delamination of the detached slab. The influx of hot asthenosphere would produce a thermal budget capable of remelting the Kisseynew rocks relatively dry from the previous metamorphism. Sub-horizontal subduction of the SC beneath the FFGC (Figure 6.1a), followed by a subduction polarity reversal and subduction of Kisseynew basement, was likely accompanied by the detachment of the distal portion of the Sask Craton through extension and necking (Sacks and Secor, 1990) of the subducting slab at the Kisseynew join (Figure 6.1b). Localization of M2 resulted from subsequent delamination of the detached SC slab and asthenospheric influx as the slab foundered (Figure 6.2). After slab detachment, foundering may take up to 30 Ma (Bird, 1979), possibly explaining the 30 Ma separation between Kisseynew subduction (~1835 Ma) and metamorphism (~1805 Ma). The absence of mantle derived magmas in the Kisseynew may be attributed to their difficulty in penetrating oceanic lithosphere (McNutt and Fisher, 1987).

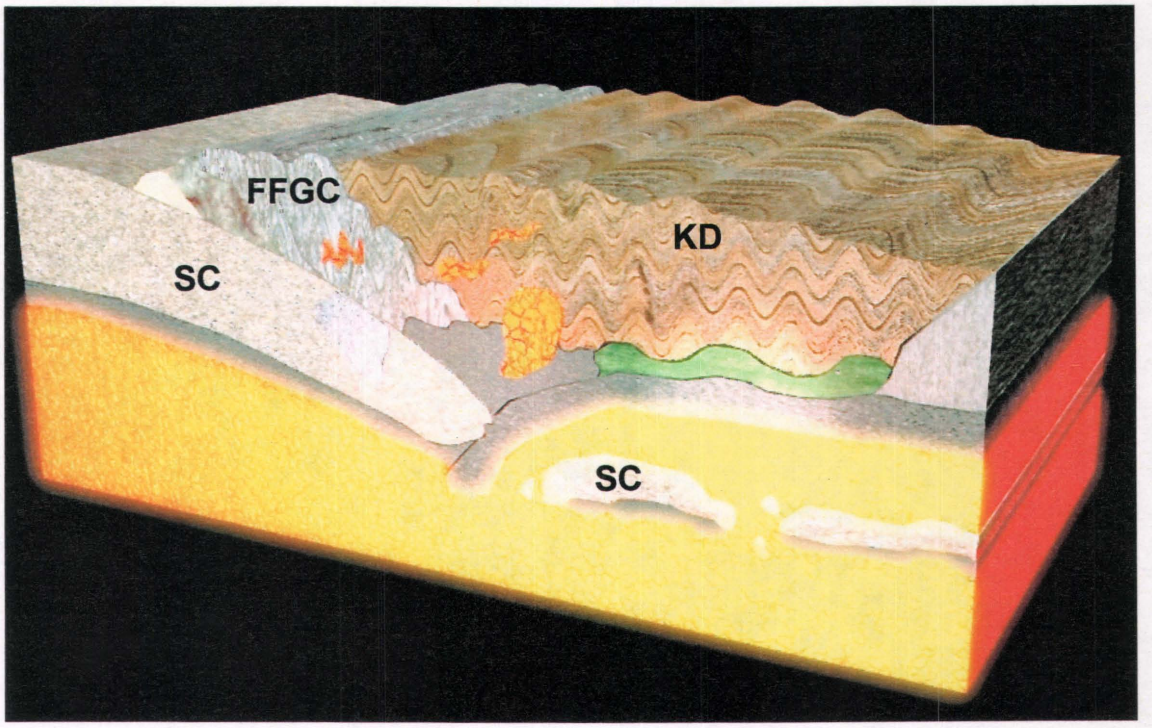

Figure 6.2. A diagram illustrating the foundering of the detached Sask Craton slab and the influx of hot asthenoshere. This results in the heating of the overlying crust causing the second metamorphic event. KD = Kisseynew Domain; SC = Sask Craton; FFGC = Flin Flon Glennie Complex

CHAPTER 7:

SUMMARY-CONCLUSIONS

7.0. Summary -Conclusions

The Reindeer Zone within the Trans-Hudson Orogen is a 400 km wide collage of Paleoproterozoic (1.92-1.83 Ga) oceanic arc and volcanic rocks, plutons, and associated molasse and basin sediments.

The Kisseynew Domain, in which the study area is situated, is comprised of mainly 1.86-1.84 Ga marine metaturbidite rocks, and represents the uppermost stratigraphic level in the Reindeer Zone. By 1837 Ma (Slimmon, 1994) marine sedimentation had ceased, indicating that uplift had begun. This is coeval with a regional period of 1840-1830 Ma plutonism, as well as collision between the Flin Flon Glennie Complex (FFGC) and the Sask Craton (SC) at ~1835 Ma. South-southwest movement along the Pelican Thrust involved overthrusting of the Paleoproterozoic rocks over the underlying Archean SC, and gave rise to the highly mylonitized Pelican Décollement Zone. This major collisional event was long lasting (1837-1825 Ma) and is believed to represent the D_2 structural characteristics within the study area. D_2 Isoclinal folding resulted in transposing an early mineral alignment (S_1), parallel the axial plane of the F_2 folds. The

position of the S_2 fabric is the most pervasive foliation throughout the area. Fabric development and collisional tectonics were accompanied by the first metamorphic event (M1), which began pre-D_2 but waned before the end of deformation at ~1825 Ma. Growth of andalusite and staurolite is documented in the lower grade area (Zone 1), along with sllimanite, garnet, cordierite, K-feldspar, and melt development in the higher grade zones (Zones 2,3,4). Chemically, the garnet and biotite interpreted to have grown during M1 yield compositions relatively higher in Mg, than the later generations. Peak metamorphism is deduced to have occurred prior to 1830 Ma and reached conditions of 720-730 °C at pressures less than 6.5 kbars. Timing is recorded in numerous 1833-1830 Ma zircon ages. This includes an 1833 Ma zircon population in the 1848 Ma granodiorite intrusive (Elliot, 1995a). A period of retrogression followed, prior to the end of D_2, evident by the D_2 deformation of replacement minerals.

M1 metamorphism is attributed to a remnant thermal anomaly associated with back arc basin crust, along with magmatism above southwards subducting Kisseynew oceanic/back arc crust, which resulted from collision of the Sask Craton and the Flin Flon-Glennie Complex.

A second metamorphic event (M2) was recognized, broadly coeval with a third deformational event (D_3). D_3 is correlated to deformation resulting from collision with the Superior Craton, beginning ~1820-1810 Ma. This deformational event

resulted in producing tight to open folds, a crenulation of the S_2 fabric and "type III" fold interference patterns in the study area. Kinematic indicators such as pinch and swell structures, asymmetric pull-aparts, and rotated tension gashes/ boudin necks indicate that D_3 had a dextral component of movement. Metamorphism resulted in growth of andalusite in Zone 1, and garnet, cordierite, sillimanite, and K-feldspar in Zones 2,3, and 4. A second generation of melt also developed; evident cross-cutting the S_2 fabric, but is present only within Zone 4. M2 mineral growth texturally overprints the S_2 fabric, and is observed oriented parallel to the axial plane of F_3 folds. Mineral chemistry of M2 minerals shows that the Fe-Mg minerals have a higher proportion of Fe to Mg than the M1 minerals. This is indicative of different metamorphic conditions during growth. Peak temperatures exceeded that of M1, upwards 741-758 °C with pressures less than 6 kbars. The presence of well formed cordierite within the second generation melt indicates that pressures likely did not exceed 5 kbars (Clemens and Wall, 1981). Peak conditions were achieved by 1805 Ma, and were followed by rapid uplift and cooling.

Source of the second metamorphic event is somewhat enigmatic, however it is believed that during the onset of Kisseynew oceanic/back arc crust subduction at ~1835 Ma, a portion of the Sask Craton detached beneath the Kisseynew Basin. Subsequent foundering of this detached slab would have allowed influx of hot asthenosphere beneath the Kisseynew, inturn creating a thermal anomaly and metamorphism.

REFERENCES

Ansdell, K. M., and Connors, K. A., 1995, Collisional processes in the eastern Trans-Hudson Orogen, Wekusko Lake, Manitoba: Geological Association of Canada; Mineralogical Association of Canada; annual meeting; program with abstracts--Association Geologique du Canada; Association Mineralogique du Canada; reunion annuelle; programme et resumes., v. 20, p. 3.

Ansdell, K. M., and Kyser, T. K., 1991, Plutonism, deformation and metamorphism in the Proterozoic Flin Flon greenstone belt, Canada: limits on timing provided by the single-zircon Pb-evaporation technique: Geology, v. 19, p. 518-521.

Ansdell, K. M., Lucas, S. B., Connors, K., and Stern, R. A., 1995a, Kisseynew metasedimentary gneiss belt, Trans-Hudson Orogen (Canada); back-arc origin and collisional inversion: Geology (Boulder), v. 23, p. 1039-1043.

Ansdell, K. M., Lucas, S. B., Connors, K. A., and Stern, R. A., 1995b, Kisseynew gneisses, Trans-Hudson Orogen; development and closure of a heavily sedimented back-arc basin: Geological Association of Canada; Mineralogical Association of Canada; annual meeting; program with abstracts--Association Geologique du Canada; Association Mineralogique du Canada; reunion annuelle; programme et resumes., v. 20, p. 3.

Ansdell, K. M., and Norman, A. R., 1995, U-Pb geochronology and tectonic development of the southern flank of the Kisseynew Domain, Trans-Hudson Orogen, Canada: Precambrian Research, v. 72, p. 147-167.

Ashton, K. E., 1999, A proposed lithotectonic domainal classification of the Southeastern Reindeer Zone in Saskatchewan: Summary of Investigations; Saskatchewan Geological Survey, v. 1, p. 92-100.

Ashton, K. E., and Balzer, S. S., 1995, Wildnest-Tabbernor transect: Pelican Lake Tabbernor Fault area (Part of 63M-3): Summary of Investigations, Saskatchewan Geological Survey, v. 95-4, p. 13-22.

Ashton, K. E., Drake, A. J., and Lewry, J. F., 1993, The Wildnest-Tabbernor transect; Attitti-Mirond lakes area (parts of NTS 63M-1 and -2): Summary of investigations 1993; Saskatchewan Geological Survey., p. 50-66.

Ashton, K. E., Hartlaub, R. P., and Lewry, J. F., 1997, The case for a Flin Flon-Glennie protocontinent: Lithoprobe; Sixth Trans-Hudson Orogen Transect workshop., p. 1-5.

Ashton, K. E., Heaman, L. m., Lewry, J. F., and Hartlaub, R. P., 1999, Age and origin of the Jan Lake Complex: a glimpse at the buried Archean craton of the Trans-Hudson Orogen: Canadian Journal of Earth Sciences, v. 36, p. 185-208.

Ashton, K. E., Hunt, P. A., and Froese, E., 1992, Age constraints on the evolution of the Flin Flon volcanic belt and Kisseynew gneiss belt, Saskatchewan and Manitoba: Radiogenic age and isotopic studies; Report 5., p. 55-69.

Ashton, K. E., and Leclair, A. D., 1991, Revision bedrock geological mapping, Wildnest-Attitti lakes area (Parts of NTS 63M-1 and -2): Summary of investigations 1991, Saskatchewan Geological Survey, p. 29-40.

Ashton, K. E., and Lewry, J. F., 1994, Vergence of the "Pelican Slide" and Sturgeon-wier Shear Zone: Lithoprobe Trans-Hudson Orogen Transect Workshop, v. 38, p. 12-17.

Ashton, K. E., and Shi, R., 1994, Wildnest-Tabbernor transect: Mirond-Pelican Lakes area (Parts of NTS 63M-2 and -3): Summary of Investigations, Saskatchewan Geological Survey, v. 94-7, p. 27-37.

Ashton, K. E., Wilcox, K. H., Wheatley, K. J., Paul, D., and Tombe, J., 1987, The boundary zone between the Flin Flon Domain, Kisseynew Gneisses and Hanson Lake Block, northern Saskatchewan: Summary of investigations 1987; Saskatchewan Geological Survey, p. 131-135.

Ashton, K. E. and Wheatley, K. J., 1986, Preliminary report on the Kisseynew gneisses in the Kisseynew-Wildnest Lakes area, Saskatchewan.: Current research, part B. Geological Survey Canada, Paper 86-1B, p. 305-317.

Bailes, A. H., and McRitchie, W. D., 1978, The transition from low to high grade metamorphism in the Kisseynew sedimentary gneiss belt, Manitoba, *in* Fraser, J. A., and Heywood, W. W., eds., Metamorphism in the Canadian Shield.: Geological Survey Canada, Paper 78-10,p. 155-178.

Balzer, S. S., and Pan, Y., 1997, Geochemistry of the Kisseynew Domain near Sandy Narrows, Saskatchewan: Summary of Investigations, Saskatchewan Geological Survey, v. 97-4, p. 150-161.

Barker, A. J., 1990, Introduction to Metamorphic Textures and Microstructures: Glasgow, Blackie, 162 p.

Bell, T. H., 1985, Deformation partitioning and porphyroblast rotation in metamorphic rocks; a radical reinterpretation: Journal of Metamorphic Geology, v. 3, p. 109-118.

Bell, T. H., and Rubenach, M. J., 1983, Sequential porphyroblast growth and crenulation cleavage development during progressive deformation, *in* Etheridge, M. A., and Cox, S. F., eds., Deformation processes in tectonics.: Tectonophysics, Amsterdam, Netherlands, Elsevier, p. 171-194.

Berman, R. G., 1988, Internally-consistent thermodynamic data for minerals in the system Na (sub 2) O-K (sub 2) O-CaO-MgO-FeO-Fe (sub 2) O (sub 3) -Al (sub 2) O (sub 3) -SiO (sub 2) -TiO (sub 2) -H (sub 2) O-CO (sub 2): Journal of Petrology, v. 29, p. 445-522.

Berman, R. G., 1991, Thermobarometry using multi-equilibrium calculations: A new technique, with petrological applications: Canadian Mineralogist, v. 29, p. 833-855.

Bhatia, M. R., 1985, Rare earth element geochemistry of Australian Paleozoic graywackes and mudrocks; Provenance and tectonic control: Sedimentary Geology, v. 45, p. 97-113.

Bhatia, M. R., and Crook, K. A. W., 1986, Trace element characteristics of graywackes and tectonic setting discrimination of sedimentary basins: Contributions to Mineralogy and Petrology, v. 92, p. 181-193.

Bickford, M. E., Collerson, K. D., Lewry, J. F., Van, S. W. R., and Chiarenzelli, J. R., 1990, Proterozoic collisional tectonism in the Trans-Hudson Orogen, Saskatchewan: Geology (Boulder), v. 18, p. 14-18.

Bickford, M. E., Van Schumas, W. R., Collerson, K. D., and Macdonald, R., 1987, U-Pb zircon geochronology project: new results and interpretations: Summary of Investigations, Saskatchewan Geological Survey, v. 87-4, p. 76-79.

Bird, P., 1979, Continental delamination and the Colorado Plateau: Journal of Geophysical Research, v. 84, p. 7561-7571.

Bird, P., and Baumgardner, J., 1979, Finite-element models of continental delamination: Eos, Transactions, American Geophysical Union, v. 60, p. 939.

Bleeker, W., 1996, The Thompson Nickel Belt and its nickel deposits: A review: Annual GAC-MAC Meeting, p. A9.

Bucher, K., and Frey, M., 1994, Petrogenesis of Metamorphic Rocks, Spinger-Verlag, 318 p.

Chappell, B. W., and White, A. J. R., 1974, Two contrasting granite types: Pacific Geology, v. 8, p. 173-174.

Clemmens, J. D., and Wall, V. J., 1981, Origin and crystallization of some peraluminous (S-type) granitic magmas: Canadian Mineralogist, v. 19, p. 111-131.

Delaney, G. D., 1987, Bedrock geological mapping, Carruthers-Uskik Lakes area (part of NTS 63M-11 and -12): Summary of Investigations, Saskatchewan Geological Survey, p. 8-17.

Dickerson, R. P., and Holdaway, M. J., 1989, Acadian metamorphism associated with the Lexington Batholith, Bingham, Maine: American Journal of Science, v. 289, p. 945-974.

Digel, S., Ashton, K. E., and Wilcox, K. H., 1991, Metamorphic P-T investigations in the southern part of Kisseynew and western part of Flin Flon Domains: Summary of Investigations, Saskatchewan Geological Survey, v. 91-4, p. 41-46.

Elliot, C. G., 1993, Structural study of the Tabbernor Fault, Nielson Lake Area: Summary of Investigations, Saskatchewan Geological Survey, v. 93-4, p. 139-141.

Elliot, C. G., 1994, Structural relationships across the Tabbernor Fault, Nielson Lake area, Trans-Hudson Orogen, Saskatchewan: Current Research, v. 1994-C, p. 113-120.

Elliot, C. G., 1995a, Bedrock geology of selected. areas along the Tabbernor Fault zone (parts of NTS 63L-14, 63M-3, -6, and -11)1: 20,000 scale prelim. map: Summary of Investigations, Saskatchewan Geological Survey, v. 95-4.

Elliot, C. G., 1995b, The Tabbernor Fault and its Proterozoic and Phanerozoic movement in Saskatchewan and Manitoba: Lithoprobe: Trans-Hudson Orogen Transect, v. 48, p. 148-154.

England, P. C., and Richardson, S. W., 1977, The influence of erosion upon the mineral facies of rocks from different metamorphic environments: Journal of the Geological Society of London, v. 134, p. 201-213.

Evans, B. W., 1965, Application of a reaction-rate method to the breakdown equilibria of muscovite and muscovite plus quartz: American Journal of Science, v. 363, p. 647-677.

Fedorowich, J. S., Kerrich, R., and Stauffer, M. R., 1993, Timing of shear zones and regional metamorphism in the central Flin Flon Domain, *in* Macdonald, R., Sibbald, T. I. I., Harper, C. T., Paterson, D. F., and Guliov, P., eds., Summary of investigations 1993; Saskatchewan Geological Survey.: Miscellaneous Report - Saskatchewan Mineral Resources, Regina, SK, Canada, Saskatchewan Mineral Resources, p. 142-152.

Ferry, J. M., and Spear, F. S., 1978, Experimental calibration of the partitioning of Fe and Mg between biotite and garnet: Contributions to Mineralogy and Petrology, v. 66, p. 113-117.

Foster, C. T., 1999, Forward modeling of metamorphic textures: Canadian Mineralogist, v. 37, p. 415-429.

Froese, E., and Gasparrini, E., 1975, Metamorphic zones in the Snow Lake Area, Manitoba. Canadian Mineralogist, v. 13, p. 162-167.

Ganguly, J., and Saxena, S. K., 1984, Mixing properties of aluminosilicate garnets; constraints from natural and experimental data, and applications to geothermo-barometry: American Mineralogist, v. 69, p. 88-97.

Gordon, T. M., 1981, Metamorphism in the Crowduck Bay area, Manitoba: Current Research, part A. Geological Survey Canada, Paper 81-1A, p. 315-316.

Gordon, T. M., 1984, Metamorphic processes in the Kisseynew sedimentary belt. 1. Initial stages of migmatite formation in the Nobel Lake area, Manitoba: Current Research, part A. Geological Survey Canada, Paper 84-1A, p. 307-312.

Gordon, T. M., 1989, Thermal evolution of the Kisseynew sedimentary gneiss belt, Manitoba; metamorphism at an early Proterozoic accretionary margin, *in* Daly, J. S., Cliff, R. A., and Yardley, B. W. D., eds., Evolution of metamorphic belts; proceedings of the 1987 joint meeting of the Metamorphic Studies Group and IGCP project 235.: Geological Society Special Publications, London, United Kingdom, Geological Society of London, p. 233-243.

Gordon, T. M., 1992, Generalized thermobarometry; Solution of the inverse chemical equilibrium problem using data for individual species: Geochimica et Cosmochimica Acta, v. 56, p. 1793-1800.

Gordon, T. M., Aranovich, L. Y., and Fed'kin, V. V., 1994, Exploratory data analysis in thermobarometry: an example from the Kisseynew sedimentary gneiss belt, Manitoba, Canada: American Mineralogist, v. 79, p. 973-982.

Gordon, T. M., and Gall, Q., 1982, Metamorphism in the Crowduck Bay area, Manitoba: Current Research, part A. Geological Survey Canada, Paper 82-1A, p. 197-201.

Gordon, T. M., Hunt, P. A., Bailes, A. H., and Syme, E. C., 1990, U-Pb ages from the Flin Flon and Kisseynew belts, Manitoba; chronology of crust formation at an early Proterozoic accretionary margin, *in* Lewry, J. F., and Stauffer, M. R., eds., The early Proterozoic Trans-Hudson Orogen of North America.: Special Paper - Geological Association of Canada, Toronto, ON, Canada, Geological Association of Canada, p. 177-199.

Grant, J. A., 1985, Phase equilibria in partial melting of pelitic rocks, *in* Ashworth, J. R., ed., Migmatites, Glasgow, Blackie, p. 86-145.

Grauch, R. I., 1989, Rare earth elements in metamorphic rocks, Geochemistry and Mineralogy of Rare Earth Elements, p. 147-167.

Grove, T. L., Baker, M. B., and Kinzler, R. J., 1984, Coupled CaAl-NaSi diffusion in plagioclase feldspar; experiments and applications to cooling rate speedometry: Geochimica et Cosmochimica Acta, v. 48, p. 2113-2121.

Guidotti, C. V., 1984, Micas in metamorphic rocks, MSA Reviews in Mineralogy, p. 357-468.

Harris, N. B. W., Pearce, J. A., and Tindle, A. G., 1986, Geochemical characteristics of collision-zone magmatism, *in* Coward, M. P., and Ries, A. C., eds., Collision tectonics.: Geological Society Special Publications, London, United Kingdom, Geological Society of London, p. 67-81.

Hartlaub, R. P., Heaman, L. M., Ashton, K. E., and Lewry, J. F., 1997, Preliminary U-Pb geochronological results from the Pelican Narrows area: Lithoprobe; Sixth Trans-Hudson Orogen Transect workshop., p. 191-196.

Hatcher, R. D., 1995, Structural geology principles, concepts, and problems: Englewood Cliffs, New Jersey, Prentice Hall, 525 p.

Heaman, L. M., and Ashton, K. E., 1996, Preliminary U-Pb results from the Attitti Lake and Pelican Lake areas: Summary of Investigations, Saskatchewan Geological Survey, p. 109-110.

Heaman, L. M., Ashton, K. E., and Lewry, J. F., 1995, U-Pb geochronology of the Pelican Window: preliminary results, *in* Hajnal, Z., and Lewry, J., eds., Lithoprobe: Trans-Hudson Transect, University of Saskatchewan, p. 143-147.

Heaman, L. M., Ashton, K. E., Reilly, B. A., Sibbald, T. I. I., Slimmon, W. L., and Thomas, D. J., 1993, 1992-93 U-Pb geochronological investigations in the Trans-Hudson Orogen, Saskatchewan: Summary of investigations 1993; Saskatchewan Geological Survey., p. 109-111.

Heaman, L. M., and Corkey, T., 1996, U-Pb Geochronology of Split Lake Block, Manitoba: Prelimanary Results: Lithoprobe Report, v. 55, p. 60-68.

Heaman, L. M., Kamo, S. L., Ashton, K. E., Reilly, B. A., Slimmon, W. L., and Thomas, D. J., 1992, U-Pb geochronological investigations in the Trans-Hudson Orogen, Saskatchewan: Summary of Investigations; Saskatchewan Geological Survey, p. 120-123.

Heaman, L. M., Kamo, S. L., Delaney, G. D., Harper, C. T., Reilly, B. A., Slimmon, W. L., and Thomas, D. J., 1991, U-Pb geochronological investigations in the Trans-Hudson Orogen, Saskatchewan: preliminary results by the ROM Laboratory in 1990-91: Summary of Investigations; Saskatchewan Geological Survey, p. 81-85.

Heaman, L. M., and LeCheminant, A. N., 1993, Paragenesis and U-Pb systematics of baddleyite (ZrO2): Chemical Geology, v. 110, p. 95-126.

Hoffman, P. E., 1989, Precambrian geology and tectonic history of North America, *in* Bally, A. W., and Palmer, A. R., eds., The geology of North America: an overview: DNAG, Geol. Soc.Am., Bounder, p. 447-512.

Holdaway, M. J., 1971, Stability of andalusite and the aluminum silicate phase diagram: American Journal of Science, v. 271, p. 97-131.

Holdaway, M. J., and Lee, S. M., 1977, Fe-Mg cordierite stability in high-grade pelitic rocks based on experimental, theoretical, and natural observations: Contributions to Mineralogy and Petrology, v. 63, p. 175-198.

Jackson, S. L., and Gordon, T. M., 1986, Metamorphic studies in the transition zone between the Lynn Lake Greenstone belt and Kisseynew gneiss

belt, Laurie Lake, Manitoba: Current research, part B. Geological Survey Canada, Paper 86-1B, p. 539-546.

Jenner, G. A., Longerich, H. P., Jackson, S. E., and Fryer, B. J., 1990, ICP-MS-a powerful tool for high precision trace element analysis in earth sciences: evidence from analysis of selected U.S.G.S. reference samples: Chemical Geology, v. 83, p. 133-148.

Johannes, W., and Holtz, F., 1990, Formation and composition of H2O-undersaturated granitic melts, *in* Ashworth, J. R., and Brown, M., eds., High-Temperature Metamorphism and Crustal Anatexis, London, Unwin Hyman, p. 87-104.

Kay, R. W., and Kay, S. M., 1993, Delamination and delamination magmatism: Tectonophysics, v. 219, p. 177-189.

Kirkland, S. J. T., 1976, The geology of the Manawan Lake area (south half); Saskatchewan: Saskatchewan Department of Mineral Resources, v. Report 175, 24 p.

Koziol, A. M., 1989, Recalibration of the garnet-plagioclase-Al2SiO5-quartz (GASP) geobarometer and application to natural parageneses: EOS Trans American Geophysical Union, v. 70, p. 493.

Koziol, A. M., and Newton, R. C., 1988, Redetermination of the anorthite breakdown reaction and improvement of the plagioclase-garnet-Al2SiO5-quartz geobarometer: American Mineralogist, v. 73, p. 216-223.

Kraus, J., and Menard, T., 1997, A thermal gradient at constant pressure: Implications for low- to medium-pressure metamorphism in a compressional tectonic setting, Flin Flon and Kisseynew Domains, Trans-Hudson Orogen, Central Canada: Canadian Mineralogist, v. 35, p. 1117-1136.

Kretz, R., 1983, Symbols for rock forming minerals: American Mineralogist, v. 68, p. 277-279.

Le Breton, N., and Thompson, A. B., 1988, Fluid absent (dehydration) melting of biotite in metapelites in the early stages of crustal anatexis: Contributions to Mineralogy and Petrology, v. 99, p. 226-237.

Lewry, J. F., 1981, Lower Proterozoic arc-microcontinent collision tectonics in the western Churchill province: Nature, v. 294, p. 69-72.

Lewry, J. F., Hajnal, Z., Green, A., Lucas, S. B., White, D., Stauffer, M. R., Ashton, K. E., Weber, W., and Clowes, R., 1994, Structure of a

Paleoproterozoic continent-continent collision zone; a Lithoprobe seismic reflection profile across the Trans-Hudson Orogen, Canada: Seismic reflection probing of the continents and their margins., v. 232, p. 143-160.

Lewry, J. F., Lucas, S., Stern, R., Ansdell, K., and Ashton, K., 1996, Tectonic assembly and orogenic closure in the Trans-Hudson Orogen: Program with Abstracts, GAC-MAC Annual Meeting, v. 21, p. A-56.

Lewry, J. F., Macdonald, R., Livesey, C., Meyer, M., Van, S. R., and Bickford, M. E., 1987, U-Pb geochronology of accreted terranes in the Trans-Hudson Orogen, northern Saskatchewan, Canada, *in* Pharaoh, T. C., Beckinsale, R. D., and Rickard, D. T., eds., Geochemistry and mineralization of Proterozoic volcanic suites.: Geological Society Special Publications, London, United Kingdom, Geological Society of London, p. 147-166.

Lewry, J. F., Sibbald, T. I. I., and Rees, C. J., 1978, Metamorphic patterns and their relation to tectonism and plutonism in the Churchill Province in northern Saskatchewan. *In* Fraser J. A., and Heywood, W. W., eds., Metamorphism in the Canadian Shield, Geological Survey Canada, Paper 78-10, p. 139-154.

Lewry, J. F., Thomas, D. J., Macdonald, R., and Chiarenzelli, J., 1990, Structural relations in accreted. terranes of the Trans-Hudson Orogen, Saskatchewan: telescoping in a collisional regime?, *in* Lewry, J. F., and Stauffer, M. R., eds., The Early Proterozoic Trans-Hudson Orogen of North America, Geological Association of Canada Special Paper 37, p. 75-94.

Longerich, H. P., Jenner, G. A., and E, J. S., 1990, Inductively coupled plasma mass spectometric analysis of geological samples: a critical evaluation based on case studies: Chemical Geology, v. 83, p. 105-118.

Loosveld, R. J. H., 1989, The synchronism of crustal thickening and low-pressure facies metamorphism in the Mount Isa Inlier, Australia. 2. Fast convective thining of mantle lithosphere during crustal thickening: Tectonophysics, v. 165, p. 191-218.

Loosveld, R. J. H., and Etheridge, M. A., 1990, A model for low-pressure facies metamorphism during crustal thickening: Journal of Metamorphic Geology, v. 8, p. 257-267.

Lucas, S. B., Green, A. G., Hajnal, Z., White, D. J., Lewry, J. F., Ashton, K. E., Weber, W., and Clowes, R. M., 1993, Deep seismic profile across a Proterozoic collision zone: surprises at depth: Nature, v. 363, p. 339-342.

Lucas, S. B., Hajnal, Z., and Lewry, J. F., 1997, Towards a synthesis of the Trans-Hudson Orogen Transect; highlights from the Phase V proposal, *in* Anonymous, ed., Lithoprobe; Sixth Trans-Hudson Orogen Transect workshop.: Lithoprobe Report, Vancouver, BC, Canada, University of British Columbia, Lithoprobe Secretariat [for the] Canadian Lithoprobe Program, p. 227-250.

Lucas, S. B., Syme, E. C., and Ashton, K. E., 1999, New perspectives on the Flin Flon Belt, Trans-Hudson Orogen, Manitoba and Saskatchewan: an introduction to the special issue on the NATMAP Shield Margin Project, Part 1: Canadian Journal of Earth Sciences, v. 36, p. 135-140.

Macdonald, R., 1974, Pelican Narrows (west) area, reconnaissance geological survey of 63M/2(W): Summary Report of Field Investigations 1974, Saskatchewan Geological Survey, p. 30-37.

Macdonald, R., 1981, Compilation bedrock geology: Pelican Narrows and Amisk Lake areas (NTS 63M, 63L and part 63N and 63K): Summary of Investigations 1981, Saskatchewan Geological Survey, v. 81-4, p. 16-23.

Macdonald, R., and Broughton, P., 1980, Geological map of Saskatchewan, scale 1: 1 000 000 provisional edition: Saskatchewan Mineral Resources.

McNicoll, V. J., Delaney, G. D., Parrish, R. R., and Heaman, L. M., 1992, U-Pb determinations from the Glennie Lake Domain, Trans-Hudson Orogen, Saskatchewan, Radiogenic age and isotopic studies; Report 6.: Paper - Geological Survey of Canada, Ottawa, ON, Canada, Geological Survey of Canada, p. 57-72.

McNutt, M. K., and Fischer, K. M., 1987, The South Pacific superswell, seamounts, islands and atolls: American Geophysical Union Geophysical Monograph, v. 43, p. 25-34.

Menard, T., and Gordon, T. M., 1997, Metamorphic P-T paths from the eastern Flin Flon Belt and Kisseynew Domain, Snow Lake, Manitoba: Canadian Mineralogist, v. 35, p. 1093-1115.

Meyer, M. T., Bickford, M. E., and Lewry, J. F., 1992, The Wathaman Batholith: An Early Proterozoic continental arc in the Trans-Hudson Orogenic Belt: Geological Society of America Bulletin, v. 104, p. 1073-1085.

Miyashiro, A., 1961, Evolution of metamorphic belts: Journal of Petrology, v. 2, p. 277-311.

Miyashiro, A., 1973, Metamorphism and Metamorphic Belts: New York, John Wiley & Sons, 492 p.

Miyashiro, A., 1994, Metamorphic Petrology: New York, John Wiley & Sons, 404 p.

Nance, W. B., and Taylor, S. R., 1977, Rare earth element patterns and crustal evolution-II. Archean sedimentary rocks from Kalgoorlie, Australia: Geochimica et Cosmochimica Acta, v. 41, p. 225-231.

Nesbit, H. W., and Young, G. M., 1982, Early Proterozoic climate and plate motions inferred from major element chemistry of lutites: Nature, v. 299, p. 715-717.

Nesbit, H. W., and Young, G. M., 1989, Formation and diagenesis of weathering profiles: Journal of Geology, v. 97, p. 129-147.

Norman, A. R., Williams, P. F., and Ansdell, K. M., 1995, Early Proterozoic deformation along the southern margin of the Kisseynew gneiss belt, Trans-Hudson Orogen: a 30 Ma progressive deformation cycle: Canadian Journal of Earth Sciences, v. 32, p. 875-984.

Parrish, R. R., 1990, U-Pb dating of monazite and its application to geological problems: Canadian Journal of Earth Sciences, v. 27, p. 1431-1450.

Pearce, J. A., Harris, N. B. W., and Tindle, A. G., 1984, Trace element discrimination diagrams for the interpretation of granitic rocks: Journal of Petrology, v. 25, p. 956-983.

Perkins, D., 1988, Glennie-Kisseynew P-T study 1988: fieldwork and preliminary results: Summary of Investigations, Saskatchewan Geological Survey, v. 88-4.

Perkins, D., 1991a, Metamorphism of the Kisseynew gneisses and related. rocks of the Reindeer Zone, Trans-Hudson Orogen, northern Saskatchewan: Canadian Journal of Earth Sciences, v. 28, p. 1664-1676.

Perkins, D., 1991b. Glennie-Kisseynew P-T study 1991: fieldwork and preliminary results: Summary of Investigations, Saskatchewan Geological Survey, v. 91-4, p. 66-68.

Platt, J. P., and England, P. C., 1993, Convective removal of lithosphere beneath mountain belts; thermal and mechanical consequences, *in* Seranne, M., and Malavieille, J., eds., Late orogenic extension in mountain belts; international meeting.: Documents - B.R.G.M., Paris,

France, Bureau de Recherches Geologiques et Minieres, (BRGM), p. 162.

Powel, C. M., 1983, Tectonic relationship between the Late Ordovician and late Silurian paleogeographies of southeastern Australia: Journal of the Geological Society of Australia, v. 30, p. 353-373.

Ramsay, J. G., 1960, The deformation of early lineation structure in areas of repeated folding: Journal of Geology, v. 68, p. 75-83.

Ramsay, J. G., 1967, Folding and Fracturing of Rocks: New York, McGraw-Hill Book Company, 568 p.

Ramsay, J. G., and Huber, M., 1987, The Techniques of Modern Structural Geology. Volume 2: Folds and Fractures: London, Academic Press, 392 p.

Rollinson, H. R., and Windley, B. F., 1980, Selective elemental depletion during metamorphism of Archean granulites, Scourie, NW Scotla: Contributions to Mineralogy and Petrology, v. 72, p. 257-263.

Sacks, P. E., and Secour, D. T., 1990, Delamination in collisional orogens: Geology, v. 18, p. 999-1002.

Schumacher, K. T., Hollocher, P. R., and Robert, J. T., 1990, Progressive reactions and melting in the Acadian metamorphic high of central Massachusetts and southwestern New Hampshire, USA, *in* Ashworth, J. R., and Brown, M., eds., High-Temperature Metamorphism and Crustal Anatexis, London, Unwin Hyman, p. 198-234.

Sibbald, T. I. I., 1978, Geology of the Sandy Narrows (east) area: Saskatchewan Department of Mineral Resources, v. Report 170, p. 49.

Slimmon, W. L., 1994, Geology of the Gee-Sadler Lakes area and its relation to the tectonics of the Glennie domain, Saskatchewan, Canada: Unpub. MSc thesis, University of Regina 111 p.

Spear, F. S., 1993, Metamorphic phase equilibria and pressure-temperature-time paths: Mineralogical Society of America Monograph, v. 1.

Spear, F. S., and Cheney, J. T., 1989, A petrogenetic grid for pelitic schists in the system Si02- A1203-FeO-MgO-K20-H20: Contributions to Mineralogy and Petrology, v. 101, p. 149-164.

Spear, F. S., and Selverstone, J., 1983, Quantitative P-T paths from zoned minerals: theory and tectonic applications: Contributions to Mineralogy and Petrology, v. 83, p. 348-357.

Spear, F. S., Selverstone, J., Hickmott, D., Crowley, P., and Hodges, K. V., 1984, P-T paths from garnet zoning: a new technique for deciphering tectonic processes in crystalline terranes: Geology, v. 12, p. 87-90.

Stauffer, M. R., 1984, Manikewan: an Early Proterozoic Ocean in central Canada, its igneous history and orogenic closure: Precambrian Research, v. 25, p. 257-281.

Stauffer, M. R., and Lewry, J. F., 1993, Regional setting and kinematic features of the Needle Falls Shear Zone, Trans-Hudson Orogen: Canadian Journal of Earth Sciences, v. 30, p. 1338-1354.

Streepey, M. M., Essene, E. J., and Van Der Pluijm, B. A., 1997, A compilation of thermobarometric data from the metasedimentary belt of the Grenville Province, Ontario and New York State: Canadian Mineralogist, v. 35, p. 1237-1247.

Sun, M., Kyser, K., Stauffer, M., Kerrich, R., and Lewry, J., 1996, Constraints on the timing of crustal imbrication in the central Trans-Hudson Orogen from single zircon 207Pb/206Pb ages of granitoid rocks from the Pelican thrust zone, Saskatchewan: Canadian Journal of Earth Sciences, v. 33, p. 1638-1647.

Symons, D. T. A., Gala, M., and Palmer, H. C., 1995, Fitting paleomagnetic data to a plate tectonic model for the Trans-Hudson Orogen with a focus on the Hanson Lake Block, *in* Hajnal, Z., and Lewry, J., eds., Lithoprobe: Trans-Hudson Orogen Transect, University of Saskatchewan, p. 66-77.

Taylor, S. R., and McClennan, S. M., 1985, The continental crust: Its composition and evolution: Oxford, Blackwell, 312 p.

Taylor, S. T., Rudnick, R. L., McClennan, S. M., and Eriksson, K. A., 1986, Rare earth element patterns in Archean high-grade metasediments and their tectonic significance: Geochimica et Cosmochimica Acta, v. 50, p. 2267-2279.

Thompson, A. B., 1982, Dehydration melting of pelitic rocks and the generation of H20-undersaturated. granitic liquids: American Journal of Science, v. 282, p. 1567-1595.

Tischendorf, G., Forster, H. J., and Trumbull, R. B., 1995, Tectonic setting and geochemistry of granitoids: the potential and problems of discrimination

diagrams: Origin of Granites and Related Rocks, U.S. Geological Survey Circular, v. 1129, p. 147-148.

Tran, H. T., 1997, Structural relations and thermotectonic history of the Medicine Rapids-Grassy Narrows area northern Saskatchewan, Canada: Unpub. MSc thesis, University of Regina 225 p.

Tran, H. T., Lewry, J. F., and Ashton, K. E., 1996, The geology of the Medicine Rapids- Grassy Narrows area: Summary of Investigations 1996; Saskatchewan Geological Survey, v. 96-4, p. 43-50.

Van Schmus, W. R., Bickford, M. E., Lewry, J. F., and Macdonald, R., 1987, U-Pb geochronology in the Trans-Hudson Orogen, northern Saskatchewan, Canada: Canadian Journal of Earth Sciences = Journal Canadien des Sciences de la Terre, v. 24, p. 407-424.

Vernon, R. H., 1976, Metamorphic Processes: Reactions and Microstructure Development: London, George Allen & Unwin Ltd., 247 p.

Vernon, R. H., 1978, Porphyroblast-matrix microstructural relationships in deformed metamorphic rocks: Geol. Rdsch, v. 67, p. 288-305.

Vernon, R. H., 1987a, Growth and concentration of fibrous sillimanite related, to heterogeneous deformation in K-feldspar-sillimanite metapelites: Journal of Metamorphic Geology, v. 5, p. 51-68.

Vernon, R. H., 1987b, Oriented growth of sillimanite in andalusite, Placitas - Juan Tabo area, New Mexico, USA: Canadian Journal of Earth Sciences, v. 24, p. 580-590.

Vernon, R. H., 1988, Sequential growth of cordierite and andalusite porphyroblasts, Cooma Complex, Australia: Microstructural evidence of a prograde reaction: Journal of Metamorphic Geology, v. 6, p. 255-269.

Vernon, R. H., 1989, Porphyroblast-matrix microstructural relationships: recent approaches and problems, *in* Daly, J. S., Cliff, R. A., and Yardley, B. W. D., eds., Evolution of Metamorphic Belts, London, Blackwell Scientific Publications, p. 83-102.

Vernon, R. H., 1999, Quartz and feldspar microstructures in metamorphic rocks: Canadian Mineralogist, v. 37, p. 513-524.

Wang, Z., and Ji, S., 1999, Deformation of silicate garnets: brittle-ductile transition and its geological implications: Canadian Mineralogist, v. 37, p. 525-541.

Wickham, S. M., 1987, Crustal anatexis and granite petrogenesis during low-pressure regional metamorphism: The Trois Seigneurs Massif, Pyrenees, France: Journal of Petrology, v. 28, p. 127-169.

Wickham, S. M., and Oxburgh, E. R., 1985, Continental rifts as a setting for regional metamorphism: Nature, v. 318, p. 330-333.

Wickham, S. M., and Oxburgh, E. R., 1987, Low pressure regional metamorphism in the Pyrenees and its implications for the thermal evolution of rifted. continental crust: Phil. Trans. R. Soc. Lond, v. A321, p. 219-243.

Wilcox, K. H., 1990, Bedrock geological mapping, Nielsen Lake Area, Tabbernor Fault Zone: Summary of Investigations 1990; Saskatchewan Geological Survey, v. 90-4, p. 74-83.

Wilcox, K. H., 1991, Geological relationships in the Wood Lake area, Tabbernor Fault Zone: Summary of Investigations 1991; Saskatchewan Geological Survey, v. 91-4, p. 135-143.

Wynne-Edwards, H. R., 1963, Flow folding: American Journal of Science, v. 261, p. 793-814.

Zielinsky, R. A., and Frey, F. A., 1974, An experimental study of the partitioning of a rare earth element (Gd) in the system diopside-aqueous vapour: Geochimica et Cosomochimica Acta, v. 38, p. 545-565.

Zwanzig, H. V., 1990, Kisseynew Gneiss Belt in Manitoba: stratigraphy, structure, and tectonic evolution, *in* Lewry, J. F., and Stauffer, M. R., eds., The Early Proterozoic Trans-Hudson Orogen of North America: Geological Association of Canada Special Paper 37, p. 95-120.

APPENDIX A: Whole Rock Geochemistry

APPENDIX A:

WHOLE ROCK GEOCHEMISTRY

A.0. Introduction

Fifteen rock samples including 13 metasedimentary and 2 granodiorite were crushed for the purpose of obtaining whole rock geochemistry. These samples were analyzed using X-Ray Flouresence with relative standard deviations of 5%, to obtain major element concentration. Inductively Coupled Plasma-Mass Spectrometry (ICP-MS; Perkins Elmer 5000) at the University of Saskatchewan following the sinter method, and using the calibration and data reduction methods from Jenner *et al*, (1990), and Longerich *et al*, (1990) was completed for the determination of trace element concentrations, including REE's. The scope of this chapter is to define the chemical nature of the Kisseynew Metaturbidites to determine a possible source and or tectonic environment. When plotting trace element diagrams the raw data must be normalized to chondrite (Table A1) to cancel the Oddo-Harkins effect. For the purpose of examining trends, the metasedimentary rocks were then plotted against Post Archean Average Shale (PAAS) from Taylor and McClennan (1985; Table A2), since it reflects the modern equivalent.

Table A.1. Chondrite (Sun and McDonough, 1989) ppm.

Th	0.029	**Gd**	0.2055
Nb	0.246	**Tb**	0.0374
La	0.237	**Dy**	0.254
Ce	0.612	**Ho**	0.0566
Pr	0.095	**Y**	1.57
Nd	0.467	**Er**	0.1655
Zr	3.87	**Tm**	0.0255
Hf	0.1066	**Yb**	0.17
Sm	0.153	**Lu**	0.0254
Eu	0.058	**Ta**	0.014
Ti	445		

Table A.2. Post Archean Average Shale (PAAS) (Taylor and McClennen, 1985) ppm.

Th	503.4483	**Eu**	18.62069	**Yb**	16.58824
Nb	77.23577	**Ti**	13.46966	**Lu**	17.04724
La	161.1814	**Gd**	22.6764	**Eu/Eu***	0.655501
Ce	130.0654	**Tb**	20.69519	**La/Sm**	4.380651
Pr	92.94737	**Dy**	18.4252	**Th/La**	3.139927
Nd	72.59101	**Ho**	17.50883	**La/Yb**	9.73478
Zr	54.26357	**Y**	17.19745	**Gd/Yb**	1.388599
Hf	46.90432	**Er**	17.22054	**Nb/Nb***	0.271846
Sm	35.94771	**Tm**	15.88235	**Ti/Ti***	0.465549

A.1. Whole Rock Geochemistry of the Metasedimentary Rocks

An important aspect of interpreting compositional data on trace elements and particularly on Rare Earth Elements (REE's) of metamorphic rocks, is whether the elements are immobile or mobile. The chemistry of sedimentary rocks is a function of the chemistry of the protolith along with sedimentary mixing with other sources, weathering, and depositional processes which may cause mineral separation. During metamorphism whole rock compositions of sediments are affected in two ways. The first is by the loss or gain of constituents due to a fluid phase. The REE content of a metamorphic rock is usually not expected to have altered significantly from its original protolith. Taylor *et al.* (1986) suggest that the REE patterns of metasedimentary rocks are not significantly altered by metamorphism, even by granulite facies conditions, and therefore are good indicators of protolith. Other studies indicate (Zielinsky and Frey, 1974; Rollinson and Windley, 1980) that only at very high water/rock ratios would the REE paterns be significantly affected. One aspect to consider when investigating the chemical pattern of a rock (including REE's) is its mineralogy; as the chemistry of a metamorphic rock is directly related to the chemical and physical conditions under which the rock evolved (Grauch, 1989). During discontinuous reactions the REE's either move into a new mineral phase or are incorporated into a metamorphic fluid. The REE pattern of a metamorphic rock will change with the mineralogy provided the REE's are removed from the system by a metamorphic fluid (Grauch, 1989). The second

process by which metasediments may have been affected by metamorphism is by partial melting of the protoliths. In situ partial melting will partition elements between the restite and melt portions of the migmatite, thereby changing the composition of the protolith. No net compositional change will be noticed in element patterns however, unless the melt has been removed for the system (Taylor *et al*, 1986). The rocks under investigation here, show anatexis in the more higher grade areas, however the melt portions are not significantly removed from the restite.

The REE's within the rocks under investigation within this study are considered to be fairly immobile for four reasons: 1) The consistency of their pattern as compared to PAAS; 2) The highest and lowest grade patterns are not inconsistent, showing similar variability; 3) The slight variation exhibited can be explained through mineralogical differences and grain size; and 4) The negative correlation of the trace elements including REE values as compared to Eu/Eu*. The Eu/Eu* [$Eu_N/SQRT(Sm_N \times Gd_N)$] value is important in interpreting REE signatures, and can be used to determine a possible source (Bhatai, 1985) as well as aid in determining whether the REE patterns of metasediments have been affected by metamorphism. Nearly all post-Archean sedimentary rocks are characterized by an Eu depletion (Taylor and McClennan, 1985). The explanation for this anomaly is that during the formation of the upper continental crust and the development of K-rich granitic melts, Eu fractionates into the lower crust. Eu depletion in sediments is then inherited from an igneous source,

where Eu^{+2} substituted for Sr^{+2} in plagioclase. Low values of Eu/Eu* (<0.85) may indicate that the source was recycled older crust, or rocks formed by intercrustal melting or plagioclase fractionation. Values of >0.85 may indicate that these processes were less important. Sediments with lower Eu/Eu* values correspond with higher concentrations of Th, Nb, Zr, Hf, and Ta. Therefore Eu/Eu* values can be plotted against these elements to determine if metamorphism has significantly altered the compositions. Figure A.1, based on values from Table A3, shows Eu/Eu* plots verses the elements mentioned above. All plots, including total REE's show a reasonable negative correlation with Eu/Eu* indicating that their concentrations are likely primary, and have not been altered by metamorphism.

Discrimination diagrams using major element concentrations can sometimes be useful for interpreting the source of the sediment, and tectonic environment. The majority of discrimination diagrams developed have been modeled on modern sediments. However, in this case, the majority of the rocks have undergone sufficient heating to cause anatexis; therefore causing the residual to be somewhat depleted in the majors with respect to modern sediments. These type of diagrams then are not useful in describing the source of tectonic environment for the rocks under investigation.

A.1.1. Chemical Signatures of Continental Weathering Processes

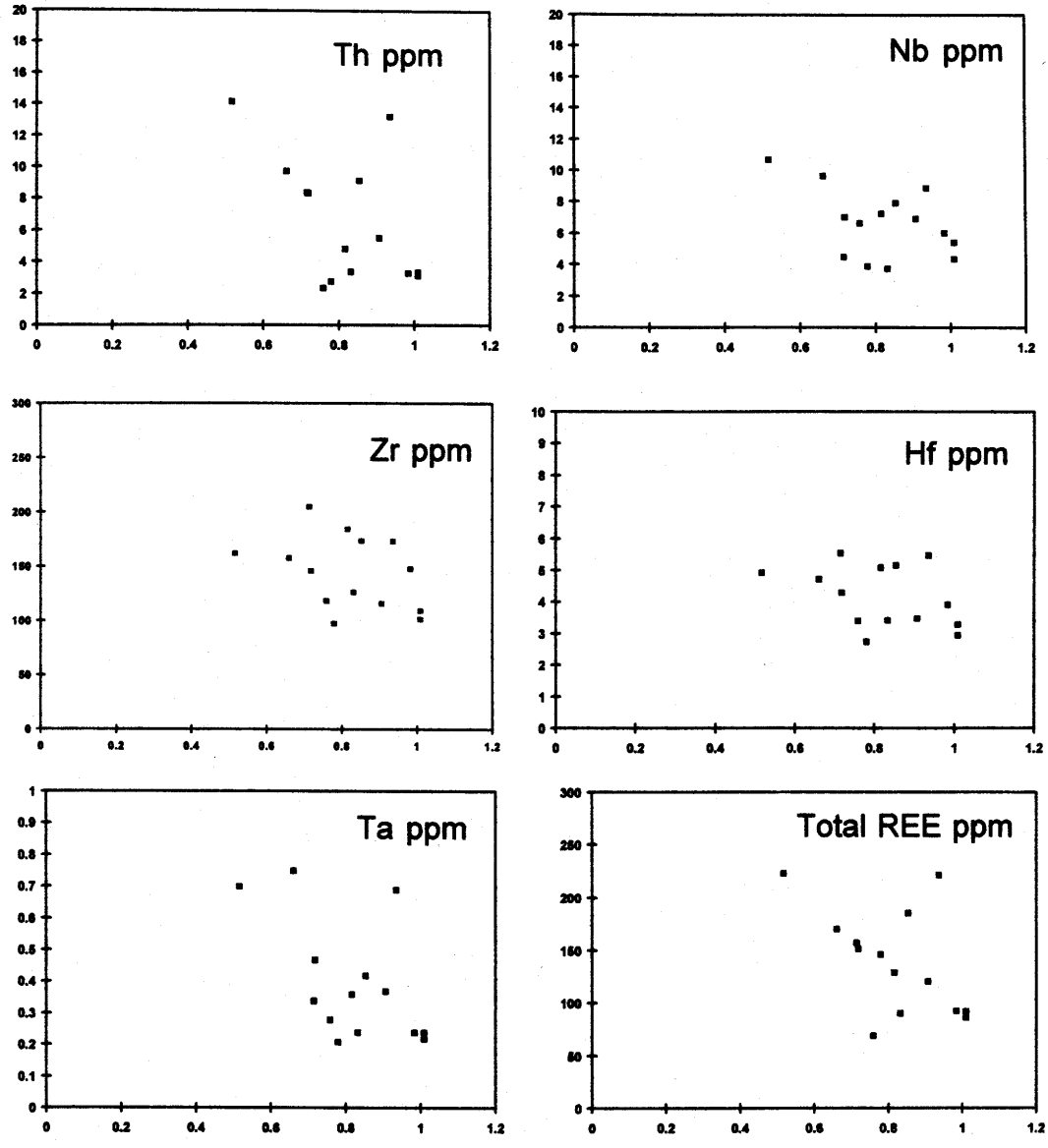

Figure A.1. Plots of trace elements against Eu/Eu* to test if metamorphic conditions have altered the compositions of the metasedimentary rocks.

Table A.3. XRF and ICP-MS Analysis of selected rock samples.

XRF	Zone 1			Zone 2			Zone 3			Zone 4				Granodiorite	
Elem./Sam.	N130	5055	5049	5038a	5100	5114	5105a	5107a	5024	7005a	7005b	5131	10a	5097	7006
SiO2 (wt.%)	65.46	65.67	63.59	68.03	67.08	70.64	65.99	69.01	59.56	65.32	60.34	58.97	61.93	65.66	61.53
TiO2	0.676	0.646	0.617	0.612	0.679	0.557	0.608	0.457	0.799	0.698	0.815	0.854	0.74	0.642	0.9
Al2O3	15.79	16.64	15.99	14.53	15.45	13.48	16.01	14.62	19.07	15.19	18.86	18.93	19.18	16.12	16.65
Fe2O3	7.16	6.42	6.49	6.17	6.05	4.86	5.93	4.27	7.3	6.3	8.06	8.89	7.78	5.71	7.64
MnO	0.016	0.042	0.044	0.061	0.059	0.049	0.033	0.021	0.037	0.045	0.032	0.096	0.038	0.045	0.084
MgO	2.77	2.46	2.51	2.09	2.07	2.14	2.21	1.83	3.06	3.22	3.56	2.83	2.94	2.52	2.77
CaO	1.83	1.39	3.13	2.89	2.82	1.87	2.9	2.3	1.64	2.51	1.66	1.61	1.15	1.96	4.51
Na2O	1.7	2.26	3.74	2.59	3.56	3.29	3.74	3.16	2.12	2.93	2.4	2.57	2.08	2.52	2.44
K2O	1.49	3	1.91	2.21	1.61	2.23	2.22	2.12	5.19	2.74	3.11	3.55	3.51	2.87	2.72
P2O5	0.113	0.171	0.155	0.148	0.167	0.161	0.164	0.183	0.176	0.217	0.161	0.131	0.149	0.165	0.182
Co (ppm)	68	70	37	89	100	110	91	116	60	75	59	78	76	74	103
Cr2O3 (ppm)	163	140	160	161	196	323	155	137	194	314	222	204	174	184	109
Cu (ppm)	19	46	68	82	117	25	73	46	70	173	73	208	46	15	50
Ni (ppm)	68	44	37	25	33	76	29	35	83	35	74	76	62	51	28
Zr (ppm)	118	153	110	132	150	199	113	140	154	163	172	160	156	154	184
FeO (%)	4.53	5.15	4.64	4.58	4.13	9.55	3	3.46	5.42	5.79	5.66	6.78	5.89	4.26	6.5
LOI	2.98	1.62	1.92	0.99	1.1	0.84	0.9	1.94	1.41	1.06	1.38	1.76	1	2.16	0.78
Total	100.03	100.57	100.14	100.37	100.7	100.19	100.75	99.95	100.42	100.3	100.44	100.26	100.55	100.42	100.26
ICP-MS															
Y (ppm)	15.81	20.23	14.44	20.14	13.01	19.25	15.31	27.1	26.37	19.06	21.81	27.03	27.08	22.92	26.18
Zr	118.72	146.21	97.73	126.57	147.94	205.24	102	157.88	173.59	184.66	173.86	116.36	162.17	151.94	201.4
Nb	6.67	7.08	3.92	3.79	6.05	4.49	5.48	9.7	8.92	7.3	7.97	6.97	10.72	7.98	9.6
La	11.29	30.52	27.79	17.16	18.79	33.47	16.4	33.89	47.01	24.79	38.01	22.03	46.55	25.59	31.42
Ce	25.36	63.27	62.37	34.91	37.18	65.93	34.23	69.45	91.53	52.21	76.8	46.18	94.77	55.51	65.38
Pr	3.42	7.47	7.76	4.26	4.52	7.86	4.26	8.41	10.94	6.51	9.26	5.68	11.06	6.76	8.09
Nd	14.02	29.3	31.13	17.13	18.66	30.38	16.83	32.41	42.46	26.18	36.36	23.3	42.19	26.92	31.38
Sm	3.2	5.42	5.42	3.43	3.43	5.23	3.42	6.18	7.62	5.16	6.82	4.9	7.52	5.32	6.31
Eu	0.8	1.15	1.17	0.91	1.01	1.13	1.07	1.24	2.14	1.29	1.72	1.44	1.15	1.22	1.21
Gd	3.26	4.44	3.9	3.27	2.88	4.49	3.08	5.35	6.43	4.54	5.58	4.83	6.2	4.63	5.71
Tb	0.48	0.6	0.46	0.51	0.4	0.59	0.41	0.77	0.84	0.63	0.74	0.81	0.82	0.67	0.8
Dy	2.87	3.8	2.63	3.35	2.29	3.55	2.68	4.9	5.1	3.67	4.31	5.13	5.04	4.21	5.17
Ho	0.6	0.77	0.52	0.72	0.47	0.69	0.56	1.03	1.05	0.69	0.82	1.02	1.02	0.87	1.06
Er	1.63	2.21	1.39	2.06	1.36	1.88	1.56	2.99	2.9	1.78	2.23	2.68	2.93	2.49	3.1
Tm	0.25	0.34	0.21	0.33	0.22	0.29	0.24	0.46	0.45	0.26	0.31	0.37	0.45	0.39	0.46
Yb	1.64	2.21	1.33	2.18	1.44	1.88	1.58	2.99	2.88	1.56	2.02	2.29	2.92	2.5	2.92
Lu	0.27	0.35	0.22	0.35	0.23	0.3	0.26	0.48	0.46	0.23	0.33	0.33	0.47	0.39	0.46
Hf	3.41	4.31	2.74	3.43	3.94	5.55	2.96	4.73	5.47	5.09	5.17	3.5	4.94	4.36	5.95
Ta	0.28	0.47	0.21	0.24	0.24	0.34	0.22	0.75	0.69	0.36	0.42	0.37	0.7	0.45	0.48
Th	2.35	8.36	2.78	3.4	3.31	8.4	3.16	9.79	13.26	4.84	9.16	5.52	14.21	6.72	9.93
Eu/Eu*	0.76	0.72	0.78	0.83	0.98	0.71	1.01	0.66	0.93	0.81	0.85	0.90	0.51	0.75	0.62
La/Sm	2.28	3.64	3.31	3.23	3.54	4.13	3.10	3.54	3.98	3.10	3.60	2.90	4.00	3.11	3.21
Th/La	1.70	2.24	0.82	1.62	1.44	2.05	1.57	2.36	2.31	1.80	1.97	2.05	2.49	2.15	2.58
La/Yb	4.94	9.91	14.99	5.65	9.36	12.77	7.45	8.13	11.71	11.40	13.50	6.90	11.44	7.34	7.72
Gd/Yb	1.64	1.66	2.43	1.24	1.65	1.98	1.61	1.48	1.85	2.41	2.29	1.74	1.76	1.53	1.62
Nb/Nb*	0.44	0.15	0.15	0.17	0.26	0.09	0.26	0.18	0.12	0.22	0.14	0.21	0.14	0.21	0.18
Ti/Ti*	0.50	0.31	0.32	0.44	0.52	0.27	0.45	0.19	0.27	0.34	0.32	0.42	0.26	0.31	0.36

Weathering products in sedimentary rocks can be quantified by a rocks chemical index of alteration (CIA; Nesbitt and Young, 1982; 1989). The CIA is expressed as CIA = [ÄAl_2O_3/(Al_2O_3+CaO*+Na_2O+K_2O)] x 100. CaO* represents the CaO with silicate phases only. These Ca within these metasediments is mainly incorporated within plagioclase and garnet, with minor amounts of apatite. Therefore negligible error is introduced using the total CaO content for calculation.

As expected the CIA values (Table A.3) within the more quartz rich psammitic samples of Zones 2 and 3 (description above) have relatively lower CAI values than the more pelitic samples of Zones 1 and 4. A ternary plot of Al_2O_3-K_2O-(CaO+Na_2O) for the rocks shows the separation of the two rock types graphically (Figure A.2). The overall signatures show that they have experienced some degree of weathering; expected with basin deposited metaturbidites. The range and average CIA values (46-76, and 64) are lower than both average shale (CIA = 72-75) and deep sea mud (CIA = 69; Nesbit and Young, 1982). The average in this case is not indicative of the rocks weathering patterns. Based on mineralogical differences the pelitic rocks range in value from CIA = 71-76, and the more psammitic samples from CIA = 46-65; expected from more quartz rich varieties. CIA values from Zone 3 samples are considerably lower than the other zones (CIA = 46-56). The rocks comprising this zone may be relatively immature compared with the other zones. This may indicate a more proximal positioning to source area.

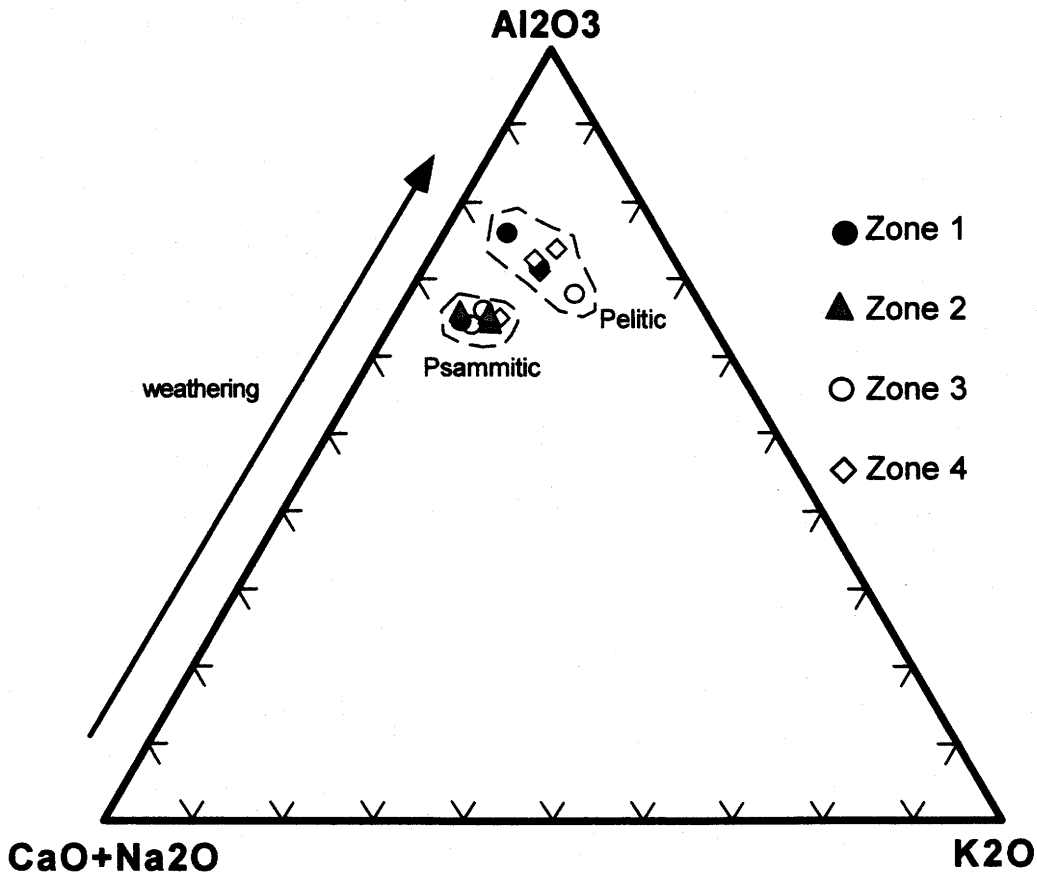

Figure A.2. Al2O3-(CaO+Na2O)-K2O ternary plot for all metasedimentary rocks analyzed within the four zones.

A.1.2. Zone 1 Metasedimentary Rocks

Table A.3 lists the chemistry of three rocks from metamorphic Zone 1 as analyzed by XRF and ICP-MS. All rock samples were collected in what has previously been interpreted as belonging to the Glennie Domain. Samples N130 and 5055 are fine grained andalusite staurolite gneiss, consisting of 40-50% quartz, 5-10% feldspar, 10-15% biotite, 5-10% chlorite, 5% muscovite, 5% staurolite, 5% andalusite, with minor cordierite and trace apatite. The protolith was a shale. Sample 5049 consists of 50% quartz, 20% chlorite, 10% feldspar, 10% biotite, 5% epidote, with trace apatite, garnet, and opaques, resembling more of a greywacke then a shale.

Figure A.3 shows the Chondrite normalized trace element pattern of the rocks described above. The data is compared to the PAAS from Taylor and McClennan (1985). The REE patterns of the metaturbidites in Zone 1 are enriched with respect to the light REE [$(La/Sm)_N$ ratios of 2.28-3.64]; and have a generally flat heavy REE pattern [$(Gd/Yb)_N$ ratio of 1.64-2.43]. Niobium shows depletion with Nb/Nb* ratios [$Nb_N/SQRT(Th_N \times La_N)$]of 0.44, 0.15, and 0.15. Eu and Ti values also exhibit depletion, with Eu/Eu* and Ti/Ti* values [$Ti/SQRT(Sm_N \times Gd_N)$] of 0.76, 0.72, 0.78, and 0.50, 0.31, 0.32.

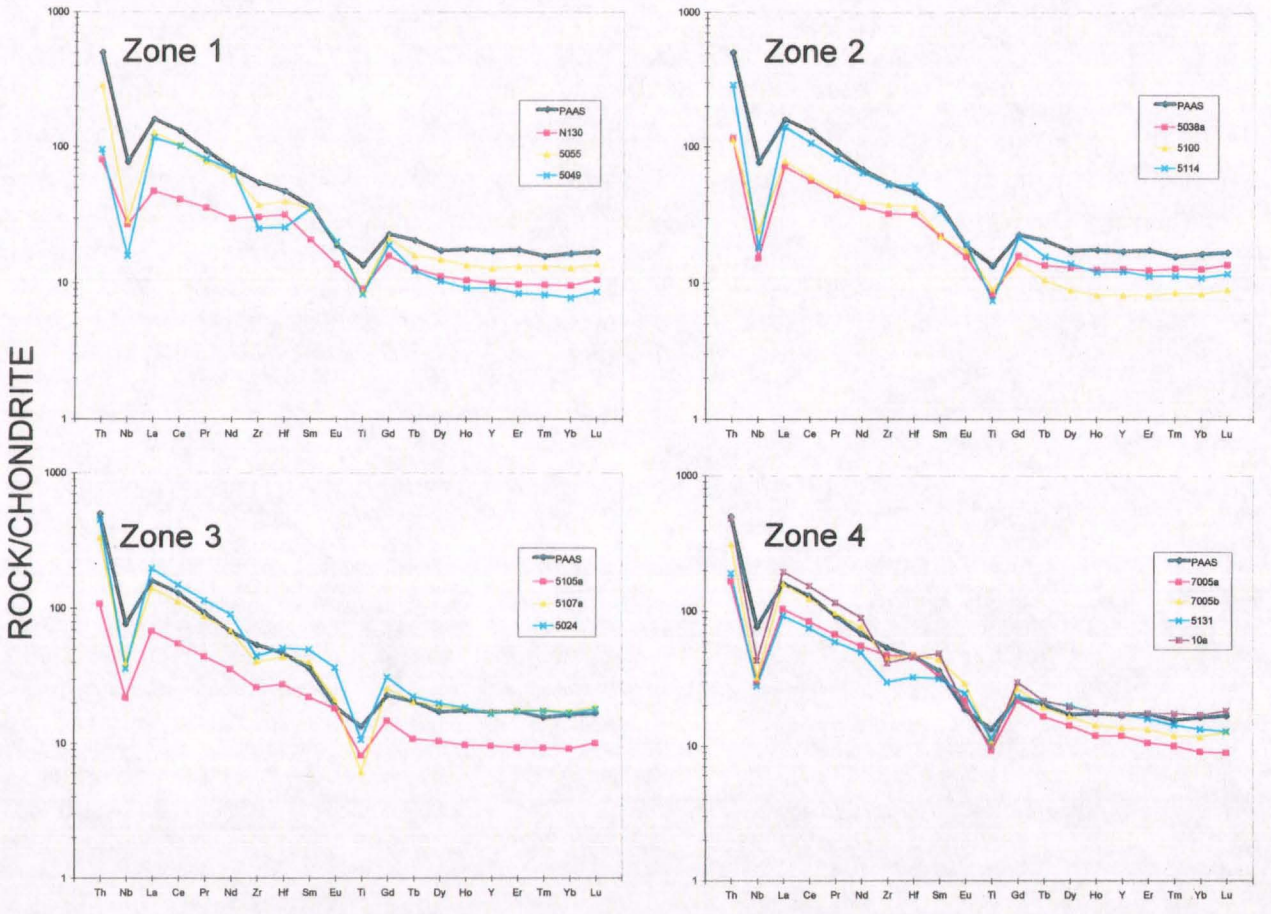

Figure A.3. Trace element spider plot for the metasedimentary rocks in Table A.3, as compared with Post Archean Average Shale.

A.1.3. Zone 2 Metasedimentary Rocks

Table A.3 lists the chemistry of three rocks from metamorphic Zone 2. All three samples are psammitic quartz-feldspar-biotite gneisses, consisting of 50-60% quartz, 20% feldspar, 15-20% biotite, minor sillimanite and muscovite, with trace apatite and opaques.

Figure A.3 shows the trace element pattern of the rocks described above. Again, the light REE's show a general enrichment, with a La/Sm ratio of 3.23 for 5038a, 3.54 for 5100, and 4.13 for sample 5114. The heavy REE's are generally flat, exhibiting fairly low Gd/Yb ratios of 1.24, 1.65, and 1.98 respectively. Niobium shows depletion with Nb/Nb* ratios of 0.17, 0.26, and 0.09. Eu and Ti values also exhibit depletion, with values of 0.83, 0.98, 0.71 for Eu/Eu*, and 0.44, 0.52, 0.27 for Ti/Ti* ratios respectively.

A.1.4. Zone 3 Metasedimentary Rocks

Table A.3 lists the whole rock chemistry of three rocks from metamorphic Zone 3. Samples 5105a and 5107a are quartz feldspar biotite gneisses, consisting of 50-60% quartz, 20% feldspar, 20% biotite, 5% cordierite, up to 2% garnet, with trace muscovite, apatite, zircon, and opaques. Sample 5024 is a sillimanite-cordierite-biotite gneiss, containing considerably less quartz (30-40%), more cordierite (10-15%) and about 5% sillimanite.

Figure A.3 shows the trace element pattern of the Zone 3 rocks described above. Again, the light REE's show a general enrichment, with La/Sm ratios of 3.10, 3.54, and 3.98 for samples 5105a, 5107a, and 5024 respectively. The heavy REE's are generally flat, exhibiting fairly low Gd/Yb ratios of 1.61, 1.48, and 1.85. Niobium shows depletion with Nb/Nb* ratios of 0.26, 0.18, and 0.12. Eu and Ti values also exhibit depletion, with values of 1.01, 0.66, 0.93 for Eu/Eu*, and 0.45, 0.19, 0.27 for Ti/Ti* ratios respectively.

A.1.5. Zone 4 Metasedimentary Rocks

Table A.3 lists the chemistry of four rocks from metamorphic Zone 4. Samples 10a, 5131, and 7005b are pelitic consisting of 25-30% quartz, 30%feldspar, 20-25% biotite, 5-10% cordierite, 5% sillimanite, 2-5% garnet, minor muscovite (1%), with trace titanite, apatite, and zircon. Sample 7005a is more psammitic in composition, consisting of 50-60% quartz, 20% feldspar, 15-20% biotite, minor sillimanite and muscovite, with trace apatite , titanite, zircon, and opaques.

Figure A.3 shows the trace element pattern of the rocks described above. Again, the light REE's show a general enrichment, with La/Sm ratios of 3.10, 3.60, 2.90, and 4.00 for samples 7005a, 7005b, 5131, and 10a respectively. The heavy REE's are generally flat, exhibiting fairly low Gd/Yb ratios of 2.41, 2.29, 1.74, and 1.76. Niobium shows depletion with Nb/Nb* ratios of 0.22, 0.14,

0.21, and 0.14. Eu and Ti values also exhibit depletion, with values of 0.81, 0.85, 0.90, and 0.51 for Eu/Eu*, and 0.34, 0.32, 0.42, and 0.26 for Ti/Ti* ratios respectively.

A.2. Geochemistry of the Granodiorite Intrusive

Two samples of Granodiorite were analyzed to aid in the interpretation of the environment at the time of emplacement (Table A.3). If the origin of the intrusive can be fingerprinted, the time at which this tectonic environment persisted could be tentatively identified. The age of Granodiorite-tonalite intrusives within the region was investigated by Elliot (1995a) and Hartlaub *et al.*, (1997,1998). A tonalite intruding volcanic rocks of the Glennie domain from Nielson Lake consistent with the Burntwood Granodiorite, yielded U/Pb zircon ages of 1848 Ma and 1833 Ma (Elliott, 1995a) based on two zircon populations. The latter is likely the result of metamorphic zircon growth, and dates an early metamorphic event.

Pearce *et al.*, (1984) developed diagrams based on trace elements of granitoids to help identify tectonic environment (Table A.4) at the time of emplacement. However, discriminating tectonic settings using granite chemistry is not an equivocal method of discerning source environments (Tischendorf *et al.*, 1995). It was found that only granitoids from within-plate settings (WPG), whether

oceanic or continental could be distinguished with confidence (Tischendorf *et al.*, 1995); and that granitoids from arc settings may span the volcanic arc (VAG)

Table A.4 Granites classified according to tectonic setting (after Pearce *et al.*, 1984; Rollinson, 1996).

Ocean Ridge Granites	Volcanic Arc Granites	Within Plate Granites	Collisional Granites
Granites associated with normal ocean ridges.	Granites in oceanic arcs dominated by tholeiitic basalt.	Granites in intracontinent ring complexes.	Syn-tectonic granites associated with continent-continent collision.
Granites associated with anomalous oceanic ridges.	Granites in oceanic arcs dominated by calc-alkali basalt.	Granites in attenuated continental crust.	Post-tectonic granites associated with continent-continent collision.
Granites associated with back-arc basin ridges.	Granites in active continental margins.	Granites in oceanic islands.	Syn-tectonic granites associated with continent-arc collision.
Granites associated with fore-arc basin ridges.			

and within-plate fields of the Pearce *et al.*, (1984) diagrams. However, it was also found that volcanic arc granites show virtually no overlap into the Syn-collisional (Syn-COLG) or ocean ridge (ORG) fields. Therefore with these premise in mind, it may be possible to interpret tectonic setting. The following interpretation of the granodiorite rock samples is cautiously examined below.

Compositional trace element data was plotted on Nb-Y and Rb-(Y+Nb) discrimination diagrams of Pearce *et al.*, (1984) (Figure A.4a and b); and Hf-Rb-Ta diagrams of Harris *et al.*, (1986) (Figure A.5a and b). Both sets of diagrams clearly show that the granodiorite has an affinity compatible with volcanic arc

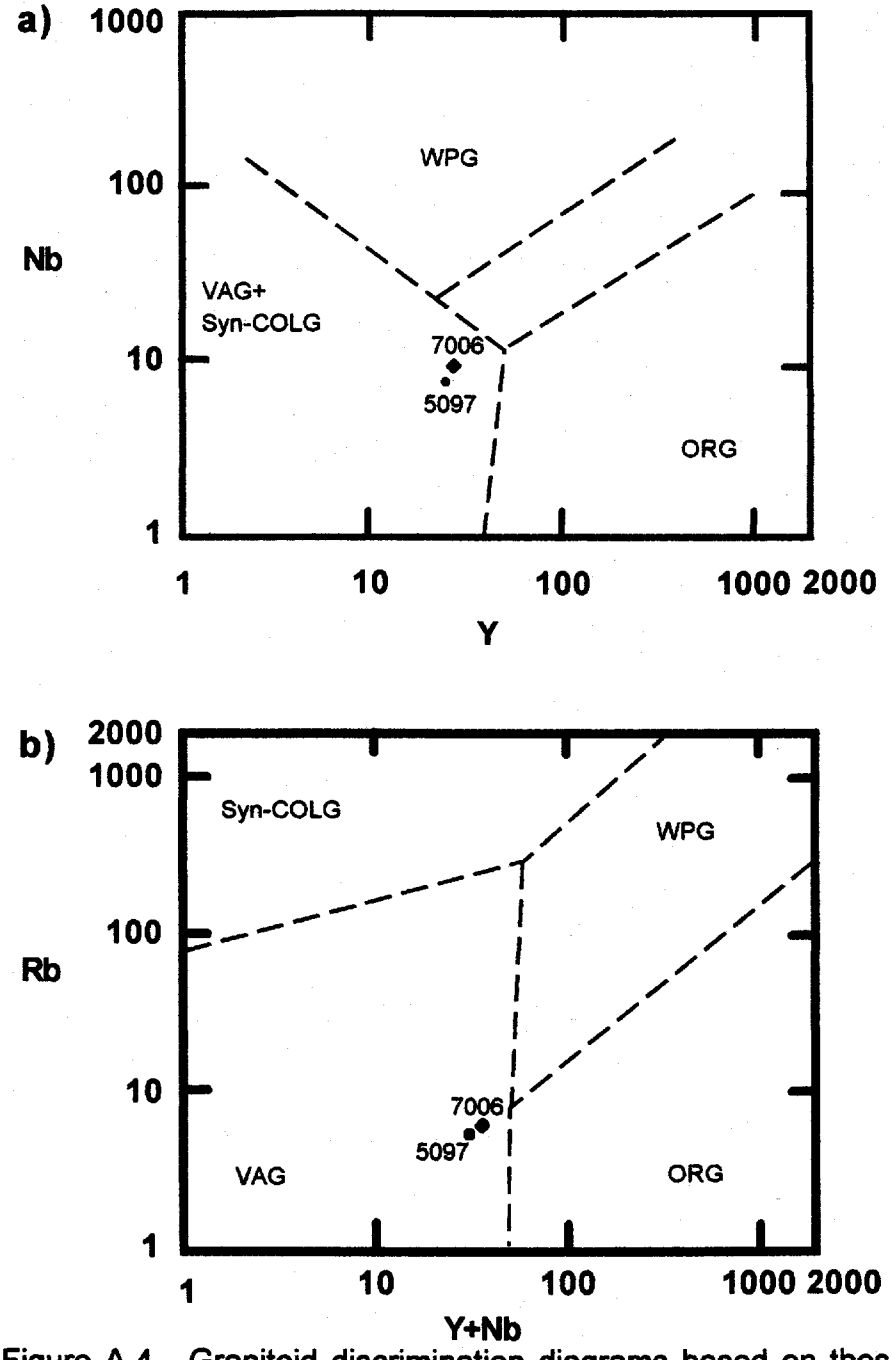

Figure A.4. Granitoid discrimination diagrams based on those developed by Pearce et al., (1984). a) Nb-Y discrimination diagram separating Volcanic Arc Granites+Syn-collisional granites (VAG+Syn-COLG), Within Plate Granites (WPG), and Ocean Ridge Granites (ORG). b) Rb-(Y+Nb) diagram further separating Syn-collisional granites from Volcanic Arc Granites.

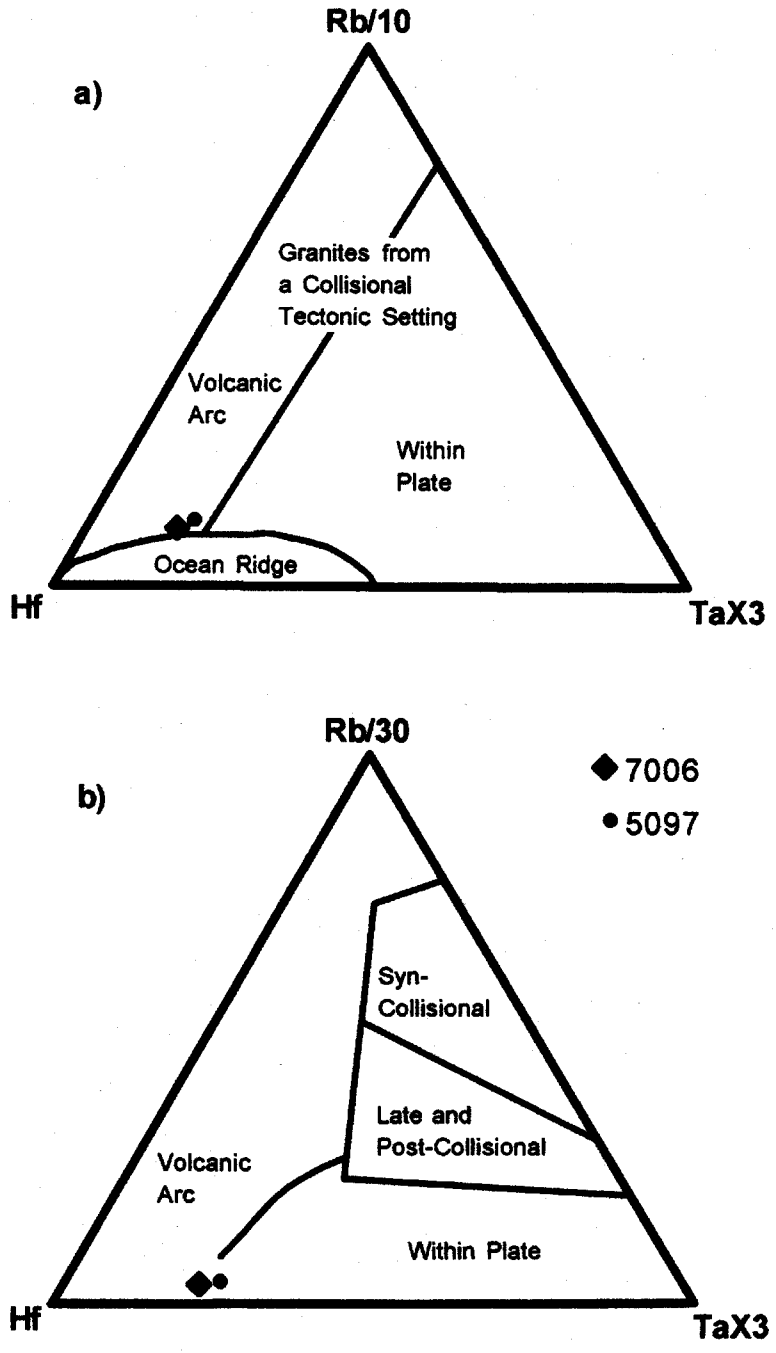

Figure A.5. Hf-Rb-Ta granitoid discrimination diagrams based of those of Harris et al., (1986). a) Diagram discriminating among Volcanic Arc, Within Plate and Ocean Ridge granites. b) Diagram allowing separation of Syn- and Post- collisional granites.

granites. When plotted on the Pearce diagrams the two samples plot completely within the VAG+Syn-COLG and VAG fields with no overlap. On the Hf-Rb-Ta diagrams however, the samples plot near the ORG field (Figure A.5a), and overlap into the WPG field (Figure A.5b). These results are consistent with the statistical findings of Tischendorf *et al.*, (1995); and lead to the assumption that this granodiorite originated from a volcanic arc setting. The granodiorite intruded into the sediments all part of an oceanic arc setting at approximately 1848 Ma (Elliott, 1995a).

A.3. Discussion of the Whole Rock Geochemistry

The slight overall depletion of the trace element patterns for samples 5100 and 5038a from Zone 2 compared to PAAS can be explained by grain size and mineralogical differences (Taylor and Mclennan, 1985). The PAAS is an average estimate of 23 post-Archean shales from Australia (Nance and Taylor, 1977) considered to be representative of the average upper crust (Taylor and McClennan, 1985). Samples 5100 and 5038a are somewhat more silica rich (68.03 and 67.08 wt percent SiO_2 respectively as compared to 62.8 percent for PAAS). The high silica content suggests a more sandy protolith, and therefore these samples exhibit a slightly depleted pattern as compared to PAAS. The same patterns are found in the analyses of rocks from Zones 1,3 and 4. Of note is the recurring Zr-Hf anomaly which is marked in the rocks of all Zones except those of Zone 2. This is not a result of incomplete dissolution of zircon since Zr

and Hf values from XRF and ICP-MS are similar (Table A.3), but derives from the sorting of grains in the protolith, and fractionation. The rocks of Zone 2 and Zone 3 are more silica rich, reflecting a protolith with a higher proportion of quartz sand and likely indicative of sorting during sedimentation/transport.

It is relatively clear from discrimination diagrams using trace elements (Figures A.6-A.7) that the turbidites originated from a protolith composed of material from an island arc tectonic setting, and predominantly oceanic island arc. The slight scatter is likely a result of the influx of older continental material, or the introduction of sediment from a more evolved arc. This is consistent with the tectonic interpretations of others (e.g. Zwanzig, 1990 Ansdell *et al.*, 1995). From Zone 1 to Zone 4 there are no marked contrasts in sedimentary types or composition with the exception that the rocks in Zone 4 exhibit patterns more closely resembling that of PAAS. This may be due to two factors. First, rocks from Zone 4 probably represent a more distal environment, therefore comprise a protolithic composition closer to that of average shale. Secondly, these rocks have undergone a higher grade of metamorphism, upper amphibolite as compared to lower amphibolite for Zone 1. Anatexis has removed quartz from the system in very small amounts causing the trace elements including the REE to be found in slightly higher concentrations. Therefore the metasediments cut by the Tabbernor Fault are part of the same package of rocks as the higher grade Kisseynew Domain metaturbidites, which in turn supports the proposed boundary change of Ashton (1999) to move the Domain boundary further west.

The difference lies only in the mineral assemblages produced by a difference in metamorphic conditions.

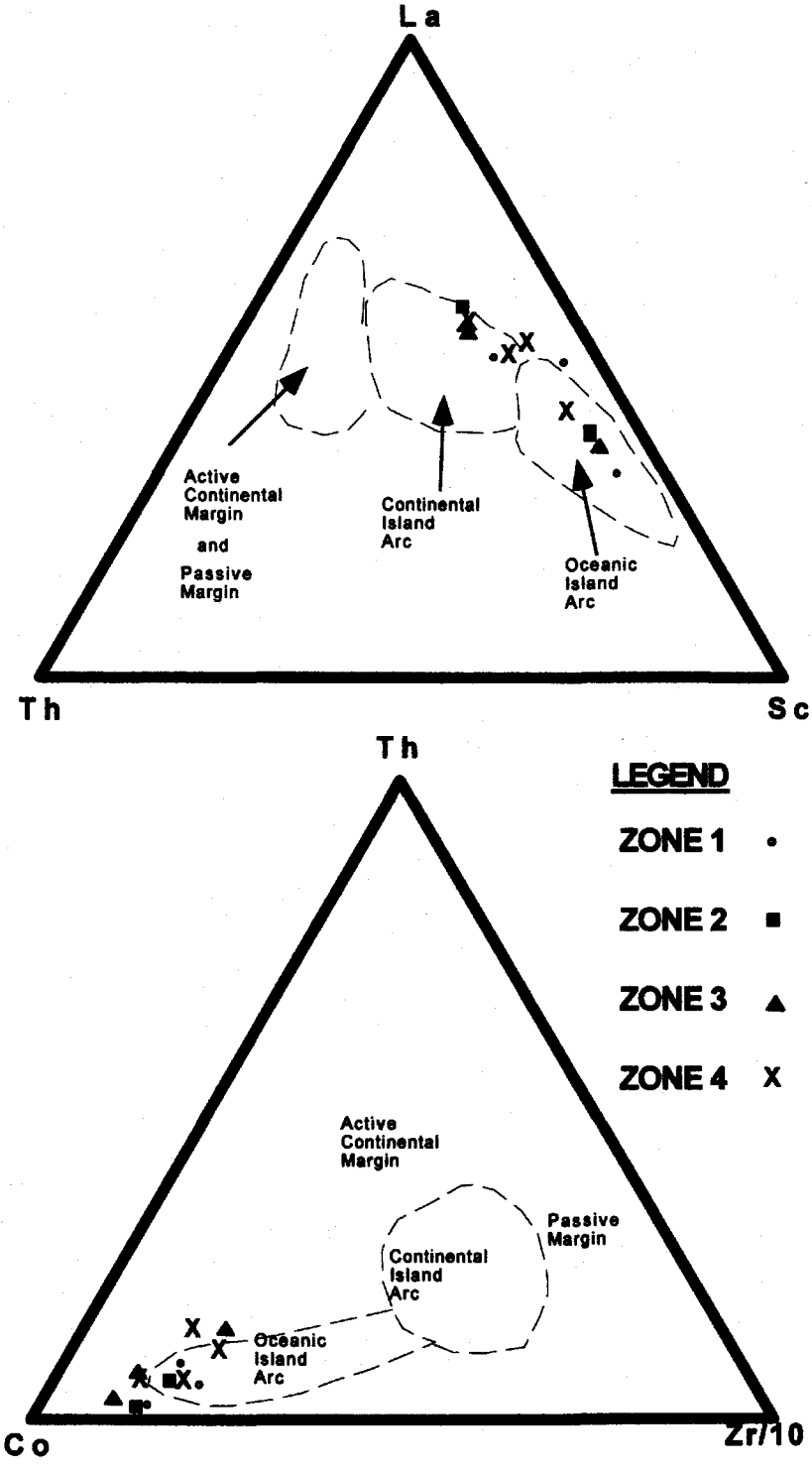

Figure A.6. La/Th/Sc and Th/Co/Zr-10 discrimmination diagrams based on those used by Bhatia and Crook (1986).

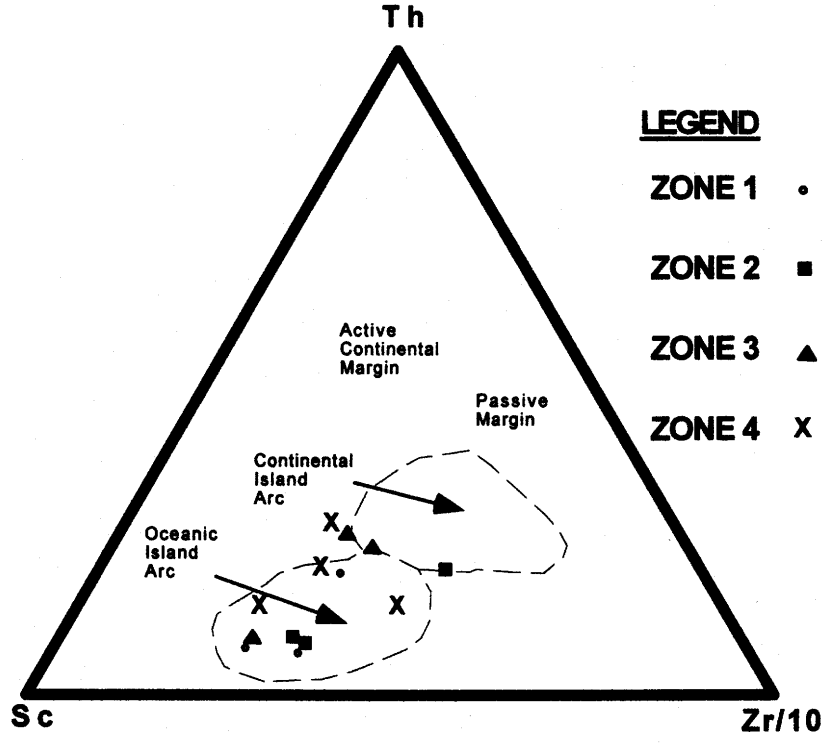

Figure A.7. Th/Sc/Zr-10 discrimmination diagram based on those used by Bhatia and Crook (1986).

APPENDIX B: Mineral Compositions From Microprobe Analysis

Appendix B.1: Garnet
Appendix B.2: Biotite
Appendix B.3: Feldspar
Appendix B.4: Cordierite
Appendix B.5: Amphibole
Appendix B.6: Mineral compositions used for quantitative pressure and temperature estimation.

B1.1. Garnet Compositional Analysis

Sample	10a core	10a rim	10a core	10a core	10a rim	10a core	10a rim	0278b rim	0278b	0278b	0278b	0278b	0278b
Oxides													
SiO2	36.97	36.15	36.83	35.65	36.86	35.22	36.55	37.69	37.44	38.33	38.28	36.94	38.05
TiO2	0.05	0.03	0.01	0.02	0.01	0.00	0.02	0.03	0.02	0.00	0.00	0.00	0.00
Al2O3	21.74	21.77	21.67	22.16	21.71	20.97	21.05	22.10	21.99	21.83	21.92	21.75	22.09
Cr2O3	0.00	0.06	0.02	0.02	0.03	0.03	0.01	0.07	0.01	0.00	0.06	0.02	0.05
FeO	35.61	36.81	35.76	35.86	36.36	35.97	35.88	32.76	32.50	32.37	31.92	32.50	33.03
MgO	3.25	2.68	3.39	3.23	2.81	3.25	2.68	4.90	5.13	5.16	5.23	5.19	5.06
MnO	1.54	1.99	1.42	1.48	1.88	1.68	2.05	0.69	0.76	0.71	0.69	0.77	0.70
CaO	0.80	0.72	0.87	0.71	0.74	0.80	0.72	1.89	2.05	1.96	1.77	1.65	1.91
Na2O	0.02	0.00	0.01	0.04	0.00	0.02	0.03	0.01	0.01	0.00	0.00	0.02	0.00
K2O	0.00	0.00	0.00	0.00	0.00	0.00	0.00	0.00	0.00	0.00	0.00	0.00	0.00
Total	99.98	100.21	99.97	99.18	100.40	97.94	98.98	100.14	99.92	100.37	99.87	98.84	100.89
Atom Proportions													
Si	5.95	5.86	5.93	5.80	5.93	5.84	5.97	5.96	5.93	6.02	6.03	5.92	5.97
Ti	0.01	0.00	0.00	0.00	0.00	0.00	0.00	0.00	0.00	0.00	0.00	0.00	0.00
Al	4.12	4.16	4.11	4.25	4.12	4.10	4.05	4.12	4.11	4.04	4.07	4.11	4.08
Cr	0.00	0.01	0.00	0.00	0.00	0.00	0.00	0.01	0.00	0.00	0.01	0.00	0.01
Fe	4.79	4.99	4.81	4.88	4.89	4.99	4.90	4.33	4.31	4.26	4.21	4.36	4.33
Mg	0.78	0.65	0.81	0.78	0.67	0.80	0.65	1.15	1.21	1.21	1.23	1.24	1.18
Mn	0.21	0.27	0.19	0.21	0.26	0.24	0.28	0.09	0.10	0.09	0.09	0.11	0.09
Ca	0.14	0.13	0.15	0.13	0.13	0.14	0.13	0.32	0.35	0.33	0.30	0.28	0.32
Na	0.01	0.00	0.00	0.01	0.00	0.01	0.01	0.00	0.00	0.00	0.00	0.01	0.00
K	0.00	0.00	0.00	0.00	0.00	0.00	0.00	0.00	0.00	0.00	0.00	0.00	0.00
O	24.00	24.00	24.00	24.00	24.00	24.00	24.00	24.00	24.00	24.00	24.00	24.00	24.00
CatTot	15.99	16.06	16.02	16.07	16.01	16.11	16.00	15.98	16.01	15.96	15.93	16.03	15.99
Total	39.99	40.06	40.02	40.07	40.01	40.11	40.00	39.98	40.01	39.96	39.93	40.03	39.99
Molar Proportions													
Grossular	0.02	0.02	0.02	0.02	0.02	0.02	0.02	0.05	0.06	0.06	0.05	0.05	0.05
Pyrope	0.13	0.11	0.14	0.13	0.11	0.13	0.11	0.20	0.20	0.21	0.21	0.21	0.20
Almandine	0.81	0.83	0.81	0.81	0.82	0.81	0.82	0.73	0.72	0.72	0.72	0.73	0.73
Spessartine	0.04	0.05	0.03	0.03	0.04	0.04	0.05	0.02	0.02	0.02	0.02	0.02	0.02
Fe/(Fe+Mg)	0.86	0.89	0.86	0.86	0.88	0.86	0.88	0.79	0.78	0.78	0.77	0.78	0.79

Sample	0278b	0278b	0278b	0278b	0278b	0278b	0278b	sbp12	sbp12	sbp12	sbp12	5000 rim adj qtz	5000 core
Oxides													
SiO2	38.20	35.11	37.60	38.15	38.20	102.61	37.37	38.65	37.50	34.99	37.63	37.24	37.27
TiO2	0.01	0.01	0.04	0.02	0.00	0.00	0.00	0.00	0.00	0.00	0.00	0.01	0.03
Al2O3	22.16	20.47	21.88	21.76	21.92	0.05	21.84	22.03	21.74	21.70	21.93	21.85	21.55
Cr2O3	0.00	0.04	0.05	0.11	0.08	0.00	0.07	0.00	0.02	0.04	0.03	0.06	0.00
FeO	32.31	30.80	32.80	32.68	32.41	0.44	33.23	35.00	34.45	34.68	34.66	35.29	34.89
MgO	4.82	4.63	4.89	4.96	5.04	0.01	4.71	3.91	3.86	4.09	4.05	3.15	3.29
MnO	0.77	0.67	0.76	0.73	0.74	0.03	0.87	1.53	1.42	1.49	1.45	1.48	1.28
CaO	1.74	1.57	1.88	1.68	1.80	0.00	1.66	0.96	0.88	0.91	0.83	0.83	1.34
Na2O	0.02	0.00	0.00	0.00	0.03	0.00	0.01	0.04	0.03	0.00	0.04	0.02	0.02
K2O	0.00	0.00	0.00	0.00	0.00	0.00	0.00	0.00	0.00	0.00	0.00	0.00	0.00
Total	100.03	93.11	99.90	100.08	100.02	103.14	99.75	100.12	99.89	97.90	100.62	99.92	99.66
Atom Proportions													
Si	6.02	5.97	5.96	6.02	6.02	11.97	5.95	5.88	5.99	5.76	5.97	5.98	5.99
Ti	0.00	0.00	0.01	0.00	0.00	0.00	0.00	0.00	0.00	0.00	0.00	0.00	0.00
Al	4.12	4.10	4.09	4.05	4.07	0.01	4.10	4.16	4.10	4.21	4.10	4.13	4.08
Cr	0.00	0.01	0.01	0.01	0.01	0.00	0.01	0.00	0.00	0.01	0.00	0.01	0.00
Fe	4.26	4.35	4.35	4.31	4.27	0.04	4.42	4.69	4.60	4.78	4.60	4.74	4.69
Mg	1.13	1.17	1.16	1.17	1.18	0.00	1.12	0.93	0.92	1.00	0.96	0.75	0.79
Mn	0.10	0.10	0.10	0.10	0.10	0.00	0.12	0.21	0.19	0.21	0.20	0.20	0.17
Ca	0.29	0.29	0.32	0.28	0.27	0.00	0.28	0.17	0.15	0.16	0.14	0.14	0.23
Na	0.01	0.00	0.00	0.00	0.01	0.00	0.00	0.01	0.01	0.00	0.01	0.01	0.01
K	0.00	0.00	0.00	0.00	0.00	0.00	0.00	0.00	0.00	0.00	0.00	0.00	0.00
O	24.00	24.00	24.00	24.00	24.00	24.00	24.00	24.00	24.00	24.00	24.00	24.00	24.00
CatTot	15.93	15.98	15.99	15.95	15.94	12.03	16.00	16.05	15.98	16.13	15.98	15.96	15.97
Total	39.93	39.98	39.99	39.95	39.94	36.03	40.00	40.05	39.98	40.13	39.98	39.96	39.97
Molar Proportions													
Grossular	0.05	0.05	0.05	0.05	0.05	0.02	0.05	0.03	0.03	0.03	0.02	0.02	0.04
Pyrope	0.20	0.20	0.20	0.20	0.20	0.02	0.19	0.16	0.16	0.16	0.16	0.13	0.13
Almandine	0.74	0.74	0.73	0.74	0.73	0.90	0.74	0.78	0.78	0.78	0.78	0.81	0.80
Spessartine	0.02	0.02	0.02	0.02	0.02	0.06	0.02	0.03	0.03	0.03	0.03	0.03	0.03
Fe/(Fe+Mg)	0.79	0.79	0.79	0.79	0.78	0.98	0.80	0.83	0.83	0.83	0.83	0.86	0.86

B1.1. Garnet Compositional Analysis

Sample	5000 rim adj plag	5000 rim adj bt	5000 adj bt incl	5000 adj bt incl	5000 adj bt incl	5000 core	5000 garn1 core	5000 garn1 rim	5000 gar2 core	5000 gar2 rim	5000 rim	5000 core	5000 rim
Oxides													
SiO2	36.67	36.96	37.05	37.28	35.73	37.37	37.43	35.58	37.64	36.16	36.88	36.39	37.03
TiO2	0.00	0.00	0.00	0.02	0.03	0.02	0.00	0.00	0.00	0.00	0.04	0.01	0.03
Al2O3	21.42	21.66	21.50	21.75	21.71	21.69	21.83	21.45	22.01	21.64	21.82	20.05	21.34
Cr2O3	0.03	0.05	0.00	0.00	0.02	0.00	0.01	0.04	0.00	0.01	0.00	0.02	0.00
FeO	35.84	36.38	35.30	36.10	35.02	35.63	35.07	35.62	34.36	35.47	34.66	32.97	34.27
MgO	2.86	2.42	2.94	2.62	2.95	2.98	3.46	2.77	3.69	3.09	2.83	3.18	3.15
MnO	1.66	1.71	1.37	1.48	1.38	1.57	1.33	1.50	0.91	1.44	1.83	1.25	1.51
CaO	0.90	0.91	0.88	0.89	0.82	0.89	0.94	0.81	1.49	0.82	0.82	1.64	0.89
Na2O	0.00	0.05	0.03	0.01	0.00	0.02	0.02	0.01	0.04	0.01	0.00	0.05	0.03
K2O	0.00	0.00	0.00	0.00	0.00	0.00	0.00	0.00	0.00	0.00	0.00	0.00	0.00
Total	99.36	100.12	99.07	100.16	97.66	100.16	100.09	97.77	100.13	98.65	98.88	96.55	98.23
Atom Proportions													
Si	5.95	5.96	6.00	5.99	5.89	5.99	5.98	5.88	5.99	5.90	5.98	6.09	6.03
Ti	0.00	0.00	0.00	0.00	0.00	0.00	0.00	0.00	0.00	0.00	0.00	0.00	0.00
Al	4.10	4.12	4.11	4.12	4.22	4.10	4.11	4.18	4.13	4.17	4.17	3.95	4.09
Cr	0.00	0.01	0.00	0.00	0.00	0.00	0.00	0.01	0.00	0.00	0.00	0.00	0.00
Fe	4.87	4.91	4.78	4.85	4.83	4.78	4.69	4.92	4.57	4.84	4.70	4.61	4.67
Mg	0.69	0.58	0.71	0.63	0.72	0.71	0.83	0.68	0.87	0.75	0.68	0.79	0.76
Mn	0.23	0.23	0.19	0.20	0.19	0.21	0.18	0.21	0.12	0.20	0.25	0.18	0.21
Ca	0.16	0.16	0.15	0.15	0.15	0.15	0.16	0.14	0.25	0.14	0.14	0.29	0.16
Na	0.00	0.02	0.01	0.00	0.00	0.01	0.01	0.00	0.01	0.00	0.00	0.02	0.01
K	0.00	0.00	0.00	0.00	0.00	0.00	0.00	0.00	0.00	0.00	0.00	0.00	0.00
O	24.00	24.00	24.00	24.00	24.00	24.00	24.00	24.00	24.00	24.00	24.00	24.00	24.00
CatTot	16.00	15.98	15.95	15.95	16.00	15.96	15.96	16.03	15.95	16.01	15.93	15.94	15.93
Total	40.00	39.98	39.95	39.95	40.00	39.96	39.96	40.03	39.95	40.01	39.93	39.94	39.93
Molar Proportions													
Grossular	0.03	0.03	0.03	0.03	0.02	0.03	0.03	0.02	0.04	0.02	0.02	0.05	0.03
Pyrope	0.12	0.10	0.12	0.11	0.12	0.12	0.14	0.11	0.15	0.13	0.12	0.13	0.13
Almandine	0.82	0.83	0.82	0.83	0.82	0.82	0.80	0.83	0.79	0.82	0.81	0.79	0.81
Spessartine	0.04	0.04	0.03	0.03	0.03	0.04	0.03	0.04	0.02	0.03	0.04	0.03	0.04
Fe/(Fe+Mg)	0.88	0.89	0.87	0.89	0.87	0.87	0.85	0.88	0.84	0.87	0.87	0.85	0.86

Sample	5000 adj bt incl	5000 rim	5000 core	5000 rim	5002	5002	5002	5002	5002	5004a gar1 core	5004a gar1 rim	5004a gar2 core	5004a gar2 rim
Oxides													
SiO2	36.85	37.13	37.53	37.56	37.45	37.45	37.05	36.91	37.35	36.92	37.12	36.91	36.28
TiO2	0.00	0.03	0.00	0.01	0.00	0.03	0.00	0.00	0.00	0.00	0.00	0.00	0.01
Al2O3	20.81	21.71	21.71	22.23	21.65	21.88	21.77	21.53	21.67	21.31	21.29	20.58	20.67
Cr2O3	0.00	0.07	0.01	0.01	0.02	0.04	0.06	0.00	0.00	0.02	0.03	0.06	0.00
FeO	34.00	34.56	34.66	33.58	34.58	33.44	34.39	33.78	34.24	34.29	34.97	34.61	33.96
MgO	2.75	3.16	3.54	3.64	3.13	3.45	3.48	3.25	3.42	3.21	3.06	3.49	2.20
MnO	1.80	1.53	1.07	1.38	2.05	1.91	2.01	2.17	1.98	1.57	1.70	1.58	2.67
CaO	0.92	1.07	1.54	0.91	0.93	1.06	1.09	1.04	1.05	0.92	0.98	1.03	1.00
Na2O	0.04	0.03	0.00	0.05	0.04	0.03	0.02	0.00	0.04	0.02	0.00	0.01	0.02
K2O	0.00	0.00	0.00	0.00	0.00	0.00	0.00	0.00	0.00	0.00	0.00	0.00	0.00
Total	96.97	99.30	100.06	99.36	99.76	99.29	99.85	98.67	99.75	98.26	99.15	98.26	96.81
Atom Proportions													
Si	6.08	5.99	5.99	6.00	6.02	6.01	5.96	5.99	5.99	6.01	6.01	6.03	6.04
Ti	0.00	0.00	0.00	0.00	0.00	0.00	0.00	0.00	0.00	0.00	0.00	0.00	0.00
Al	4.05	4.13	4.09	4.19	4.08	4.14	4.12	4.12	4.10	4.09	4.06	3.96	4.06
Cr	0.00	0.01	0.00	0.00	0.00	0.01	0.01	0.00	0.00	0.00	0.00	0.01	0.00
Fe	4.69	4.66	4.63	4.49	4.65	4.49	4.62	4.58	4.59	4.67	4.74	4.73	4.73
Mg	0.68	0.76	0.84	0.87	0.75	0.82	0.83	0.79	0.82	0.78	0.74	0.85	0.55
Mn	0.22	0.21	0.15	0.19	0.28	0.26	0.27	0.30	0.27	0.22	0.23	0.22	0.38
Ca	0.16	0.18	0.26	0.16	0.16	0.18	0.19	0.18	0.18	0.16	0.17	0.18	0.18
Na	0.01	0.01	0.00	0.02	0.01	0.01	0.01	0.00	0.01	0.01	0.00	0.00	0.01
K	0.00	0.00	0.00	0.00	0.00	0.00	0.00	0.00	0.00	0.00	0.00	0.00	0.00
O	24.00	24.00	24.00	24.00	24.00	24.00	24.00	24.00	24.00	24.00	24.00	24.00	24.00
CatTot	15.90	15.95	15.96	15.91	15.95	15.92	15.99	15.95	15.96	15.94	15.96	15.98	15.93
Total	39.90	39.95	39.96	39.91	39.95	39.92	39.99	39.95	39.96	39.94	39.96	39.98	39.93
Molar Proportions													
Grossular	0.03	0.03	0.04	0.03	0.03	0.03	0.03	0.03	0.03	0.03	0.03	0.03	0.03
Pyrope	0.12	0.13	0.14	0.15	0.13	0.14	0.14	0.13	0.14	0.13	0.13	0.14	0.09
Almandine	0.82	0.80	0.79	0.79	0.80	0.78	0.78	0.78	0.78	0.80	0.81	0.79	0.81
Spessartine	0.04	0.04	0.02	0.03	0.05	0.05	0.05	0.05	0.05	0.04	0.04	0.04	0.06
Fe/(Fe+Mg)	0.87	0.86	0.85	0.84	0.86	0.84	0.85	0.85	0.85	0.86	0.87	0.85	0.90

B1.1. Garnet Compositional Analysis

Sample	5007 garl core	5007 garn1 rim	5008 garl core	5008 garl rim	5011 core	5011 rim	5011 core	5011 rim	5011 core	5011 adj incl1	5011 adj incl2	5011 rim adj bt	5011 adj bt incl
Oxides													
SiO2	35.82	36.74	36.63	36.37	36.33	37.19	37.03	37.02	36.66	36.61	37.81	36.77	37.19
TiO2	0.00	0.00	0.00	0.00	0.00	0.02	0.00	0.01	0.01	0.01	0.03	0.06	0.04
Al2O3	20.73	21.19	21.18	21.24	21.59	21.58	22.33	22.20	21.26	21.80	22.30	21.45	21.80
Cr2O3	0.00	0.00	0.00	0.01	0.00	0.07	0.00	0.04	0.04	0.02	0.00	0.10	0.00
FeO	32.78	32.74	30.27	30.40	34.13	34.64	34.22	34.56	30.49	34.46	33.35	35.05	33.62
MgO	3.64	2.91	2.89	2.79	3.79	3.49	3.74	3.50	3.94	3.69	3.89	3.35	3.74
MnO	3.43	4.03	5.90	6.67	1.03	1.05	0.93	1.22	0.77	0.92	0.96	0.96	0.98
CaO	0.93	1.08	0.96	0.93	1.99	1.51	1.75	1.72	1.76	1.65	1.57	1.46	1.68
Na2O	0.00	0.04	0.00	0.04	0.01	0.01	0.00	0.00	0.01	0.02	0.01	0.00	0.02
K2O	0.00	0.00	0.00	0.00	0.00	0.00	0.00	0.00	0.00	0.00	0.00	0.00	0.00
Total	97.32	98.70	97.83	98.46	98.88	99.56	100.00	100.26	94.95	99.18	99.92	99.22	99.07
Atom Proportions													
Si	5.93	5.99	6.01	5.96	5.89	5.98	5.91	5.91	6.07	5.91	6.00	5.95	5.98
Ti	0.00	0.00	0.00	0.00	0.00	0.00	0.00	0.00	0.00	0.00	0.00	0.01	0.00
Al	4.04	4.07	4.09	4.10	4.13	4.09	4.20	4.18	4.15	4.15	4.17	4.09	4.13
Cr	0.00	0.00	0.00	0.00	0.00	0.01	0.00	0.01	0.01	0.00	0.00	0.01	0.00
Fe	4.54	4.46	4.15	4.16	4.63	4.66	4.57	4.61	4.22	4.65	4.42	4.74	4.52
Mg	0.90	0.71	0.71	0.68	0.92	0.84	0.89	0.83	0.97	0.89	0.92	0.81	0.90
Mn	0.48	0.56	0.82	0.92	0.14	0.14	0.13	0.17	0.11	0.13	0.13	0.13	0.13
Ca	0.17	0.19	0.17	0.16	0.35	0.26	0.30	0.29	0.31	0.29	0.27	0.25	0.29
Na	0.00	0.01	0.00	0.01	0.01	0.00	0.00	0.00	0.00	0.01	0.00	0.00	0.01
K	0.00	0.00	0.00	0.00	0.00	0.00	0.00	0.00	0.00	0.00	0.00	0.00	0.00
O	24.00	24.00	24.00	24.00	24.00	24.00	24.00	24.00	24.00	24.00	24.00	24.00	24.00
CatTot	16.06	15.98	15.95	16.00	16.05	15.97	15.99	16.00	15.85	16.02	15.92	15.99	15.96
Total	40.06	39.98	39.95	40.00	40.05	39.97	39.99	40.00	39.85	40.02	39.92	39.99	39.96
Molar Proportions													
Grossular	0.03	0.03	0.03	0.03	0.06	0.04	0.05	0.05	0.06	0.05	0.05	0.04	0.05
Pyrope	0.15	0.12	0.12	0.11	0.15	0.14	0.15	0.14	0.17	0.15	0.16	0.14	0.15
Almandine	0.75	0.76	0.71	0.70	0.77	0.79	0.78	0.78	0.75	0.78	0.77	0.80	0.77
Spessartine	0.08	0.09	0.14	0.16	0.02	0.02	0.02	0.03	0.02	0.02	0.02	0.02	0.02
Fe(Fe+Mg)	0.83	0.86	0.86	0.86	0.83	0.85	0.84	0.85	0.81	0.84	0.83	0.85	0.83

Sample	5011 rim	5011 core	5011 rim	5011 rim adj bt	5011 rim	5011 core	5011 rim	5011 adj bt incl	5023	5023	5023	5023	5023
Oxides													
SiO2	37.90	37.13	36.78	36.86	37.88	38.32	100.75	101.31	37.76	37.53	38.88	37.32	38.07
TiO2	0.00	0.00	2.36	1.65	0.03	0.00	0.00	0.00	0.00	0.01	0.02	0.00	0.00
Al2O3	22.03	21.43	19.29	19.46	22.05	22.31	0.04	0.06	21.81	21.62	21.51	21.99	21.99
Cr2O3	0.00	0.05	0.05	0.04	0.04	0.01	0.02	0.02	0.00	0.03	0.00	0.00	0.00
FeO	33.67	33.25	19.14	19.82	33.11	31.96	0.09	0.23	35.30	34.31	34.89	35.68	35.13
MgO	3.55	3.88	10.79	10.71	3.99	4.23	0.00	0.00	3.41	3.94	3.68	3.78	4.04
MnO	1.07	1.04	0.00	0.01	1.16	0.99	0.05	0.01	1.51	1.39	1.52	1.51	1.31
CaO	1.73	1.73	0.00	0.06	1.38	1.96	0.01	0.01	1.08	1.05	1.01	1.03	1.03
Na2O	0.01	0.02	0.25	0.20	0.03	0.00	0.00	0.00	0.07	0.01	0.02	0.02	0.00
K2O	0.00	0.00	7.75	7.68	0.00	0.00	0.00	0.00	0.00	0.00	0.00	0.00	0.00
Total	99.98	98.53	96.42	96.49	99.67	99.77	100.97	101.64	100.94	99.89	99.43	101.35	101.56
Atom Proportions													
Si	6.03	6.00	5.94	5.96	6.02	6.05	11.99	11.98	5.99	6.00	5.95	5.92	5.99
Ti	0.00	0.00	0.29	0.20	0.00	0.00	0.00	0.00	0.00	0.00	0.00	0.00	0.00
Al	4.13	4.08	3.67	3.71	4.13	4.15	0.01	0.01	4.08	4.07	4.09	4.11	4.08
Cr	0.00	0.01	0.01	0.00	0.01	0.00	0.00	0.00	0.00	0.00	0.00	0.00	0.00
Fe	4.48	4.49	2.59	2.68	4.40	4.22	0.01	0.02	4.69	4.59	4.71	4.73	4.62
Mg	0.84	0.94	2.60	2.58	0.95	1.00	0.00	0.00	0.81	0.94	0.86	0.89	0.95
Mn	0.15	0.14	0.00	0.00	0.16	0.13	0.01	0.00	0.20	0.19	0.21	0.20	0.17
Ca	0.30	0.30	0.00	0.01	0.24	0.33	0.00	0.00	0.18	0.18	0.18	0.18	0.17
Na	0.00	0.01	0.08	0.06	0.01	0.00	0.00	0.00	0.02	0.00	0.01	0.01	0.00
K	0.00	0.00	1.60	1.59	0.00	0.00	0.00	0.00	0.00	0.00	0.00	0.00	0.00
O	24.00	24.00	24.00	24.00	24.00	24.00	24.00	24.00	24.00	24.00	24.00	24.00	24.00
CatTot	15.91	15.96	16.77	16.80	15.91	15.88	12.01	12.02	15.98	15.97	16.00	16.03	15.98
Total	39.91	39.96	40.77	40.80	39.91	39.88	36.01	36.02	39.98	39.97	40.00	40.03	39.98
Molar Proportions													
Grossular	0.05	0.05	0.00	0.00	0.04	0.06	0.07	0.08	0.03	0.03	0.03	0.03	0.03
Pyrope	0.15	0.16	0.50	0.49	0.16	0.18	0.00	0.00	0.14	0.16	0.14	0.15	0.16
Almandine	0.78	0.77	0.50	0.51	0.77	0.74	0.60	0.88	0.80	0.78	0.79	0.79	0.78
Spessartine	0.03	0.02	0.00	0.00	0.03	0.02	0.33	0.04	0.03	0.03	0.03	0.03	0.03
Fe(Fe+Mg)	0.84	0.83	0.50	0.51	0.82	0.81	1.00	1.00	0.85	0.83	0.85	0.84	0.83

B1.1. Garnet Compositional Analysis

Sample	5023	5088 gar core	5088 gar core	5088 gar core	5088 gar cl to rim	5088 gar near rim	5088 gar rim	5088 gar rim	5088 gar rim	5088 gar rim	5088 gar2 core	5088 gar2 rim	5088 gar2 rim
Oxides													
SiO2	38.13	37.66	36.88	35.24	37.30	36.99	35.92	35.75	36.47	35.82	36.18	36.13	34.94
TiO2	0.00	0.00	0.00	0.00	0.00	0.00	0.00	0.00	0.00	0.01	0.00	0.02	0.03
Al2O3	21.84	22.01	21.63	21.85	22.07	21.70	21.93	21.78	22.25	21.78	21.71	21.53	21.78
Cr2O3	0.00	0.03	0.00	0.00	0.06	0.02	0.00	0.01	0.00	0.05	0.00	0.03	0.10
FeO	35.16	34.79	33.67	34.41	34.62	35.20	35.19	34.65	35.37	35.51	35.00	35.70	35.60
MgO	3.99	3.94	3.92	3.89	3.77	3.47	2.87	3.14	2.75	2.35	3.60	2.62	2.83
MnO	1.24	1.59	1.46	1.53	1.50	1.73	2.07	2.01	2.31	2.62	1.70	2.28	2.11
CaO	0.97	0.89	0.99	0.86	0.95	0.88	0.88	0.92	0.93	0.91	0.91	0.94	0.92
Na2O	0.05	0.00	0.01	0.04	0.02	0.03	0.00	0.04	0.01	0.01	0.04	0.00	0.00
K2O	0.00	0.00	0.00	0.00	0.00	0.00	0.00	0.00	0.00	0.00	0.00	0.00	0.00
Total	101.38	100.92	98.56	97.82	100.27	100.02	98.86	98.29	100.09	99.07	99.13	99.14	98.31
Atom Proportions													
Si	6.01	5.97	5.97	5.80	5.95	5.94	5.86	5.86	5.88	5.86	5.87	5.90	5.77
Ti	0.00	0.00	0.00	0.00	0.00	0.00	0.00	0.00	0.00	0.00	0.00	0.00	0.00
Al	4.06	4.11	4.13	4.24	4.15	4.11	4.22	4.21	4.23	4.20	4.15	4.14	4.24
Cr	0.00	0.00	0.00	0.00	0.01	0.00	0.00	0.00	0.00	0.01	0.00	0.00	0.01
Fe	4.63	4.61	4.56	4.73	4.62	4.73	4.80	4.75	4.77	4.86	4.75	4.86	4.92
Mg	0.94	0.93	0.95	0.95	0.89	0.83	0.70	0.77	0.66	0.57	0.87	0.61	0.70
Mn	0.17	0.21	0.20	0.21	0.20	0.23	0.29	0.28	0.32	0.36	0.23	0.32	0.30
Ca	0.17	0.15	0.17	0.15	0.16	0.15	0.15	0.16	0.16	0.16	0.16	0.16	0.16
Na	0.01	0.00	0.00	0.01	0.01	0.01	0.00	0.01	0.00	0.00	0.01	0.00	0.00
K	0.00	0.00	0.00	0.00	0.00	0.00	0.00	0.00	0.00	0.00	0.00	0.00	0.00
O	24.00	24.00	24.00	24.00	24.00	24.00	24.00	24.00	24.00	24.00	24.00	24.00	24.00
CatTot	15.97	15.98	15.97	16.09	15.96	16.01	16.03	16.04	16.01	16.03	16.06	16.02	16.10
Total	39.97	39.98	39.97	40.09	39.96	40.01	40.03	40.04	40.01	40.03	40.06	40.02	40.10
Molar Proportions													
Grossular	0.03	0.03	0.03	0.02	0.03	0.03	0.03	0.03	0.03	0.03	0.03	0.03	0.03
Pyrope	0.16	0.16	0.16	0.16	0.15	0.14	0.12	0.13	0.11	0.10	0.14	0.10	0.11
Almandine	0.79	0.78	0.78	0.78	0.79	0.80	0.81	0.80	0.81	0.82	0.79	0.82	0.81
Spessartine	0.03	0.04	0.03	0.04	0.03	0.04	0.05	0.05	0.05	0.06	0.04	0.05	0.05
Fe/(Fe+Mg)	0.83	0.83	0.83	0.83	0.84	0.85	0.87	0.86	0.86	0.89	0.85	0.89	0.88

Sample	5088 gar3 core	5088 gar3 rim	5088 gar4 core	5088 gar4 near rim	5088 gar4 rim	5088 gar5 core	5088 gar5 rim	5088 core	5088 rim near biot2	5100 core	5100 adj bt15039	5100 core	5100 rim
Oxides													
SiO2	34.31	35.02	35.84	37.35	36.31	34.00	36.16	37.14	36.69	37.33	37.27	37.35	37.50
TiO2	0.00	0.01	0.00	0.00	0.00	0.00	0.04	0.00	0.00	0.00	0.01	0.01	0.00
Al2O3	21.68	21.89	21.66	21.71	21.61	22.05	21.83	21.37	21.35	21.59	21.91	21.55	21.52
Cr2O3	0.02	0.02	0.00	0.07	0.03	0.03	0.10	0.02	0.00	0.00	0.01	0.06	0.00
FeO	33.95	34.89	34.92	34.97	35.74	34.20	34.40	32.90	32.44	33.25	33.41	33.72	33.78
MgO	3.79	3.29	3.47	3.35	2.68	3.95	3.36	3.97	3.40	3.12	2.83	3.05	2.76
MnO	1.56	1.90	1.97	2.09	2.42	1.54	1.88	2.17	2.30	2.27	2.48	2.38	2.73
CaO	0.84	0.94	0.98	0.98	0.89	0.93	0.89	1.80	2.90	1.70	1.70	1.81	1.81
Na2O	0.03	0.02	0.01	0.04	0.00	0.02	0.00	0.00	0.03	0.00	0.01	0.02	0.00
K2O	0.00	0.00	0.00	0.00	0.00	0.00	0.00	0.00	0.00	0.00	0.00	0.00	0.00
Total	96.18	97.96	98.85	100.54	99.67	96.71	98.66	99.36	99.10	99.26	99.63	99.95	99.90
Atom Proportions													
Si	5.75	5.78	5.85	5.97	5.90	5.67	5.89	5.97	5.93	6.01	5.99	5.99	6.02
Ti	0.00	0.00	0.00	0.00	0.00	0.00	0.00	0.00	0.00	0.00	0.00	0.00	0.00
Al	4.28	4.26	4.17	4.09	4.14	4.34	4.19	4.05	4.07	4.10	4.15	4.07	4.07
Cr	0.00	0.00	0.00	0.01	0.00	0.00	0.01	0.00	0.00	0.00	0.00	0.01	0.00
Fe	4.76	4.81	4.77	4.67	4.86	4.77	4.68	4.42	4.39	4.48	4.49	4.52	4.54
Mg	0.95	0.81	0.85	0.80	0.65	0.98	0.81	0.95	0.82	0.75	0.68	0.73	0.66
Mn	0.22	0.27	0.27	0.28	0.33	0.22	0.26	0.30	0.31	0.31	0.34	0.32	0.37
Ca	0.15	0.17	0.17	0.16	0.16	0.17	0.16	0.31	0.50	0.29	0.29	0.31	0.28
Na	0.01	0.01	0.00	0.01	0.00	0.01	0.00	0.00	0.01	0.00	0.00	0.01	0.00
K	0.00	0.00	0.00	0.00	0.00	0.00	0.00	0.00	0.00	0.00	0.00	0.00	0.00
O	24.00	24.00	24.00	24.00	24.00	24.00	24.00	24.00	24.00	24.00	24.00	24.00	24.00
CatTot	16.12	16.10	16.07	15.99	16.03	16.16	16.01	16.00	16.04	15.94	15.94	15.97	15.94
Total	40.12	40.10	40.07	39.99	40.03	40.16	40.01	40.00	40.04	39.94	39.94	39.97	39.94
Molar Proportions													
Grossular	0.02	0.03	0.03	0.03	0.03	0.03	0.03	0.05	0.08	0.05	0.05	0.06	0.05
Pyrope	0.16	0.13	0.14	0.14	0.11	0.16	0.14	0.16	0.14	0.13	0.12	0.12	0.11
Almandine	0.78	0.79	0.79	0.79	0.81	0.78	0.79	0.74	0.73	0.77	0.77	0.77	0.78
Spessartine	0.04	0.04	0.04	0.05	0.06	0.04	0.04	0.05	0.05	0.05	0.06	0.05	0.06
Fe/(Fe+Mg)	0.83	0.86	0.85	0.85	0.88	0.83	0.85	0.82	0.84	0.86	0.87	0.86	0.87

B1.1. Garnet Compositional Analysis

Sample	5100 rim	5100 core	5100 rim	5100 rim	5100 core	5100 rim	5100 rim adj to bt	5100	5100	5100	5100	5100 rim	5100 rim gar 2
Oxides													
SiO2	37.48	36.33	37.37	36.31	37.13	36.82	37.36	36.77	36.77	36.68	37.53	37.65	37.06
TiO2	0.00	0.02	0.01	0.02	0.05	0.05	0.00	0.04	0.00	0.05	0.00	0.00	0.00
Al2O3	21.83	21.42	21.42	21.47	21.51	21.29	21.24	21.08	20.95	21.22	22.10	21.76	21.56
Cr2O3	0.00	0.02	0.05	0.01	0.08	0.00	0.03	0.00	0.03	0.04	0.06	0.09	0.08
FeO	32.27	31.94	33.00	32.81	32.42	32.38	33.23	30.77	31.24	30.85	31.86	32.61	33.80
MgO	2.86	3.13	2.63	2.85	3.14	2.91	2.96	3.25	2.99	3.19	3.29	3.08	3.20
MnO	2.70	2.64	3.02	2.67	2.51	2.54	2.65	2.65	2.36	2.67	2.88	2.75	2.65
CaO	1.59	1.60	1.63	1.61	1.57	1.53	1.77	1.43	1.64	1.56	1.76	1.59	1.59
Na2O	0.02	0.00	0.01	0.00	0.00	0.01	0.03	0.03	0.04	0.02	0.00	0.01	0.03
K2O	0.00	0.00	0.00	0.00	0.00	0.00	0.00	0.00	0.00	0.00	0.00	0.00	0.00
Total	98.75	97.10	99.13	97.75	98.40	97.53	99.27	96.01	96.01	96.30	99.48	99.54	99.78
Atom Proportions													
Si	6.05	5.96	6.04	5.96	6.02	6.03	6.03	6.08	6.09	6.05	6.00	6.03	5.96
Ti	0.00	0.00	0.00	0.00	0.01	0.01	0.00	0.00	0.00	0.01	0.00	0.00	0.00
Al	4.15	4.15	4.08	4.15	4.11	4.11	4.04	4.11	4.09	4.13	4.17	4.11	4.09
Cr	0.00	0.00	0.01	0.00	0.01	0.00	0.00	0.00	0.00	0.01	0.01	0.01	0.01
Fe	4.36	4.39	4.46	4.50	4.40	4.43	4.49	4.25	4.33	4.26	4.26	4.37	4.52
Mg	0.69	0.77	0.63	0.70	0.76	0.71	0.71	0.80	0.74	0.78	0.79	0.74	0.77
Mn	0.37	0.37	0.41	0.37	0.34	0.35	0.36	0.37	0.33	0.37	0.39	0.37	0.36
Ca	0.28	0.28	0.28	0.28	0.27	0.27	0.31	0.25	0.29	0.28	0.30	0.27	0.27
Na	0.01	0.00	0.00	0.00	0.00	0.01	0.01	0.01	0.01	0.01	0.00	0.01	0.01
K	0.00	0.00	0.00	0.00	0.00	0.00	0.00	0.00	0.00	0.00	0.00	0.00	0.00
O	24.00	24.00	24.00	24.00	24.00	24.00	24.00	24.00	24.00	24.00	24.00	24.00	24.00
CatTot	15.88	15.96	15.92	15.97	15.92	15.91	15.96	15.87	15.87	15.88	15.91	15.91	15.99
Total	39.88	39.96	39.92	39.97	39.92	39.91	39.96	39.87	39.87	39.88	39.91	39.91	39.99
Molar Proportions													
Grossular	0.05	0.05	0.05	0.05	0.05	0.05	0.05	0.04	0.05	0.05	0.05	0.05	0.05
Pyrope	0.12	0.13	0.11	0.12	0.13	0.12	0.12	0.14	0.13	0.14	0.14	0.13	0.13
Almandine	0.77	0.76	0.77	0.77	0.76	0.77	0.76	0.75	0.76	0.75	0.74	0.76	0.76
Spessartine	0.06	0.06	0.07	0.06	0.06	0.06	0.06	0.07	0.06	0.07	0.07	0.07	0.06
Fe/(Fe+Mg)	0.86	0.85	0.88	0.87	0.85	0.86	0.86	0.84	0.85	0.84	0.84	0.86	0.85

Sample	5100 gar 2 core	5100 gar2 rim adj bt	5131 garcore1	5131 garrim1	5131 garcore1b	5131 garrim1b	5131 garcore2	5131 gar2 near biot	5131 gar2 rim	5131 gar3 core	5131 gar3 near biot	5131 gar3 rim	7006b core
Oxides													
SiO2	36.90	37.35	37.21	36.85	36.86	37.06	37.01	36.83	36.25	36.78	36.84	36.61	35.64
TiO2	0.00	0.00	0.04	0.01	0.00	0.00	0.00	0.03	0.06	0.00	0.00	0.00	0.00
Al2O3	21.71	21.97	21.72	21.51	21.72	21.62	21.76	21.53	21.06	21.80	21.06	21.62	22.07
Cr2O3	0.00	0.00	0.07	0.07	0.00	0.04	0.07	0.01	0.05	0.00	0.02	0.07	0.01
FeO	31.88	32.15	33.90	33.56	34.52	34.90	32.50	33.30	33.67	33.90	33.78	34.22	34.77
MgO	3.25	2.92	3.73	3.31	3.14	2.43	3.68	3.63	3.30	3.86	3.74	3.03	3.23
MnO	2.57	2.58	2.31	2.33	2.46	3.19	1.96	2.06	2.25	1.89	1.96	2.37	2.61
CaO	1.74	1.71	0.91	0.88	0.93	0.88	0.93	0.81	0.89	0.88	0.87	0.86	0.88
Na2O	0.00	0.05	0.04	0.53	0.00	0.04	0.06	0.02	0.05	0.05	0.01	0.04	0.03
K2O	0.00	0.00	0.00	0.00	0.00	0.00	0.00	0.00	0.00	0.00	0.00	0.00	0.00
Total	98.05	98.73	99.91	99.05	99.62	100.14	97.96	98.23	97.56	98.96	98.26	98.82	99.24
Atom Proportions													
Si	6.00	6.02	5.96	5.97	5.95	5.97	6.00	5.99	5.97	5.95	6.00	5.95	5.80
Ti	0.00	0.00	0.00	0.00	0.00	0.00	0.00	0.00	0.01	0.00	0.00	0.00	0.00
Al	4.16	4.18	4.10	4.11	4.13	4.11	4.16	4.12	4.08	4.12	4.04	4.14	4.24
Cr	0.00	0.00	0.01	0.01	0.00	0.00	0.01	0.00	0.01	0.00	0.00	0.01	0.00
Fe	4.33	4.34	4.54	4.54	4.66	4.71	4.41	4.53	4.63	4.58	4.80	4.65	4.74
Mg	0.79	0.70	0.89	0.80	0.75	0.58	0.89	0.88	0.81	0.93	0.91	0.74	0.78
Mn	0.35	0.35	0.31	0.32	0.33	0.44	0.27	0.28	0.31	0.26	0.27	0.33	0.36
Ca	0.30	0.30	0.16	0.15	0.16	0.16	0.16	0.14	0.16	0.15	0.15	0.15	0.15
Na	0.00	0.01	0.01	0.17	0.00	0.01	0.02	0.01	0.02	0.01	0.00	0.01	0.01
K	0.00	0.00	0.00	0.00	0.00	0.00	0.00	0.00	0.00	0.00	0.00	0.00	0.00
O	24.00	24.00	24.00	24.00	24.00	24.00	24.00	24.00	24.00	24.00	24.00	24.00	24.00
CatTot	15.93	15.90	15.99	16.06	15.99	15.97	15.92	15.96	15.99	16.00	15.98	15.98	16.08
Total	39.93	39.90	39.99	40.06	39.99	39.97	39.92	39.96	39.99	40.00	39.98	39.98	40.08
Molar Proportions													
Grossular	0.05	0.05	0.03	0.03	0.03	0.03	0.03	0.02	0.03	0.03	0.03	0.03	0.03
Pyrope	0.14	0.12	0.15	0.14	0.13	0.10	0.16	0.15	0.14	0.16	0.15	0.13	0.13
Almandine	0.75	0.76	0.77	0.78	0.79	0.80	0.77	0.78	0.78	0.77	0.78	0.79	0.79
Spessartine	0.06	0.06	0.05	0.05	0.06	0.07	0.05	0.05	0.05	0.04	0.05	0.06	0.06
Fe/(Fe+Mg)	0.85	0.86	0.84	0.85	0.86	0.89	0.83	0.84	0.85	0.83	0.84	0.86	0.86

B1.1. Garnet Compositional Analysis

Sample	7006b rim
Oxides	
SiO2	36.85
TiO2	0.00
Al2O3	21.64
Cr2O3	0.00
FeO	34.74
MgO	3.14
MnO	2.41
CaO	0.83
Na2O	0.02
K2O	0.00
Total	99.64
Atom Proportions	
Si	5.95
Ti	0.00
Al	4.12
Cr	0.00
Fe	4.69
Mg	0.76
Mn	0.33
Ca	0.14
Na	0.01
K	0.00
O	24.00
CatTot	15.99
Total	39.99
Molar Proportions	
Grossular	0.02
Pyrope	0.13
Almandine	0.79
Spessartine	0.06
Fe/(Fe+Mg)	0.86

Sample
Oxides
SiO2
TiO2
Al2O3
Cr2O3
FeO
MgO
MnO
CaO
Na2O
K2O
Total
Atom Proportions
Si
Ti
Al
Cr
Fe
Mg
Mn
Ca
Na
K
O
CatTot
Total
Molar Proportions
Grossular
Pyrope
Almandine
Spessartine
Fe/(Fe+Mg)

B1.2. Compositional Analysis of Garnet Profiles

Sample	5000 garnet profile	5000 garnet profile	5000 garnet profile	5000 garnet profile	5000 garnet profile	5000 garnet profile	5000 garnet profile	5000 garnet profile	5000 garnet profile	5000 garnet profile	5000 garnet profile	5000 garnet profile	5000 garnet profile	5000 garnet profile
Scan #	scan #1	scan #1	scan #1	scan #1	scan #1	scan #1	scan #1	scan #1	scan #1	scan #1	scan #1	scan #1	scan #1	scan #1
Oxides														
SiO2	37.00	36.95	37.01	36.52	37.27	37.31	36.53	37.17	37.30	37.05	37.43	37.28	34.77	37.57
TiO2	0.00	0.01	0.01	0.00	0.00	0.00	0.00	0.00	0.00	0.02	0.01	0.00	0.03	0.00
Al2O3	21.71	21.76	22.01	22.06	22.35	21.86	22.04	21.86	22.24	21.92	22.07	21.91	21.67	22.24
Cr2O3	0.00	0.02	0.00	0.03	0.02	0.00	0.05	0.04	0.01	0.00	0.00	0.00	0.03	0.01
FeO	36.98	36.43	36.28	36.86	36.42	35.11	36.83	36.45	36.21	36.42	36.40	36.02	34.84	36.30
MgO	3.36	3.40	3.37	3.46	3.44	3.40	3.50	3.48	3.40	3.48	3.48	3.48	3.08	2.99
MnO	1.43	1.50	1.82	1.34	1.80	1.46	1.39	1.30	1.34	1.30	1.39	1.27	1.24	1.40
CaO	0.94	0.91	0.92	0.98	1.01	1.14	1.21	1.25	1.34	1.31	1.36	1.31	1.28	1.51
Na2O	0.05	0.03	0.00	0.02	0.00	0.00	0.05	0.00	0.01	0.05	0.02	0.02	0.02	0.04
K2O	0.00	0.00	0.00	0.00	0.00	0.00	0.00	0.00	0.00	0.00	0.00	0.00	0.00	0.00
Total	100.46	100.00	101.20	100.27	102.01	100.09	100.40	100.52	100.84	100.56	101.17	100.19	97.74	101.87
Atom Proportions														
Si	5.93	5.94	5.90	5.87	5.88	5.96	5.86	5.94	5.93	5.92	5.94	5.96	5.75	5.96
Ti	0.00	0.00	0.00	0.00	0.00	0.00	0.00	0.00	0.00	0.00	0.00	0.00	0.00	0.00
Al	4.10	4.12	4.13	4.18	4.16	4.09	4.17	4.11	4.17	4.13	4.12	4.11	4.22	4.16
Cr	0.00	0.00	0.00	0.00	0.00	0.00	0.01	0.01	0.00	0.00	0.00	0.00	0.00	0.00
Fe	4.82	4.76	4.83	4.82	4.81	4.71	4.76	4.74	4.68	4.73	4.70	4.68	4.81	4.68
Mg	0.80	0.82	0.80	0.83	0.81	0.81	0.84	0.82	0.81	0.83	0.82	0.83	0.85	0.71
Mn	0.19	0.20	0.22	0.18	0.20	0.20	0.19	0.18	0.18	0.18	0.19	0.17	0.17	0.19
Ca	0.16	0.16	0.16	0.17	0.17	0.20	0.21	0.21	0.23	0.22	0.23	0.22	0.23	0.26
Na	0.01	0.01	0.00	0.01	0.00	0.00	0.02	0.00	0.00	0.02	0.01	0.01	0.01	0.01
K	0.00	0.00	0.00	0.00	0.00	0.00	0.00	0.00	0.00	0.00	0.00	0.00	0.00	0.00
O	24.00	24.00	24.00	24.00	24.00	24.00	24.00	24.00	24.00	24.00	24.00	24.00	24.00	24.00
CatTot	16.03	16.01	16.04	16.05	16.04	15.98	16.06	16.01	15.98	16.02	16.00	15.98	16.14	15.97
Total	40.03	40.01	40.04	40.05	40.04	39.98	40.06	40.01	39.98	40.02	40.00	39.98	40.14	39.97
Molar Proportions														
Grossular	0.03	0.03	0.03	0.03	0.03	0.03	0.03	0.04	0.04	0.04	0.04	0.04	0.04	0.04
Pyrope	0.13	0.14	0.13	0.14	0.14	0.14	0.14	0.14	0.14	0.14	0.14	0.14	0.15	0.12
Almandine	0.81	0.80	0.80	0.80	0.80	0.80	0.79	0.80	0.79	0.79	0.79	0.79	0.78	0.80
Spessartine	0.03	0.03	0.04	0.03	0.03	0.03	0.03	0.03	0.03	0.03	0.03	0.03	0.03	0.03
Fe/Fe+Mg	0.86	0.85	0.86	0.85	0.86	0.85	0.85	0.85	0.85	0.85	0.85	0.85	0.84	0.87

Sample	5000 garnet profile	5000 garnet profile	5000 garnet profile	5000 garnet profile	5000 garnet profile	5000 garnet profile	5000 garnet profile	5000 garnet profile	5000 garnet profile	5000 garnet profile	5000 garnet profile	5000 garnet profile	5000 garnet profile	5000 garnet profile
Scan #	scan #1	scan #1	scan #1	scan #1	scan #1	scan #1	scan #1	scan #1	scan #1	scan #1	scan #1	scan #2	scan #2	scan #2
Oxides														
SiO2	37.00	36.98	36.67	36.71	37.36	37.10	37.24	37.31	37.07	36.49	37.04	37.11	37.07	37.18
TiO2	0.01	0.00	0.02	0.03	0.00	0.01	0.00	0.00	0.00	0.01	0.00	0.00	0.02	0.00
Al2O3	21.74	21.47	21.69	21.86	21.70	21.98	21.94	21.86	21.85	21.20	21.73	21.87	21.45	21.91
Cr2O3	0.01	0.01	0.01	0.01	0.00	0.00	0.00	0.00	0.04	0.00	0.00	0.00	0.00	0.02
FeO	34.88	35.00	35.17	34.52	35.14	34.34	35.16	34.97	35.19	35.88	35.82	35.00	35.30	34.67
MgO	3.29	3.37	3.45	3.47	3.43	3.35	3.42	3.45	3.33	3.18	3.17	3.48	3.44	3.50
MnO	1.25	1.30	1.36	1.26	1.42	1.40	1.43	1.43	1.31	1.47	1.55	1.45	1.56	1.45
CaO	1.47	1.49	1.35	1.33	1.31	1.18	1.24	1.14	1.08	1.03	0.96	0.83	0.88	0.83
Na2O	0.01	0.01	0.03	0.00	0.01	0.00	0.01	0.02	0.03	0.01	0.03	0.00	0.02	0.03
K2O	0.00	0.00	0.00	0.00	0.00	0.00	0.00	0.00	0.00	0.00	0.00	0.00	0.00	0.00
Total	99.63	99.61	99.79	99.19	100.36	99.33	100.15	100.16	99.90	99.28	100.21	100.34	99.86	99.70
Atom Proportions														
Si	5.96	5.96	5.91	5.93	5.97	5.97	5.97	5.97	5.96	5.93	5.95	5.94	5.97	5.97
Ti	0.00	0.00	0.00	0.00	0.00	0.00	0.00	0.00	0.00	0.00	0.00	0.00	0.00	0.00
Al	4.12	4.08	4.12	4.16	4.08	4.16	4.09	4.12	4.13	4.06	4.11	4.13	4.07	4.14
Cr	0.00	0.00	0.00	0.00	0.00	0.00	0.00	0.00	0.01	0.00	0.00	0.00	0.00	0.00
Fe	4.69	4.72	4.74	4.66	4.70	4.62	4.71	4.68	4.72	4.88	4.81	4.77	4.76	4.65
Mg	0.79	0.81	0.83	0.83	0.82	0.80	0.82	0.82	0.80	0.78	0.76	0.83	0.83	0.84
Mn	0.17	0.18	0.19	0.17	0.19	0.19	0.19	0.18	0.18	0.20	0.21	0.20	0.21	0.20
Ca	0.25	0.26	0.23	0.23	0.22	0.20	0.21	0.20	0.19	0.18	0.15	0.14	0.15	0.16
Na	0.00	0.00	0.01	0.00	0.00	0.00	0.00	0.01	0.01	0.00	0.01	0.00	0.01	0.01
K	0.00	0.00	0.00	0.00	0.00	0.00	0.00	0.00	0.00	0.00	0.00	0.00	0.00	0.00
O	24.00	24.00	24.00	24.00	24.00	24.00	24.00	24.00	24.00	24.00	24.00	24.00	24.00	24.00
CatTot	15.98	16.00	16.03	15.98	15.98	15.95	15.98	15.98	15.98	15.86	16.03	16.00	15.98	15.97
Total	39.98	40.00	40.03	39.98	39.98	39.95	39.98	39.98	39.98	39.89	40.03	40.00	39.98	39.97
Molar Proportions														
Grossular	0.04	0.04	0.04	0.04	0.04	0.03	0.04	0.03	0.03	0.03	0.02	0.02	0.03	0.03
Pyrope	0.13	0.14	0.14	0.14	0.14	0.14	0.14	0.14	0.14	0.13	0.13	0.14	0.14	0.14
Almandine	0.79	0.79	0.79	0.79	0.79	0.79	0.79	0.79	0.80	0.81	0.81	0.80	0.80	0.80
Spessartine	0.03	0.03	0.03	0.03	0.03	0.03	0.03	0.03	0.03	0.03	0.04	0.03	0.03	0.03
Fe/Fe+Mg	0.86	0.85	0.85	0.85	0.85	0.85	0.85	0.85	0.86	0.86	0.86	0.85	0.85	0.85

B1.2. Compositional Analysis of Garnet Profiles

Sample	5000 garnet profile	5000 garnet profile	5000 garnet profile	5000 garnet profile	5000 garnet profile	5000 garnet profile	5000 garnet profile	5000 garnet profile	5000 garnet profile	5000 garnet profile	5000 garnet profile	5000 garnet profile	5000 garnet profile	5000 garnet profile
Scan #	scan #2	scan #2	scan #2	scan #2	scan #2	scan #2	scan #2	scan #2	scan #2	scan #2	scan #2	scan #2	scan #2	scan #2
Oxides														
SiO2	37.49	37.17	37.13	37.30	37.10	36.85	37.18	37.33	37.00	37.05	36.88	36.95	36.87	32.57
TiO2	0.01	0.00	0.01	0.00	0.00	0.00	0.00	0.01	0.00	0.00	0.00	0.03	0.04	0.00
Al2O3	21.80	22.02	22.02	21.85	21.62	21.55	21.87	21.98	21.51	21.56	21.65	21.31	21.47	21.80
Cr2O3	0.03	0.00	0.01	0.01	0.02	0.00	0.00	0.00	0.01	0.04	0.00	0.03	0.03	0.00
FeO	35.50	35.27	35.87	34.48	34.79	34.18	34.36	34.86	34.54	34.62	33.89	35.10	34.11	34.48
MgO	3.36	3.43	3.31	3.23	3.40	3.28	3.29	3.47	3.55	3.49	3.43	3.47	3.29	4.37
MnO	1.41	1.40	1.41	1.40	1.37	1.24	1.29	1.24	1.16	1.19	1.28	1.08	1.14	0.93
CaO	1.00	1.08	1.19	1.21	1.25	1.28	1.27	1.36	1.35	1.38	1.39	1.50	1.50	0.91
Na2O	0.00	0.04	0.03	0.08	0.01	0.01	0.09	0.00	0.06	0.03	0.02	0.00	0.03	0.02
K2O	0.00	0.00	0.00	0.00	0.00	0.00	0.00	0.00	0.00	0.00	0.00	0.00	0.00	0.00
Total	100.60	100.39	100.97	99.36	99.57	99.51	99.57	100.26	99.18	99.36	98.54	99.48	98.48	94.90
Atom Proportions														
Si	5.98	5.94	5.92	6.00	5.97	6.00	6.04	5.98	5.97	5.97	5.98	5.99	5.99	5.57
Ti	0.00	0.00	0.00	0.00	0.00	0.00	0.00	0.00	0.00	0.00	0.00	0.00	0.01	0.00
Al	4.10	4.15	4.14	4.11	4.10	4.12	4.03	4.13	4.09	4.10	4.14	4.05	4.11	4.35
Cr	0.00	0.00	0.00	0.00	0.00	0.00	0.00	0.00	0.00	0.01	0.00	0.00	0.00	0.00
Fe	4.73	4.71	4.78	4.84	4.68	4.84	4.67	4.85	4.66	4.67	4.58	4.74	4.63	4.93
Mg	0.80	0.82	0.78	0.78	0.82	0.80	0.80	0.83	0.85	0.84	0.83	0.83	0.80	1.11
Mn	0.19	0.19	0.19	0.19	0.19	0.17	0.18	0.17	0.16	0.16	0.18	0.15	0.16	0.14
Ca	0.17	0.19	0.20	0.21	0.22	0.22	0.22	0.24	0.23	0.24	0.24	0.26	0.26	0.17
Na	0.00	0.01	0.01	0.02	0.00	0.00	0.03	0.00	0.02	0.01	0.01	0.00	0.01	0.01
K	0.00	0.00	0.00	0.00	0.00	0.00	0.00	0.00	0.00	0.00	0.00	0.00	0.00	0.00
O	24.00	24.00	24.00	24.00	24.00	24.00	24.00	24.00	24.00	24.00	24.00	24.00	24.00	24.00
CatTot	15.97	16.00	16.02	15.95	15.99	15.95	15.96	15.99	15.99	15.99	15.96	16.00	15.96	16.26
Total	39.97	40.00	40.02	39.95	39.99	39.95	39.99	39.99	39.99	39.99	39.96	40.00	39.96	40.26
Molar Proportions														
Grossular	0.03	0.03	0.03	0.04	0.04	0.04	0.04	0.04	0.04	0.04	0.04	0.04	0.04	0.05
Pyrope	0.14	0.14	0.13	0.13	0.14	0.14	0.14	0.14	0.14	0.14	0.14	0.14	0.14	0.18
Almandine	0.80	0.80	0.80	0.80	0.79	0.80	0.80	0.79	0.79	0.79	0.79	0.79	0.79	0.79
Spessartine	0.03	0.03	0.03	0.03	0.03	0.03	0.03	0.03	0.03	0.03	0.03	0.02	0.03	0.02
Fe/(Fe+Mn)	0.86	0.86	0.86	0.86	0.85	0.86	0.86	0.86	0.85	0.86	0.85	0.85	0.85	0.82

Sample	5000 garnet profile	5000 garnet profile	5000 garnet profile	5000 garnet profile	5000 garnet profile	5000 garnet profile	5000 garnet profile	5000 garnet profile	5000 garnet profile	5000 garnet profile	5000 garnet profile	5000 garnet profile	5000 garnet profile	5000 garnet profile
Scan #	scan #2	scan #2	scan #2	scan #2	scan #2	scan #2	scan #2	scan #2	scan #2	scan #2	scan #2	scan #2	scan #2	scan #2
Oxides														
SiO2	37.20	37.03	36.86	37.40	37.21	36.15	36.72	36.85	33.77	35.23	37.21	45.08	37.08	37.13
TiO2	0.00	0.00	0.03	0.00	0.01	0.00	0.02	0.00	0.00	0.01	0.00	0.06	0.00	0.01
Al2O3	20.93	21.15	21.09	21.92	21.62	21.09	21.91	20.81	21.39	21.16	21.82	18.62	21.92	22.27
Cr2O3	0.00	0.00	0.00	0.02	0.00	0.00	0.00	0.03	0.05	0.00	0.00	0.04	0.00	0.01
FeO	34.04	33.99	34.21	34.55	33.58	34.12	34.48	36.83	31.17	32.83	34.22	7.99	34.90	33.89
MgO	3.39	3.43	3.43	3.48	3.48	3.41	2.99	2.23	2.91	2.95	3.84	1.37	3.78	3.75
MnO	1.07	1.09	1.12	1.09	1.08	1.05	1.04	1.21	0.85	0.97	1.00	0.26	1.03	1.02
CaO	1.80	1.70	1.70	1.81	1.83	1.70	1.82	1.84	1.82	1.27	1.83	4.73	1.44	1.38
Na2O	0.02	0.01	0.02	0.02	0.02	0.00	0.07	0.00	0.04	0.02	0.04	3.37	0.02	0.03
K2O	0.00	0.00	0.00	0.00	0.00	0.00	0.00	0.00	0.00	0.00	0.00	0.00	0.00	0.00
Total	98.25	98.39	98.20	100.31	99.42	98.12	98.85	98.39	91.20	94.15	99.55	81.52	100.17	99.26
Atom Proportions														
Si	6.05	6.02	5.93	5.98	6.02	5.99	5.95	6.02	5.99	5.97	5.97	7.70	5.93	5.95
Ti	0.00	0.00	0.00	0.00	0.00	0.00	0.00	0.00	0.00	0.00	0.00	0.01	0.00	0.00
Al	4.01	4.05	4.18	4.12	4.10	4.18	4.18	4.03	4.39	4.22	4.12	3.75	4.13	4.21
Cr	0.00	0.00	0.00	0.00	0.00	0.00	0.00	0.00	0.01	0.00	0.00	0.01	0.00	0.00
Fe	4.63	4.62	4.61	4.61	4.54	4.66	4.67	4.82	4.56	4.82	4.58	1.14	4.67	4.61
Mg	0.82	0.83	0.82	0.83	0.84	0.83	0.72	0.55	0.76	0.76	0.87	0.35	0.90	0.90
Mn	0.15	0.15	0.15	0.15	0.14	0.15	0.14	0.17	0.13	0.13	0.14	0.04	0.14	0.14
Ca	0.28	0.30	0.29	0.31	0.29	0.30	0.28	0.29	0.19	0.23	0.28	0.87	0.25	0.24
Na	0.01	0.00	0.01	0.01	0.01	0.00	0.02	0.00	0.01	0.01	0.01	1.12	0.01	0.01
K	0.00	0.00	0.00	0.00	0.00	0.00	0.00	0.00	0.00	0.00	0.00	0.00	0.00	0.00
O	24.00	24.00	24.00	24.00	24.00	24.00	24.00	24.00	24.00	24.00	24.00	24.00	24.00	24.00
CatTot	15.95	15.98	15.98	15.99	15.83	16.01	15.97	15.97	15.82	15.92	15.99	14.97	16.01	15.95
Total	39.95	39.98	39.98	39.99	39.93	40.01	39.97	39.97	39.82	39.92	39.99	38.97	40.01	39.95
Molar Proportions														
Grossular	0.05	0.05	0.05	0.05	0.05	0.06	0.05	0.05	0.03	0.04	0.05	0.38	0.04	0.04
Pyrope	0.14	0.14	0.14	0.14	0.14	0.14	0.12	0.09	0.13	0.13	0.15	0.15	0.15	0.15
Almandine	0.78	0.78	0.78	0.78	0.78	0.78	0.80	0.83	0.81	0.81	0.78	0.48	0.78	0.78
Spessartine	0.03	0.03	0.03	0.02	0.02	0.02	0.02	0.03	0.02	0.02	0.02	0.02	0.02	0.02
Fe/(Fe+Mn)	0.85	0.85	0.85	0.85	0.84	0.85	0.87	0.90	0.85	0.86	0.84	0.77	0.84	0.83

B1.2. Compositional Analysis of Garnet Profiles

Sample	5000 garnet profile	5000 garnet profile	5000 garnet profile	5000 garnet profile	5000 garnet profile	5000 garnet profile	5000 garnet profile	5000 garnet profile	5000 garnet profile	5000 garnet profile	5000 garnet profile	5000 garnet profile	5000 garnet profile	5000 garnet profile
Scan #	scan #2	scan #2	scan #2	scan #2	scan #2	scan #2	scan #2	scan #2	scan #2	scan #2	scan #2	scan #2	scan #2	scan #2
Oxides														
SiO2	37.20	37.04	37.31	37.23	37.25	37.24	37.45	37.36	37.01	37.54	37.47	36.69	37.31	36.80
TiO2	0.00	0.00	0.00	0.00	0.00	0.01	0.00	0.03	0.00	0.00	0.00	0.00	0.00	0.00
Al2O3	20.98	21.62	21.27	22.22	21.83	21.76	22.06	22.09	21.98	22.12	21.62	20.81	21.62	21.72
Cr2O3	0.02	0.00	0.01	0.00	0.04	0.04	0.00	0.03	0.05	0.05	0.00	0.04	0.04	0.00
FeO	34.44	34.18	34.88	36.09	34.91	34.50	34.73	34.13	34.13	34.97	34.84	35.20	34.56	34.51
MgO	3.73	3.75	3.61	3.67	3.87	3.78	3.65	3.82	3.82	3.82	3.85	3.60	3.82	3.82
MnO	1.06	0.99	0.97	1.00	0.98	1.04	1.01	1.02	1.04	1.05	0.96	0.95	0.99	1.02
CaO	1.32	1.24	1.32	1.27	1.29	1.31	1.29	1.20	1.20	1.22	1.25	1.30	1.26	1.25
Na2O	0.03	0.02	0.02	0.02	0.00	0.01	0.00	0.00	0.02	0.02	0.02	0.01	0.01	0.00
K2O	0.00	0.00	0.00	0.00	0.00	0.00	0.00	0.00	0.00	0.00	0.00	0.00	0.00	0.00
Total	99.02	99.84	99.17	100.50	100.27	99.99	100.19	99.67	99.05	100.79	99.71	99.60	99.42	99.23
Mass Proportions														
Si	6.02	5.98	6.02	5.93	5.94	5.97	5.97	5.97	5.96	5.95	6.00	5.98	5.99	5.95
Ti	0.00	0.00	0.00	0.00	0.00	0.00	0.00	0.00	0.00	0.00	0.00	0.00	0.00	0.00
Al	4.01	4.11	4.04	4.17	4.11	4.11	4.14	4.16	4.17	4.13	4.08	4.00	4.09	4.12
Cr	0.00	0.00	0.00	0.00	0.01	0.01	0.00	0.00	0.01	0.01	0.00	0.01	0.01	0.00
Fe	4.66	4.61	4.68	4.67	4.66	4.62	4.63	4.56	4.60	4.64	4.62	4.80	4.64	4.65
Mg	0.90	0.90	0.87	0.87	0.92	0.90	0.87	0.91	0.87	0.90	0.92	0.86	0.87	0.92
Mn	0.15	0.14	0.13	0.14	0.13	0.14	0.14	0.14	0.14	0.14	0.13	0.13	0.14	0.14
Ca	0.23	0.22	0.23	0.22	0.22	0.22	0.22	0.21	0.21	0.21	0.22	0.23	0.22	0.22
Na	0.01	0.01	0.01	0.01	0.03	0.00	0.00	0.00	0.01	0.01	0.01	0.00	0.00	0.00
K	0.00	0.00	0.00	0.00	0.00	0.00	0.00	0.00	0.00	0.00	0.00	0.00	0.00	0.00
O	24.00	24.00	24.00	24.00	24.00	24.00	24.00	24.00	24.00	24.00	24.00	24.00	24.00	24.00
CatTot	15.98	15.97	15.97	15.98	16.01	15.98	15.98	15.95	15.98	15.98	15.97	16.02	15.98	15.99
Total	39.98	39.97	39.97	39.98	40.01	39.98	39.98	39.95	39.98	39.98	39.97	40.02	39.98	39.99
Molar Proportions														
Grossular	0.04	0.04	0.04	0.04	0.04	0.04	0.04	0.04	0.04	0.04	0.04	0.04	0.04	0.04
Pyrope	0.15	0.15	0.15	0.15	0.16	0.15	0.15	0.16	0.15	0.15	0.16	0.15	0.15	0.15
Almandine	0.78	0.78	0.78	0.78	0.78	0.78	0.78	0.78	0.78	0.78	0.79	0.80	0.79	0.79
Spessartine	0.02	0.02	0.02	0.02	0.02	0.02	0.02	0.02	0.02	0.02	0.02	0.02	0.02	0.02
Fe/(Fe+Mg)	0.84	0.84	0.84	0.84	0.83	0.84	0.84	0.83	0.84	0.84	0.83	0.85	0.84	0.84

Sample	5000 garnet profile	5000 garnet profile	5000 garnet profile	5000 garnet profile	5000 garnet profile	5000 garnet profile	5000 garnet profile	5000 garnet profile	5000 garnet profile	5000 garnet profile	5000 garnet profile	5000 garnet profile	5000 garnet profile	5000 garnet profile
Scan #	scan #2	scan #2	scan #2	scan #2	scan #2	scan #2	scan #2	scan #2	scan #2	scan #2	scan #2	scan #2	scan #2	scan #2
Oxides														
SiO2	37.15	37.63	36.93	36.89	37.05	37.26	37.20	37.33	37.09	36.04	37.11	36.96	40.50	36.44
TiO2	0.00	0.00	0.00	0.00	0.01	0.00	0.00	0.01	0.00	0.00	0.00	0.00	0.00	0.00
Al2O3	21.89	21.74	21.49	21.66	21.74	21.47	21.61	22.16	21.87	21.27	21.26	21.66	26.21	22.03
Cr2O3	0.01	0.00	0.01	0.06	0.01	0.01	0.11	0.01	0.03	0.06	0.01	0.01	0.06	0.03
FeO	35.30	35.28	34.90	34.51	34.56	34.54	35.01	34.84	35.39	34.64	34.92	36.36	28.04	35.26
MgO	3.65	3.71	3.77	3.50	3.61	3.73	3.58	3.74	3.47	3.46	3.51	3.62	2.97	3.31
MnO	1.05	1.12	1.02	0.92	1.08	1.10	1.09	1.00	1.05	1.19	1.10	1.28	1.10	1.32
CaO	1.27	1.28	1.28	1.23	1.27	1.23	1.13	1.14	1.10	0.82	0.91	0.90	0.73	0.79
Na2O	0.00	0.02	0.01	0.03	0.05	0.00	0.00	0.00	0.01	0.02	0.03	0.03	0.04	0.03
K2O	0.00	0.00	0.00	0.00	0.00	0.00	0.00	0.00	0.00	0.00	0.00	0.00	0.00	0.00
Total	100.44	100.79	99.41	98.75	99.38	99.35	99.74	100.22	100.02	97.69	99.70	99.80	99.65	99.21
Mass Proportions														
Si	5.93	5.98	5.95	5.97	5.96	5.99	5.97	5.95	5.96	5.93	6.02	5.94	6.19	5.90
Ti	0.00	0.00	0.00	0.00	0.00	0.00	0.00	0.00	0.00	0.00	0.00	0.00	0.00	0.00
Al	4.14	4.07	4.08	4.13	4.12	4.07	4.08	4.16	4.13	4.12	4.06	4.11	4.72	4.20
Cr	0.00	0.00	0.00	0.00	0.00	0.00	0.01	0.00	0.00	0.01	0.00	0.00	0.01	0.00
Fe	4.71	4.69	4.70	4.67	4.65	4.65	4.70	4.64	4.75	4.77	4.74	4.76	3.58	4.77
Mg	0.87	0.88	0.91	0.85	0.87	0.89	0.86	0.89	0.83	0.85	0.85	0.87	0.68	0.80
Mn	0.14	0.15	0.14	0.13	0.15	0.15	0.15	0.14	0.14	0.17	0.15	0.17	0.14	0.18
Ca	0.22	0.22	0.22	0.21	0.22	0.21	0.19	0.19	0.19	0.16	0.14	0.15	0.12	0.14
Na	0.00	0.01	0.00	0.01	0.02	0.00	0.00	0.00	0.00	0.01	0.01	0.01	0.01	0.01
K	0.00	0.00	0.00	0.00	0.00	0.00	0.00	0.00	0.00	0.00	0.00	0.00	0.00	0.00
O	24.00	24.00	24.00	24.00	24.00	24.00	24.00	24.00	24.00	24.00	24.00	24.00	24.00	24.00
CatTot	16.00	15.99	16.01	15.97	15.98	15.97	15.98	15.97	15.99	16.01	15.96	16.01	15.45	16.00
Total	40.00	39.99	40.01	39.97	39.98	39.97	39.98	39.97	39.99	40.01	39.96	40.01	39.45	40.00
Molar Proportions														
Grossular	0.04	0.04	0.04	0.04	0.04	0.04	0.03	0.03	0.03	0.03	0.02	0.03	0.03	0.02
Pyrope	0.15	0.15	0.15	0.14	0.15	0.15	0.15	0.15	0.14	0.14	0.14	0.15	0.15	0.14
Almandine	0.79	0.79	0.79	0.80	0.79	0.79	0.80	0.79	0.80	0.80	0.81	0.80	0.79	0.81
Spessartine	0.02	0.03	0.02	0.02	0.03	0.03	0.03	0.02	0.02	0.03	0.03	0.03	0.03	0.03
Fe/(Fe+Mg)	0.84	0.84	0.84	0.85	0.84	0.84	0.85	0.84	0.85	0.85	0.86	0.85	0.84	0.86

Sample	5000 garnet profile
Scan #	scan #2
Oxides	
SiO2	36.87
TiO2	0.00
Al2O3	21.47
Cr2O3	0.03
FeO	35.88
MgO	2.79
MnO	1.40
CaO	0.86
Na2O	0.04
K2O	0.00
Total	99.44
Atom Proportions	
Si	5.97
Ti	0.00
Al	4.10
Cr	0.00
Fe	4.86
Mg	0.67
Mn	0.21
Ca	0.15
Na	0.01
K	0.00
O	24.00
CatTot	15.98
Total	39.99
Molar Proportions	
Grossular	0.03
Pyrope	0.11
Almandine	0.83
Spessartine	0.03
Fe/(Fe+Mg)	0.88

Sample
Scan #
Oxides
SiO2
TiO2
Al2O3
Cr2O3
FeO
MgO
MnO
CaO
Na2O
K2O
Total
Atom Proportions
Si
Ti
Al
Cr
Fe
Mg
Mn
Ca
Na
K
O
CatTot
Total
Molar Proportions
Grossular
Pyrope
Almandine
Spessartine
Fe/(Fe+Mg)

B1.3. Spot Analysis for a Single Grain in Sample 5011

Sample	5011	5011	5011	5011	5011	5011	5011	5011	5011	5011	5011	5011	5011	5011	5011	5011	5011	5011	5011	5011	5011	5011	5011	5011	5011	5011
Point #	1	2	3	4	5	6	7	8	9	10	11	12	13	14	15	16	17	18	19	20	21	22	23	24	25	26
Oxides																										
SiO2	37.60	37.58	37.78	36.42	36.81	37.05	36.05	36.94	37.73	38.09	36.01	37.56	38.10	37.78	36.09	37.62	37.23	37.23	36.78	37.22	37.88	37.00	37.10	37.61	37.24	37.83
TiO2	0.00	0.00	0.00	0.01	0.00	0.00	0.00	0.00	0.02	0.00	0.00	0.00	0.00	0.00	0.00	0.00	0.04	0.00	0.00	0.05	0.00	0.00	0.00	0.00	0.03	0.09
Al2O3	21.95	22.17	22.32	22.04	22.13	21.92	21.82	21.99	22.09	22.12	22.14	22.34	21.62	22.24	22.11	21.99	22.02	22.05	21.95	22.29	22.29	21.78	21.84	22.00	22.08	21.66
Cr2O3	0.03	0.05	0.10	0.00	0.10	0.06	0.02	0.03	0.03	0.02	0.02	0.01	0.10	0.00	0.00	0.01	0.00	0.05	0.00	0.08	0.04	0.01	0.02	0.11	0.04	0.10
FeO	34.96	35.17	35.21	35.19	34.79	34.62	33.82	34.22	34.31	34.57	34.84	34.65	34.20	34.31	34.19	34.27	34.10	34.34	34.40	33.96	34.27	33.84	34.78	34.14	35.34	35.39
MgO	3.21	3.54	3.84	3.39	3.77	3.57	3.78	3.77	3.71	3.70	3.84	3.79	3.85	3.89	3.71	3.80	4.03	4.01	3.94	3.97	4.00	3.84	3.91	3.84	3.83	3.77
MnO	1.23	1.03	1.12	1.21	1.12	1.04	1.04	1.07	1.06	1.20	1.11	1.05	0.95	1.07	1.14	1.03	1.14	1.13	0.98	1.00	0.99	1.07	1.00	1.06	0.98	1.13
CaO	1.46	1.69	1.61	1.50	1.73	1.49	1.53	1.59	1.75	1.76	1.87	1.49	1.68	1.63	1.75	1.63	1.68	1.85	1.47	1.69	1.93	2.01	1.87	1.70	1.73	1.41
Na2O	0.01	0.01	0.03	0.04	0.02	0.04	0.00	0.01	0.00	0.00	0.01	0.01	0.02	0.03	0.00	0.06	0.03	0.00	0.08	0.03	0.06	0.00	0.02	0.01	0.01	0.04
K2O	0.00	0.00	0.00	0.00	0.00	0.00	0.00	0.00	0.00	0.00	0.00	0.00	0.00	0.00	0.00	0.00	0.00	0.00	0.00	0.00	0.00	0.00	0.00	0.00	0.00	0.00
Total	100.46	101.26	101.92	99.80	100.28	99.79	100.07	99.61	100.70	101.46	99.84	100.90	100.52	100.95	99.99	100.42	100.28	100.66	99.60	100.31	101.47	99.55	100.34	100.46	101.29	101.43
Atom Proportions																										
Si	5.99	5.94	5.93	5.87	5.86	5.94	6.04	5.92	5.97	5.99	5.80	5.94	6.04	5.96	5.84	5.97	5.93	5.91	5.91	5.91	5.95	5.94	5.92	5.97	5.90	5.98
Ti	0.00	0.00	0.00	0.00	0.00	0.00	0.00	0.00	0.00	0.00	0.00	0.00	0.00	0.00	0.00	0.00	0.00	0.00	0.00	0.01	0.00	0.00	0.00	0.00	0.00	0.01
Al	4.12	4.13	4.13	4.18	4.17	4.14	4.08	4.16	4.12	4.10	4.20	4.16	4.04	4.14	4.22	4.12	4.13	4.13	4.15	4.17	4.13	4.12	4.11	4.11	4.12	4.03
Cr	0.00	0.01	0.01	0.00	0.01	0.01	0.00	0.00	0.00	0.00	0.00	0.00	0.01	0.00	0.00	0.00	0.00	0.01	0.00	0.01	0.01	0.00	0.00	0.01	0.01	0.01
Fe	4.66	4.65	4.62	4.74	4.66	4.64	4.49	4.59	4.54	4.55	4.69	4.58	4.53	4.53	4.63	4.55	4.54	4.56	4.62	4.51	4.50	4.54	4.64	4.53	4.68	4.68
Mg	0.76	0.84	0.90	0.82	0.90	0.85	0.90	0.90	0.88	0.87	0.92	0.89	0.91	0.92	0.89	0.90	0.96	0.95	0.94	0.94	0.94	0.92	0.93	0.91	0.90	0.89
Mn	0.17	0.14	0.15	0.17	0.15	0.14	0.14	0.15	0.14	0.16	0.15	0.14	0.13	0.14	0.16	0.14	0.15	0.15	0.13	0.14	0.13	0.15	0.14	0.14	0.13	0.15
Ca	0.25	0.29	0.26	0.26	0.30	0.26	0.26	0.27	0.30	0.30	0.32	0.25	0.29	0.28	0.30	0.28	0.29	0.32	0.25	0.29	0.33	0.35	0.29	0.29	0.29	0.24
Na	0.00	0.00	0.01	0.01	0.01	0.01	0.00	0.00	0.00	0.00	0.00	0.00	0.01	0.01	0.00	0.02	0.01	0.00	0.02	0.01	0.02	0.00	0.01	0.01	0.00	0.01
K	0.00	0.00	0.00	0.00	0.00	0.00	0.00	0.00	0.00	0.00	0.00	0.00	0.00	0.00	0.00	0.00	0.00	0.00	0.00	0.00	0.00	0.00	0.00	0.00	0.00	0.00
O	24.00	24.00	24.00	24.00	24.00	24.00	24.00	24.00	24.00	24.00	24.00	24.00	24.00	24.00	24.00	24.00	24.00	24.00	24.00	24.00	24.00	24.00	24.00	24.00	24.00	24.00
CatTot	15.95	15.99	16.01	16.05	16.05	15.99	15.92	16.00	15.96	15.98	16.10	15.98	15.94	15.97	16.05	15.98	16.01	16.02	16.03	15.99	15.99	16.01	16.03	15.97	16.04	16.00
Total	39.95	39.99	40.01	40.05	40.05	39.99	39.92	40.00	39.96	39.96	40.10	39.96	39.94	39.97	40.05	39.96	40.01	40.02	40.03	39.99	39.99	40.01	40.03	39.97	40.04	40.00
Molar Proportions																										
Grossular	0.04	0.05	0.04	0.04	0.05	0.04	0.05	0.05	0.05	0.05	0.05	0.04	0.05	0.05	0.05	0.05	0.05	0.05	0.04	0.05	0.06	0.06	0.05	0.05	0.05	0.04
Pyrope	0.13	0.14	0.15	0.14	0.15	0.14	0.15	0.15	0.15	0.15	0.15	0.15	0.16	0.16	0.15	0.16	0.16	0.16	0.16	0.16	0.16	0.15	0.16	0.15	0.15	0.15
Almandine	0.80	0.79	0.78	0.79	0.78	0.79	0.78	0.78	0.78	0.77	0.77	0.78	0.77	0.77	0.77	0.78	0.78	0.78	0.78	0.77	0.76	0.78	0.77	0.77	0.78	0.79
Spessartine	0.03	0.02	0.03	0.03	0.03	0.02	0.02	0.02	0.02	0.03	0.02	0.02	0.02	0.02	0.03	0.02	0.03	0.03	0.02	0.02	0.02	0.02	0.02	0.02	0.02	0.03
Fe/(Fe+Mg)	0.86	0.85	0.84	0.85	0.84	0.84	0.83	0.84	0.84	0.84	0.84	0.84	0.83	0.83	0.84	0.83	0.83	0.83	0.83	0.83	0.83	0.83	0.83	0.83	0.84	0.84

Sample	5011	5011	5011	5011	5011	5011	5011	5011	5011	5011	5011	5011	5011	5011	5011	5011	5011	5011	5011	5011	5011	5011	5011	5011	5011	5011
Point #	27	28	29	30	31	32	33	34	35	36	37	38	39	40	41	42	43	44	45	46	47	48	49	50	51	52
Oxides																										
SiO2	37.66	37.46	37.38	38.06	37.54	36.91	37.75	33.96	35.38	38.21	37.55	36.33	37.49	38.01	37.53	36.58	33.85	35.71	35.30	35.04	36.73	36.97	36.49	37.84	37.76	37.81
TiO2	0.05	0.01	0.04	0.04	0.01	0.00	0.00	0.01	0.03	0.01	0.02	0.00	0.00	0.00	0.00	0.02	0.00	0.00	0.00	0.00	0.01	0.00	0.02	0.02	0.01	0.03
Al2O3	22.08	21.33	21.81	22.00	21.40	22.03	21.24	20.61	21.24	22.09	22.13	22.10	22.03	22.25	21.92	21.90	22.14	21.66	21.74	21.88	21.86	22.19	22.19	22.04	21.83	22.09
Cr2O3	0.07	0.07	0.11	0.00	0.00	0.00	0.00	0.00	0.06	0.06	0.00	0.01	0.03	0.02	0.02	0.00	0.00	0.00	0.00	0.00	0.07	0.06	0.06	0.10	0.00	0.00
FeO	36.13	35.35	34.91	34.43	35.81	34.94	35.43	35.13	34.60	34.85	32.77	33.16	33.32	34.07	34.02	34.15	33.01	33.32	33.17	33.83	33.69	33.37	34.12	34.65	34.36	34.58
MgO	3.78	3.77	3.98	3.85	3.72	3.76	3.73	3.92	3.92	4.01	3.97	3.97	3.99	3.90	4.03	3.85	3.79	3.87	3.90	4.03	3.93	4.04	3.99	3.92	3.96	3.87
MnO	1.10	1.16	1.06	1.00	1.11	1.14	1.00	0.91	1.09	1.00	0.96	1.04	1.08	1.11	1.01	1.12	1.00	1.02	0.97	0.97	0.85	0.93	1.07	0.99	1.11	1.12
CaO	1.38	1.50	1.67	1.86	1.66	1.65	2.01	1.73	1.79	1.84	1.74	1.58	1.43	1.64	1.60	1.56	1.74	1.45	1.63	1.43	1.76	1.91	1.61	1.72	1.56	1.71
Na2O	0.03	0.00	0.05	0.01	0.00	0.04	0.01	0.02	0.00	0.00	0.01	0.02	0.02	0.00	0.02	0.01	0.00	0.00	0.01	0.00	0.00	0.05	0.01	0.01	0.04	0.01
K2O	0.00	0.00	0.00	0.00	0.00	0.00	0.00	0.00	0.00	0.00	0.00	0.00	0.00	0.00	0.00	0.00	0.00	0.00	0.00	0.00	0.00	0.00	0.00	0.00	0.00	0.00
Total	102.27	100.66	101.01	101.26	101.25	100.48	101.17	96.29	98.06	102.06	99.23	98.20	99.37	101.01	100.14	99.22	95.52	97.03	96.71	97.16	96.88	96.52	99.55	101.09	100.62	101.22
Atom Proportions																										
Si	5.92	5.97	5.93	5.99	5.96	5.89	5.99	5.73	5.82	5.97	5.98	5.89	5.99	5.99	5.97	5.90	5.69	5.88	5.84	5.78	5.92	5.83	5.86	5.95	5.99	5.96
Ti	0.01	0.00	0.01	0.00	0.00	0.00	0.00	0.00	0.00	0.00	0.00	0.00	0.00	0.00	0.00	0.00	0.00	0.00	0.00	0.00	0.00	0.00	0.00	0.00	0.00	0.00
Al	4.09	4.01	4.08	4.08	4.01	4.14	3.97	4.10	4.12	4.07	4.16	4.22	4.15	4.13	4.11	4.16	4.39	4.20	4.24	4.25	4.16	4.24	4.20	4.11	4.08	4.11
Cr	0.01	0.01	0.01	0.00	0.00	0.00	0.00	0.00	0.00	0.01	0.01	0.00	0.00	0.00	0.00	0.00	0.00	0.00	0.00	0.00	0.01	0.01	0.01	0.01	0.00	0.00
Fe	4.75	4.71	4.63	4.53	4.76	4.66	4.70	4.96	4.76	4.56	4.38	4.50	4.45	4.49	4.53	4.61	4.84	4.59	4.59	4.67	4.54	4.53	4.58	4.58	4.56	4.56
Mg	0.88	0.90	0.94	0.90	0.88	0.89	0.88	0.99	0.96	0.94	0.95	0.96	0.95	0.92	0.96	0.93	0.96	0.95	0.96	0.99	0.94	0.96	0.96	0.92	0.94	0.91
Mn	0.15	0.16	0.14	0.13	0.15	0.16	0.13	0.13	0.15	0.13	0.13	0.14	0.15	0.15	0.14	0.15	0.14	0.14	0.14	0.14	0.12	0.13	0.15	0.13	0.15	0.15
Ca	0.23	0.26	0.26	0.31	0.26	0.26	0.34	0.31	0.32	0.31	0.30	0.28	0.25	0.28	0.27	0.27	0.31	0.26	0.29	0.25	0.30	0.33	0.28	0.29	0.26	0.29
Na	0.01	0.00	0.02	0.00	0.00	0.01	0.00	0.01	0.00	0.00	0.00	0.01	0.01	0.00	0.01	0.00	0.00	0.00	0.00	0.00	0.00	0.02	0.00	0.00	0.01	0.00
K	0.00	0.00	0.00	0.00	0.00	0.00	0.00	0.00	0.00	0.00	0.00	0.00	0.00	0.00	0.00	0.00	0.00	0.00	0.00	0.00	0.00	0.00	0.00	0.00	0.00	0.00
O	24.00	24.00	24.00	24.00	24.00	24.00	24.00	24.00	24.00	24.00	24.00	24.00	24.00	24.00	24.00	24.00	24.00	24.00	24.00	24.00	24.00	24.00	24.00	24.00	24.00	24.00
CatTot	16.04	16.02	16.03	15.97	16.04	16.04	16.03	16.22	16.12	15.99	15.92	16.00	15.94	15.95	15.98	16.02	16.12	16.02	16.05	16.09	16.00	16.05	16.03	15.99	15.98	15.98
Total	40.04	40.02	40.03	39.97	40.04	40.04	40.03	40.22	40.12	39.99	39.92	40.00	39.94	39.95	39.98	40.02	40.12	40.02	40.05	40.09	40.00	40.05	40.03	39.99	39.98	39.98
Molar Proportions																										
Grossular	0.04	0.04	0.05	0.05	0.05	0.05	0.06	0.05	0.05	0.05	0.06	0.05	0.04	0.05	0.05	0.05	0.05	0.04	0.05	0.04	0.05	0.06	0.05	0.05	0.04	0.05
Pyrope	0.15	0.15	0.16	0.15	0.15	0.15	0.15	0.15	0.16	0.16	0.16	0.16	0.16	0.16	0.16	0.16	0.16	0.16	0.16	0.16	0.16	0.16	0.16	0.16	0.16	0.15
Almandine	0.79	0.78	0.77	0.77	0.78	0.78	0.78	0.78	0.77	0.77	0.76	0.77	0.77	0.77	0.77	0.77	0.77	0.77	0.77	0.77	0.77	0.76	0.77	0.77	0.77	0.77
Spessartine	0.02	0.03	0.02	0.02	0.02	0.03	0.02	0.02	0.02	0.02	0.02	0.02	0.03	0.03	0.02	0.03	0.02	0.02	0.02	0.02	0.02	0.02	0.02	0.02	0.03	0.03
Fe/(Fe+Mg)	0.84	0.84	0.83	0.83	0.84	0.84	0.84	0.83	0.83	0.83	0.82	0.82	0.82	0.83	0.83	0.83	0.83	0.83	0.83	0.82	0.83	0.82	0.83	0.83	0.83	0.83

B1.3. Spot Analysis for a Single Grain in Sample 5011

Sample	5011	5011	5011	5011	5011	5011	5011	5011	5011	5011	5011	5011	5011	5011	5011	5011	5011	5011	5011	5011	5011	5011	5011	5011	5011
Point #	53	54	55	56	57	58	59	60	61	62	63	64	65	66	67	68	69	70	71	72	73	74	75	76	77	78
Oxides																										
SiO2	36.97	37.78	37.88	38.04	36.48	37.53	38.09	37.48	36.59	37.80	36.70	37.40	37.99	37.19	37.42	36.81	37.42	37.55	37.62	37.90	37.76	37.22	37.97	38.53	37.22	37.63
TiO2	0.00	0.00	0.00	0.00	0.00	0.02	0.00	0.00	0.04	0.00	0.02	0.05	0.03	0.00	0.00	0.02	0.00	0.04	0.04	0.00	0.05	0.03	0.00	0.00	0.00	0.01
Al2O3	22.33	22.03	21.78	22.33	21.80	22.01	22.15	22.03	22.02	22.25	21.91	21.87	21.96	22.20	22.15	21.91	21.87	22.42	22.22	22.08	22.07	22.12	22.18	22.31	21.82	22.22
Cr2O3	0.01	0.00	0.00	0.06	0.05	0.09	0.05	0.01	0.03	0.11	0.04	0.05	0.02	0.02	0.04	0.12	0.06	0.13	0.04	0.00	0.04	0.08	0.00	0.07	0.01	0.02
FeO	34.71	34.90	34.91	34.79	35.36	34.39	34.78	34.05	34.90	34.44	35.19	34.60	34.27	33.73	34.38	33.56	33.77	33.60	34.02	34.22	34.76	35.10	34.47	34.65	34.87	34.42
MgO	3.46	3.41	3.66	4.07	4.04	4.06	4.06	3.95	3.88	3.94	3.95	3.95	3.97	4.01	4.03	3.99	3.88	4.06	4.05	4.10	4.02	4.04	3.96	4.02	3.70	4.01
MnO	1.18	1.06	1.20	1.01	1.03	1.11	1.06	1.06	1.04	1.09	1.01	0.98	1.10	1.01	0.96	1.01	1.13	1.01	0.95	0.98	1.05	1.03	1.12	1.11	1.15	1.04
CaO	1.63	1.62	1.74	1.71	1.71	1.86	1.66	1.66	1.57	1.56	1.63	1.50	1.50	1.58	1.65	1.69	1.47	1.61	1.50	1.71	1.53	1.53	1.46	1.60	1.65	1.56
Na2O	0.00	0.00	0.00	0.00	0.00	0.02	0.03	0.00	0.00	0.00	0.00	0.00	0.00	0.02	0.01	0.03	0.00	0.02	0.00	0.04	0.00	0.00	0.02	0.00	0.01	0.00
K2O	0.00	0.00	0.00	0.00	0.00	0.00	0.00	0.00	0.00	0.00	0.00	0.00	0.00	0.00	0.00	0.00	0.00	0.00	0.00	0.00	0.00	0.00	0.00	0.00	0.00	0.00
Total	100.32	100.79	101.17	102.00	100.47	101.10	101.87	100.25	100.06	101.20	100.46	100.39	100.83	99.77	100.86	99.14	99.60	100.44	100.43	101.02	101.31	101.15	101.18	102.28	100.43	100.92
Atom Proportions																										
Si	5.90	5.99	5.99	5.95	5.84	5.93	5.97	5.96	5.87	5.96	5.87	5.95	6.00	5.93	5.93	5.92	5.96	5.94	5.96	5.97	5.95	5.89	5.96	6.00	5.94	5.95
Ti	0.00	0.00	0.00	0.00	0.00	0.00	0.00	0.00	0.01	0.00	0.00	0.01	0.00	0.00	0.00	0.00	0.00	0.01	0.01	0.00	0.01	0.00	0.00	0.00	0.00	0.00
Al	4.20	4.12	4.06	4.12	4.12	4.10	4.09	4.13	4.16	4.13	4.13	4.10	4.09	4.18	4.14	4.15	4.12	4.18	4.15	4.10	4.10	4.13	4.12	4.09	4.10	4.14
Cr	0.00	0.00	0.00	0.01	0.01	0.01	0.01	0.00	0.00	0.01	0.01	0.01	0.00	0.00	0.01	0.02	0.01	0.02	0.00	0.00	0.01	0.01	0.00	0.01	0.00	0.00
Fe	4.63	4.63	4.62	4.55	4.74	4.54	4.56	4.53	4.68	4.54	4.71	4.60	4.53	4.50	4.56	4.51	4.52	4.45	4.51	4.51	4.58	4.65	4.54	4.51	4.65	4.55
Mg	0.83	0.81	0.86	0.95	0.96	0.96	0.95	0.94	0.93	0.93	0.94	0.94	0.93	0.95	0.95	0.96	0.92	0.96	0.96	0.96	0.95	0.95	0.93	0.93	0.88	0.95
Mn	0.16	0.14	0.16	0.13	0.14	0.16	0.14	0.14	0.14	0.15	0.14	0.13	0.15	0.14	0.13	0.14	0.15	0.14	0.13	0.13	0.14	0.14	0.15	0.15	0.16	0.14
Ca	0.28	0.28	0.30	0.29	0.29	0.31	0.28	0.28	0.27	0.26	0.28	0.26	0.25	0.27	0.28	0.29	0.25	0.27	0.28	0.29	0.26	0.26	0.26	0.27	0.28	0.26
Na	0.00	0.00	0.00	0.00	0.00	0.01	0.01	0.00	0.00	0.00	0.00	0.00	0.00	0.01	0.00	0.01	0.00	0.01	0.00	0.01	0.00	0.00	0.01	0.00	0.00	0.00
K	0.00	0.00	0.00	0.00	0.00	0.00	0.00	0.00	0.00	0.00	0.00	0.00	0.00	0.00	0.00	0.00	0.00	0.00	0.00	0.00	0.00	0.00	0.00	0.00	0.00	0.00
O	24.00	24.00	24.00	24.00	24.00	24.00	24.00	24.00	24.00	24.00	24.00	24.00	24.00	24.00	24.00	24.00	24.00	24.00	24.00	24.00	24.00	24.00	24.00	24.00	24.00	24.00
CatTot	16.00	15.96	15.96	15.99	16.10	16.02	15.99	15.98	16.05	15.97	16.07	15.99	15.95	15.98	16.00	16.00	15.95	15.96	15.98	15.98	15.99	16.03	15.97	15.95	16.01	15.98
Total	40.00	39.95	39.98	39.99	40.10	40.02	39.99	39.98	40.05	39.97	40.07	39.99	39.95	39.98	40.00	40.00	39.95	39.96	39.98	39.98	39.99	40.03	39.97	39.95	40.01	39.98
Molar Proportions																										
Grossular	0.05	0.05	0.05	0.05	0.05	0.05	0.05	0.05	0.04	0.04	0.05	0.04	0.04	0.05	0.05	0.05	0.04	0.05	0.04	0.05	0.04	0.04	0.04	0.05	0.05	0.04
Pyrope	0.14	0.14	0.15	0.16	0.16	0.16	0.16	0.16	0.15	0.16	0.16	0.16	0.16	0.16	0.16	0.16	0.16	0.16	0.16	0.16	0.16	0.16	0.16	0.16	0.15	0.16
Almandine	0.79	0.79	0.78	0.77	0.77	0.76	0.77	0.77	0.78	0.77	0.78	0.78	0.77	0.77	0.77	0.77	0.77	0.76	0.77	0.77	0.77	0.77	0.77	0.77	0.78	0.77
Spessartine	0.03	0.02	0.03	0.02	0.02	0.02	0.02	0.02	0.02	0.02	0.02	0.02	0.03	0.02	0.02	0.02	0.03	0.02	0.02	0.02	0.02	0.02	0.03	0.02	0.03	0.02
Fe/(Fe+Mg)	0.85	0.85	0.84	0.83	0.83	0.83	0.83	0.83	0.83	0.83	0.83	0.83	0.83	0.83	0.83	0.83	0.83	0.82	0.82	0.82	0.83	0.83	0.83	0.83	0.84	0.83

Sample	5011	5011	5011	5011	5011	5011	5011	5011	5011	5011	5011	5011	5011	5011	5011	5011	5011	5011	5011	5011	5011	5011	5011	5011	5011	5011
Point #	79	80	81	82	83	84	27	2	3	10	21	25	27	30	31	34	35	35	36	38	43	44	45	46	47	48
Oxides																										
SiO2	37.10	38.00	37.13	37.71	34.88	37.49	37.72	37.72	37.96	37.63	37.85	37.97	37.45	37.38	37.97	37.35	38.16	37.96	37.45	37.85	37.76	37.07	37.76	38.06	37.96	38.19
TiO2	0.00	0.00	0.01	0.04	0.01	0.01	0.07	0.00	0.03	0.00	0.00	0.01	0.03	0.03	0.00	0.01	0.00	0.00	0.00	0.03	0.00	0.00	0.03	0.02	0.00	0.01
Al2O3	22.01	22.05	21.54	22.10	21.60	21.91	21.95	21.52	21.91	21.79	21.90	21.97	22.16	21.79	22.14	21.92	22.47	22.30	21.72	22.06	22.04	21.83	22.16	21.99	22.13	22.08
Cr2O3	0.00	0.01	0.01	0.00	0.08	0.07	0.02	0.05	0.05	0.06	0.04	0.08	0.00	0.00	0.01	0.13	0.02	0.06	0.07	0.04	0.04	0.06	0.02	0.01	0.00	0.07
FeO	34.17	34.67	33.76	33.81	34.14	34.45	35.31	33.77	34.09	33.48	32.44	33.31	34.66	33.34	33.77	33.18	33.45	33.48	33.03	33.02	33.94	33.27	33.59	33.59	33.58	33.29
MgO	3.96	3.93	3.94	4.07	3.93	4.05	4.05	3.79	4.19	4.03	4.22	4.09	4.01	4.23	4.12	4.27	4.37	4.37	4.38	4.39	4.16	4.28	4.37	4.34	4.48	4.36
MnO	1.16	1.02	0.99	1.07	1.01	0.96	1.16	1.16	1.03	1.00	1.07	1.06	1.09	1.03	1.07	1.01	0.95	1.07	0.96	1.06	1.12	1.03	1.03	1.00	1.07	0.96
CaO	1.67	1.68	1.67	1.71	1.66	1.56	1.38	1.65	1.47	1.84	1.88	1.63	1.39	1.68	1.81	1.96	1.79	1.87	1.97	1.76	1.79	1.65	1.46	1.72	1.61	1.69
Na2O	0.00	0.00	0.00	0.04	0.03	0.00	0.01	0.00	0.01	0.00	0.02	0.04	0.00	0.00	0.05	0.00	0.00	0.01	0.01	0.03	0.03	0.00	0.00	0.04	0.00	0.03
K2O	0.00	0.00	0.00	0.00	0.00	0.00	0.00	0.00	0.00	0.00	0.00	0.00	0.00	0.00	0.00	0.00	0.00	0.00	0.00	0.00	0.00	0.00	0.00	0.00	0.00	0.00
Total	100.08	101.37	99.03	100.54	97.37	100.50	101.66	99.85	100.72	99.83	99.42	100.17	100.77	99.49	100.95	99.83	101.21	101.13	99.58	100.23	100.91	99.19	100.42	100.76	100.62	100.66
Atom Proportions																										
Si	5.92	5.98	5.98	5.97	5.77	5.95	5.94	6.03	6.00	5.99	6.02	6.01	5.93	5.97	5.98	5.95	5.98	5.96	5.97	5.99	5.96	5.95	5.97	6.00	5.98	6.01
Ti	0.00	0.00	0.00	0.01	0.00	0.00	0.01	0.00	0.00	0.00	0.00	0.00	0.00	0.00	0.00	0.00	0.00	0.00	0.00	0.00	0.00	0.00	0.00	0.00	0.00	0.00
Al	4.14	4.09	4.09	4.12	4.21	4.10	4.07	4.05	4.08	4.09	4.11	4.10	4.14	4.10	4.11	4.11	4.15	4.13	4.08	4.11	4.10	4.13	4.13	4.08	4.11	4.10
Cr	0.00	0.00	0.00	0.00	0.01	0.01	0.00	0.01	0.01	0.01	0.01	0.01	0.00	0.00	0.00	0.02	0.00	0.01	0.01	0.01	0.01	0.01	0.00	0.00	0.00	0.01
Fe	4.56	4.56	4.55	4.47	4.72	4.58	4.65	4.51	4.50	4.46	4.32	4.41	4.59	4.46	4.45	4.42	4.38	4.40	4.41	4.37	4.48	4.46	4.44	4.43	4.42	4.38
Mg	0.94	0.92	0.96	0.96	0.97	0.96	0.95	0.90	0.99	0.96	1.00	0.97	0.95	1.01	0.97	1.01	1.02	1.02	1.04	1.03	0.96	1.02	1.03	1.02	1.05	1.02
Mn	0.16	0.14	0.13	0.14	0.14	0.13	0.16	0.16	0.14	0.14	0.14	0.14	0.15	0.14	0.14	0.14	0.13	0.14	0.13	0.14	0.15	0.14	0.14	0.13	0.14	0.13
Ca	0.29	0.28	0.29	0.29	0.29	0.27	0.23	0.28	0.25	0.31	0.32	0.28	0.24	0.29	0.31	0.34	0.30	0.32	0.34	0.30	0.30	0.28	0.25	0.29	0.27	0.28
Na	0.00	0.00	0.00	0.01	0.01	0.00	0.00	0.00	0.00	0.00	0.01	0.01	0.00	0.00	0.02	0.00	0.00	0.00	0.00	0.01	0.01	0.00	0.00	0.01	0.00	0.01
K	0.00	0.00	0.00	0.00	0.00	0.00	0.00	0.00	0.00	0.00	0.00	0.00	0.00	0.00	0.00	0.00	0.00	0.00	0.00	0.00	0.00	0.00	0.00	0.00	0.00	0.00
O	24.00	24.00	24.00	24.00	24.00	24.00	24.00	24.00	24.00	24.00	24.00	24.00	24.00	24.00	24.00	24.00	24.00	24.00	24.00	24.00	24.00	24.00	24.00	24.00	24.00	24.00
CatTot	16.01	15.96	15.98	15.97	16.13	15.99	16.02	15.94	15.96	15.96	15.93	15.94	16.00	15.97	15.97	15.99	15.95	15.97	15.98	15.96	15.99	15.99	15.96	15.96	15.97	15.94
Total	40.01	39.96	39.96	39.97	40.13	39.99	40.02	39.94	39.96	39.96	39.93	39.94	40.00	39.97	39.97	39.99	39.95	39.97	39.98	39.96	39.99	39.99	39.96	39.96	39.97	39.94
Molar Proportions																										
Grossular	0.05	0.05	0.05	0.05	0.05	0.04	0.04	0.05	0.04	0.05	0.06	0.05	0.04	0.05	0.05	0.06	0.05	0.05	0.06	0.05	0.06	0.05	0.04	0.05	0.05	0.05
Pyrope	0.16	0.16	0.16	0.16	0.16	0.16	0.16	0.15	0.17	0.16	0.17	0.17	0.16	0.17	0.17	0.17	0.17	0.17	0.18	0.18	0.17	0.17	0.18	0.17	0.18	0.18
Almandine	0.77	0.77	0.77	0.76	0.77	0.77	0.78	0.77	0.77	0.76	0.76	0.76	0.78	0.76	0.76	0.75	0.75	0.75	0.75	0.75	0.76	0.76	0.76	0.76	0.75	0.75
Spessartine	0.03	0.02	0.02	0.02	0.02	0.02	0.03	0.03	0.02	0.02	0.02	0.02	0.02	0.02	0.02	0.02	0.02	0.02	0.02	0.02	0.03	0.02	0.02	0.02	0.02	0.02
Fe/(Fe+Mg)	0.83	0.83	0.83	0.82	0.83	0.83	0.83	0.83	0.82	0.82	0.81	0.82	0.83	0.82	0.82	0.81	0.81	0.81	0.81	0.81	0.82	0.81	0.81	0.81	0.81	0.81

B1.3. Spot Analysis for a Single Grain in Sample 5011

Sample	5011	5011	5011	5011	5011	5011	5011	5011	5011	5011	5011	5011	5011	5011	5011	5011	5011	5011	5011	5011	5011	5011	5011	5011	5011	5011
Point #	52	82	59	56	58	69	73	78	80	85	86	87	88	89	90	91	92	93	94	95	96	97	98	99	100	101
Oxides																										
SiO2	38.02	37.07	36.74	36.58	36.67	37.95	37.51	37.31	37.90	36.98	37.18	36.95	37.11	37.91	35.27	37.40	37.62	37.93	38.24	36.81	38.26	37.87	37.58	37.86	38.27	37.61
TiO2	0.00	0.04	0.00	0.00	0.00	0.01	0.00	0.00	0.01	0.00	0.00	0.00	0.00	0.03	0.02	0.00	0.02	0.00	0.01	0.04	0.00	0.03	0.00	0.00	0.00	0.00
Al2O3	22.33	21.47	21.14	21.68	21.71	21.96	22.04	21.95	22.27	21.53	21.65	22.07	21.43	21.72	22.09	21.58	21.95	21.74	22.24	21.77	21.59	21.97	22.08	22.05	22.07	22.02
Cr2O3	0.05	0.00	0.04	0.00	0.03	0.00	0.06	0.01	0.03	0.00	0.00	0.06	0.02	0.05	0.03	0.00	0.00	0.01	0.00	0.00	0.00	0.00	0.00	0.00	0.02	0.07
FeO	33.80	33.56	33.18	33.68	33.67	32.85	33.49	33.18	33.34	33.63	33.19	33.35	33.53	33.60	33.58	33.87	33.63	33.38	33.05	32.95	33.53	32.95	33.12	33.65	33.03	33.51
MgO	4.36	4.28	4.06	4.01	4.17	4.32	4.43	4.28	4.43	4.30	4.16	4.20	3.99	4.00	3.95	3.86	3.60	3.83	4.23	4.15	4.30	4.24	4.26	4.41	4.29	4.38
MnO	1.14	1.20	1.18	1.04	1.08	0.94	1.04	0.95	1.04	1.07	0.99	1.13	0.94	1.11	1.06	0.97	1.10	1.03	1.05	1.08	1.06	0.95	1.05	0.97	1.04	0.95
CaO	1.63	1.62	1.64	1.81	1.95	1.76	1.70	1.62	1.74	1.62	1.60	1.61	1.57	1.84	1.77	1.67	1.57	1.78	1.77	1.72	1.79	1.94	1.68	1.67	2.02	1.80
Na2O	0.01	0.00	0.00	0.03	0.02	0.00	0.01	0.01	0.01	0.05	0.01	0.00	0.05	0.03	0.04	0.03	0.02	0.01	0.02	0.00	0.02	0.00	0.06	0.04	0.01	0.03
K2O	0.00	0.00	0.00	0.00	0.00	0.00	0.00	0.00	0.00	0.00	0.00	0.00	0.00	0.00	0.00	0.00	0.00	0.00	0.00	0.00	0.00	0.00	0.00	0.00	0.00	0.00
Total	101.34	99.24	97.98	98.83	99.28	99.78	100.27	99.30	100.77	99.19	98.77	99.38	98.66	100.29	97.80	99.38	99.51	99.71	100.61	96.51	100.54	99.96	99.81	100.64	100.74	100.37
Atom Proportions																										
Si	5.96	5.98	5.98	5.91	5.90	6.02	5.95	5.97	5.97	5.95	5.98	5.92	5.99	6.01	5.78	6.00	6.01	6.04	6.02	5.94	6.04	6.00	5.97	5.98	6.02	5.96
Ti	0.00	0.01	0.00	0.00	0.00	0.00	0.00	0.00	0.00	0.00	0.00	0.00	0.00	0.00	0.00	0.00	0.00	0.00	0.00	0.01	0.00	0.00	0.00	0.00	0.00	0.00
Al	4.13	4.07	4.06	4.13	4.12	4.10	4.12	4.14	4.13	4.08	4.11	4.17	4.08	4.06	4.27	4.08	4.14	4.08	4.12	4.14	4.02	4.10	4.13	4.10	4.09	4.11
Cr	0.01	0.00	0.01	0.00	0.00	0.00	0.01	0.00	0.00	0.00	0.00	0.01	0.00	0.01	0.00	0.00	0.00	0.00	0.00	0.00	0.00	0.00	0.00	0.00	0.00	0.01
Fe	4.43	4.51	4.52	4.55	4.53	4.36	4.44	4.44	4.39	4.52	4.47	4.47	4.53	4.46	4.60	4.54	4.49	4.45	4.35	4.45	4.43	4.37	4.40	4.44	4.34	4.44
Mg	1.02	1.03	0.99	0.97	1.00	1.02	1.05	1.02	1.04	1.03	1.00	1.00	0.96	0.95	0.96	0.92	0.86	0.91	0.99	1.00	1.01	1.00	1.01	1.04	1.01	1.03
Mn	0.15	0.16	0.16	0.14	0.14	0.13	0.14	0.13	0.14	0.15	0.14	0.16	0.13	0.15	0.16	0.13	0.15	0.14	0.14	0.15	0.14	0.13	0.14	0.13	0.14	0.13
Ca	0.27	0.28	0.29	0.31	0.34	0.30	0.29	0.28	0.29	0.28	0.28	0.28	0.27	0.31	0.31	0.29	0.27	0.30	0.30	0.30	0.30	0.33	0.29	0.28	0.34	0.31
Na	0.00	0.00	0.00	0.01	0.01	0.00	0.00	0.00	0.00	0.02	0.00	0.00	0.02	0.01	0.01	0.01	0.01	0.00	0.01	0.00	0.01	0.00	0.02	0.01	0.00	0.01
K	0.00	0.00	0.00	0.00	0.00	0.00	0.00	0.00	0.00	0.00	0.00	0.00	0.00	0.00	0.00	0.00	0.00	0.00	0.00	0.00	0.00	0.00	0.00	0.00	0.00	0.00
O	24.00	24.00	24.00	24.00	24.00	24.00	24.00	24.00	24.00	24.00	24.00	24.00	24.00	24.00	24.00	24.00	24.00	24.00	24.00	24.00	24.00	24.00	24.00	24.00	24.00	24.00
CatTot	15.97	16.01	15.99	16.03	16.04	15.93	15.99	15.97	15.97	16.02	15.97	15.99	15.98	15.96	16.09	15.97	15.92	15.92	15.93	15.98	15.95	15.94	15.97	15.98	15.94	15.99
Total	39.97	40.01	39.99	40.03	40.04	39.93	39.99	39.97	39.97	40.02	39.97	39.99	39.98	39.96	40.09	39.97	39.92	39.92	39.93	39.98	39.95	39.94	39.97	39.98	39.94	39.99
Molar Proportions																										
Grossular	0.05	0.05	0.05	0.05	0.06	0.05	0.05	0.05	0.05	0.05	0.06	0.06	0.05	0.05	0.05	0.05	0.05	0.05	0.05	0.05	0.05	0.06	0.05	0.05	0.06	0.05
Pyrope	0.17	0.17	0.17	0.16	0.17	0.18	0.18	0.17	0.18	0.17	0.17	0.17	0.16	0.16	0.16	0.16	0.15	0.16	0.17	0.17	0.17	0.17	0.17	0.18	0.17	0.18
Almandine	0.75	0.75	0.76	0.76	0.75	0.75	0.75	0.76	0.75	0.76	0.76	0.76	0.77	0.76	0.76	0.77	0.78	0.77	0.75	0.76	0.75	0.75	0.75	0.75	0.75	0.75
Spessartine	0.03	0.03	0.03	0.02	0.02	0.02	0.02	0.02	0.02	0.02	0.02	0.03	0.02	0.03	0.02	0.02	0.03	0.02	0.02	0.02	0.02	0.02	0.02	0.02	0.02	0.02
Fe/(Fe+Mg)	0.81	0.81	0.82	0.82	0.82	0.81	0.81	0.81	0.81	0.81	0.82	0.82	0.82	0.83	0.83	0.83	0.84	0.83	0.81	0.82	0.81	0.81	0.81	0.81	0.81	0.81

Sample	5011	5011	5011	5011	5011	5011	5011	5011	5011	5011	5011	5011	5011	5011	5011	5011	5011	5011	5011	5011	5011	5011	5011	5011	5011	5011
Point #	102	103	104	105	106	107	108	109	110	111	112	113	114	115	116	117	118	119	120	121	122	123	124	125	126	127
Oxides																										
SiO2	37.76	37.89	37.99	37.86	38.07	37.77	37.81	37.82	37.97	37.89	37.61	38.12	36.48	36.02	37.27	36.79	35.85	36.78	36.47	37.35	37.99	38.06	38.20	36.40	37.82	36.76
TiO2	0.01	0.00	0.00	0.00	0.00	0.02	0.00	0.00	0.00	0.02	0.01	0.00	0.00	0.03	0.06	0.00	0.01	0.00	0.00	0.00	0.02	0.00	0.00	0.00	0.00	0.00
Al2O3	22.15	21.96	22.02	21.90	21.94	22.02	22.14	22.18	22.14	22.38	22.11	21.99	21.45	21.58	21.33	21.43	21.50	21.91	21.84	21.86	21.59	21.89	22.08	22.12	21.61	22.06
Cr2O3	0.01	0.04	0.00	0.05	0.01	0.04	0.00	0.07	0.08	0.02	0.03	0.00	0.02	0.07	0.09	0.02	0.00	0.00	0.01	0.03	0.07	0.05	0.02	0.00	0.01	0.10
FeO	33.49	33.92	33.51	33.97	33.83	32.93	34.21	33.42	33.73	33.20	32.85	33.61	32.50	32.24	32.64	32.54	32.91	32.62	32.25	32.22	32.99	32.68	33.05	33.56	32.50	33.18
MgO	4.35	4.24	4.32	4.25	4.18	4.13	3.81	4.20	4.22	4.33	4.44	4.38	4.44	4.39	4.29	4.14	4.07	4.32	4.35	4.34	4.55	4.48	4.49	4.23	4.34	4.25
MnO	1.02	1.09	1.04	1.04	1.09	1.11	1.08	1.09	1.09	0.93	0.98	1.00	1.06	0.95	1.00	1.03	1.03	1.05	0.93	0.93	1.02	1.00	1.05	0.94	1.13	1.05
CaO	1.85	1.71	1.85	1.71	1.72	1.74	1.67	1.68	1.70	1.80	2.00	2.07	1.77	1.86	1.85	1.87	1.77	1.75	1.64	1.77	1.89	1.89	2.36	2.21	1.80	1.88
Na2O	0.00	0.00	0.03	0.00	0.05	0.02	0.00	0.00	0.00	0.00	0.01	0.02	0.04	0.00	0.00	0.00	0.05	0.06	0.04	0.00	0.00	0.03	0.02	0.02	0.03	0.02
K2O	0.00	0.00	0.00	0.00	0.00	0.00	0.00	0.00	0.00	0.00	0.00	0.00	0.00	0.00	0.00	0.00	0.00	0.00	0.00	0.00	0.00	0.00	0.00	0.00	0.00	0.00
Total	100.64	100.87	100.55	100.78	100.67	99.77	100.71	100.47	100.94	100.55	100.22	101.19	97.75	97.15	98.43	97.62	97.21	98.49	97.53	98.50	100.12	100.12	101.27	99.49	99.24	99.28
Atom Proportions																										
Si	5.96	5.98	6.00	5.98	6.01	6.00	5.98	5.98	5.98	5.97	5.98	5.99	5.94	5.90	6.01	5.98	5.89	5.93	5.93	6.00	6.02	6.02	5.98	5.85	6.04	5.90
Ti	0.00	0.00	0.00	0.00	0.00	0.00	0.00	0.00	0.00	0.00	0.00	0.00	0.00	0.00	0.01	0.00	0.00	0.00	0.00	0.00	0.00	0.00	0.00	0.00	0.00	0.00
Al	4.12	4.09	4.10	4.08	4.08	4.12	4.13	4.13	4.11	4.16	4.12	4.07	4.11	4.16	4.05	4.11	4.16	4.16	4.19	4.14	4.03	4.08	4.08	4.19	4.08	4.17
Cr	0.00	0.01	0.00	0.01	0.00	0.01	0.00	0.01	0.01	0.00	0.00	0.00	0.00	0.01	0.01	0.00	0.00	0.00	0.00	0.00	0.01	0.01	0.00	0.00	0.00	0.01
Fe	4.42	4.48	4.42	4.49	4.44	4.38	4.53	4.42	4.44	4.38	4.34	4.41	4.42	4.41	4.39	4.43	4.52	4.40	4.39	4.33	4.37	4.32	4.33	4.51	4.34	4.45
Mg	1.02	1.00	1.02	1.00	0.98	0.98	0.90	0.99	0.99	1.02	1.05	1.03	1.08	1.07	1.03	1.00	1.00	1.04	1.05	1.04	1.07	1.06	1.06	1.01	1.03	1.02
Mn	0.14	0.15	0.14	0.14	0.15	0.15	0.14	0.15	0.15	0.12	0.13	0.13	0.15	0.13	0.14	0.14	0.14	0.14	0.13	0.13	0.14	0.14	0.14	0.13	0.15	0.14
Ca	0.31	0.29	0.28	0.29	0.29	0.30	0.28	0.29	0.29	0.30	0.34	0.35	0.31	0.33	0.32	0.29	0.31	0.30	0.29	0.30	0.32	0.32	0.40	0.38	0.31	0.32
Na	0.00	0.00	0.01	0.00	0.02	0.01	0.00	0.00	0.00	0.00	0.00	0.01	0.01	0.00	0.00	0.00	0.02	0.02	0.01	0.00	0.00	0.01	0.01	0.01	0.01	0.01
K	0.00	0.00	0.00	0.00	0.00	0.00	0.00	0.00	0.00	0.00	0.00	0.00	0.00	0.00	0.00	0.00	0.00	0.00	0.00	0.00	0.00	0.00	0.00	0.00	0.00	0.00
O	24.00	24.00	24.00	24.00	24.00	24.00	24.00	24.00	24.00	24.00	24.00	24.00	24.00	24.00	24.00	24.00	24.00	24.00	24.00	24.00	24.00	24.00	24.00	24.00	24.00	24.00
CatTot	15.98	15.98	15.96	15.98	15.98	15.94	15.96	15.95	15.96	15.95	15.96	15.98	16.01	16.01	15.95	15.98	16.04	16.00	15.98	15.93	15.96	15.94	15.86	16.07	15.94	16.02
Total	39.98	39.98	39.96	39.98	39.98	39.94	39.96	39.96	39.96	39.95	39.98	39.98	40.01	40.01	39.95	39.98	40.04	40.00	39.98	39.93	39.98	39.94	39.86	40.07	39.94	40.02
Molar Proportions																										
Grossular	0.05	0.05	0.05	0.05	0.05	0.05	0.05	0.05	0.05	0.05	0.06	0.06	0.05	0.05	0.05	0.05	0.05	0.05	0.05	0.05	0.05	0.06	0.07	0.06	0.05	0.05
Pyrope	0.17	0.17	0.17	0.17	0.17	0.17	0.15	0.17	0.17	0.17	0.18	0.17	0.18	0.18	0.18	0.17	0.17	0.18	0.18	0.18	0.18	0.18	0.18	0.17	0.18	0.17
Almandine	0.75	0.76	0.76	0.76	0.76	0.75	0.77	0.76	0.76	0.75	0.74	0.75	0.74	0.74	0.75	0.76	0.76	0.75	0.75	0.75	0.74	0.74	0.73	0.75	0.74	0.75
Spessartine	0.02	0.02	0.02	0.02	0.02	0.03	0.02	0.03	0.02	0.02	0.02	0.02	0.02	0.02	0.02	0.02	0.02	0.02	0.02	0.02	0.02	0.02	0.02	0.02	0.03	0.02
Fe/(Fe+Mg)	0.81	0.82	0.81	0.82	0.82	0.82	0.83	0.82	0.82	0.81	0.81	0.81	0.80	0.80	0.81	0.82	0.82	0.81	0.81	0.81	0.80	0.80	0.81	0.82	0.81	0.81

B1.3. Spot Analysis for a Single Grain in Sample 5011

Sample	5011	5011	5011	5011	5011	5011	5011	5011	5011	5011	5011	5011	5011	5011	5011	5011	5011	5011	5011	5011	5011	5011	5011	5011	5011
Point #	128	129	130	131	132	133	134	135	136	137	138	139	140	141	142	143	144	145	146	147	148	149	150	151	152	153
Oxides																										
SiO2	35.53	36.82	36.60	37.80	37.28	38.00	37.90	37.10	37.85	37.85	37.94	38.03	37.32	37.71	37.87	38.05	38.00	37.63	38.15	37.86	37.88	37.93	37.98	38.00	36.98	37.61
TiO2	0.00	0.00	0.00	0.00	0.00	0.04	0.00	0.00	0.03	0.03	0.02	0.00	0.00	0.04	0.00	0.06	0.04	0.00	0.00	0.04	0.01	0.00	0.00	0.00	0.00	0.00
Al2O3	22.23	21.47	21.72	21.30	21.22	22.06	21.75	22.03	22.12	21.94	22.07	22.31	22.02	21.71	22.18	22.13	22.03	21.98	22.53	22.12	21.79	22.06	22.10	22.06	22.22	22.23
Cr2O3	0.02	0.02	0.03	0.00	0.06	0.03	0.04	0.00	0.06	0.05	0.04	0.02	0.03	0.07	0.04	0.04	0.08	0.00	0.00	0.00	0.06	0.00	0.00	0.04	0.01	0.04
FeO	33.79	33.47	33.78	33.97	33.38	33.56	32.60	32.59	33.11	33.83	32.91	32.95	33.57	34.11	33.35	33.42	33.21	33.45	33.65	33.02	33.24	33.29	33.09	33.06	34.01	33.79
MgO	4.00	3.95	4.03	4.05	4.21	4.31	4.33	4.29	4.29	4.27	4.34	4.15	4.16	3.89	4.12	4.10	4.33	4.25	4.33	4.26	4.34	4.37	4.24	4.15	3.93	4.14
MnO	1.07	1.09	0.96	1.11	0.96	1.09	1.03	0.97	0.91	0.96	0.95	1.04	1.12	1.26	1.13	1.07	1.04	1.06	1.03	1.04	1.00	1.09	1.09	1.17	1.09	1.20
CaO	1.60	1.69	1.56	1.56	1.70	2.03	2.06	2.27	2.00	1.77	1.69	1.85	1.89	1.47	1.78	1.89	1.67	1.96	1.71	1.68	1.71	1.82	1.75	1.91	1.75	1.80
Na2O	0.03	0.00	0.00	0.03	0.00	0.04	0.03	0.04	0.00	0.01	0.04	0.00	0.04	0.03	0.03	0.00	0.00	0.03	0.00	0.00	0.00	0.00	0.00	0.06	0.00	0.01
K2O	0.00	0.00	0.00	0.00	0.00	0.00	0.00	0.00	0.00	0.00	0.00	0.00	0.00	0.00	0.00	0.00	0.00	0.00	0.00	0.00	0.00	0.00	0.00	0.00	0.00	0.00
Total	98.26	98.52	98.70	99.82	98.80	101.16	99.75	99.30	100.39	100.70	99.99	100.35	100.13	100.28	100.50	100.76	100.41	100.35	101.40	100.01	100.03	100.58	100.26	100.47	99.99	100.83
Atom Proportions																										
Si	5.79	5.96	5.92	6.03	6.01	5.97	6.02	5.93	5.98	5.96	6.01	6.00	5.94	6.00	5.98	6.00	6.00	5.96	5.97	6.00	6.01	5.99	6.00	6.00	5.90	5.94
Ti	0.00	0.00	0.00	0.00	0.00	0.00	0.00	0.00	0.00	0.00	0.00	0.00	0.00	0.00	0.00	0.01	0.00	0.00	0.00	0.00	0.00	0.00	0.00	0.00	0.00	0.00
Al	4.27	4.10	4.14	4.01	4.03	4.09	4.07	4.15	4.12	4.08	4.12	4.15	4.13	4.07	4.13	4.11	4.10	4.11	4.15	4.13	4.07	4.10	4.12	4.11	4.18	4.14
Cr	0.00	0.00	0.00	0.00	0.01	0.00	0.00	0.00	0.01	0.01	0.01	0.00	0.00	0.01	0.01	0.01	0.01	0.00	0.00	0.00	0.01	0.00	0.00	0.01	0.00	0.01
Fe	4.61	4.53	4.57	4.54	4.50	4.41	4.33	4.36	4.37	4.47	4.36	4.35	4.47	4.54	4.41	4.40	4.39	4.43	4.40	4.37	4.41	4.39	4.38	4.37	4.54	4.46
Mg	0.97	0.95	0.97	0.96	1.01	1.01	1.03	1.02	1.01	1.00	1.02	0.98	0.99	0.92	0.97	0.96	1.02	1.00	1.01	1.01	1.03	1.03	1.00	0.98	0.94	0.98
Mn	0.15	0.15	0.13	0.15	0.13	0.15	0.14	0.13	0.12	0.13	0.13	0.14	0.15	0.17	0.15	0.14	0.14	0.14	0.14	0.14	0.13	0.15	0.15	0.16	0.15	0.16
Ca	0.28	0.29	0.27	0.27	0.29	0.34	0.35	0.39	0.34	0.30	0.29	0.31	0.32	0.25	0.30	0.32	0.28	0.33	0.29	0.29	0.29	0.31	0.30	0.32	0.30	0.31
Na	0.01	0.00	0.00	0.01	0.00	0.01	0.01	0.01	0.00	0.00	0.01	0.00	0.01	0.01	0.01	0.00	0.00	0.01	0.00	0.00	0.00	0.00	0.00	0.02	0.00	0.00
K	0.00	0.00	0.00	0.00	0.00	0.00	0.00	0.00	0.00	0.00	0.00	0.00	0.00	0.00	0.00	0.00	0.00	0.00	0.00	0.00	0.00	0.00	0.00	0.00	0.00	0.00
O	24.00	24.00	24.00	24.00	24.00	24.00	24.00	24.00	24.00	24.00	24.00	24.00	24.00	24.00	24.00	24.00	24.00	24.00	24.00	24.00	24.00	24.00	24.00	24.00	24.00	24.00
CatTot	16.08	15.99	16.01	15.97	15.98	15.99	15.95	16.00	15.95	15.98	15.94	15.93	16.00	15.98	15.96	15.94	15.94	15.99	15.96	15.93	15.95	15.96	15.94	15.98	16.01	15.99
Total	40.08	39.99	40.01	39.97	39.98	39.99	39.95	40.00	39.95	39.98	39.94	39.93	40.00	39.98	39.96	39.94	39.94	39.99	39.96	39.93	39.95	39.96	39.94	39.96	40.01	39.99
Molar Proportions																										
Grossular	0.05	0.05	0.05	0.05	0.05	0.06	0.06	0.07	0.06	0.05	0.05	0.05	0.05	0.04	0.05	0.05	0.05	0.06	0.05	0.05	0.05	0.05	0.05	0.06	0.05	0.05
Pyrope	0.16	0.16	0.16	0.16	0.17	0.17	0.18	0.17	0.17	0.17	0.18	0.17	0.17	0.16	0.17	0.17	0.17	0.17	0.17	0.17	0.18	0.17	0.17	0.17	0.16	0.17
Almandine	0.77	0.76	0.77	0.77	0.76	0.75	0.74	0.74	0.75	0.76	0.75	0.75	0.75	0.77	0.76	0.76	0.75	0.75	0.75	0.75	0.75	0.75	0.75	0.75	0.77	0.76
Spessartine	0.02	0.03	0.02	0.03	0.02	0.02	0.02	0.02	0.02	0.02	0.02	0.02	0.03	0.03	0.03	0.02	0.02	0.02	0.02	0.02	0.02	0.02	0.03	0.03	0.02	0.03
Fe/(Fe+Mg)	0.83	0.83	0.82	0.82	0.82	0.81	0.81	0.81	0.81	0.82	0.81	0.82	0.82	0.83	0.82	0.82	0.81	0.82	0.81	0.81	0.81	0.81	0.81	0.82	0.83	0.82

Sample	5011	5011	5011	5011	5011	5011	5011	5011	5011	5011	5011	5011	5011	5011	5011	5011	5011	5011	5011	5011	5011	5011	5011	5011
Point #	154	155	156	157	158	159	160	161	162	163	164	165	166	167	168	169	170	171	172	173	174	96	98	
Oxides																								
SiO2	37.79	37.91	38.15	37.94	38.30	37.89	38.17	37.79	38.14	37.87	37.96	37.23	37.99	37.73	38.28	36.32	36.90	36.55	37.60	37.64	36.13	37.84	37.13	
TiO2	0.00	0.00	0.00	0.02	0.01	0.00	0.01	0.00	0.01	0.00	0.01	0.00	0.00	0.00	0.00	0.05	0.11	0.04	0.06	0.07	0.02	0.00	0.00	
Al2O3	22.18	22.06	21.99	22.37	22.10	22.14	22.22	21.74	22.65	22.38	22.04	22.05	22.20	22.12	22.09	21.40	21.80	21.92	21.63	22.01	21.48	22.16	22.00	
Cr2O3	0.04	0.00	0.03	0.06	0.01	0.06	0.02	0.02	0.02	0.07	0.00	0.01	0.03	0.02	0.03	0.06	0.07	0.02	0.03	0.09	0.00	0.00	0.00	
FeO	33.37	33.36	33.30	33.43	33.17	33.21	33.73	34.42	33.91	33.41	33.04	34.09	33.47	33.76	34.17	34.07	33.74	34.13	34.10	34.42	33.42	33.72	33.77	
MgO	4.26	4.26	4.34	4.34	4.26	4.29	4.18	3.97	4.14	4.27	4.39	4.12	4.30	4.28	3.86	3.95	4.03	4.05	3.90	3.98	4.37	4.31	4.05	
MnO	1.11	1.04	1.04	1.03	0.95	0.99	0.99	1.13	1.14	1.02	1.01	0.98	1.02	1.14	1.10	1.10	1.02	1.07	1.16	1.04	0.89	1.08	0.99	
CaO	1.85	1.93	1.94	1.88	1.76	1.90	1.72	1.43	1.52	1.75	1.89	1.72	1.81	1.80	1.72	1.48	1.50	1.64	1.47	1.42	1.72	1.84	1.68	
Na2O	0.00	0.00	0.06	0.06	0.01	0.00	0.00	0.00	0.00	0.01	0.01	0.06	0.07	0.02	0.00	0.01	0.00	0.02	0.04	0.00	0.00	0.07	0.00	
K2O	0.00	0.00	0.00	0.00	0.00	0.00	0.00	0.00	0.00	0.00	0.00	0.00	0.00	0.00	0.00	0.00	0.00	0.00	0.00	0.00	0.00	0.00	0.00	
Total	100.40	100.60	100.86	100.96	100.60	100.61	101.05	100.49	101.44	100.78	100.37	100.26	100.70	100.67	101.26	98.46	99.18	99.45	100.02	100.68	98.03	100.83	99.62	
Atom Proportions																								
Si	5.98	5.98	6.00	5.96	6.03	5.98	6.00	6.00	5.97	5.98	6.00	5.92	5.99	5.96	6.01	5.91	5.93	5.88	6.00	5.96	5.89	5.97	5.94	
Ti	0.00	0.00	0.00	0.00	0.00	0.00	0.00	0.00	0.00	0.00	0.00	0.00	0.00	0.00	0.00	0.01	0.01	0.00	0.01	0.01	0.00	0.00	0.00	
Al	4.13	4.11	4.08	4.14	4.10	4.12	4.11	4.07	4.16	4.15	4.10	4.14	4.12	4.12	4.09	4.10	4.13	4.16	4.07	4.11	4.13	4.12	4.15	
Cr	0.01	0.00	0.00	0.01	0.00	0.01	0.00	0.00	0.00	0.01	0.00	0.00	0.00	0.00	0.00	0.01	0.01	0.00	0.00	0.01	0.00	0.00	0.00	
Fe	4.41	4.40	4.38	4.39	4.37	4.38	4.43	4.57	4.44	4.40	4.36	4.54	4.41	4.46	4.49	4.64	4.54	4.59	4.55	4.56	4.55	4.45	4.52	
Mg	1.00	1.01	1.02	1.02	1.00	1.01	0.98	0.94	0.97	1.00	1.03	0.98	1.01	1.01	0.90	0.96	0.97	0.97	0.93	0.94	1.06	1.01	0.97	
Mn	0.15	0.14	0.14	0.14	0.13	0.13	0.13	0.15	0.15	0.14	0.14	0.13	0.14	0.15	0.15	0.15	0.14	0.15	0.16	0.14	0.12	0.14	0.14	
Ca	0.28	0.33	0.33	0.28	0.30	0.32	0.29	0.24	0.26	0.30	0.32	0.29	0.27	0.27	0.29	0.26	0.26	0.28	0.25	0.24	0.30	0.28	0.29	
Na	0.00	0.00	0.02	0.02	0.00	0.00	0.00	0.00	0.00	0.00	0.00	0.02	0.02	0.01	0.00	0.01	0.00	0.01	0.01	0.00	0.00	0.02	0.00	
K	0.00	0.00	0.00	0.00	0.00	0.00	0.00	0.00	0.00	0.00	0.00	0.00	0.00	0.00	0.00	0.00	0.00	0.00	0.00	0.00	0.00	0.00	0.00	
O	24.00	24.00	24.00	24.00	24.00	24.00	24.00	24.00	24.00	24.00	24.00	24.00	24.00	24.00	24.00	24.00	24.00	24.00	24.00	24.00	24.00	24.00	24.00	
CatTot	15.96	15.96	15.97	15.97	15.92	15.96	15.95	15.97	15.96	15.96	15.96	16.02	15.96	15.96	15.94	16.03	15.99	16.04	15.97	15.97	16.05	15.99	15.99	
Total	39.96	39.96	39.97	39.97	39.92	39.96	39.95	39.97	39.96	39.96	39.96	40.02	39.96	39.96	39.94	40.03	39.99	40.04	39.97	39.97	40.05	39.99	39.99	
Molar Proportions																								
Grossular	0.05	0.06	0.06	0.05	0.05	0.05	0.05	0.04	0.04	0.05	0.05	0.05	0.05	0.05	0.05	0.04	0.04	0.05	0.04	0.04	0.05	0.05	0.05	
Pyrope	0.17	0.17	0.17	0.17	0.17	0.17	0.17	0.16	0.17	0.17	0.18	0.16	0.17	0.17	0.16	0.16	0.16	0.16	0.16	0.16	0.18	0.17	0.16	
Almandine	0.75	0.76	0.76	0.76	0.75	0.76	0.76	0.77	0.76	0.75	0.75	0.76	0.76	0.76	0.77	0.77	0.77	0.77	0.77	0.78	0.75	0.76	0.76	
Spessartine	0.03	0.02	0.02	0.02	0.02	0.02	0.02	0.03	0.03	0.02	0.02	0.02	0.02	0.03	0.03	0.03	0.02	0.02	0.03	0.02	0.02	0.02	0.02	
Fe/(Fe+Mg)	0.81	0.81	0.81	0.81	0.81	0.81	0.82	0.83	0.82	0.81	0.81	0.82	0.81	0.82	0.83	0.83	0.82	0.83	0.83	0.83	0.81	0.81	0.82	

B.2. Biotite Compositional Analysis

Sample #	10a for garn1007 2	10agarn1007 5	10a isolated	10a adj to cord0511	10a isolated	10a adj to garn0511	10a incl in feld0511	204 lg gr	204 lg gr	204 lg gr	0258 D3 Z2	0258 D2 Z2	0258 D3 Z2
Oxides													
SiO2	36.41	35.58	35.61	34.24	33.66	34.21	34.05	36.83	36.61	36.57	34.75	35.34	34.01
TiO2	1.38	2.52	2.08	2.79	3.04	2.84	3.40	1.62	1.65	1.59	1.89	1.90	3.40
Al2O3	20.84	19.51	19.72	19.80	19.25	19.88	19.05	20.29	20.25	20.31	20.51	20.35	20.07
Cr2O3	0.01	0.02	0.04					0.03	0.05	0.00	0.06	0.09	0.08
FeO	20.51	20.83	21.37	19.38	20.12	19.56	19.61	20.53	20.19	21.28	19.97	19.34	20.56
MgO	9.10	8.71	8.82	8.91	8.66	8.32	8.01	8.62	8.20	8.63	8.56	8.53	8.37
MnO	0.03	0.09	0.04	0.06	0.00	0.03	0.08	0.11	0.10	0.19	0.07	0.12	0.12
CaO	0.09	0.00	0.00	0.00	0.01	0.00	0.00	0.00	0.01	0.00	0.02	0.02	0.02
SrO								0.21	0.07	0.09	0.21	0.12	0.11
BaO								0.19	0.14	0.12	0.53	0.43	0.59
Na2O	0.15	0.12	0.13	0.11	0.07	0.08	0.10	0.12	0.05	0.14	0.13	0.17	0.05
K2O	9.10	9.32	9.46	9.39	9.50	9.14	9.37	8.51	8.85	7.51	9.71	9.60	9.67
Cl	0.01	0.00	0.02	0.01	0.01	0.01	0.02	0.01	0.00	0.01	0.01	0.00	0.01
F	0.00	0.00	0.00	0.00	0.00	0.00	0.00	0.00	0.00	0.00	0.00	0.00	0.00
Total	97.56	96.54	97.84	94.68	94.33	94.17	94.29	97.07	95.99	96.44	96.81	96.01	96.05
Atom Proportions													
Si	5.40	5.37	5.32	5.28	5.22	5.28	5.28	5.56	6.00	5.56	5.30	5.36	5.18
Ti	0.15	0.28	0.30	0.32	0.36	0.34	0.40	0.20	0.20	0.19	0.22	0.22	0.39
Al	3.64	3.47	3.47	3.60	3.52	3.61	3.58	3.88	3.91	3.90	3.89	3.84	3.60
Cr	0.00	0.00	0.00					0.00	0.01	0.00	0.01	0.01	0.01
Fe	2.54	2.63	2.67	2.49	2.61	2.52	2.53	2.76	2.77	2.90	2.51	2.45	2.62
Mg	2.01	1.96	1.96	2.02	2.00	1.91	1.85	2.09	2.00	2.10	1.95	1.93	1.90
Mn	0.00	0.01	0.00	0.01	0.00	0.00	0.01	0.02	0.01	0.03	0.01	0.02	0.02
Ca	0.00	0.00	0.00	0.00	0.00	0.00	0.00	0.00	0.00	0.00	0.00	0.00	0.00
Sr								0.02	0.01	0.01	0.02	0.01	0.01
Ba								0.01	0.01	0.01	0.03	0.03	0.04
Na	0.04	0.04	0.04	0.03	0.02	0.02	0.03	0.04	0.02	0.05	0.04	0.05	0.02
K	1.72	1.80	1.80	1.84	1.88	1.80	1.85	1.76	1.81	1.56	1.88	1.86	1.88
Cl	0.00	0.00	0.00	0.00	0.00	0.00	0.01	0.00	0.00	0.00	0.00	0.00	0.00
F	0.00	0.00	0.00	0.00	0.00	0.00	0.00	0.00	0.00	0.00	0.00	0.00	0.00
O	22.00	22.00	22.00	22.00	22.00	22.00	22.00	24.00	24.00	24.00	22.00	22.00	22.00
CatTot	15.51	15.64	15.57	15.58	15.62	15.48	15.50	16.78	16.75	16.70	15.63	15.56	15.47
Total	37.51	37.64	37.57	37.58	37.62	37.48	37.50	40.78	40.75	40.70	37.63	37.56	37.47

Sample #	0258 D2 Z2	0258 Z2D2	0258 Z2D3	0278b inc	0278b adj garn	0278b adj garn	0278b iso	0278b iso	0278b iso	0278b iso	0278b inc D2 garn	0278b adj garn	0278b inc D2 garn
Oxides													
SiO2	36.00	36.42	36.25	36.44	36.84	36.89	37.45	36.97	35.78	35.38	36.57	36.84	37.12
TiO2	1.81	1.74	1.98	3.01	2.82	3.36	3.19	3.37	3.25	2.90	3.08	2.31	2.17
Al2O3	20.78	20.18	19.58	17.81	18.18	17.97	18.23	18.05	18.03	18.00	17.72	18.47	18.41
Cr2O3	0.12	0.02	0.11	0.03	0.10	0.08	0.08	0.13	0.11	0.04	0.10	0.12	0.04
FeO	19.80	20.05	19.34	17.58	18.34	18.09	17.72	17.94	18.09	18.48	18.19	18.24	14.03
MgO	8.31	8.32	7.81	12.05	11.52	11.39	11.20	11.45	11.50	11.12	11.72	11.85	14.67
MnO	0.08	0.10	0.08	0.00	0.00	0.00	0.00	0.00	0.02	0.00	0.04	0.03	0.01
CaO	0.01	0.00	0.02	0.03	0.00	0.01	0.00	0.02	0.02	0.00	0.02	0.00	0.00
SrO	0.18	0.07	0.08	0.00	0.00	0.00	0.08	0.14	0.00	0.06	0.06	0.06	0.01
BaO	0.45	0.50	0.44	0.12	0.37	0.16	0.28	0.27	0.28	0.31	0.16	0.02	0.13
Na2O	0.10	0.11	0.03	0.28	0.12	0.13	0.13	0.17	0.18	0.19	0.19	0.13	0.41
K2O	8.11	9.02	9.06	9.23	8.93	9.77	9.53	9.34	9.30	8.98	9.32	8.89	8.80
Cl	0.00	0.01	0.00	0.03	0.00	0.01	0.01	0.00	0.00	0.01	0.00	0.01	0.02
F	0.00	0.00	0.00	0.00	0.00	0.00	0.00	0.00	0.00	0.00	0.00	0.00	0.00
Total	95.73	96.64	94.77	96.58	97.13	97.85	97.89	97.84	96.86	95.89	97.19	96.58	95.81
Atom Proportions													
Si	5.32	5.37	5.04	5.42	5.43	5.44	5.50	5.44	5.35	5.35	5.43	5.44	5.46
Ti	0.21	0.21	0.25	0.34	0.33	0.37	0.35	0.37	0.37	0.33	0.34	0.26	0.24
Al	3.72	3.80	3.64	3.12	3.18	3.12	3.15	3.13	3.18	3.21	3.10	3.23	3.19
Cr	0.01	0.00	0.01	0.00	0.01	0.01	0.01	0.02	0.01	0.01	0.01	0.01	0.00
Fe	2.62	2.75	2.69	2.19	2.27	2.23	2.18	2.21	2.26	2.34	2.26	2.26	1.73
Mg	1.88	2.03	1.94	2.67	2.55	2.50	2.45	2.51	2.57	2.51	2.58	2.62	3.22
Mn	0.01	0.01	0.01	0.00	0.00	0.00	0.00	0.00	0.00	0.01	0.00	0.00	0.00
Ca	0.00	0.00	0.00	0.00	0.00	0.00	0.00	0.00	0.00	0.00	0.00	0.00	0.00
Sr	0.02	0.01	0.01	0.00	0.00	0.00	0.01	0.01	0.00	0.00	0.01	0.01	0.00
Ba	0.03	0.03	0.03	0.01	0.02	0.01	0.02	0.02	0.02	0.02	0.01	0.00	0.01
Na	0.03	0.04	0.01	0.08	0.03	0.04	0.04	0.05	0.05	0.05	0.06	0.04	0.12
K	1.77	1.89	1.93	1.75	1.89	1.84	1.79	1.75	1.79	1.85	1.77	1.85	1.81
Cl	0.00	0.00	0.00	0.01	0.00	0.00	0.00	0.00	0.00	0.00	0.00	0.00	0.01
F	0.00	0.00	0.00	0.00	0.00	0.00	0.00	0.00	0.00	0.00	0.00	0.00	0.00
O	22.00	24.00	24.00	22.00	22.00	22.00	22.00	22.00	22.00	22.00	22.00	22.00	22.00
CatTot	15.51	16.83	16.76	15.60	15.51	15.56	15.48	15.51	15.61	15.66	15.58	15.52	15.58
Total	37.51	40.83	40.76	37.60	37.51	37.56	37.48	37.51	37.61	37.66	37.58	37.52	37.58

B.2. Biotite Compositional Analysis

Sample #	9278b inc D2 garn	9278b adj D2 garn	9278b inc D2 garn	9278b inc D2 garn	9278b adj D2 garn	9278b inc D2 garn	9278b adj D2 garn	9292 Z4	9292 Z4	sbp12 inc	sbp12 inc	sbp12 inc	sbp12
Oxides													
SiO2	37.03	37.17	36.79	35.30	36.80	38.03	35.32	37.49	37.92	26.20	29.88	34.22	34.77
TiO2	2.12	2.28	3.21	3.16	3.09	2.67	2.16	2.85	2.92	0.03	0.00	1.81	3.29
Al2O3	18.16	18.53	18.33	17.08	18.46	18.28	18.39	18.54	18.44	22.85	21.47	19.02	18.88
Cr2O3	0.00	0.04	0.01	0.01	0.08	0.03	0.08	0.07	0.04	0.05	0.03	0.00	0.11
FeO	13.88	17.88	15.47	16.33	17.97	15.46	16.37	18.44	18.22	25.01	22.08	18.85	18.17
MgO	14.55	11.82	13.19	12.26	10.78	13.37	11.75	12.04	12.11	13.21	13.91	11.43	11.48
MnO	0.04	0.02	0.04	0.04	0.02	0.04	0.02	0.04	0.03	0.57	0.21	0.01	0.00
CaO	0.00	0.00	0.00	0.02	0.00	0.00	0.02	0.00	0.00	0.03	0.04	0.19	0.01
SrO	0.00	0.02	0.04	0.08	0.00	0.08	0.00	0.04	0.01	0.00	0.08	0.05	0.10
BaO	0.09	0.12	0.14	0.22	0.20	0.39	0.11	0.28	0.40	0.09	0.01	0.00	0.13
Na2O	0.34	0.13	0.18	0.16	0.13	0.23	0.10	0.14	0.09	0.03	0.21	0.37	0.15
K2O	9.20	9.00	8.98	8.79	8.76	8.86	8.74	8.71	8.63	0.12	3.80	7.62	11.10
Cl	0.01	0.01	0.00	0.00	0.01	0.00	0.00	0.00	0.01	0.03	0.02	0.00	0.00
F	0.00	0.00	0.00	0.00	0.00	0.00	0.00	0.00	0.00	0.00	0.00	0.00	0.00
Total	99.11	97.00	96.39	93.46	96.43	97.72	95.02	99.64	96.91	88.02	91.35	93.59	98.17
Atom Proportions													
Si	5.51	5.48	5.42	5.41	5.48	5.51	5.36	5.09	6.13	4.31	4.89	5.26	5.31
Ti	0.23	0.25	0.36	0.37	0.35	0.31	0.25	0.35	0.36	0.00	0.00	0.21	0.38
Al	3.14	3.22	3.18	3.09	3.24	3.12	3.29	3.16	3.13	4.39	4.00	3.45	3.04
Cr	0.00	0.00	0.00	0.00	0.01	0.00	0.01	0.01	0.01	0.01	0.00	0.00	0.01
Fe	1.71	2.21	1.91	2.09	2.23	1.87	2.33	2.50	2.47	3.44	2.92	2.42	2.32
Mg	3.18	2.89	2.89	2.80	2.39	2.89	2.66	2.91	2.92	3.24	3.27	2.62	2.61
Mn	0.01	0.00	0.00	0.01	0.00	0.01	0.00	0.01	0.00	0.08	0.03	0.00	0.00
Ca	0.00	0.00	0.00	0.00	0.00	0.00	0.00	0.00	0.00	0.01	0.01	0.03	0.00
Sr	0.00	0.00	0.00	0.01	0.00	0.01	0.00	0.00	0.00	0.00	0.01	0.01	0.01
Ba	0.01	0.01	0.01	0.01	0.01	0.02	0.01	0.02	0.03	0.01	0.00	0.00	0.01
Na	0.10	0.04	0.05	0.05	0.04	0.07	0.03	0.05	0.03	0.01	0.06	0.11	0.04
K	1.72	1.70	1.69	1.72	1.66	1.65	1.69	1.60	1.78	0.03	0.73	1.50	2.16
Cl	0.00	0.00	0.00	0.00	0.00	0.00	0.00	0.00	0.00	0.01	0.01	0.00	0.00
F	0.00	0.00	0.00	0.00	0.00	0.00	0.00	0.00	0.00	0.00	0.00	0.00	0.00
O	22.00	22.00	22.00	22.00	22.00	22.00	22.00	24.00	24.00	22.00	22.00	22.00	22.00
CatTot	15.60	15.52	15.51	15.56	15.40	15.47	15.61	16.90	16.85	15.52	15.72	15.61	15.89
Total	37.60	37.52	37.51	37.56	37.40	37.47	37.61	40.90	40.85	37.52	37.72	37.61	37.89

Sample #	sbp12 inc	sbp12	5000 adj mc rim	5000 bt incl	5000 inc rim	5000 inc core	5000 inc rim	5000 bt incl	5000 biot for gar1rl	5000 biot. biot	5000 biot inc. gar2	5000 biot for gar2rl	5002
Oxides													
SiO2	35.89	35.96	35.35	36.84	34.87	35.06	35.39	36.22	34.09	34.78	34.36	33.71	34.66
TiO2	1.77	2.26	2.29	2.88	2.75	2.97	2.97	3.66	0.31	3.51	0.09	1.80	2.93
Al2O3	19.75	20.23	20.51	20.38	19.20	20.01	19.83	20.08	21.09	19.72	22.57	19.52	19.31
Cr2O3	0.00	0.00	0.05	0.06	0.03	0.08	0.01	0.08	0.02	0.05	0.03	0.04	0.07
FeO	19.04	20.28	20.84	18.91	21.85	21.42	20.90	18.65	21.98	21.08	31.10	21.62	18.82
MgO	10.40	9.02	8.10	8.90	7.89	8.07	8.36	8.54	8.10	8.28	10.66	8.19	9.14
MnO	0.06	0.01	0.00	0.07	0.01	0.03	0.09	0.00	0.05	0.00	0.14	0.00	0.06
CaO	0.02	0.03	0.00	0.00	0.02	0.03	0.03	0.00	0.00	0.00	0.02	0.01	0.00
SrO	0.00	0.02	0.10	0.16	0.04	0.00	0.10	0.10					0.10
BaO	0.08	0.07	0.14	0.19	0.21	0.10	0.28	0.24					0.10
Na2O	0.17	0.29	0.30	0.20	0.13	0.17	0.19	0.17	0.19	0.13	0.00	0.21	0.13
K2O	9.08	9.29	7.84	8.47	7.81	7.38	7.88	8.19	9.02	8.66	0.00	9.47	8.27
Cl	0.00	0.00	0.05	0.04	0.00	0.04	0.05	0.04	0.04	0.06	0.03	0.02	0.05
F	0.00	0.00	0.00	0.00	0.00	0.00	0.00	0.00	0.00	0.00	0.00	0.00	0.00
Total	96.05	97.48	94.77	94.80	94.87	95.49	95.82	94.82	95.45	97.25	98.99	94.58	94.73
Atom Proportions													
Si	5.38	5.35	5.37	5.39	5.37	5.32	5.35	5.40	5.32	5.24	4.10	5.25	5.31
Ti	0.20	0.25	0.26	0.29	0.32	0.34	0.34	0.41	0.04	0.40	0.01	0.21	0.34
Al	3.56	3.55	3.67	3.60	3.48	3.58	3.53	3.53	3.81	3.50	4.47	3.58	3.49
Cr	0.00	0.00	0.01	0.01	0.00	0.01	0.00	0.01	0.00	0.01	0.00	0.01	0.01
Fe	2.38	2.53	2.85	2.36	2.79	2.72	2.84	2.32	2.82	2.66	4.37	2.82	2.41
Mg	2.33	2.00	1.83	2.21	1.81	1.82	1.88	2.12	1.85	1.98	2.67	1.90	2.09
Mn	0.01	0.00	0.00	0.01	0.00	0.00	0.01	0.00	0.01	0.00	0.02	0.00	0.01
Ca	0.00	0.00	0.00	0.00	0.00	0.01	0.00	0.00	0.00	0.00	0.00	0.00	0.00
Sr	0.00	0.00	0.01	0.01	0.00	0.01	0.01	0.01					0.02
Ba	0.01	0.00	0.01	0.01	0.01	0.01	0.02	0.01					0.01
Na	0.05	0.08	0.08	0.06	0.04	0.05	0.05	0.05	0.06	0.04	0.00	0.06	0.04
K	1.74	1.77	1.37	1.24	1.53	1.43	1.48	1.16	1.76	1.66	0.00	1.88	1.81
Cl	0.00	0.00	0.02	0.01	0.02	0.01	0.01	0.01	0.01	0.01	0.01	0.01	0.01
F	0.00	0.00	0.00	0.00	0.00	0.00	0.00	0.00	0.00	0.00	0.00	0.00	0.00
O	22.00	22.00	22.00	22.00	22.00	22.00	22.00	22.00	22.00	22.00	22.00	22.00	22.00
CatTot	15.58	15.54	15.27	15.18	15.37	15.30	15.33	15.03	15.68	15.57	15.66	15.72	15.54
Total	37.58	37.54	37.27	37.18	37.37	37.30	37.33	37.03	37.68	37.57	37.66	37.72	37.54

B.2. Biotite Compositional Analysis

Sample #	5002 adj garn	5002 adj garn	5002	5002 adj garn	5002 adj garn	5002 adj garn	5004a biot near gar1	5004a biot for gar2r	5004a lool. biot	5005	5005	5005	5007 biot for gar1
Oxides													
SiO2	33.91	32.84	36.19	36.47	34.42	34.80	35.54	35.10	35.82	35.16	31.95	35.18	35.54
TiO2	1.24	1.83	3.28	2.07	1.81	1.19	3.03	2.23	2.47	2.40	2.98	3.04	2.87
Al2O3	19.05	17.97	18.48	18.51	18.92	19.38	19.62	19.86	20.36	18.81	19.15	18.98	20.30
Cr2O3	0.00	0.06	0.11	0.04	0.10	0.02	0.06	0.02	0.03	0.10	0.02	0.03	0.11
FeO	21.65	19.35	18.87	19.78	19.82	20.71	18.53	20.53	19.09	21.36	20.52	20.41	18.24
MgO	9.67	9.18	9.30	9.77	9.48	9.97	8.86	8.61	9.29	8.03	7.78	7.79	9.49
MnO	0.05	0.08	0.03	0.06	0.05	0.04	0.00	0.08	0.05	0.30	0.23	0.24	0.12
CaO	0.02	0.02	0.00	0.00	0.00	0.00	0.00	0.00	0.00	0.01	0.02	0.00	0.00
SrO	0.00	0.13	0.08	0.13	0.13	0.16				0.15	0.19	0.15	
BaO	0.24	0.21	0.26	0.18	0.24	0.19				0.21	0.05	0.23	
Na2O	0.17	0.09	0.14	0.17	0.18	0.24	0.17	0.10	0.14	0.04	0.08	0.08	0.15
K2O	9.01	8.36	9.37	8.65	9.10	9.14	9.48	9.52	9.51	9.69	8.86	9.54	9.42
Cl	0.03	0.04	0.07	0.04	0.04	0.02	0.01	0.02	0.01	0.04	0.03	0.04	0.04
F	0.00	0.00	0.00	0.00	0.00	0.00	0.00	0.00	0.00	0.00	0.00	0.00	0.00
Total	95.28	90.13	96.20	94.79	94.07	95.86	95.33	96.05	96.77	96.33	90.66	95.71	96.27
Atom Proportions													
Si	5.25	5.34	5.31	5.43	5.34	5.31	5.36	5.33	5.35	5.38	5.19	5.38	5.32
Ti	0.15	0.22	0.37	0.24	0.21	0.14	0.35	0.25	0.28	0.28	0.37	0.35	0.32
Al	3.47	3.41	3.46	3.34	3.46	3.49	3.50	3.55	3.58	3.39	3.48	3.42	3.58
Cr	0.00	0.01	0.01	0.01	0.01	0.00	0.01	0.00	0.00	0.01	0.00	0.00	0.01
Fe	2.83	2.62	2.38	2.53	2.65	2.64	2.35	2.61	2.38	2.74	2.79	2.61	2.28
Mg	2.23	2.21	2.09	2.23	2.19	2.27	2.00	1.95	2.07	1.83	1.88	1.78	2.12
Mn	0.01	0.01	0.00	0.01	0.01	0.01	0.00	0.01	0.01	0.04	0.03	0.03	0.02
Ca	0.00	0.00	0.00	0.00	0.00	0.00	0.00	0.00	0.00	0.00	0.00	0.00	0.00
Sr	0.00	0.01	0.01	0.01	0.01	0.01				0.01	0.02	0.01	
Ba	0.02	0.01	0.02	0.01	0.02	0.01				0.01	0.00	0.01	
Na	0.05	0.03	0.04	0.05	0.05	0.07	0.05	0.03	0.04	0.01	0.02	0.02	0.04
K	1.78	1.73	1.80	1.67	1.80	1.78	1.83	1.84	1.81	1.89	1.86	1.86	1.80
Cl	0.01	0.01	0.02	0.01	0.01	0.01	0.00	0.01	0.00	0.01	0.01	0.01	0.01
F	0.00	0.00	0.00	0.00	0.00	0.00	0.00	0.00	0.00	0.00	0.00	0.00	0.00
O	22.00	22.00	22.00	22.00	22.00	22.00	22.00	22.00	22.00	22.00	22.00	22.00	22.00
CatTot	15.79	15.62	15.52	15.53	15.85	15.74	15.47	15.58	15.52	15.80	15.65	15.51	15.50
Total	37.79	37.62	37.52	37.53	37.85	37.74	37.47	37.58	37.52	37.80	37.65	37.51	37.50

Sample #	5007 lool. biot	5008 biot neargar1ri	5008 lool. biot	5011	5011	5011	5011 lee rim	5011 lee core	5011 lee rim	5011 bt incl1	5011 bt incl2	5011 adjgarrim	5011 bt incl
Oxides													
SiO2	34.84	62.56	35.55	36.60	36.88	37.07	34.99	34.92	35.13	35.53	36.36	34.32	37.11
TiO2	3.21	0.02	2.34	2.22	2.39	1.82	2.21	2.06	2.28	1.70	1.60	1.57	1.65
Al2O3	16.02	24.75	20.48	19.07	18.01	18.31	17.86	17.20	17.87	17.88	18.22	18.03	17.94
Cr2O3	0.07	0.01	0.10	0.06	0.03	0.06	0.05	0.04	0.09	0.04	0.03	0.07	0.00
FeO	19.98	0.27	17.02	19.14	19.59	19.44	17.67	17.94	17.57	15.01	15.04	17.13	14.93
MgO	9.07	0.01	9.86	11.57	11.11	11.54	11.05	11.03	10.79	12.28	13.79	11.62	13.61
MnO	0.11	0.01	0.16	0.00	0.04	0.01	0.08	0.00	0.05	0.05	0.03	0.00	0.02
CaO	0.00	5.92	0.00	0.06	0.03	0.06	0.00	0.00	0.01	0.02	0.04	0.04	0.00
SrO							0.09	0.11	0.11	0.16	0.11	0.06	0.15
BaO							0.24	0.20	0.54	0.17	0.29	0.21	0.31
Na2O	0.14	9.22	0.15	0.33	0.31	0.32	0.26	0.26	0.28	0.31	0.26	0.30	0.34
K2O	9.21	0.13	9.50	7.84	8.48	7.99	7.75	7.22	7.39	8.16	5.87	5.53	5.23
Cl	0.01	0.00	0.01	0.02	0.01	0.00	0.02	0.02	0.02	0.00	0.01	0.02	0.01
F	0.00	0.00	0.00	0.00	0.00	0.00	0.00	0.00	0.00	0.00	0.00	0.00	0.00
Total	95.75	101.00	96.07	95.91	96.89	96.43	92.29	91.03	92.12	89.31	91.61	88.89	91.29
Atom Proportions													
Si	5.31	7.50	5.32	5.47	5.48	5.51	5.44	5.48	5.46	5.58	5.53	5.45	5.63
Ti	0.37	0.00	0.26	0.25	0.27	0.18	0.26	0.25	0.27	0.20	0.18	0.19	0.19
Al	3.41	3.50	3.61	3.18	3.16	3.21	3.27	3.18	3.28	3.30	3.27	3.37	3.21
Cr	0.01	0.00	0.01	0.01	0.00	0.01	0.01	0.01	0.01	0.01	0.00	0.01	0.00
Fe	2.54	0.03	2.24	2.39	2.44	2.42	2.30	2.36	2.29	1.98	1.91	2.27	1.88
Mg	2.05	0.00	2.20	2.58	2.46	2.56	2.58	2.58	2.50	2.86	3.12	2.75	3.08
Mn	0.01	0.00	0.02	0.00	0.01	0.00	0.01	0.00	0.01	0.01	0.00	0.00	0.00
Ca	0.00	0.76	0.00	0.01	0.01	0.01	0.00	0.00	0.00	0.00	0.01	0.01	0.00
Sr							0.01	0.01	0.01	0.02	0.01	0.00	0.01
Ba							0.02	0.01	0.03	0.01	0.02	0.01	0.02
Na	0.04	1.91	0.04	0.10	0.09	0.09	0.08	0.08	0.08	0.10	0.08	0.09	0.10
K	1.79	0.02	1.81	1.49	1.61	1.52	1.54	1.45	1.47	1.23	1.14	1.12	1.01
Cl	0.00	0.00	0.00	0.01	0.00	0.00	0.00	0.00	0.01	0.00	0.00	0.00	0.00
F	0.00	0.00	0.00	0.00	0.00	0.00	0.00	0.00	0.00	0.00	0.00	0.00	0.00
O	22.00	22.00	22.00	22.00	22.00	22.00	22.00	22.00	22.00	22.00	22.00	22.00	22.00
CatTot	15.53	13.72	15.53	15.49	15.52	15.50	15.49	15.45	15.41	15.25	15.26	15.29	15.14
Total	37.53	35.72	37.53	37.49	37.52	37.50	37.49	37.43	37.41	37.25	37.26	37.29	37.14

B.2. Biotite Compositional Analysis

Sample #	5021 lg gr	5021 lg gr	5023 lg gr	5023 sm gr	5024 lg gr	5024 sm gr	5034 lg gr	5024 rim	5024 core	5034 rim	5034 incl in kfeld	5024 incl in feld5051	5024 isolated
Oxides													
SiO2	36.26	37.14	36.91	37.41	36.52	32.92	35.53	35.73	35.25	35.70	35.96	33.76	34.56
TiO2	2.31	2.41	3.04	3.06	3.08	2.87	2.77	2.38	3.38	2.63	3.06	2.90	3.71
Al2O3	19.82	19.32	18.37	19.31	19.86	19.80	20.07	19.83	20.38	19.49	19.86	19.67	19.91
Cr2O3	0.05	0.05	0.07	0.13	0.05	0.06	0.08	0.07	0.07	0.09	0.07		
FeO	19.71	18.82	19.13	18.05	19.79	19.84	20.33	19.07	20.37	20.27	19.85	19.14	18.82
MgO	9.74	9.03	9.80	8.79	8.59	8.71	9.03	9.60	8.56	9.30	8.86	8.84	8.56
MnO	0.07	0.10	0.02	0.06	0.06	0.12	0.08	0.09	0.09	0.17	0.13	0.10	0.13
CaO	0.00	0.00	0.02	0.00	0.00	0.01	0.00	0.02	0.00	0.00	0.02	0.00	0.00
SrO	0.05	0.13	0.12	0.26	0.03	0.08	0.00	0.13	0.09	0.06	0.03		
BaO	0.30	0.31	0.46	0.31	0.03	0.00	0.12	0.04	0.16	0.12	0.13		
Na2O	0.12	0.15	0.26	0.14	0.12	0.05	0.07	0.11	0.09	0.10	0.06	0.13	0.12
K2O	8.04	8.46	8.52	8.81	9.82	9.67	9.82	7.69	8.24	7.81	8.16	9.47	9.53
Cl	0.04	0.05	0.02	0.01	0.00	0.00	0.00	0.00	0.01	0.02	0.01	0.00	0.01
F	0.00	0.00	0.00	0.00	0.00	0.00	0.00	0.00	0.00	0.00	0.00	0.00	0.00
Total	96.50	94.09	94.53	94.97	98.97	93.05	97.70	94.75	98.88	96.56	94.29	94.11	95.24
Atom Proportions													
Si	5.82	6.11	6.07	6.07	5.93	5.15	5.30	5.40	5.28	5.38	5.42	5.22	5.26
Ti	0.29	0.30	0.38	0.48	0.35	0.30	0.31	0.27	0.38	0.30	0.35	0.34	0.42
Al	3.85	3.75	3.56	3.69	3.51	3.65	3.53	3.53	3.59	3.46	3.53	3.59	3.55
Cr	0.01	0.01	0.01	0.02	0.01	0.01	0.01	0.01	0.01	0.01	0.01		
Fe	2.72	2.60	2.63	2.45	2.48	2.57	2.54	2.41	2.55	2.56	2.50	2.48	2.48
Mg	2.38	2.21	2.35	2.12	1.92	2.03	2.01	2.16	1.91	2.09	2.01	2.06	1.94
Mn	0.01	0.02	0.00	0.01	0.01	0.02	0.01	0.01	0.01	0.02	0.02	0.01	0.02
Ca	0.00	0.00	0.00	0.00	0.00	0.00	0.00	0.00	0.00	0.00	0.00	0.00	0.00
Sr	0.01	0.01	0.01	0.02	0.00	0.01	0.00	0.01	0.01	0.01	0.00		
Ba	0.02	0.02	0.03	0.02	0.00	0.00	0.01	0.00	0.01	0.01	0.01		
Na	0.04	0.05	0.08	0.04	0.04	0.02	0.02	0.03	0.03	0.03	0.02	0.04	0.04
K	1.69	1.38	1.37	1.37	1.69	1.83	1.83	1.48	1.57	1.46	1.19	1.67	1.85
Cl	0.01	0.02	0.01	0.00	0.00	0.00	0.00	0.00	0.00	0.00	0.00	0.00	0.00
F	0.00	0.00	0.00	0.00	0.00	0.00	0.00	0.00	0.00	0.00	0.00	0.00	0.00
O	24.00	24.00	24.00	24.00	22.00	22.00	22.00	22.00	22.00	22.00	22.00	22.00	22.00
CatTot	16.84	16.44	16.50	16.30	15.52	15.69	15.55	15.32	15.34	15.33	15.06	15.60	15.48
Total	40.84	40.44	40.50	40.30	37.52	37.69	37.55	37.32	37.34	37.33	37.06	37.60	37.48

Sample #	5030 lg gr	5030 lg gr	5030 sm gr	5030 lg gr	5030 lg gr	5030 lg gr	5030 lg gr	5030 adj to feld5011	5032 lg gr	5032 lg gr	5032 lg gr	5032 lg gr	5038a
Oxides													
SiO2	36.91	36.99	36.53	36.12	37.19	37.26	36.73	33.78	34.57	35.82	35.73	36.09	35.20
TiO2	1.88	2.44	2.16	2.47	1.99	2.08	1.94	2.35	2.98	2.58	2.61	2.59	2.61
Al2O3	20.22	20.12	20.03	19.88	20.34	20.30	20.06	20.14	18.47	19.04	19.03	19.05	18.82
Cr2O3	0.03	0.04	0.00	0.06	0.00	0.02	0.06		0.07	0.04	0.01	0.06	0.14
FeO	20.67	20.22	19.25	19.88	20.38	19.97	20.52	19.16	20.63	20.97	20.26	20.27	20.91
MgO	8.98	8.54	8.85	8.44	8.83	8.61	8.60	8.47	8.36	8.70	8.71	8.86	8.52
MnO	0.19	0.18	0.24	0.14	0.14	0.17	0.16	0.14	0.10	0.09	0.11	0.08	0.15
CaO	0.00	0.00	0.00	0.00	0.00	0.01	0.00	0.00	0.00	0.00	0.00	0.02	0.01
SrO	0.21	0.21	0.01	0.07	0.13	0.16	0.10		0.20	0.13	0.21	0.16	0.07
BaO	0.18	0.13	0.07	0.05	0.05	0.16	0.07		0.08	0.21	0.07	0.11	0.33
Na2O	0.12	0.13	0.11	0.12	0.14	0.12	0.15	0.12	0.09	0.16	0.18	0.15	0.23
K2O	9.44	8.71	9.39	8.83	9.29	9.87	9.75	9.51	9.78	9.81	9.32	9.83	8.93
Cl	0.05	0.07	0.07	0.06	0.04	0.06	0.06	0.06	0.03	0.01	0.03	0.00	0.02
F	0.00	0.00	0.00	0.00	0.00	0.00	0.00	0.00	0.00	0.00	0.00	0.00	0.00
Total	97.88	97.77	96.70	95.91	97.82	98.82	98.21	93.72	95.32	97.27	96.28	97.05	95.65
Atom Proportions													
Si	5.95	5.98	5.95	5.94	5.98	5.97	5.94	5.25	5.82	5.88	5.95	5.91	5.89
Ti	0.23	0.30	0.27	0.31	0.24	0.25	0.24	0.28	0.37	0.32	0.32	0.32	0.30
Al	3.84	3.82	3.85	3.82	3.85	3.83	3.82	3.69	3.66	3.69	3.79	3.68	3.36
Cr	0.00	0.01	0.00	0.01	0.00	0.00	0.01		0.01	0.01	0.00	0.01	0.02
Fe	2.79	2.73	2.62	2.73	2.74	2.68	2.77	2.49	2.80	2.84	2.80	2.78	2.68
Mg	2.15	2.05	2.15	2.07	2.14	2.06	2.07	1.98	2.10	2.13	2.14	2.16	1.94
Mn	0.03	0.03	0.03	0.02	0.02	0.02	0.02	0.02	0.01	0.01	0.02	0.01	0.02
Ca	0.00	0.00	0.00	0.00	0.00	0.00	0.00	0.00	0.00	0.00	0.00	0.00	0.00
Sr	0.02	0.02	0.00	0.01	0.01	0.02	0.01		0.02	0.01	0.02	0.02	0.01
Ba	0.01	0.01	0.01	0.00	0.00	0.01	0.01		0.00	0.01	0.01	0.01	0.02
Na	0.04	0.04	0.04	0.04	0.04	0.04	0.05	0.04	0.03	0.05	0.06	0.05	0.07
K	1.74	1.79	1.95	1.86	1.70	2.02	2.01	1.98	2.10	2.06	1.96	2.01	1.74
Cl	0.01	0.02	0.02	0.02	0.01	0.02	0.02	0.02	0.01	0.00	0.01	0.00	0.01
F	0.00	0.00	0.00	0.00	0.00	0.00	0.00	0.00	0.00	0.00	0.00	0.00	0.00
O	24.00	24.00	24.00	24.00	24.00	24.00	24.00	22.00	24.00	24.00	24.00	24.00	22.00
CatTot	16.80	16.78	16.87	16.81	16.74	16.91	16.96	15.61	17.04	17.01	16.94	16.96	15.54
Total	40.80	40.78	40.87	40.81	40.74	40.91	40.96	37.61	41.04	41.01	40.94	40.96	37.54

B.2. Biotite Compositional Analysis

Sample #	5038a D3 Z3	5038a D3 Z3	5038a D3 Z3	5038a D3 Z3	5061	5061	e2e1 biot in stau1	e2e1 biot:stau2	5055 Z1	5055 Z1	5055 biot1	NH30	NH30
Oxides													
SiO2	33.45	34.15	33.72	34.73	32.49	36.81	36.48	36.48	36.29	35.90	36.56	36.87	36.79
TiO2	2.43	2.46	2.38	2.50	1.38	1.44	1.48	1.57	1.73	1.57	0.12	1.66	1.47
Al2O3	18.29	18.19	17.97	18.72	15.92	19.34	20.48	19.65	19.43	19.28	19.42	19.80	19.20
Cr2O3	0.06	0.03	0.00	0.06	0.08	0.02	0.03	0.00	0.02	0.00	0.01	0.05	0.00
FeO	20.56	21.21	21.44	21.01	20.33	19.79	19.21	19.79	19.80	20.59	28.78	20.67	19.47
MgO	8.63	9.05	8.99	8.58	10.94	10.80	10.08	10.29	8.66	8.98	12.94	9.12	9.16
MnO	0.25	0.23	0.23	0.17	0.07	0.06	0.03	0.03	0.22	0.13	0.17	0.06	0.01
CaO	0.00	0.00	0.02	0.02	0.07	0.03	0.00	0.00	0.00	0.02	0.02	0.01	0.00
SrO	0.15	0.15	0.11	0.16	0.05	0.26			0.25	0.11		0.20	0.05
BaO	0.37	0.28	0.21	0.21	0.25	0.21			0.02	0.16		0.32	0.10
Na2O	0.17	0.15	0.18	0.21	0.14	0.07	0.32	0.38	0.42	0.37	0.05	0.27	0.31
K2O	8.54	8.48	7.77	8.53	8.35	8.86	8.88	8.89	9.03	8.28	0.09	8.31	9.08
Cl	0.03	0.02	0.03	0.03	0.01	0.01	0.00	0.01	0.00	0.00	0.04	0.00	0.00
F	0.00	0.00	0.00	0.00	0.00	0.00	0.00	0.00	0.00	0.00	0.00	0.00	0.00
Total	92.95	94.39	93.10	94.93	91.09	94.49	96.99	96.10	96.66	95.41	98.19	94.39	95.83
Atom Proportions													
Si	5.29	5.32	5.31	5.35	5.76	6.17	5.33	5.35	5.99	5.95	4.45	6.05	6.06
Ti	0.29	0.29	0.28	0.29	0.19	0.18	0.17	0.18	0.21	0.20	0.01	0.21	0.18
Al	3.41	3.34	3.34	3.40	3.34	3.23	3.63	3.49	3.78	3.76	3.84	3.83	3.72
Cr	0.01	0.00	0.01	0.01	0.01	0.00	0.00	0.00	0.00	0.01	0.00	0.01	0.00
Fe	2.72	2.76	2.83	2.71	3.02	2.78	2.41	2.49	2.71	2.88	4.03	2.84	2.68
Mg	2.04	2.10	2.11	1.97	2.80	2.65	2.26	2.31	2.14	2.21	3.23	2.23	2.25
Mn	0.03	0.03	0.03	0.02	0.01	0.01	0.00	0.00	0.03	0.02	0.02	0.01	0.00
Ca	0.00	0.00	0.00	0.00	0.01	0.01	0.00	0.00	0.00	0.00	0.00	0.00	0.00
Sr	0.01	0.01	0.01	0.02	0.01	0.03			0.02	0.01		0.02	0.00
Ba	0.02	0.02	0.01	0.01	0.02	0.01			0.00	0.01		0.02	0.01
Na	0.05	0.04	0.05	0.06	0.05	0.02	0.09	0.11	0.13	0.12	0.02	0.09	0.10
K	1.72	1.69	1.56	1.69	2.12	1.90	1.70	1.71	1.90	1.75	0.02	1.11	1.91
Cl	0.01	0.01	0.01	0.01	0.00	0.00	0.00	0.00	0.00	0.00	0.01	0.00	0.00
F	0.00	0.00	0.00	0.00	0.00	0.00	0.00	0.00	0.00	0.00	0.00	0.00	0.00
O	22.00	22.00	22.00	22.00	24.00	24.00	22.00	22.00	24.00	24.00	22.00	24.00	24.00
CatTot	15.61	15.60	15.56	15.53	17.45	16.99	15.58	15.65	16.82	16.90	15.84	16.42	16.91
Total	37.61	37.60	37.56	37.53	41.45	40.99	37.58	37.65	40.82	40.90	37.84	40.42	40.91

Sample #	5068	5068	5068	5068 lg gr	5068 lg gr	5068 sm gr	5068 inc	5068 adj garn	5068	5068 adj garn	5068	5068 adj garn	5068 biot rim
Oxides													
SiO2	35.48	34.58	33.44	34.57	35.35	34.20	34.87	34.66	32.93	34.32	34.51	35.57	35.54
TiO2	0.04	1.84	2.30	2.88	2.06	3.12	2.91	1.94	2.82	2.29	2.99	2.39	2.46
Al2O3	22.72	19.34	19.29	20.02	19.80	18.85	19.00	20.17	19.44	19.71	19.22	20.01	19.33
Cr2O3	0.05	0.04	0.00	0.08	0.04	0.09	0.05	0.02	0.07	0.03	0.07	0.09	0.08
FeO	25.88	19.38	19.77	19.77	20.04	20.31	19.74	19.89	19.19	19.72	19.80	19.83	18.29
MgO	12.43	11.58	9.66	8.87	9.54	9.58	9.51	9.28	9.81	9.94	9.05	8.99	8.65
MnO	0.50	0.00	0.05	0.05	0.01	0.07	0.01	0.03	0.03	0.05	0.07	0.02	0.01
CaO	0.02	0.13	0.08	0.00	0.00	0.02	0.01	0.00	0.04	0.04	0.03	0.00	0.00
SrO	0.00	0.11	0.03	0.00	0.03	0.02	0.02	0.02	0.11	0.17	0.17	0.15	
BaO	0.19	0.12	0.26	0.00	0.24	0.21	0.18	0.22	0.26	0.14	0.26	0.07	
Na2O	0.03	0.25	0.21	0.16	0.13	0.15	0.15	0.16	0.20	0.19	0.15	0.20	0.13
K2O	0.00	9.13	11.32	9.26	9.66	7.81	9.21	9.28	9.56	9.37	9.82	9.39	9.54
Cl	0.02	0.00	0.01	0.02	0.01	0.02	0.00	0.01	0.02	0.01	0.01	0.01	0.00
F	0.00	0.00	0.00	0.00	0.00	0.00	0.00	0.00	0.00	0.00	0.00	0.00	0.00
Total	97.34	95.48	96.41	95.69	96.90	94.49	94.64	95.66	93.69	94.96	95.13	96.51	94.11
Atom Proportions													
Si	4.25	5.24	5.14	5.28	5.32	5.26	5.34	5.30	5.15	5.27	5.28	5.35	5.70
Ti	0.01	0.21	0.27	0.33	0.34	0.36	0.34	0.22	0.34	0.26	0.34	0.27	0.30
Al	4.46	3.48	3.50	3.58	3.52	3.42	3.43	3.61	3.58	3.57	3.47	3.55	3.65
Cr	0.01	0.01	0.00	0.01	0.00	0.01	0.01	0.00	0.01	0.00	0.01	0.01	0.01
Fe	3.61	2.45	2.54	2.51	2.52	2.61	2.40	2.50	2.51	2.53	2.54	2.47	2.45
Mg	3.09	2.62	2.22	2.01	1.92	2.20	2.17	2.10	2.08	2.05	2.07	2.01	2.07
Mn	0.07	0.00	0.01	0.01	0.00	0.01	0.00	0.00	0.00	0.01	0.01	0.00	0.00
Ca	0.00	0.02	0.01	0.00	0.00	0.00	0.00	0.00	0.01	0.01	0.01	0.00	0.01
Sr	0.00	0.01	0.00	0.00	0.00	0.00	0.00	0.00	0.01	0.02	0.02	0.01	
Ba	0.01	0.01	0.02	0.00	0.01	0.01	0.01	0.01	0.02	0.01	0.02	0.00	
Na	0.01	0.07	0.08	0.05	0.04	0.05	0.05	0.05	0.06	0.06	0.04	0.06	0.04
K	0.00	1.67	2.22	1.80	1.86	1.53	1.80	1.80	1.91	1.84	1.72	1.80	1.95
Cl	0.01	0.00	0.00	0.01	0.00	0.01	0.00	0.00	0.01	0.00	0.00	0.00	0.00
F	0.00	0.00	0.00	0.00	0.00	0.00	0.00	0.00	0.00	0.00	0.00	0.00	0.00
O	22.00	22.00	22.00	22.00	22.00	22.00	22.00	22.00	22.00	22.00	22.00	22.00	23.00
CatTot	15.52	15.65	15.80	15.58	15.53	15.46	15.53	15.60	15.70	15.62	15.52	15.54	16.17
Total	37.52	37.65	37.80	37.58	37.53	37.46	37.53	37.60	37.70	37.62	37.52	37.54	38.17

B.2. Biotite Compositional Analysis

Sample #	5008 biot rim	5008 biot near rim	5008 biot core	5008 biot	5008 biot2	5008 biot2 rim for q	5008 biot rim for qa	5008 biot core for q	5008 biot rim for qa	5008 biot core for q	5008 biot for garb	5008 rim	5008 core
Oxides													
SiO2	36.62	35.23	36.04	37.03	36.10	36.22	33.65	33.64	33.57	33.19	35.98	36.48	36.46
TiO2	2.76	2.68	2.48	1.21	2.41	2.37	2.09	2.48	1.91	3.02	3.46	3.86	4.30
Al2O3	19.34	18.75	18.49	20.65	18.37	18.70	19.52	19.14	19.21	18.58	19.25	15.38	15.07
Cr2O3	0.05	0.08	0.08	0.04	0.10	0.05	0.05	0.07	0.07	0.09	0.08	0.00	0.00
FeO	19.15	19.87	19.12	20.13	19.71	18.57	20.12	19.81	20.12	20.98	19.12	18.91	19.16
MgO	9.46	9.37	9.11	9.60	9.34	8.77	8.20	8.27	9.90	8.57	9.72	11.16	11.06
MnO	0.04	0.01	0.04	0.03	0.00	0.05	0.08	0.04	0.02	0.07	0.06	0.12	0.08
CaO	0.02	0.00	0.02	0.02	0.02	0.00	0.01	0.03	0.01	0.00	0.00	0.00	0.00
SrO												0.06	0.08
BaO												0.46	0.31
Na2O	0.16	0.15	0.15	0.12	0.20	0.18	0.20	0.18	0.18	0.16	0.14	0.09	0.09
K2O	8.18	8.70	7.62	7.44	7.61	7.42	7.67	8.09	7.68	8.70	8.39	8.15	8.80
Cl	0.01	0.00	0.00	0.00	0.01	0.01	0.00	0.01	0.00	0.01	0.01	0.05	0.02
F	0.00	0.00	0.00	0.00	0.00	0.00	0.00	0.00	0.00	0.00	0.00	0.00	0.00
Total	96.70	94.85	94.19	96.17	94.18	92.35	92.59	91.55	92.69	92.96	96.29	94.73	95.45
Atom Proportions													
Si	5.72	5.63	5.72	5.74	5.81	5.84	5.50	5.54	5.49	5.47	5.57	5.57	5.55
Ti	0.32	0.31	0.30	0.14	0.29	0.29	0.26	0.30	0.23	0.37	0.41	0.44	0.49
Al	3.56	3.53	3.64	3.78	3.65	3.55	3.76	3.72	3.70	3.61	3.58	2.77	2.71
Cr	0.01	0.01	0.01	0.01	0.01	0.01	0.01	0.01	0.01	0.01	0.01	0.00	0.00
Fe	2.50	2.66	2.54	2.61	2.64	2.50	2.75	2.56	2.76	2.83	2.62	2.42	2.44
Mg	2.21	2.23	2.15	2.22	2.23	2.11	2.24	2.27	2.41	2.10	2.05	2.54	2.51
Mn	0.01	0.00	0.01	0.00	0.00	0.01	0.01	0.01	0.00	0.01	0.01	0.02	0.01
Ca	0.00	0.00	0.00	0.00	0.00	0.00	0.00	0.01	0.00	0.00	0.00	0.00	0.00
Sr												0.01	0.01
Ba												0.03	0.02
Na	0.05	0.05	0.05	0.04	0.06	0.06	0.06	0.06	0.06	0.05	0.04	0.03	0.03
K	1.63	1.78	1.54	1.47	1.61	1.53	1.60	1.70	1.60	1.83	1.69	1.59	1.71
Cl	0.00	0.00	0.00	0.00	0.00	0.00	0.00	0.00	0.00	0.00	0.00	0.01	0.01
F	0.00	0.00	0.00	0.00	0.00	0.00	0.00	0.00	0.00	0.00	0.00	0.00	0.00
O	23.00	23.00	23.00	23.00	23.00	23.00	23.00	23.00	23.00	23.00	23.00	22.00	22.00
CatTot	16.02	16.21	15.99	15.99	16.11	15.89	16.19	16.18	16.29	16.29	15.99	15.42	15.48
Total	39.02	39.21	38.99	38.99	39.11	38.89	39.19	39.18	39.29	39.29	38.99	37.42	37.48

Sample #	5008 rim	5008 rim adj plag	5008 shown musc inte	5008 adj to garn5011	5008 incl in garn501	5008 incl in garn501	5100 adj gar rim	5100 lee rim	5100 lee core	5100 lee rim	5100 adj garn50837	5100a 23	5100a 23
Oxides													
SiO2	38.66	38.93	34.86	36.22	34.83	35.18	36.45	36.76	36.57	35.46	37.21	36.47	36.98
TiO2	2.74	3.48	3.62	3.64	4.46	4.37	1.90	1.71	1.92	1.88	1.82	2.61	2.31
Al2O3	18.11	15.69	15.06	15.21	15.89	15.28	18.28	18.20	17.97	17.89	18.23	17.67	18.07
Cr2O3	0.07	0.02					0.09	0.11	0.09	0.13	0.13	0.06	0.00
FeO	18.43	18.95	21.47	20.91	18.85	18.55	19.56	19.93	20.22	19.89	18.13	20.23	20.26
MgO	12.74	11.65	10.54	10.82	11.52	11.42	10.70	10.89	10.46	10.42	10.88	9.05	9.23
MnO	0.12	0.11	0.15	0.05	0.06	0.06	0.09	0.08	0.09	0.04	0.05	0.18	0.15
CaO	0.03	0.02	0.04	0.01	0.00	0.02	0.04	0.00	0.01	0.06	0.03	0.02	0.00
SrO	0.16	0.09					0.07	0.26	0.10	0.07	0.10	0.21	0.18
BaO	0.38	0.34					0.26	0.27	0.58	0.49	0.49	0.27	0.33
Na2O	0.17	0.08	0.09	0.19	0.22	0.24	0.22	0.28	0.26	0.20	0.25	0.21	0.11
K2O	8.47	7.27	9.26	8.92	8.84	9.08	8.42	8.70	7.08	7.21	8.34	9.41	9.04
Cl	0.04	0.03	0.03	0.03	0.03	0.03	0.01	0.02	0.03	0.03	0.01	0.03	0.01
F	0.00	0.00	0.00	0.00	0.00	0.00	0.00	0.00	0.00	0.00	0.00	0.00	0.00
Total	99.01	94.67	95.13	96.01	94.58	94.22	94.00	95.19	95.36	93.87	94.87	96.40	96.66
Atom Proportions													
Si	5.70	5.80	5.42	5.44	5.36	5.43	5.53	5.53	5.53	5.48	5.59	5.63	5.66
Ti	0.30	0.40	0.42	0.42	0.52	0.51	0.22	0.19	0.22	0.22	0.21	0.32	0.29
Al	2.81	2.80	2.76	2.77	2.84	2.78	3.27	3.23	3.20	3.27	3.23	3.44	3.48
Cr	0.01	0.00					0.01	0.01	0.01	0.02	0.02	0.01	0.00
Fe	2.28	2.48	2.79	2.78	2.43	2.38	2.48	2.51	2.56	2.54	2.41	2.80	2.78
Mg	2.81	2.63	2.44	2.49	2.64	2.63	2.42	2.44	2.38	2.39	2.44	2.23	2.26
Mn	0.02	0.01	0.02	0.01	0.01	0.01	0.01	0.01	0.01	0.01	0.01	0.03	0.02
Ca	0.00	0.00	0.01	0.00	0.01	0.00	0.01	0.00	0.00	0.01	0.01	0.00	0.00
Sr	0.01	0.01					0.01	0.02	0.01	0.01	0.01	0.02	0.02
Ba	0.02	0.02					0.02	0.02	0.03	0.03	0.03	0.02	0.02
Na	0.05	0.02	0.03	0.05	0.07	0.07	0.06	0.09	0.07	0.06	0.07	0.07	0.04
K	1.22	1.41	1.84	1.76	1.74	1.79	1.24	1.28	1.36	1.42	1.22	1.88	1.86
Cl	0.01	0.01	0.01	0.01	0.01	0.01	0.00	0.01	0.01	0.01	0.00	0.01	0.00
F	0.00	0.00	0.00	0.00	0.00	0.00	0.00	0.00	0.00	0.00	0.00	0.00	0.00
O	22.00	22.00	22.00	22.00	22.00	22.00	22.00	22.00	22.00	22.00	22.00	24.00	24.00
CatTot	15.24	15.32	15.72	15.67	15.61	15.61	15.27	15.34	15.37	15.42	15.23	16.98	16.87
Total	37.24	37.32	37.72	37.67	37.61	37.61	37.27	37.34	37.37	37.42	37.23	40.98	40.87

B.2. Biotite Compositional Analysis

Sample #	5107a	5107a	5107a cen gr	5107a cen gr	5114 lg gr	5114 lg gr	5114 lg gr	5114 adj to fsh09511	5114 isolated	5115 b rim adj plag	5115 b core	5115 b rim adj plag/bi	5115 b adj plg
Oxides													
SiO2	35.09	33.55	35.78	35.09	36.89	37.30	36.64	99.14	35.09	35.61	36.12	35.89	35.38
TiO2	2.84	2.10	1.85	2.08	2.75	2.38	2.71	0.02	2.17	2.33	2.19	2.35	0.11
Al2O3	18.24	18.84	19.10	19.77	19.71	19.14	18.80	0.02	19.00	19.84	19.95	19.95	22.90
Cr2O3	0.00	0.06	0.07	0.03	0.12	0.11	0.15			0.00	0.04	0.06	0.00
FeO	19.11	18.42	19.40	17.74	17.45	18.04	18.91	0.14	17.74	19.87	19.97	20.03	25.64
MgO	9.28	9.42	10.05	9.42	9.71	9.80	9.33	0.00	10.14	9.06	9.45	9.23	14.12
MnO	0.14	0.14	0.16	0.12	0.21	0.24	0.23	0.00	0.21	0.19	0.12	0.12	0.18
CaO	0.00	0.04	0.05	0.06	0.00	0.00	0.00	0.01	0.00	0.01	0.00	0.00	0.04
SrO	0.04	0.12	0.19	0.12	0.13	0.27	0.12			0.11	0.12	0.13	0.03
BaO	0.35	0.15	0.02	0.16	0.47	0.57	0.46			0.24	0.44	0.24	0.00
Na2O	0.17	0.17	0.09	0.16	0.10	0.10	0.12	0.05	0.13	0.20	0.24	0.21	0.01
K2O	10.44	10.18	9.41	10.01	8.18	8.32	8.66	8.47	9.41	7.37	7.37	7.97	0.00
Cl	0.04	0.02	0.01	0.01	0.01	0.01	0.00	0.01	0.02	0.01	0.02	0.02	0.01
F	0.00	0.00	0.00	0.00	0.00	0.00	0.00	0.90	0.00	0.00	0.00	0.00	0.00
Total	95.84	93.29	96.87	95.89	93.85	96.26	96.13	100.86	93.91	93.84	98.01	96.19	99.51
Atom Proportions													
Si	5.86	5.74	5.90	5.92	6.13	6.06	6.00	10.76	5.38	5.44	5.41	5.38	4.16
Ti	0.36	0.27	0.21	0.26	0.34	0.29	0.33	0.00	0.25	0.27	0.24	0.27	0.01
Al	3.59	3.82	3.71	3.93	3.67	3.86	3.83	0.00	3.44	3.53	3.52	3.53	4.42
Cr	0.01	0.01	0.01	0.00	0.02	0.01	0.02			0.00	0.01	0.01	0.01
Fe	2.67	2.84	2.68	2.44	2.43	2.45	2.59	0.01	2.28	2.43	2.50	2.51	3.51
Mg	2.31	2.40	2.47	2.31	2.16	2.37	2.28	0.00	2.32	2.08	2.11	2.06	3.45
Mn	0.02	0.02	0.02	0.02	0.03	0.03	0.03	0.00	0.03	0.02	0.02	0.02	0.03
Ca	0.00	0.01	0.01	0.01	0.00	0.00	0.00	0.00	0.00	0.00	0.00	0.00	0.01
Sr	0.00	0.01	0.02	0.01	0.01	0.03	0.01			0.01	0.01	0.01	0.00
Ba	0.02	0.01	0.00	0.01	0.03	0.04	0.03			0.01	0.03	0.01	0.00
Na	0.05	0.06	0.03	0.05	0.03	0.03	0.04	0.01	0.04	0.06	0.07	0.06	0.00
K	2.22	2.22	1.98	2.10	1.72	1.72	1.81	0.90	1.84	1.44	1.41	1.53	0.00
Cl	0.01	0.01	0.00	0.00	0.00	0.00	0.00	0.00	0.01	0.00	0.01	0.01	0.00
F	0.00	0.00	0.00	0.00	0.00	0.00	0.00	0.00	0.00	0.00	0.00	0.00	0.00
O	24.00	24.00	24.00	24.00	24.00	24.00	24.00	22.00	22.00	22.00	22.00	22.00	22.00
CatTot	17.13	17.22	17.04	16.88	16.56	16.70	16.77	11.86	15.58	15.28	15.33	15.38	15.61
Total	41.13	41.22	41.04	40.88	40.56	40.70	40.77	33.86	37.58	37.28	37.33	37.38	37.61

Sample #	5115b	5115b	5131 for cen1	5131 for cen1b	5131 inc. in an	5131 rev rimcor	5131 incl. in a	5131 near rim c	5131 24	5131 24	7005b isolated	7005b forgarn10 11	7005b anc all
Oxides													
SiO2	36.37	36.50	36.80	36.75	38.23	36.18	36.76	36.98	35.91	36.10	35.73	36.52	36.51
TiO2	2.07	2.01	2.78	2.56	0.00	1.98	3.04	0.33	3.09	3.32	2.22	1.84	2.45
Al2O3	19.20	19.74	19.03	18.88	21.08	18.85	18.40	20.83	19.76	19.27	20.36	20.40	20.88
Cr2O3	0.00	0.09	0.08	0.08	0.05	0.08	0.00	0.04	0.11	0.15	0.05	0.10	0.11
FeO	20.85	19.88	20.27	22.19	38.56	22.46	18.54	23.58	19.09	19.95	19.73	18.62	18.63
MgO	8.80	8.94	10.50	9.14	3.78	9.15	10.87	9.55	8.05	8.24	9.23	9.60	9.38
MnO	0.13	0.13	0.04	0.07	1.83	0.01	0.04	0.08	0.13	0.08	0.06	0.07	0.08
CaO	0.04	0.00	0.00	0.01	0.93	0.00	0.03	0.05	0.00	0.01	0.00	0.03	0.05
SrO	0.14	0.11							0.19	0.17			0.12
BaO	0.19	0.21							0.22	0.27			0.24
Na2O	0.15	0.21	0.14	0.11	0.00	0.07	0.17	0.21	0.16	0.08	0.18	0.06	0.24
K2O	9.36	9.56	9.54	9.81	0.06	9.50	9.52	9.49	8.55	9.08	9.35	9.60	9.08
Cl	0.01	0.02	0.00	0.00	0.00	0.01	0.01	0.01	0.02	0.01	0.03	0.03	0.04
F	0.00	0.00	0.00	0.00	0.00	0.00	0.00	0.00	0.00	0.00	0.00	0.00	0.00
Total	96.42	96.20	99.15	99.59	104.54	97.09	97.38	100.09	95.28	96.74	96.94	96.66	96.63
Atom Proportions													
Si	5.66	5.66	5.51	5.53	5.45	5.54	5.50	5.29	5.53	5.61	5.54	5.53	5.51
Ti	0.29	0.25	0.31	0.29	0.00	0.22	0.34	0.04	0.38	0.41	0.25	0.18	0.28
Al	3.75	3.84	3.33	3.32	3.54	3.34	3.39	3.61	3.85	3.72	3.58	3.61	3.64
Cr	0.00	0.01	0.01	0.01	0.01	0.01	0.00	0.00	0.01	0.02	0.01	0.01	0.01
Fe	2.80	2.72	2.51	2.77	4.60	2.85	2.30	2.90	2.64	2.73	2.46	2.46	2.33
Mg	2.17	2.20	2.32	2.03	0.80	2.07	2.40	2.08	1.88	2.01	2.08	2.15	2.09
Mn	0.02	0.02	0.01	0.01	0.23	0.00	0.00	0.01	0.02	0.01	0.01	0.01	0.01
Ca	0.01	0.00	0.00	0.00	0.14	0.00	0.00	0.01	0.00	0.00	0.00	0.00	0.01
Sr	0.01	0.01							0.02	0.02			0.01
Ba	0.01	0.01							0.01	0.02			0.01
Na	0.05	0.07	0.04	0.03	0.00	0.02	0.05	0.06	0.05	0.03	0.05	0.02	0.07
K	1.86	2.01	1.80	1.87	0.00	1.84	1.80	1.78	1.80	1.80	1.78	1.84	1.73
Cl	0.00	0.01	0.00	0.00	0.00	0.00	0.00	0.00	0.01	0.00	0.01	0.01	0.01
F	0.00	0.00	0.00	0.00	0.00	0.00	0.00	0.00	0.00	0.00	0.00	0.00	0.00
O	24.00	24.00	22.00	22.00	22.00	22.00	22.00	22.00	24.00	24.00	22.00	22.00	22.00
CatTot	17.03	17.01	15.84	15.66	14.78	15.70	15.59	15.78	16.68	16.78	15.54	15.82	15.56
Total	41.03	41.01	37.84	37.66	36.78	37.70	37.59	37.78	40.68	40.78	37.54	37.82	37.56

B.2. Biotite Compositional Analysis

Sample #	7086b
Oxides	
SiO2	35.36
TiO2	2.83
Al2O3	19.91
Cr2O3	0.10
FeO	19.57
MgO	8.94
MnO	0.06
CaO	0.00
SrO	0.11
BaO	0.09
Na2O	0.11
K2O	9.20
Cl	0.01
F	0.00
Total	96.30
Atom Proportions	
Si	5.32
Ti	0.32
Al	3.53
Cr	0.01
Fe	2.46
Mg	2.01
Mn	0.01
Ca	0.00
Sr	0.01
Ba	0.01
Na	0.03
K	1.77
Cl	0.00
F	0.00
O	22.00
CatTot	15.49
Total	37.49

Sample #
Oxides
SiO2
TiO2
Al2O3
Cr2O3
FeO
MgO
MnO
CaO
SrO
BaO
Na2O
K2O
Cl
F
Total
Atom Proportions
Si
Ti
Al
Cr
Fe
Mg
Mn
Ca
Sr
Ba
Na
K
Cl
F
O
CatTot
Total

B.3.1. Feldspar Compositional Analysis

Sample	10a	10a	10a adj to cord0511	10a adj to garn0511	10a incl in garn0511	10a kspar adj to gar	10a kspar with biot	204	204	250	250
Oxides											
SiO2	62.77	61.51	62.83	62.61	64.57	63.58	66.00	63.01	61.28	62.52	63.52
TiO2	0.05	0.00	0.00	0.03	0.03	0.05	0.00	0.00	0.00	0.01	0.00
Al2O3	22.31	22.47	22.56	22.73	18.12	18.21	18.40	23.85	23.33	22.98	23.32
Fe2O3	0.05	0.06	0.00	0.11	0.82	0.07	0.00	0.17	0.18	0.15	0.02
CaO	4.41	4.50	4.70	4.68	0.04	0.00	0.01	5.31	5.90	4.30	4.43
BaO	0.00	0.00	0.00	0.04	0.82	0.73	0.78	0.44	0.00	0.00	0.21
SrO	0.22	0.26	0.24	0.35	0.26	0.34	0.38	0.26	0.37	0.23	0.21
Na2O	8.94	8.75	8.13	7.96	1.40	1.05	1.50	8.42	8.11	0.09	9.12
K2O	0.20	0.22	0.21	0.17	13.22	14.24	13.36	0.04	0.07	0.17	0.09
Total	98.96	97.76	98.67	98.66	99.29	98.27	99.42	101.50	99.23	99.46	100.92
Atom Proportions											
Si	11.24	11.16	11.25	11.22	11.98	11.96	12.02	11.04	10.99	11.15	11.16
Ti	0.01	0.00	0.00	0.00	0.00	0.01	0.00	0.00	0.00	0.00	0.00
Al	4.71	4.80	4.76	4.80	3.96	4.04	4.01	4.93	4.93	4.83	4.83
Fe	0.01	0.01	0.00	0.01	0.12	0.01	0.00	0.02	0.03	0.20	0.00
Ca	0.85	0.88	0.90	0.90	0.01	0.00	0.00	1.00	1.13	0.82	0.83
Ba	0.00	0.00	0.00	0.00	0.06	0.05	0.06	0.03	0.00	0.00	0.02
Sr	0.02	0.03	0.03	0.04	0.03	0.04	0.04	0.03	0.04	0.24	0.02
Na	3.10	3.08	2.82	2.77	0.51	0.38	0.54	2.86	2.82	3.14	3.11
K	0.05	0.05	0.05	0.04	3.13	3.42	3.15	0.01	0.02	0.40	0.02
O	32.00	32.00	32.00	32.00	32.00	32.00	32.00	32.00	32.00	32.00	32.00
CatTot	19.98	20.00	19.81	19.77	19.79	19.91	19.82	19.92	19.95	20.02	19.99
Total	51.98	52.00	51.81	51.77	51.79	51.91	51.82	51.92	51.95		
An	0.21	0.22	0.24	0.24	0.00	0.00	0.00	0.25	0.28	0.18	0.21
Ab	0.77	0.76	0.74	0.74	0.14	0.10	0.14	0.73	0.70	0.68	0.78
Or	0.01	0.01	0.01	0.01	0.84	0.88	0.83	0.00	0.00	0.09	0.01

Sample	0278b	0278b	0278b	0278b	0278b adj D2 garn	0278b adj garn	0278b inc. in D2 garn	0278b inc. in D2 garn	0278b inc. in D2 garn	0278b inc. in D2 garn	292
Oxides											
SiO2	58.38	59.72	58.96	59.36	59.36	58.42	57.63	58.01	59.81	59.60	58.10
TiO2	0.02	0.00	0.04	0.00	0.01	0.01	0.00	0.01	0.01	0.00	0.00
Al2O3	25.89	25.56	25.66	25.81	25.66	25.85	26.46	26.47	25.44	25.60	26.10
Fe2O3	0.18	0.08	0.03	0.04	0.13	0.00	0.22	0.04	0.74	0.67	0.00
CaO	7.83	7.57	7.73	7.67	7.68	7.71	8.57	8.67	7.37	7.69	8.31
BaO	0.00	0.00	0.00	0.32	0.00	0.00	0.00	0.07	0.00	0.06	0.34
SrO	0.37	0.34	0.38	0.40	0.38	0.35	0.29	0.33	0.25	0.35	0.30
Na2O	6.96	7.01	6.96	6.81	6.92	6.79	6.42	6.40	6.89	6.98	6.48
K2O	0.06	0.10	0.12	0.11	0.08	0.05	0.08	0.07	0.16	0.03	0.05
Total	99.68	100.37	99.89	100.52	100.22	99.18	99.66	100.07	100.68	100.99	99.67
Atom Proportions											
Si	10.49	10.63	10.56	10.57	10.59	10.52	10.37	10.39	10.62	10.57	10.45
Ti	0.00	0.00	0.01	0.00	0.00	0.00	0.00	0.00	0.00	0.00	0.00
Al	5.48	5.36	5.42	5.42	5.39	5.49	5.61	5.59	5.32	5.35	5.53
Fe	0.02	0.01	0.00	0.01	0.02	0.00	0.03	0.01	0.10	0.09	0.00
Ca	1.51	1.44	1.48	1.46	1.47	1.49	1.65	1.66	1.40	1.46	1.60
Ba	0.00	0.00	0.00	0.02	0.00	0.00	0.00	0.01	0.00	0.00	0.02
Sr	0.04	0.04	0.04	0.04	0.04	0.04	0.03	0.03	0.03	0.04	0.03
Na	2.42	2.42	2.42	2.35	2.39	2.37	2.24	2.23	2.37	2.40	2.26
K	0.02	0.02	0.03	0.03	0.02	0.01	0.02	0.02	0.04	0.01	0.01
O	32.00	32.00	32.00	32.00	32.00	32.00	32.00	32.00	32.00	32.00	32.00
CatTot	19.98	19.91	19.95	19.90	19.91	19.92	19.94	19.93	19.88	19.92	19.92
Total	51.98	51.91	51.95	51.90	51.91	51.92	51.94	51.93	51.88	51.92	51.92
An	0.38	0.37	0.37	0.38	0.37	0.38	0.42	0.42	0.37	0.37	0.41
Ab	0.61	0.62	0.61	0.60	0.61	0.61	0.57	0.56	0.62	0.61	0.58
Or	0.00	0.01	0.01	0.01	0.00	0.00	0.00	0.00	0.01	0.00	0.00

B.3.1. Feldspar Compositional Analysis

Sample	282	5000 core	5000 rim for po14	5000 rim for po14	5002 adj garn	5002	5005 kspar	5005 plag	5011 iso	5011 iso
Oxides										
SiO2	58.30	60.83	62.44	62.01	60.01	60.25	63.34	61.26	28.10	58.74
TiO2	0.02	0.00	0.00	0.01	0.00	0.00	0.05	0.00	0.17	0.00
Al2O3	26.36	23.58	23.38	23.51	23.78	24.01	18.45	24.74	17.09	24.68
Fe2O3	0.08	0.00	0.06	0.03	0.21	0.06	0.00	0.03	40.80	0.04
CaO	8.46	4.97	4.77	5.04	5.52	5.37	0.03	6.29	0.18	6.73
BaO	0.00	0.00	0.05	0.09	0.00	0.07	0.93	0.00	0.00	0.00
SrO	0.22	0.24	0.23	0.22	0.32	0.14	0.14	0.12	0.03	0.21
Na2O	6.49	8.91	8.20	8.72	8.25	8.38	1.10	7.80	0.32	7.43
K2O	0.07	0.19	1.17	0.09	0.14	0.16	14.72	0.21	7.60	0.08
Total	99.99	98.72	100.31	99.71	98.22	98.46	98.76	100.45	94.30	97.91
Atom Proportions										
Si	10.43	10.96	11.09	11.04	10.88	10.89	11.90	10.84	6.51	10.70
Ti	0.00	0.00	0.00	0.00	0.00	0.00	0.01	0.00	0.03	0.00
Al	5.56	5.01	4.89	4.93	5.08	5.11	4.09	5.16	4.67	5.30
Fe	0.01	0.00	0.01	0.00	0.03	0.01	0.00	0.00	7.11	0.01
Ca	1.62	0.96	0.91	0.96	1.07	1.04	0.01	1.19	0.05	1.31
Ba	0.00	0.00	0.00	0.01	0.00	0.01	0.07	0.00	0.00	0.00
Sr	0.02	0.03	0.02	0.02	0.03	0.01	0.02	0.01	0.00	0.02
Na	2.25	3.11	2.82	3.01	2.90	2.94	0.40	2.68	0.14	2.62
K	0.02	0.04	0.27	0.02	0.03	0.04	3.53	0.05	2.25	0.02
O	32.00	32.00	32.00	32.00	32.00	32.00	32.00	32.00	32.00	32.00
CatTot	19.92	20.11	20.01	20.00	20.03	20.04	20.01	19.94	20.76	19.97
Total	51.92	52.11	52.01	52.00					52.76	51.97
An	0.41	0.23	0.23	0.24	0.27	0.26	0.00	0.30	0.02	0.33
Ab	0.58	0.75	0.70	0.75	0.72	0.73	0.10	0.68	0.06	0.66
Or	0.00	0.01	0.07	0.00	0.01	0.01	0.88	0.01	0.92	0.00

Sample	5011 nr gr	5011 iso	5011 nr gr	5011 adj garn	5011 iso	5011	5011	5011	5011	5011
Oxides										
SiO2	57.96	60.79	60.11	60.17	52.85	60.78	85.24	59.65	59.73	60.11
TiO2	0.00	0.00	0.04	0.00	0.00	0.00	0.00	0.00	0.01	0.00
Al2O3	24.57	25.06	24.82	24.91	24.44	25.09	10.67	23.09	24.00	25.05
Fe2O3	0.36	0.01	0.31	0.10	0.00	0.25	0.13	0.00	0.07	0.19
CaO	6.94	6.86	6.87	6.90	6.98	7.08	2.24	6.82	6.71	6.77
BaO	0.07	0.00	0.00	0.00	0.00	0.00	0.00	0.00	0.01	0.00
SrO	0.24	0.33	0.30	0.26	0.33	0.18	0.24	0.33	0.30	0.24
Na2O	7.32	7.57	7.27	7.34	6.97	7.40	4.20	7.53	7.65	7.63
K2O	0.04	0.08	0.06	0.03	0.07	0.04	0.03	0.03	0.07	0.06
Total	97.50	100.70	99.78	99.71	91.64	100.84	102.74	97.45	98.57	100.06
Atom Proportions										
Si	10.63	10.76	10.74	10.75	10.35	10.74	13.91	10.91	10.81	10.71
Ti	0.00	0.00	0.01	0.00	0.00	0.00	0.00	0.00	0.00	0.00
Al	5.31	5.23	5.23	5.24	5.64	5.23	2.05	4.98	5.12	5.26
Fe	0.05	0.00	0.04	0.01	0.00	0.03	0.02	0.00	0.01	0.03
Ca	1.36	1.30	1.32	1.32	1.47	1.34	0.39	1.34	1.30	1.29
Ba	0.01	0.00	0.00	0.00	0.00	0.00	0.00	0.00	0.00	0.00
Sr	0.03	0.03	0.03	0.03	0.04	0.02	0.02	0.04	0.03	0.03
Na	2.60	2.60	2.52	2.54	2.65	2.54	1.33	2.67	2.69	2.64
K	0.01	0.02	0.02	0.01	0.02	0.01	0.01	0.01	0.02	0.01
O	32.00	32.00	32.00	32.00	32.00	32.00	32.00	32.00	32.00	32.00
CatTot	20.00	19.94	19.89	19.90	20.16	19.90	17.72	19.94	19.98	19.97
Total	52.00	51.94	51.89	51.90	52.16			51.94	51.98	51.97
An	0.34	0.33	0.34	0.34	0.35	0.34	0.22	0.33	0.32	0.33
Ab	0.65	0.66	0.65	0.65	0.64	0.65	0.76	0.66	0.67	0.66
Or	0.00	0.00	0.00	0.00	0.00	0.00	0.00	0.00	0.00	0.00

B.3.1. Feldspar Compositional Analysis

Sample	5011	5011	5011 core	5011 iso	5011 rim	5011 rim	5021	5021	5023	5023	5023
Oxides											
SiO2	59.50	60.63	60.11	58.78	60.97	60.04	61.58	60.46	59.56	62.75	60.66
TiO2	0.00	0.00	0.02	0.00	0.00	0.00	0.00	0.00	0.01	0.00	0.00
Al2O3	24.58	25.43	25.40	25.41	25.61	25.31	23.69	23.68	24.01	24.18	23.86
Fe2O3	0.04	0.25	0.04	0.08	0.04	0.12	0.05	0.00	0.02	0.01	0.03
CaO	6.73	6.99	7.08	7.40	0.02	6.89	5.60	5.29	5.50	5.68	5.48
BaO	0.00	0.15	0.00	0.46	0.02	0.00	0.00	0.00	0.43	0.00	0.17
SrO	0.16	0.40	0.23	0.22	0.11	0.12	0.20	0.25	0.25	0.34	0.31
Na2O	7.69	7.52	7.51	7.20	7.46	7.62	8.07	8.23	8.22	8.00	8.35
K2O	0.07	0.05	0.08	0.07	0.06	0.05	0.24	0.25	0.10	0.16	0.13
Total	98.77	101.43	100.48	99.62	94.28	100.15	99.44	98.16	98.11	101.11	98.98
Atom Proportions											
Si	10.74	10.68	10.67	10.58	11.17	10.68	10.95	11.00	10.84	11.01	10.92
Ti	0.00	0.00	0.00	0.00	0.00	0.00	0.00	0.00	0.00	0.00	0.00
Al	5.23	5.28	5.32	5.39	5.53	5.31	5.05	4.99	5.15	5.00	5.06
Fe	0.01	0.03	0.01	0.01	0.01	0.02	0.00	0.01	0.00	0.00	0.00
Ca	1.30	1.32	1.35	1.43	0.00	1.31	1.03	1.07	1.07	1.07	1.06
Ba	0.00	0.01	0.00	0.03	0.00	0.00	0.00	0.00	0.03	0.00	0.01
Sr	0.02	0.04	0.02	0.02	0.01	0.01	0.03	0.02	0.03	0.03	0.03
Na	2.69	2.57	2.59	2.51	2.65	2.63	2.89	2.80	2.90	2.72	2.91
K	0.02	0.01	0.02	0.02	0.02	0.01	0.06	0.05	0.02	0.04	0.03
O	32.00	32.00	32.00	32.00	32.00	32.00	32.00	32.00	32.00	32.00	32.00
CatTot	20.00	19.95	19.97	19.99	19.39	19.97	20.00	19.93	20.05	19.87	20.02
Total	52.00	51.95	51.97		51.39	51.97	52.00	51.93	52.05	51.87	52.02
An	0.32	0.33	0.34	0.36	0.00	0.33	0.26	0.27	0.26	0.28	0.26
Ab	0.67	0.65	0.65	0.63	0.99	0.66	0.72	0.71	0.72	0.71	0.72
Or	0.00	0.00	0.00	0.00	0.01	0.00	0.01	0.01	0.01	0.01	0.01

Sample	5023	5023	5023	5023	5023	5023	5023 adj garn	5023 adj garn	5023 adj garn	5024	5024
Oxides											
SiO2	60.22	63.50	65.44	53.44	62.26	61.97	59.90	60.25	62.82	62.16	61.58
TiO2	0.04	0.05	0.05	0.08	0.01	0.00	0.01	0.00	0.00	0.00	0.00
Al2O3	23.33	18.53	18.51	28.75	23.98	23.73	23.90	23.49	23.34	24.00	23.90
Fe2O3	0.02	0.16	0.16	0.52	0.07	0.02	0.55	0.60	0.55	0.03	0.04
CaO	5.56	0.01	0.01	11.70	5.38	5.54	5.18	5.15	5.24	5.22	5.35
BaO	0.19	1.52	1.52	0.51	0.04	0.00	0.24	0.00	0.21	0.00	0.00
SrO	0.23	0.41	0.41	0.27	0.25	0.21	0.29	0.26	0.24	0.31	0.33
Na2O	8.01	2.78	2.78	4.29	8.20	8.21	8.32	8.51	8.48	8.06	8.18
K2O	0.10	12.03	12.03	0.33	0.14	0.12	0.07	0.04	0.10	0.28	0.19
Total	97.71	98.99	100.92	99.90	100.35	99.80	98.46	98.31	100.99	100.06	99.57
Atom Proportions											
Si	10.96	11.87	11.96	9.74	11.01	11.02	10.85	10.91	11.07	11.02	10.98
Ti	0.01	0.01	0.01	0.01	0.00	0.00	0.00	0.00	0.00	0.00	0.00
Al	5.01	4.08	3.99	6.17	5.00	4.97	5.10	5.02	4.85	5.01	5.02
Fe	0.00	0.02	0.02	0.07	0.01	0.00	0.08	0.08	0.07	0.00	0.01
Ca	1.09	0.00	0.00	2.28	1.02	1.06	1.01	1.00	0.99	0.99	1.02
Ba	0.01	0.11	0.11	0.04	0.00	0.00	0.02	0.00	0.02	0.00	0.00
Sr	0.03	0.04	0.04	0.03	0.03	0.02	0.03	0.03	0.03	0.03	0.03
Na	2.83	1.01	0.99	1.52	2.81	2.83	2.92	2.99	2.90	2.77	2.83
K	0.02	2.87	2.81	0.08	0.03	0.03	0.02	0.01	0.02	0.06	0.04
O	32.00	32.00	32.00	32.00	32.00	32.00	32.00	32.00	32.00	32.00	32.00
CatTot	19.95	20.01	19.92	19.93	19.91	19.93	20.03	20.04	19.93	19.89	19.94
Total	51.95	52.01	51.92	51.93	51.91	51.93	52.03	52.04	51.93	51.89	51.94
An	0.27	0.00	0.00	0.58	0.26	0.27	0.25	0.25	0.25	0.26	0.26
Ab	0.71	0.25	0.25	0.38	0.72	0.72	0.73	0.74	0.73	0.72	0.72
Or	0.01	0.71	0.71	0.02	0.01	0.01	0.00	0.00	0.01	0.02	0.01

B.3.1. Feldspar Compositional Analysis

Sample	5024 kfeld	5024 kfeld adj ecan2	5024 kfeld adj to 2	5024 kfeld adj to ec	5024 kfld	5024 kaper with incl	5024 myrmeketic rim	5024 plag	5024 plag myrmeketic	5024 plag rim	5030 isolated plag
Oxides											
SiO2	63.10	63.63	63.23	63.63	65.06	64.92	61.99	62.45	98.05	62.50	61.65
TiO2	0.02	0.07	0.03	0.03	0.04	0.01	0.00	0.00	0.00	0.00	0.00
Al2O3	18.51	18.23	18.47	18.47	18.55	18.39	21.56	23.21	1.20	23.42	22.87
Fe2O3	0.05	0.00	0.02	0.00	0.04	0.00	0.03	0.02	0.04	0.10	0.00
CaO	0.03	0.04	0.01	0.01	0.02	0.07	3.31	5.19	0.19	4.76	5.08
BeO	0.70	1.51	0.67	0.77	0.49	0.38	0.11	0.00	0.00	0.01	0.02
SrO	0.20	0.25	0.29	0.29	0.42	0.32	0.22	0.35	0.31	0.24	0.28
Na2O	1.38	0.86	1.19	1.22	1.05	1.57	8.48	7.87	0.35	8.90	7.71
K2O	14.36	14.34	14.73	14.94	14.74	13.15	1.54	0.17	0.05	0.18	0.24
Total	98.33	98.94	98.65	99.37	100.39	98.80	97.25	99.27	100.19	100.11	97.85
Atom Proportions											
Si	11.88	11.95	11.89	11.90	11.97	12.03	11.33	11.14	15.77	11.08	11.15
Ti	0.00	0.01	0.01	0.00	0.01	0.00	0.00	0.00	0.00	0.00	0.00
Al	4.11	4.04	4.09	4.07	4.02	4.02	4.65	4.88	0.23	4.89	4.87
Fe	0.01	0.00	0.00	0.00	0.01	0.00	0.00	0.00	0.00	0.01	0.00
Ca	0.01	0.01	0.00	0.00	0.00	0.01	0.65	0.99	0.03	0.91	0.98
Be	0.05	0.11	0.05	0.06	0.04	0.03	0.01	0.00	0.00	0.00	0.00
Sr	0.02	0.03	0.03	0.03	0.05	0.04	0.02	0.04	0.03	0.03	0.03
Na	0.50	0.31	0.44	0.44	0.37	0.56	3.01	2.72	0.11	3.06	2.71
K	3.45	3.44	3.53	3.56	3.46	3.11	0.36	0.04	0.01	0.04	0.06
O	32.00	32.00	32.00	32.00	32.00	32.00	32.00	32.00	32.00	32.00	32.00
CatTot	20.03	19.90	20.04	20.07	19.92	19.80	20.03	19.80	16.18	20.02	19.80
Total	52.03	51.90	52.04	52.07	51.92	51.80	52.03	51.80	48.18	52.02	51.80
An	0.00	0.00	0.00	0.00	0.00	0.00	0.16	0.26	0.18	0.22	0.26
Ab	0.12	0.08	0.11	0.11	0.10	0.15	0.74	0.72	0.60	0.76	0.72
Or	0.86	0.88	0.87	0.87	0.88	0.83	0.09	0.01	0.06	0.01	0.01

Sample	5030 isolated plag	5032	5032	5038a	5038a	5061	5061	5065 kfld	5065 kfld	5065 Z1	5065 Z1
Oxides											
SiO2	61.68	62.55	62.06	59.60	60.11	61.30	63.23	67.49	63.99	62.94	62.85
TiO2	0.00	0.03	0.00	0.03	0.00	0.00	0.03	0.00	0.05	0.00	0.00
Al2O3	22.60	23.45	23.13	25.57	24.96	24.28	23.18	18.53	18.27	23.13	23.82
Fe2O3	0.05	0.05	0.01	0.04	0.07	0.10	0.23	0.14	0.11	0.02	0.00
CaO	4.57	5.01	4.71	6.97	6.77	6.33	4.71	0.01	0.00	4.74	5.04
BeO	0.00	0.36	0.33	0.00	0.00	0.48	0.00	0.78	0.70	0.00	0.00
SrO	0.31	0.16	0.35	0.28	0.25	0.27	0.34	0.28	0.35	0.26	0.26
Na2O	7.65	8.39	8.56	7.45	7.56	7.68	8.53	0.36	0.28	7.63	8.19
K2O	0.21	0.26	0.26	0.05	0.10	0.05	0.16	15.74	15.89	0.08	0.07
Total	97.06	100.26	99.42	100.00	99.85	100.49	100.41	103.31	99.64	98.82	100.23
Atom Proportions											
Si	11.22	11.09	11.10	10.63	10.73	10.88	11.16	12.08	11.95	11.22	11.09
Ti	0.00	0.00	0.00	0.00	0.00	0.00	0.00	0.00	0.01	0.00	0.00
Al	4.84	4.90	4.88	5.38	5.26	5.08	4.82	3.91	4.02	4.86	4.95
Fe	0.01	0.01	0.00	0.01	0.01	0.01	0.03	0.02	0.02	0.00	0.00
Ca	0.89	0.95	0.90	1.33	1.30	1.21	0.89	0.00	0.00	0.91	0.95
Be	0.00	0.03	0.02	0.00	0.00	0.03	0.00	0.06	0.05	0.00	0.00
Sr	0.03	0.02	0.04	0.03	0.03	0.03	0.04	0.03	0.04	0.03	0.03
Na	2.70	2.88	2.97	2.58	2.62	2.64	2.92	0.12	0.10	2.64	2.80
K	0.05	0.06	0.06	0.01	0.02	0.01	0.04	3.59	3.78	0.02	0.02
O	32.00	32.00	32.00	32.00	32.00	32.00	32.00	32.00	32.00	32.00	32.00
CatTot	19.73	19.93	19.97	19.97	19.96	19.90	19.89	19.81	19.97	19.67	19.84
Total	51.73	51.93	51.97			51.90	51.89	51.81	51.97	51.67	51.84
An	0.24	0.24	0.23	0.34	0.33	0.31	0.23	0.00	0.00	0.25	0.26
Ab	0.74	0.73	0.74	0.65	0.66	0.67	0.75	0.03	0.03	0.73	0.74
Or	0.01	0.01	0.02	0.00	0.01	0.00	0.01	0.95	0.95	0.01	0.00

B.3.1. Feldspar Compositional Analysis

Sample	5055 Z1	5088	5088	5088	5088	5088 adj to biot1	5088 adj to garn0511	5088 core	5088 rim	5088 rim	5100
Oxides											
SiO2	61.84	59.85	61.77	61.51	60.01	59.72	58.57	57.33	56.74	58.05	61.81
TiO2	0.02	0.01	0.03	0.01	0.00	0.00	0.00	0.00	0.00	0.03	0.02
Al2O3	23.56	24.14	23.88	23.86	23.96	24.59	25.48	26.95	26.97	26.92	24.49
Fe2O3	0.03	0.15	0.02	0.07	0.00	0.09	0.17	0.05	0.07	0.02	0.02
CaO	4.91	5.57	5.61	5.59	5.47	7.19	8.10	8.50	8.76	9.01	5.66
BaO	0.00	0.02	0.00	0.00	0.00	0.01	0.02	0.00	0.09	0.00	0.00
SrO	0.22	0.13	0.29	0.26	0.21	0.26	0.25	0.22	0.25	0.24	0.32
Na2O	8.40	8.26	8.14	8.17	8.22	7.09	6.51	6.57	6.29	6.51	8.11
K2O	0.09	0.15	0.18	0.33	0.27	0.10	0.13	0.16	0.11	0.11	0.06
Total	99.07	98.27	99.92	99.81	98.14	99.06	99.22	99.80	99.28	100.89	100.50
Atom Proportions											
Si	11.06	10.84	10.98	10.96	10.88	10.75	10.55	10.30	10.26	10.32	10.92
Ti	0.00	0.00	0.00	0.00	0.00	0.00	0.00	0.00	0.00	0.00	0.00
Al	4.97	5.15	5.00	5.01	5.12	5.22	5.41	5.71	5.75	5.64	5.10
Fe	0.00	0.02	0.00	0.01	0.00	0.01	0.02	0.01	0.01	0.00	0.00
Ca	0.94	1.08	1.07	1.07	1.06	1.39	1.56	1.64	1.70	1.72	1.07
Ba	0.00	0.00	0.00	0.00	0.00	0.00	0.00	0.00	0.01	0.00	0.00
Sr	0.02	0.01	0.03	0.03	0.02	0.03	0.03	0.02	0.03	0.03	0.03
Na	2.91	2.90	2.81	2.82	2.89	2.47	2.27	2.29	2.21	2.25	2.78
K	0.02	0.04	0.04	0.08	0.06	0.02	0.03	0.04	0.03	0.03	0.01
O	32.00	32.00	32.00	32.00	32.00	32.00	32.00	32.00	32.00	32.00	32.00
CatTot	19.92	20.04	19.94	19.98	20.04	19.89	19.88	20.01	19.98	19.99	19.92
Total	51.92		51.94	51.98		51.89	51.88	52.01	51.98	51.99	
An	0.24	0.27	0.27	0.27	0.26	0.35	0.40	0.41	0.43	0.43	0.28
Ab	0.75	0.72	0.71	0.71	0.72	0.63	0.58	0.57	0.56	0.56	0.71
Or	0.01	0.01	0.01	0.02	0.02	0.01	0.01	0.01	0.01	0.01	0.00

Sample	5100	5100 adj garn	5100 adj garn	5100	5100	5100 core	5100 kfeld at rim	5100 kfeld inclusion	5100 rim	5100 rim	5105a
Oxides											
SiO2	60.12	60.81	60.77	63.00	60.80	62.06	68.53	63.48	61.36	61.45	58.74
TiO2	0.00	0.00	0.02	0.01	0.00	0.00	0.00	0.01	0.01	0.00	0.01
Al2O3	23.31	23.66	24.33	24.17	24.34	24.82	19.93	24.06	24.82	24.71	24.31
Fe2O3	0.09	0.12	0.31	0.05	0.04	0.11	0.34	0.25	0.12	0.10	0.06
CaO	5.93	5.90	5.91	6.15	5.92	5.91	0.01	0.47	6.02	5.89	5.95
BaO	0.00	0.35	0.00	0.46	0.05	0.00	0.53	0.23	0.02	0.00	0.00
SrO	0.26	0.27	0.29	0.21	0.30	0.20	0.19	0.24	0.28	0.18	0.33
Na2O	7.86	7.98	7.92	7.56	8.07	7.96	0.19	0.94	8.23	8.22	7.71
K2O	0.06	0.06	0.04	0.07	0.07	0.03	15.40	12.79	0.04	0.05	0.11
Total	97.63	99.15	99.58	101.68	99.60	101.10	105.12	102.47	100.91	100.60	97.22
Atom Proportions											
Si	10.96	10.93	10.86	11.01	10.86	10.89	11.98	11.31	10.83	10.86	10.76
Ti	0.00	0.00	0.00	0.00	0.00	0.00	0.00	0.00	0.00	0.00	0.00
Al	5.00	5.01	5.12	4.98	5.13	5.14	4.11	5.05	5.16	5.15	5.25
Fe	0.01	0.02	0.04	0.01	0.01	0.02	0.05	0.03	0.02	0.01	0.01
Ca	1.16	1.14	1.13	1.15	1.13	1.11	0.00	0.09	1.14	1.12	1.17
Ba	0.00	0.03	0.00	0.03	0.00	0.00	0.04	0.02	0.00	0.00	0.00
Sr	0.03	0.03	0.03	0.02	0.03	0.02	0.02	0.03	0.03	0.02	0.04
Na	2.77	2.78	2.74	2.56	2.77	2.71	0.07	0.33	2.82	2.82	2.74
K	0.01	0.01	0.01	0.02	0.02	0.01	3.44	2.91	0.01	0.01	0.03
O	32.00	32.00	32.00	32.00	32.00	32.00	32.00	32.00	32.00	32.00	32.00
CatTot	19.94	19.96	19.93	19.78	19.98	19.89	19.69	19.76	20.00	19.98	19.99
Total						51.89	51.69	51.76	52.00	51.98	51.99
An	0.29	0.29	0.29	0.30	0.29	0.29	0.00	0.03	0.28	0.28	0.29
Ab	0.70	0.70	0.70	0.68	0.70	0.70	0.02	0.10	0.71	0.71	0.69
Or	0.00	0.00	0.00	0.00	0.00	0.00	0.97	0.86	0.00	0.00	0.01

B.3.1. Feldspar Compositional Analysis

Sample	5105a	5105a	5105a	5107a lg gr	5107a lg gr	5107a lg gr	5107a lg gr	5114 isolated feldsp	5114	5114	5114
Oxides											
SiO2	61.13	59.08	61.61	60.14	62.71	60.08	62.28	62.60	63.19	61.87	63.36
TiO2	0.01	0.01	0.02	0.01	0.00	0.00	0.00	0.03	0.00	0.00	0.00
Al2O3	24.43	24.08	23.94	24.19	23.97	23.92	23.51	22.06	22.26	22.54	22.36
Fe2O3	0.05	0.00	0.02	0.07	0.02	0.00	0.00	0.05	0.00	0.02	0.05
CaO	6.00	5.78	5.84	5.36	5.42	5.29	5.24	4.19	4.14	3.99	4.16
BaO	0.34	0.37	0.00	0.00	0.01	0.49	0.20	0.00	0.00	0.15	0.00
SrO	0.29	0.30	0.33	0.25	0.21	0.31	0.24	0.32	0.25	0.37	0.32
Na2O	7.93	7.97	7.97	8.02	7.86	8.20	8.00	8.53	8.75	8.75	8.66
K2O	0.08	0.13	0.10	0.25	0.30	0.25	0.22	0.13	0.17	0.16	0.17
Total	100.26	97.71	99.83	98.29	100.51	98.54	99.69	97.90	98.76	97.84	99.09
Atom Proportions											
Si	10.87	10.80	10.96	10.88	11.05	10.89	11.06	11.30	11.30	11.20	11.30
Ti	0.00	0.00	0.00	0.00	0.00	0.00	0.00	0.00	0.00	0.00	0.00
Al	5.12	5.19	5.02	5.16	4.98	5.11	4.93	4.69	4.69	4.81	4.70
Fe	0.01	0.00	0.00	0.01	0.00	0.00	0.00	0.01	0.00	0.00	0.01
Ca	1.14	1.13	1.11	1.04	1.02	1.03	1.00	0.81	0.79	0.77	0.80
Ba	0.02	0.03	0.00	0.00	0.00	0.04	0.01	0.00	0.00	0.01	0.00
Sr	0.03	0.03	0.03	0.03	0.02	0.03	0.03	0.03	0.03	0.04	0.03
Na	2.73	2.82	2.76	2.81	2.89	2.88	2.76	2.98	3.04	3.07	3.00
K	0.02	0.03	0.02	0.06	0.07	0.06	0.05	0.03	0.04	0.04	0.04
O	32.00	32.00	32.00	32.00	32.00	32.00	32.00	32.00	32.00	32.00	32.00
CatTot	19.94	20.03	19.91	19.98	19.83	20.03	19.86	19.86	19.89	19.95	19.87
Total	51.94	52.03	51.91	51.98	51.83	52.03	51.86	51.86	51.89		
An	0.29	0.28	0.28	0.26	0.27	0.25	0.26	0.21	0.20	0.20	0.21
Ab	0.69	0.70	0.70	0.71	0.71	0.71	0.72	0.77	0.78	0.78	0.78
Or	0.00	0.01	0.01	0.02	0.02	0.01	0.01	0.01	0.01	0.01	0.01

Sample	5114	5115b core	5115b kfeld	5115b plag adj po9	5115b plag inphoto 9	5115b rim	5115b rim adjmusc	5131 adj garn	5131 iso	5131	7005b
Oxides											
SiO2	63.36	62.35	64.45	62.85	62.71	63.26	61.93	61.81	61.96	62.71	62.39
TiO2	0.00	0.01	0.03	0.00	0.00	0.00	0.02	0.02	0.00	0.00	0.00
Al2O3	22.36	23.10	18.20	23.12	23.14	22.72	23.05	23.74	23.78	23.60	23.69
Fe2O3	0.05	0.06	0.05	0.00	0.08	0.02	0.02	0.02	0.00	0.00	0.06
CaO	4.16	4.45	0.05	4.47	4.61	3.47	4.39	5.31	5.03	5.03	4.83
BaO	0.00	0.07	0.03	0.00	0.00	0.00	0.00	0.00	0.13	0.19	0.00
SrO	0.32	0.14	0.25	0.26	0.17	0.19	0.15	0.23	0.34	0.30	0.14
Na2O	8.66	9.08	0.15	8.92	9.07	9.04	8.92	8.03	8.33	8.38	8.76
K2O	0.17	0.10	16.43	0.21	0.10	0.60	0.11	0.26	0.28	0.27	0.18
Total	99.09	99.36	99.64	99.83	99.89	99.32	98.59	99.42	99.86	100.47	100.03
Atom Proportions											
Si		11.12	11.99	11.16	11.13	11.27	11.12	11.02	11.02	11.08	11.06
Ti		0.00	0.00	0.00	0.00	0.00	0.00	0.00	0.00	0.00	0.00
Al		4.86	3.99	4.84	4.84	4.77	4.88	4.99	4.99	4.92	4.95
Fe		0.01	0.01	0.00	0.01	0.00	0.00	0.00	0.00	0.00	0.01
Ca		0.85	0.01	0.85	0.88	0.66	0.85	1.01	0.96	0.95	0.92
Ba		0.01	0.00	0.00	0.00	0.00	0.00	0.00	0.01	0.01	0.00
Sr		0.01	0.03	0.03	0.02	0.02	0.02	0.02	0.04	0.03	0.01
Na		3.14	0.05	3.07	3.12	3.12	3.11	2.78	2.87	2.87	3.01
K		0.02	3.90	0.05	0.02	0.14	0.03	0.06	0.07	0.06	0.04
O		32.00	32.00	32.00	32.00	32.00	32.00	32.00	32.00	32.00	32.00
CatTot		20.02	19.98	19.99	20.02	19.98	20.00	19.89	19.95	19.93	19.99
Total		52.02	51.98	51.99	52.02	51.98	52.00	51.89	51.95	51.93	
An		0.21	0.00	0.21	0.22	0.17	0.21	0.26	0.24	0.24	0.23
Ab		0.78	0.01	0.77	0.77	0.79	0.78	0.72	0.73	0.73	0.76
Or		0.01	0.98	0.01	0.01	0.03	0.01	0.02	0.02	0.02	0.01

B.3.1. Feldespar Compositional Analysis

Sample	7006b	7006b	7006b	7006b	7006b adj biot1906 10	7006b kspar	N130	N130	sbp12 lg grain	sbp12 lg grain
Oxides										
SiO2	60.06	62.36	61.12	60.92	62.76	62.60	60.20	59.89	63.07	62.36
TiO2	0.00	0.00	0.00	0.00	0.00	0.05	0.01	0.00	0.02	0.01
Al2O3	22.95	22.14	23.48	23.38	23.61	19.10	24.38	25.04	23.48	23.48
Fe2O3	0.01	0.06	0.04	0.02	0.12	0.02	0.05	0.04	0.06	0.00
CaO	5.20	4.45	5.42	5.28	4.97	0.01	6.79	7.02	5.19	4.71
BaO	0.02	0.00	0.00	0.10	0.12	1.21	0.00	0.00	0.00	0.00
SrO	0.28	0.22	0.29	0.28	0.25	0.32	0.25	0.21	0.30	0.26
Na2O	8.48	8.96	8.37	8.35	8.71	1.72	7.25	7.31	8.09	8.20
K2O	0.29	0.20	0.31	0.28	0.10	13.49	0.17	0.09	0.50	0.36
Total	97.29	98.39	99.03	98.60	100.85	98.54	99.09	99.60	100.70	99.38
Atom Proportions										
Si	10.99	11.23	10.98	11.00	11.06	11.78	10.82	10.71	11.11	11.11
Ti	0.00	0.00	0.00	0.00	0.00	0.01	0.00	0.00	0.00	0.00
Al	4.95	4.70	4.97	4.97	4.94	4.24	5.16	5.28	4.88	4.93
Fe	0.00	0.01	0.01	0.00	0.02	0.00	0.01	0.01	0.01	0.00
Ca	1.02	0.86	1.04	1.02	0.94	0.00	1.31	1.35	0.98	0.90
Ba	0.00	0.00	0.00	0.01	0.01	0.09	0.00	0.00	0.00	0.00
Sr	0.03	0.02	0.03	0.03	0.03	0.04	0.03	0.02	0.03	0.03
Na	3.01	3.13	2.92	2.92	2.97	0.63	2.52	2.54	2.76	2.83
K	0.07	0.05	0.07	0.07	0.02	3.24	0.04	0.02	0.11	0.08
O	32.00	32.00	32.00	32.00	32.00	32.00	32.00	32.00	32.00	32.00
CatTot	20.07	20.00	20.02	20.01	19.97	20.02	19.88	19.92	19.88	19.88
Total	52.07	52.00	52.02	52.01			51.88	51.92	51.88	51.88
An	0.25	0.21	0.26	0.26	0.24	0.00	0.34	0.34	0.26	0.23
Ab	0.73	0.77	0.72	0.72	0.75	0.16	0.65	0.65	0.71	0.74
Or	0.02	0.01	0.02	0.02	0.01	0.81	0.01	0.01	0.03	0.02

Sample
Oxides
SiO2
TiO2
Al2O3
Fe2O3
CaO
BaO
SrO
Na2O
K2O
Total
Atom Proportions
Si
Ti
Al
Fe
Ca
Ba
Sr
Na
K
O
CatTot
Total
An
Ab
Or

B.3.2. Feldspar Profile 1302a from Sample 5024

Sample	Fel1302a	5024 scan 1	0.88mm long	0.022mm apart											
	1	2	3	4	5	6	7	8	9	10	11	12	13	14	15
Oxides															
SiO2	60.95	61.58	49.32	61.16	60.82	61.30	59.78	61.39	61.63	60.97	61.05	59.33	61.44	60.77	61.48
TiO2	0.02	0.01	0.00	0.00	0.00	0.00	0.03	0.00	0.03	0.00	0.00	0.01	0.00	0.00	0.01
Al2O3	23.82	24.03	21.90	24.18	24.09	24.01	23.92	24.10	23.96	24.22	23.99	24.26	24.16	23.88	24.25
Fe2O3	0.06	0.05	0.40	0.04	0.04	0.00	0.03	0.02	0.00	0.02	0.06	0.04	0.06	0.00	0.07
CaO	5.26	5.31	4.49	5.63	5.55	5.53	5.41	5.45	5.39	5.55	5.59	5.51	5.65	5.54	5.61
BaO	0.00	0.05	0.00	0.00	0.00	0.01	0.05	0.00	0.11	0.04	0.00	0.00	0.00	0.03	0.00
SrO	0.29	0.31	0.25	0.27	0.31	0.21	0.31	0.23	0.32	0.27	0.24	0.31	0.20	0.18	0.28
Na2O	8.57	8.37	6.41	8.21	8.42	8.33	8.01	8.25	8.12	8.25	8.31	8.28	8.24	8.21	8.33
K2O	0.18	0.20	0.31	0.26	0.23	0.26	0.30	0.28	0.57	0.32	0.30	0.30	0.29	0.31	0.30
Total	99.17	99.91	83.08	99.75	99.46	99.66	97.84	99.71	100.13	99.64	99.54	98.04	100.05	98.91	100.32
Atom Proportions															
Si	10.94	10.96	10.58	10.91	10.89	10.94	10.88	10.94	10.96	10.89	10.92	10.79	10.92	10.93	10.91
Ti	0.00	0.00	0.00	0.00	0.00	0.00	0.00	0.00	0.00	0.00	0.00	0.00	0.00	0.00	0.00
Al	5.04	5.04	5.54	5.08	5.09	5.05	5.13	5.06	5.02	5.10	5.06	5.20	5.06	5.06	5.07
Fe	0.01	0.01	0.07	0.01	0.01	0.00	0.01	0.00	0.00	0.00	0.01	0.01	0.01	0.00	0.01
Ca	1.02	1.01	1.03	1.08	1.06	1.06	1.05	1.04	1.03	1.06	1.07	1.07	1.06	1.07	1.07
Ba	0.00	0.00	0.00	0.00	0.00	0.00	0.00	0.00	0.01	0.00	0.00	0.00	0.00	0.00	0.00
Sr	0.03	0.03	0.03	0.03	0.03	0.02	0.03	0.02	0.03	0.03	0.03	0.03	0.02	0.02	0.03
Na	2.98	2.89	2.67	2.84	2.93	2.88	2.83	2.85	2.80	2.86	2.88	2.92	2.84	2.86	2.87
K	0.04	0.05	0.09	0.06	0.05	0.06	0.07	0.06	0.13	0.07	0.07	0.07	0.07	0.07	0.07
O	32.00	32.00	32.00	32.00	32.00	32.00	32.00	32.00	32.00	32.00	32.00	32.00	32.00	32.00	32.00
CatTot	20.05	19.98	20.00	20.00	20.05	20.01	20.00	19.98	19.99	20.02	20.03	20.10	20.00	20.01	20.02
Total	52.05	51.98	52.00	52.00	52.05	52.01	52.00	51.98	51.99	52.02	52.03	52.10	52.00	52.01	52.02
An	0.25	0.25	0.27	0.27	0.26	0.26	0.26	0.26	0.26	0.26	0.26	0.26	0.27	0.27	0.26
Ab	0.73	0.73	0.70	0.71	0.72	0.72	0.71	0.72	0.70	0.71	0.71	0.71	0.71	0.71	0.71
Or	0.01	0.01	0.02	0.01	0.01	0.01	0.02	0.02	0.03	0.02	0.02	0.02	0.02	0.02	0.02

Sample															
	16	17	18	19	20	21	22	23	24	25	26	27	28	29	30
Oxides															
SiO2	60.60	60.52	61.35	59.80	61.37	61.41	60.63	59.78	61.89	61.95	61.05	61.99	61.75	61.76	61.06
TiO2	0.00	0.00	0.00	0.00	0.01	0.00	0.00	0.00	0.02	0.00	0.01	0.02	0.00	0.01	0.00
Al2O3	24.19	23.82	24.11	24.40	24.12	24.03	24.00	25.32	24.50	23.69	23.49	23.24	24.03	24.14	24.08
Fe2O3	0.02	0.03	0.03	0.03	0.03	0.04	0.12	0.11	0.44	0.08	0.09	0.04	0.07	0.01	0.02
CaO	5.52	5.54	5.63	5.56	5.49	5.52	5.38	4.86	2.94	5.23	4.48	4.74	5.35	5.46	5.43
BaO	0.00	0.01	0.07	0.00	0.04	0.00	0.00	0.00	0.05	0.00	0.08	0.01	0.00	0.00	0.00
SrO	0.31	0.22	0.20	0.26	0.31	0.29	0.27	0.29	0.22	0.28	0.23	0.29	0.30	0.20	0.23
Na2O	8.17	8.08	8.26	8.26	8.27	8.40	8.27	8.45	8.14	8.42	7.71	7.70	8.34	8.37	8.25
K2O	0.30	0.29	0.25	0.29	0.28	0.28	0.24	0.22	1.76	0.19	1.16	1.51	0.26	0.28	0.30
Total	99.10	98.48	99.90	98.61	99.91	99.97	96.90	99.04	99.95	99.84	98.27	99.54	100.11	100.23	99.37
Atom Proportions															
Si	10.88	10.93	10.93	10.81	10.93	10.93	10.91	10.74	11.01	11.02	11.04	11.09	10.98	10.95	10.93
Ti	0.00	0.00	0.00	0.00	0.00	0.00	0.00	0.00	0.00	0.00	0.00	0.00	0.00	0.00	0.00
Al	5.12	5.07	5.06	5.20	5.06	5.04	5.09	5.36	5.14	4.97	5.01	4.90	5.03	5.05	5.08
Fe	0.00	0.00	0.00	0.00	0.00	0.01	0.02	0.02	0.06	0.01	0.01	0.01	0.01	0.00	0.00
Ca	1.06	1.07	1.07	1.08	1.05	1.05	1.04	0.94	0.56	1.00	0.87	0.91	1.02	1.04	1.04
Ba	0.00	0.00	0.01	0.00	0.00	0.00	0.00	0.00	0.00	0.00	0.00	0.00	0.00	0.00	0.00
Sr	0.03	0.02	0.02	0.03	0.03	0.03	0.03	0.03	0.02	0.03	0.02	0.03	0.03	0.02	0.02
Na	2.84	2.82	2.85	2.89	2.86	2.90	2.88	2.94	2.81	2.90	2.70	2.67	2.87	2.88	2.86
K	0.07	0.07	0.06	0.07	0.06	0.06	0.06	0.05	0.40	0.04	0.27	0.35	0.06	0.06	0.07
O	32.00	32.00	32.00	32.00	32.00	32.00	32.00	32.00	32.00	32.00	32.00	32.00	32.00	32.00	32.00
CatTot	20.01	19.98	20.00	20.07	20.00	20.02	20.01	20.07	20.00	19.97	19.93	19.96	19.98	20.00	20.00
Total	52.01	51.98	52.00	52.07	52.00	52.02	52.01	52.07	52.00	51.97	51.93	51.96	51.98	52.00	52.00
An	0.26	0.27	0.27	0.26	0.26	0.26	0.26	0.24	0.15	0.25	0.22	0.23	0.26	0.26	0.26
Ab	0.71	0.71	0.71	0.71	0.71	0.72	0.72	0.74	0.74	0.73	0.70	0.68	0.72	0.72	0.72
Or	0.02	0.02	0.01	0.02	0.02	0.02	0.01	0.01	0.10	0.01	0.07	0.09	0.02	0.02	0.02

B.3.2. Feldspar Profile 1302a from Sample 5024

Sample	31	32	33	34	35	36	37	38	39	40
Oxides										
SiO2	61.52	61.15	61.33	61.36	61.07	60.51	61.30	61.95	60.33	62.16
TiO2	0.00	0.00	0.00	0.00	0.01	0.00	0.00	0.00	0.00	0.00
Al2O3	24.07	24.27	23.53	24.19	24.25	24.12	24.23	24.05	23.86	24.08
Fe2O3	0.01	0.02	0.02	0.00	0.00	0.00	0.00	0.02	0.03	0.05
CaO	5.47	5.38	4.92	5.65	5.60	5.62	5.57	5.33	5.32	5.33
BaO	0.00	0.02	0.33	0.00	0.00	0.00	0.00	0.02	0.03	0.04
SrO	0.23	0.23	0.26	0.31	0.24	0.23	0.21	0.32	0.29	0.23
Na2O	8.46	8.37	7.50	8.17	8.20	8.26	8.34	8.54	8.29	8.49
K2O	0.26	0.29	1.54	0.27	0.25	0.21	0.25	0.25	0.22	0.25
Total	100.03	99.72	99.44	99.95	99.63	98.95	99.90	100.49	98.37	100.62
Atom Proportions										
Si	10.94	10.91	11.02	10.92	10.90	10.88	10.91	10.97	10.91	10.98
Ti	0.00	0.00	0.00	0.00	0.00	0.00	0.00	0.00	0.00	0.00
Al	5.04	5.10	4.98	5.07	5.10	5.11	5.08	5.02	5.09	5.01
Fe	0.00	0.00	0.00	0.00	0.00	0.00	0.00	0.00	0.01	0.01
Ca	1.04	1.03	0.95	1.08	1.07	1.08	1.08	1.01	1.03	1.01
Ba	0.00	0.00	0.02	0.00	0.00	0.00	0.00	0.00	0.00	0.00
Sr	0.02	0.02	0.03	0.03	0.03	0.02	0.02	0.03	0.03	0.02
Na	2.92	2.90	2.61	2.82	2.84	2.88	2.88	2.93	2.91	2.91
K	0.06	0.07	0.35	0.06	0.06	0.05	0.06	0.06	0.05	0.06
O	32.00	32.00	32.00	32.00	32.00	32.00	32.00	32.00	32.00	32.00
CatTot	20.03	20.02	19.97	19.98	20.00	20.03	20.02	20.02	20.02	20.00
Total	52.03	52.02	51.97	51.98	52.00	52.03	52.02	52.02	52.02	52.00
An	0.26	0.26	0.24	0.27	0.27	0.27	0.26	0.25	0.26	0.25
Ab	0.72	0.72	0.66	0.71	0.71	0.71	0.72	0.73	0.72	0.73
Or	0.01	0.02	0.09	0.02	0.01	0.01	0.01	0.01	0.01	0.01

Sample
Oxides
SiO2
TiO2
Al2O3
Fe2O3
CaO
BaO
SrO
Na2O
K2O
Total
Atom Proportions
Si
Ti
Al
Fe
Ca
Ba
Sr
Na
K
O
CatTot
Total
An
Ab
Or

B.3.3. Feldspar Profile 1302b from Sample 6024

Sample	Fel1302b	6024 scan2	0.219 mm long	0.024 mm apart						
	1	2	3	4	5	6	7	8	9	10
Oxides										
SiO2	71.41	71.12	61.76	61.48	61.12	60.50	61.66	60.74	61.62	61.67
TiO2	0.03	0.00	0.00	0.00	0.00	0.02	0.00	0.00	0.00	0.00
Al2O3	18.02	17.37	23.17	23.33	23.54	23.84	23.99	23.43	23.72	23.16
Fe2O3	0.03	0.01	0.00	0.00	0.03	0.02	0.02	0.05	0.05	0.02
CaO	2.25	2.32	4.34	4.79	4.72	5.40	5.37	5.26	4.92	4.79
BaO	0.02	0.03	0.05	0.02	0.00	0.03	0.00	0.04	0.00	0.01
SrO	0.33	0.30	0.21	0.27	0.23	0.32	0.24	0.22	0.25	0.29
Na2O	8.44	7.12	9.13	8.60	8.19	8.49	8.37	8.37	8.79	8.73
K2O	0.05	1.07	0.09	0.16	0.88	0.17	0.19	0.16	0.12	0.15
Total	100.58	99.33	98.75	98.64	98.72	98.80	99.83	98.27	99.48	98.82
Atom Proportions										
Si	12.31	12.42	11.09	11.06	11.01	10.91	10.97	10.98	11.00	11.08
Ti	0.00	0.00	0.00	0.00	0.00	0.00	0.00	0.00	0.00	0.00
Al	3.66	3.58	4.91	4.94	5.00	5.07	5.03	4.99	4.99	4.90
Fe	0.00	0.00	0.00	0.00	0.00	0.00	0.00	0.01	0.01	0.00
Ca	0.42	0.43	0.83	0.92	0.91	1.04	1.02	1.02	0.94	0.92
Ba	0.00	0.00	0.00	0.00	0.00	0.00	0.00	0.00	0.00	0.00
Sr	0.03	0.03	0.02	0.03	0.02	0.03	0.03	0.02	0.03	0.03
Na	2.82	2.41	3.18	3.00	2.86	2.97	2.89	2.93	3.04	3.04
K	0.01	0.24	0.02	0.04	0.20	0.04	0.04	0.04	0.03	0.03
O	32.00	32.00	32.00	32.00	32.00	32.00	32.00	32.00	32.00	32.00
CatTot	19.27	19.11	20.06	19.99	20.02	20.06	19.96	20.00	20.04	20.01
Total	51.27	51.11	52.06	51.99	52.02	52.06	51.96	52.00	52.04	52.01
An	0.13	0.14	0.21	0.23	0.23	0.26	0.26	0.25	0.23	0.23
Ab	0.86	0.77	0.78	0.75	0.72	0.73	0.73	0.73	0.75	0.75
Or	0.00	0.08	0.00	0.01	0.05	0.01	0.01	0.01	0.01	0.01

B.3.4. Feldspar Profile 1302c from Sample 5115b

Sample	Fel1302c	5115b scan1	0.264 mm long	0.024mm apart								
	1	2	3	4	5	6	7	8	9	10	11	12
Oxides												
SiO2	63.16	61.97	62.93	62.72	62.92	62.59	62.90	63.27	63.32	62.79	62.58	62.45
TiO2	0.02	0.01	0.00	0.00	0.00	0.00	0.00	0.00	0.00	0.00	0.00	0.00
Al2O3	23.07	22.92	22.49	23.28	23.10	23.53	23.08	23.05	23.01	22.72	22.30	23.05
Fe2O3	0.00	0.00	0.00	0.02	0.00	0.00	0.00	0.00	0.02	0.00	0.04	0.00
CaO	4.40	4.28	4.42	4.50	4.55	4.72	4.35	4.36	4.30	4.25	4.04	4.39
BaO	0.00	0.04	0.00	0.00	0.01	0.03	0.04	0.00	0.00	0.04	0.01	0.00
SrO	0.35	0.22	0.24	0.25	0.24	0.32	0.30	0.22	0.29	0.22	0.25	0.27
Na2O	8.99	9.13	8.96	8.93	9.05	9.06	8.90	9.33	9.19	8.99	8.56	9.09
K2O	0.26	0.11	0.09	0.14	0.16	0.13	0.15	0.15	0.13	0.29	1.38	0.10
Total	100.24	99.69	99.13	99.83	100.04	100.38	99.72	100.39	100.26	99.30	99.16	99.35
Atom Proportions												
Si	11.17	11.13	11.24	11.13	11.15	11.07	11.17	11.17	11.19	11.20	11.23	11.14
Ti	0.00	0.00	0.00	0.00	0.00	0.00	0.00	0.00	0.00	0.00	0.00	0.00
Al	4.81	4.85	4.73	4.87	4.82	4.91	4.83	4.80	4.79	4.78	4.72	4.85
Fe	0.00	0.00	0.00	0.00	0.00	0.00	0.00	0.00	0.00	0.00	0.01	0.00
Ca	0.83	0.82	0.85	0.86	0.86	0.89	0.83	0.83	0.82	0.81	0.78	0.84
Ba	0.00	0.00	0.00	0.00	0.00	0.00	0.00	0.00	0.00	0.00	0.00	0.00
Sr	0.04	0.02	0.03	0.03	0.03	0.03	0.03	0.02	0.03	0.02	0.03	0.03
Na	3.08	3.18	3.10	3.07	3.11	3.11	3.06	3.20	3.15	3.11	2.98	3.14
K	0.06	0.03	0.02	0.03	0.04	0.03	0.03	0.03	0.03	0.07	0.32	0.02
O	32.00	32.00	32.00	32.00	32.00	32.00	32.00	32.00	32.00	32.00	32.00	32.00
CatTot	19.99	20.04	19.96	19.99	20.01	20.04	19.96	20.04	20.01	20.00	20.06	20.02
Total	51.99	52.04	51.96	51.99	52.01	52.04	51.96	52.04	52.01	52.00	52.06	52.02
An	0.21	0.20	0.21	0.21	0.21	0.22	0.21	0.20	0.20	0.20	0.19	0.21
Ab	0.77	0.78	0.78	0.77	0.77	0.76	0.77	0.78	0.78	0.77	0.73	0.78
Or	0.01	0.01	0.00	0.01	0.01	0.01	0.01	0.01	0.01	0.02	0.08	0.01

B.3.5. Feldspar Profile 1302d from Sample 5000

Sample	Fel1302d	5000 scan 1	0.283 mm long	0.024 mm apart									
	1	2	3	4	5	6	7	8	9	10	11	12	13
Oxides													
SiO2													
TiO2													
Al2O3													
Fe2O3													
CaO													
BaO													
SrO													
Na2O													
K2O													
Total													
Atom Proportions													
Si	11.00	10.99	10.94	10.97	10.88	10.92	10.95	10.98	11.01	11.02	11.02	11.04	11.02
Ti	0.00	0.00	0.00	0.01	0.00	0.00	0.00	0.00	0.00	0.00	0.00	0.00	0.00
Al	4.97	4.96	5.03	5.01	5.09	5.06	5.04	5.00	4.98	4.97	4.96	4.93	4.93
Fe	0.02	0.02	0.01	0.00	0.01	0.01	0.00	0.01	0.01	0.02	0.01	0.01	0.03
Ca	0.95	1.05	1.04	1.01	1.09	1.05	1.05	1.02	0.96	0.97	0.98	0.99	0.97
Ba	0.00	0.00	0.00	0.00	0.00	0.00	0.00	0.00	0.00	0.00	0.00	0.00	0.00
Sr	0.02	0.02	0.02	0.02	0.02	0.03	0.02	0.02	0.02	0.02	0.01	0.02	0.02
Na	3.05	2.95	2.97	2.82	2.90	2.91	2.87	2.97	3.02	2.96	2.99	2.98	3.02
K	0.03	0.03	0.04	0.19	0.05	0.04	0.04	0.03	0.02	0.03	0.03	0.03	0.02
O	32.00	32.00	32.00	32.00	32.00	32.00	32.00	32.00	32.00	32.00	32.00	32.00	32.00
CatTot	20.05	20.01	20.04	20.02	20.04	20.02	19.98	20.02	20.02	19.98	20.01	20.00	20.02
Total	52.05	52.01	52.04	52.02	52.04	52.02	51.98	52.02	52.02	51.98	52.01	52.00	52.02
An	0.23	0.26	0.26	0.25	0.27	0.26	0.26	0.25	0.24	0.24	0.24	0.25	0.24
Ab	0.75	0.73	0.73	0.70	0.71	0.72	0.72	0.73	0.75	0.74	0.74	0.74	0.75
Or	0.01	0.01	0.01	0.05	0.01	0.01	0.01	0.01	0.01	0.01	0.01	0.01	0.01

B.3.6. Feldspar Profile 1402a from Sample 5066

Sample	Fel1402a scan	5066	0.486mm long	0.0222mm apart	psammitic								
	1	2	3	4	5	6	7	8	9	10	11	12	13
Oxides													
SiO2	57.12	57.90	58.54	58.07	57.84	55.62	56.25	56.41	55.74	55.86	56.11	56.58	56.11
TiO2	0.00	0.01	0.02	0.00	0.00	0.01	0.06	0.00	0.02	0.00	0.00	0.01	0.03
Al2O3	27.18	26.78	26.80	26.72	27.07	27.21	27.26	27.44	27.69	27.77	27.81	27.98	27.66
Fe2O3	0.09	0.12	0.04	0.11	0.06	0.00	0.06	0.07	0.02	0.03	0.05	0.04	0.05
CaO	8.87	8.60	8.40	8.55	8.89	9.29	9.54	9.83	9.81	9.93	9.91	9.93	9.86
BaO	0.00	0.00	0.04	0.03	0.02	0.04	0.00	0.00	0.00	0.00	0.00	0.02	0.05
SrO	0.17	0.15	0.21	0.23	0.19	0.19	0.25	0.29	0.31	0.26	0.23	0.27	0.22
Na2O	6.36	6.75	6.68	6.62	6.50	6.26	6.04	5.95	5.88	5.78	5.67	5.83	5.77
K2O	0.12	0.11	0.12	0.15	0.15	0.13	0.15	0.13	0.15	0.12	0.16	0.13	0.13
Total	99.93	100.43	100.86	100.48	100.74	98.74	99.61	100.12	99.61	99.74	99.92	100.79	99.88
Atom Proportions													
Si	10.25	10.34	10.39	10.36	10.30	10.14	10.16	10.14	10.08	10.08	10.10	10.10	10.11
Ti	0.00	0.00	0.00	0.00	0.00	0.00	0.01	0.00	0.00	0.00	0.00	0.00	0.00
Al	5.75	5.64	5.61	5.62	5.68	5.85	5.80	5.82	5.90	5.91	5.90	5.89	5.87
Fe	0.01	0.02	0.01	0.01	0.01	0.00	0.01	0.01	0.00	0.00	0.01	0.01	0.01
Ca	1.71	1.65	1.60	1.64	1.70	1.81	1.85	1.89	1.90	1.92	1.91	1.90	1.91
Ba	0.00	0.00	0.00	0.00	0.00	0.00	0.00	0.00	0.00	0.00	0.00	0.00	0.00
Sr	0.02	0.02	0.02	0.02	0.02	0.02	0.03	0.03	0.03	0.03	0.02	0.03	0.02
Na	2.22	2.34	2.30	2.29	2.25	2.21	2.12	2.07	2.06	2.02	1.98	2.02	2.02
K	0.03	0.03	0.03	0.03	0.04	0.03	0.04	0.03	0.04	0.03	0.04	0.03	0.03
O	32.00	32.00	32.00	32.00	32.00	32.00	32.00	32.00	32.00	32.00	32.00	32.00	32.00
CatTot	19.99	20.02	19.96	19.98	19.99	20.06	20.00	20.00	20.02	19.99	19.96	19.97	19.97
Total	51.99	52.02	51.96	51.98	51.99	52.06	52.00	52.00	52.02	51.99	51.96	51.97	51.97
An	0.43	0.41	0.40	0.41	0.42	0.44	0.46	0.47	0.47	0.48	0.48	0.48	0.48
Ab	0.56	0.58	0.58	0.57	0.56	0.54	0.53	0.52	0.51	0.51	0.50	0.51	0.51
Or	0.01	0.01	0.01	0.01	0.01	0.01	0.01	0.01	0.01	0.01	0.01	0.01	0.01

Sample	14	15	16	17	18	19	20	21	22	23
Oxides										
SiO2	56.07	56.46	56.83	57.56	58.23	57.97	57.30	58.71	57.85	58.03
TiO2	0.00	0.03	0.00	0.00	0.00	0.01	0.00	0.00	0.02	0.03
Al2O3	27.87	27.46	27.37	27.32	27.24	26.55	26.96	26.49	26.59	26.67
Fe2O3	0.05	0.07	0.08	0.08	0.08	0.15	0.06	0.11	0.07	0.18
CaO	9.86	9.86	9.57	9.29	8.87	7.31	8.51	8.49	8.51	8.58
BaO	0.02	0.06	0.02	0.00	0.00	0.00	0.00	0.00	0.01	0.00
SrO	0.24	0.35	0.25	0.18	0.29	0.28	0.22	0.23	0.26	0.31
Na2O	5.97	5.80	6.05	6.30	6.11	6.14	6.60	6.64	6.67	6.51
K2O	0.12	0.13	0.17	0.14	0.14	1.03	0.18	0.15	0.14	0.07
Total	100.21	100.22	100.33	100.86	100.96	99.44	99.84	100.82	100.13	100.39
Atom Proportions										
Si	10.08	10.15	10.19	10.25	10.33	10.44	10.30	10.43	10.36	10.36
Ti	0.00	0.00	0.00	0.00	0.00	0.00	0.00	0.00	0.00	0.00
Al	5.90	5.82	5.78	5.73	5.70	5.64	5.71	5.55	5.61	5.61
Fe	0.01	0.01	0.01	0.01	0.01	0.02	0.01	0.01	0.01	0.03
Ca	1.90	1.90	1.84	1.77	1.69	1.41	1.64	1.62	1.63	1.64
Ba	0.00	0.00	0.00	0.00	0.00	0.00	0.00	0.00	0.00	0.00
Sr	0.03	0.04	0.03	0.02	0.03	0.03	0.02	0.02	0.03	0.03
Na	2.08	2.02	2.10	2.17	2.10	2.14	2.30	2.29	2.32	2.25
K	0.03	0.03	0.04	0.03	0.03	0.24	0.04	0.03	0.03	0.02
O	32.00	32.00	32.00	32.00	32.00	32.00	32.00	32.00	32.00	32.00
CatTot	20.02	19.96	19.99	19.98	19.89	19.92	20.02	19.95	20.00	19.95
Total	52.02	51.96	51.99	51.98	51.89	51.92	52.02	51.95	52.00	51.95
An	0.47	0.48	0.46	0.44	0.44	0.37	0.41	0.41	0.41	0.42
Ab	0.52	0.51	0.52	0.54	0.55	0.56	0.57	0.58	0.58	0.57
Or	0.01	0.01	0.01	0.01	0.01	0.06	0.01	0.01	0.01	0.00

B.3.7 Feldspar Profile 1402b from Sample 5100

Sample	Fel1402b scan	5100	0.109mm long	0.027mm apart	psammitic
	1	2	3	4	5
Oxides					
SiO2	62.61	61.44	61.65	61.38	61.79
TiO2	0.02	0.01	0.05	0.03	0.00
Al2O3	24.91	24.95	24.89	24.65	24.98
Fe2O3	0.08	0.01	0.01	0.05	0.09
CaO	5.91	5.83	5.86	6.02	6.22
BaO	0.06	0.03	0.00	0.01	0.01
SrO	0.24	0.15	0.27	0.29	0.21
Na2O	8.05	7.90	7.97	7.93	7.99
K2O	0.04	0.06	0.08	0.05	0.05
Total	101.92	100.39	100.78	100.40	101.34
Atom Proportions					
Si	10.91	10.86	10.86	10.87	10.84
Ti	0.00	0.00	0.01	0.00	0.00
Al	5.11	5.20	5.17	5.14	5.16
Fe	0.01	0.00	0.00	0.01	0.01
Ca	1.10	1.10	1.11	1.14	1.17
Ba	0.00	0.00	0.00	0.00	0.00
Sr	0.02	0.02	0.03	0.03	0.02
Na	2.72	2.71	2.72	2.72	2.72
K	0.01	0.01	0.02	0.01	0.01
O	32.00	32.00	32.00	32.00	32.00
CatTot	19.89	19.90	19.92	19.92	19.94
Total	51.89	51.90	51.92	51.92	51.94
An	0.29	0.29	0.29	0.29	0.30
Ab	0.70	0.70	0.70	0.70	0.69
Or	0.00	0.00	0.00	0.00	0.00

B.3.8 Feldspar Profile 1402c from Sample 5100

Sample	Fel1402c scan	5100	0.093 mm long	0.023 mm apart	psammitic
	1	2	3	4	5
Oxides					
SiO2	61.45	61.94	61.62	61.98	61.23
TiO2	0.00	0.00	0.00	0.03	0.02
Al2O3	25.02	25.06	25.20	24.90	25.13
Fe2O3	0.32	0.18	0.04	0.15	0.29
CaO	6.06	5.92	5.82	6.00	6.06
BaO	0.00	0.00	0.00	0.00	0.00
SrO	0.31	0.28	0.22	0.31	0.19
Na2O	8.18	8.06	8.12	7.77	7.83
K2O	0.05	0.04	0.05	0.02	0.05
Total	101.39	101.48	101.08	101.14	100.81
Atom Proportions					
Si	10.80	10.85	10.83	10.88	10.80
Ti	0.00	0.00	0.00	0.00	0.00
Al	5.18	5.17	5.22	5.15	5.22
Fe	0.04	0.02	0.01	0.02	0.04
Ca	1.14	1.11	1.10	1.13	1.14
Ba	0.00	0.00	0.00	0.00	0.00
Sr	0.03	0.03	0.02	0.03	0.02
Na	2.79	2.74	2.77	2.65	2.68
K	0.01	0.01	0.01	0.00	0.01
O	32.00	32.00	32.00	32.00	32.00
CatTot	19.99	19.93	19.95	19.86	19.91
Total	51.99	51.93	51.95	51.86	51.91
An	0.29	0.29	0.28	0.30	0.30
Ab	0.70	0.70	0.71	0.69	0.69
Or	0.00	0.00	0.00	0.00	0.00

B.3.9. Feldspar Profile 1402d from Sample 5011

Sample	Fel1402d scan	5011	0.322 mm long	0.023 mm apart	peammitic						KFELD			
	1	2	3	4	5	6	7	8	9	10	11	12	13	14
Oxides														
SiO2	61.33	60.94	60.56	60.02	60.38	61.00	60.56	59.83	61.02	56.04	61.12	60.73	61.03	61.02
TiO2	0.00	0.00	0.00	0.00	0.00	0.01	0.01	0.00	0.00	0.33	0.00	0.03	0.03	0.01
Al2O3	25.90	25.38	25.43	25.26	25.73	25.39	25.65	25.68	25.81	22.87	25.66	25.52	25.73	25.83
Fe2O3	0.00	0.06	0.02	0.10	0.05	0.04	0.00	0.02	0.05	0.05	0.02	0.06	0.00	0.06
CaO	6.79	6.70	6.68	6.85	6.87	6.80	7.02	6.68	6.85	0.19	6.75	6.83	6.72	6.72
BaO	0.03	0.07	0.06	0.05	0.00	0.00	0.00	0.00	0.04	14.19	0.00	0.00	0.05	0.00
SrO	0.30	0.24	0.18	0.20	0.22	0.19	0.19	0.18	0.15	0.13	0.13	0.15	0.24	0.17
Na2O	7.55	7.39	7.65	7.72	7.60	7.41	7.45	7.06	7.64	0.17	7.74	7.55	7.50	7.42
K2O	0.04	0.04	0.07	0.04	0.03	0.07	0.05	0.05	0.06	9.12	0.07	0.07	0.09	0.09
Total	101.95	100.82	100.62	100.25	100.87	100.92	100.93	99.50	101.62	103.09	101.49	100.93	101.38	101.35
Atom Proportions														
Si	10.71	10.75	10.72	10.68	10.67	10.75	10.68	10.68	10.69	10.88	10.72	10.71	10.71	10.71
Ti	0.00	0.00	0.00	0.00	0.00	0.00	0.00	0.00	0.00	0.05	0.00	0.00	0.00	0.00
Al	5.33	5.28	5.30	5.30	5.36	5.27	5.34	5.40	5.33	5.23	5.30	5.30	5.32	5.34
Fe	0.00	0.01	0.00	0.01	0.01	0.01	0.00	0.00	0.01	0.01	0.00	0.01	0.00	0.01
Ca	1.27	1.27	1.27	1.31	1.30	1.29	1.33	1.28	1.29	0.04	1.27	1.29	1.28	1.28
Ba	0.00	0.01	0.00	0.00	0.00	0.00	0.00	0.00	0.00	1.08	0.00	0.00	0.00	0.00
Sr	0.03	0.03	0.02	0.02	0.02	0.02	0.02	0.02	0.02	0.02	0.01	0.02	0.02	0.02
Na	2.55	2.53	2.62	2.66	2.60	2.53	2.55	2.44	2.60	0.06	2.63	2.58	2.55	2.52
K	0.01	0.01	0.02	0.01	0.01	0.02	0.01	0.01	0.01	2.26	0.02	0.02	0.02	0.02
O	32.00	32.00	32.00	32.00	32.00	32.00	32.00	32.00	32.00	32.00	32.00	32.00	32.00	32.00
CatTot	19.91	19.87	19.95	20.00	19.96	19.88	19.93	19.84	19.94	19.62	19.95	19.93	19.91	19.89
Total	51.91	51.87	51.95	52.00	51.96	51.88	51.93	51.84	51.94	51.62	51.95	51.93	51.91	51.89
An	0.33	0.33	0.32	0.33	0.33	0.33	0.34	0.34	0.33	0.01	0.32	0.33	0.33	0.33
Ab	0.66	0.66	0.67	0.67	0.66	0.66	0.65	0.65	0.66	0.02	0.67	0.66	0.66	0.66
Or	0.00	0.00	0.00	0.00	0.00	0.00	0.00	0.00	0.00	0.65	0.00	0.00	0.01	0.01

Sample	15
Oxides	
SiO2	60.46
TiO2	0.01
Al2O3	25.51
Fe2O3	0.03
CaO	6.76
BaO	0.00
SrO	0.10
Na2O	7.48
K2O	0.07
Total	100.41
Atom Proportions	
Si	10.71
Ti	0.00
Al	5.33
Fe	0.00
Ca	1.28
Ba	0.00
Sr	0.01
Na	2.57
K	0.02
O	32.00
CatTot	19.92
Total	51.92
An	0.33
Ab	0.66
Or	0.00

B.4. Cordierite Compositional Analysis

Sample	10a	10a	10a	10a	10a	10a	10a	10a	10a	10a	10a 1st po	10a 2nd po	10a 3rd po	10a 4th po	10a core
Oxides															
SiO2	45.10	46.86	45.67	41.45	44.08	35.38	37.50	47.00	46.92	44.92	37.98	45.71	43.86	48.04	47.68
TiO2	0.01	0.01	0.03	0.00	0.01	0.02	0.00	0.00	0.00	0.00	0.00	0.01	0.02	0.01	0.03
Al2O3	32.86	32.94	32.96	33.21	32.63	50.51	31.52	31.65	32.09	32.08	59.65	32.70	33.24	33.18	32.43
CrO3	0.00	0.00	0.00	0.00	0.00	0.04	0.00	0.01	0.04	0.00	0.08	0.00	0.00	0.02	0.00
FeO	8.85	8.79	8.37	8.73	8.76	4.23	8.83	9.08	8.96	9.02	1.50	8.55	8.75	8.81	9.63
MgO	7.35	6.90	7.03	7.07	7.01	3.09	6.78	7.01	7.00	6.89	0.72	7.72	7.65	7.38	7.06
MnO	0.14	0.10	0.11	0.15	0.07	0.04	0.10	0.12	0.15	0.10	0.00	0.11	0.13	0.15	0.15
CaO	0.00	0.04	0.03	0.07	0.01	0.00	0.04	0.00	0.01	0.00	0.00	0.02	0.00	0.00	0.02
Na2O	0.21	0.17	0.14	0.21	0.21	0.10	0.15	0.19	0.14	0.18	0.00	0.17	0.14	0.20	0.17
K2O	0.00	0.00	0.00	0.00	0.00	0.00	0.00	0.00	0.00	0.00	0.00	0.00	0.00	0.00	0.00
Total	94.52	95.82	94.35	90.90	92.77	93.40	84.92	95.06	95.31	93.20	99.93	94.99	93.79	97.78	97.17
Atom Proportions															
Si	4.86	4.96	4.91	4.67	4.84	3.78	4.55	5.03	5.00	4.91	3.72	4.89	4.77	4.99	5.00
Ti	0.00	0.00	0.00	0.00	0.00	0.00	0.00	0.00	0.00	0.00	0.00	0.00	0.00	0.00	0.00
Al	4.18	4.11	4.18	4.41	4.22	6.36	4.50	3.99	4.03	4.13	6.88	4.13	4.26	4.06	4.01
Cr	0.00	0.00	0.00	0.00	0.00	0.00	0.00	0.00	0.00	0.00	0.01	0.00	0.00	0.00	0.00
Fe	0.80	0.78	0.75	0.82	0.80	0.38	0.90	0.81	0.80	0.83	0.12	0.77	0.80	0.76	0.85
Mg	1.18	1.09	1.13	1.19	1.15	0.49	1.23	1.12	1.11	1.12	0.11	1.23	1.24	1.14	1.10
Mn	0.01	0.01	0.01	0.02	0.01	0.00	0.01	0.01	0.01	0.01	0.00	0.01	0.01	0.01	0.01
Ca	0.00	0.01	0.00	0.01	0.00	0.00	0.01	0.00	0.00	0.00	0.00	0.00	0.00	0.00	0.00
Na	0.04	0.04	0.03	0.05	0.05	0.02	0.04	0.04	0.03	0.04	0.00	0.04	0.03	0.04	0.03
K	0.00	0.00	0.00	0.00	0.00	0.00	0.00	0.00	0.00	0.00	0.00	0.00	0.00	0.00	0.00
O	18.00	18.00	18.00	18.00	18.00	18.00	18.00	18.00	18.00	18.00	18.00	18.00	18.00	18.00	18.00
CatTot	11.07	11.00	11.01	11.15	11.07	11.04	11.22	11.00	10.99	11.04	10.84	11.06	11.11	11.00	11.01
Total	29.07	29.00	29.01	29.15	29.07	29.04	29.22	29.00	28.99	29.04	28.84	29.06	29.11	29.00	29.01

Sample	10a rim	5004a	5004a	5004a	5023	5023	5023	5023	5131	5131	5131	5131	5131	5131	5131
Oxides															
SiO2	47.83	42.35	47.90	48.23	47.60	47.60	46.76	49.27	45.10	45.36	44.13	43.94	44.17	47.93	48.08
TiO2	0.01	0.04	0.01	0.03	0.00	0.00	0.01	0.01	0.00	0.02	0.00	0.02	0.03	0.03	0.00
Al2O3	32.61	30.70	33.76	33.62	33.81	33.81	32.11	34.03	32.54	33.50	33.61	33.07	33.03	33.44	33.20
CrO3	0.00	0.00	0.00	0.00	0.00	0.00	0.00	0.00	0.01	0.08	0.03	0.02	0.00	0.02	0.02
FeO	9.26	9.09	8.66	8.70	7.76	7.76	8.25	8.43	9.03	8.96	9.06	8.89	8.73	8.72	9.26
MgO	7.38	7.34	7.69	7.70	8.61	8.61	8.68	8.38	7.36	7.28	7.19	7.27	7.30	7.27	7.34
MnO	0.16	0.10	0.16	0.18	0.17	0.17	0.10	0.03	0.15	0.16	0.17	0.17	0.15	0.15	0.18
CaO	0.03	0.02	0.00	0.01	0.00	0.00	0.00	0.01	0.05	0.00	0.02	0.00	0.05	0.03	0.04
Na2O	0.24	0.19	0.16	0.14	0.28	0.28	0.25	0.26	0.13	0.19	0.16	0.18	0.16	0.20	0.14
K2O	0.00	0.00	0.00	0.00	0.00	0.00	0.00	0.00	0.00	0.00	0.00	0.00	0.00	0.00	0.00
Total	97.51	89.83	98.34	98.61	98.23	98.23	96.18	100.42	94.37	95.57	94.36	93.56	93.62	97.80	98.26
Atom Proportions															
Si	4.99	4.83	4.94	4.96	6.54	4.90	4.94	4.97	4.87	4.84	4.78	4.79	4.81	4.97	4.98
Ti	0.00	0.00	0.00	0.00	0.00	0.00	0.00	0.00	0.00	0.00	0.00	0.00	0.00	0.00	0.00
Al	4.01	4.13	4.10	4.08	5.47	4.11	4.00	4.04	4.14	4.21	4.29	4.25	4.24	4.09	4.05
Cr	0.00	0.00	0.00	0.00	0.00	0.00	0.00	0.00	0.00	0.01	0.00	0.00	0.00	0.00	0.00
Fe	0.81	0.87	0.75	0.75	0.89	0.67	0.73	0.71	0.82	0.80	0.82	0.81	0.80	0.76	0.80
Mg	1.15	1.25	1.18	1.18	1.76	1.32	1.37	1.26	1.19	1.16	1.16	1.18	1.19	1.12	1.13
Mn	0.01	0.01	0.01	0.02	0.02	0.02	0.01	0.00	0.01	0.01	0.02	0.02	0.01	0.01	0.02
Ca	0.00	0.00	0.00	0.00	0.00	0.00	0.00	0.00	0.01	0.00	0.00	0.00	0.01	0.00	0.01
Na	0.05	0.04	0.03	0.03	0.06	0.06	0.05	0.05	0.03	0.04	0.03	0.04	0.03	0.04	0.03
K	0.00	0.00	0.00	0.00	0.00	0.00	0.00	0.00	0.00	0.00	0.00	0.00	0.00	0.00	0.00
O	18.00	18.00	18.00	18.00	24.00	18.00	18.00	18.00	18.00	18.00	18.00	18.00	18.00	18.00	18.00
CatTot	11.03	11.13	11.02	11.01	14.76	11.07	11.09	11.04	11.07	11.07	11.10	11.10	11.09	11.00	11.01
Total	29.03	29.13	29.02	29.01	38.76	29.07	29.09	29.04	29.07	29.07	29.10	29.10	29.09	29.00	29.01

Sample	7005b	7005b 2nd po	7005b first po	SBP12 1st po	SBP12 2nd po	SBP12 3rd po
Oxides						
SiO2	44.20	48.72	49.11	48.46	48.65	48.41
TiO2	0.05	0.00	0.00	0.02	0.01	0.00
Al2O3	32.98	34.05	34.22	33.62	34.03	33.21
CrO3	0.00	0.02	0.02	0.01	0.00	0.01
FeO	8.82	8.72	8.54	8.69	9.08	8.50
MgO	7.67	8.05	8.36	7.94	7.75	7.70
MnO	0.16	0.15	0.18	0.15	0.15	0.09
CaO	0.03	0.00	0.00	0.00	0.00	0.00
Na2O	0.12	0.13	0.11	0.28	0.20	0.21
K2O	0.00	0.00	0.00	0.00	0.00	0.00
Total	94.03	99.65	100.54	99.17	99.86	98.13
Atom Proportions						
Si	4.80	4.95	4.95	4.96	4.95	5.00
Ti	0.00	0.00	0.00	0.00	0.00	0.00
Al	4.22	4.08	4.06	4.06	4.08	4.04
Cr	0.00	0.00	0.00	0.00	0.00	0.00
Fe	0.80	0.74	0.72	0.74	0.77	0.73
Mg	1.24	1.22	1.26	1.21	1.18	1.18
Mn	0.02	0.01	0.02	0.01	0.01	0.01
Ca	0.00	0.00	0.00	0.00	0.00	0.00
Na	0.03	0.03	0.02	0.06	0.04	0.04
K	0.00	0.00	0.00	0.00	0.00	0.00
O	18.00	18.00	18.00	18.00	18.00	18.00
CatTot	11.10	11.03	11.03	11.04	11.03	11.01
Total	29.10	29.03	29.03	29.04	29.03	29.01

Sample
Oxides
SiO2
TiO2
Al2O3
CrO3
FeO
MgO
MnO
CaO
Na2O
K2O
Total
Atom Proportions
Si
Ti
Al
Cr
Fe
Mg
Mn
Ca
Na
K
O
CatTot
Total

B.5. Amphibole Compositional Analysis

Sample	5124 rim	5124 rim	5124 core	5124 rim opposite Pt 1	5124 rim adj plag	5124 rim adj apatite	5027 rim adj biotite	5027 core	5027 core
Oxides									
SiO2	48.94	50.46	49.48	50.05	50.13	49.28	45.62	44.65	45.02
TiO2	0.59	0.44	0.46	0.48	0.37	0.60	0.78	0.84	0.86
Al2O3	6.48	4.84	5.12	5.12	5.38	6.00	9.44	9.87	9.79
Cr2O3	0.08	0.00	0.04	0.08	0.03	0.00	0.07	0.00	0.07
FeO	18.95	18.63	18.79	18.49	19.00	18.76	20.14	20.10	20.33
MgO	10.94	11.71	11.76	11.74	11.54	11.42	9.44	8.97	8.98
MnO	0.34	0.41	0.43	0.38	0.38	0.26	0.40	0.31	0.37
ZnO	0.00	0.00	0.07	0.03	0.07	0.00	0.08	0.06	0.02
CaO	11.42	11.27	11.36	11.38	11.21	11.76	11.07	11.14	11.19
Na2O	0.60	0.49	0.53	0.56	0.51	0.61	1.09	1.12	1.08
K2O	0.09	0.00	0.00	0.03	0.00	0.00	0.21	0.19	0.23
Cl	0.02	0.01	0.00	0.00	0.01	0.00	0.02	0.04	0.04
F	0.00	0.00	0.00	0.00	0.00	0.00	0.00	0.00	0.00
Total	98.45	98.27	98.05	98.33	98.64	96.70	98.37	97.30	97.98
Atom Proportions									
Si	7.23	7.44	7.34	7.38	7.38	7.26	6.83	6.77	6.78
Ti	0.07	0.05	0.05	0.05	0.04	0.07	0.09	0.10	0.10
Al	1.13	0.84	0.89	0.89	0.93	1.04	1.67	1.76	1.74
Cr	0.01	0.00	0.01	0.01	0.00	0.00	0.01	0.00	0.01
Fe	2.34	2.30	2.33	2.28	2.34	2.31	2.52	2.55	2.56
Mg	2.41	2.57	2.60	2.58	2.53	2.51	2.11	2.03	2.02
Mn	0.04	0.05	0.05	0.05	0.05	0.03	0.05	0.04	0.05
Zn	0.00	0.00	0.01	0.00	0.01	0.00	0.01	0.01	0.00
Ca	1.81	1.78	1.80	1.80	1.77	1.86	1.78	1.81	1.81
Na	0.17	0.14	0.15	0.16	0.15	0.17	0.32	0.33	0.32
K	0.02	0.00	0.00	0.00	0.00	0.00	0.04	0.04	0.04
Cl	0.01	0.00	0.00	0.00	0.00	0.00	0.01	0.01	0.01
F	0.00	0.00	0.00	0.00	0.00	0.00	0.00	0.00	0.00
O	23.00	23.00	23.00	23.00	23.00	23.00	23.00	23.00	23.00
CatTot	15.23	15.17	15.24	15.20	15.19	15.24	15.43	15.44	15.44
Total	38.23	38.17	38.24	38.20	38.19	38.24	38.43	38.44	38.44

Sample	5027 rim opposite Pt 6	5027 small gr surr. by Bt	5027 core of larger grain	5027 rim of grain in Pt 10	5124 adj Pt 1	5124 core of a new grain	5124 rim of lg grain adj Qtz	5124 core of same gr in Pt 14	5124 rim opposite Pt 14
Oxides									
SiO2	45.50	45.60	45.07	44.75	49.91	49.06	48.07	47.71	47.06
TiO2	0.76	0.77	0.73	0.78	0.46	0.42	0.48	0.45	0.59
Al2O3	9.36	9.76	9.89	9.76	5.24	5.68	5.56	5.73	6.96
Cr2O3	0.06	0.02	0.00	0.03	0.03	0.09	0.04	0.13	0.05
FeO	20.20	19.95	20.55	19.73	18.54	20.36	21.88	22.15	22.19
MgO	9.61	9.21	8.87	8.88	11.88	9.93	9.73	9.43	8.93
MnO	0.33	0.36	0.00	0.41	0.36	0.50	0.38	0.45	0.29
ZnO	0.03	0.07	0.10	0.00	0.00	0.03	0.03	0.11	0.03
CaO	11.12	11.38	10.94	11.24	11.47	11.22	11.36	11.30	11.35
Na2O	1.02	1.14	1.16	1.11	0.50	0.64	0.53	0.60	0.73
K2O	0.19	0.24	0.23	0.19	0.00	0.01	0.00	0.06	0.04
Cl	0.03	0.04	0.04	0.03	0.19	0.00	0.00	0.01	0.00
F	0.00	0.00	0.00	0.00	0.00	0.00	0.00	0.00	0.00
Total	98.21	98.53	97.37	96.91	98.58	97.94	98.04	98.13	98.24
Atom Proportions									
Si	6.83	6.82	6.83	6.80	7.35	7.34	7.25	7.21	7.10
Ti	0.09	0.09	0.08	0.09	0.05	0.05	0.05	0.05	0.07
Al	1.66	1.72	1.73	1.75	0.91	1.00	0.99	1.02	1.24
Cr	0.01	0.00	0.00	0.00	0.00	0.01	0.00	0.02	0.01
Fe	2.53	2.49	2.60	2.51	2.29	2.55	2.76	2.80	2.80
Mg	2.15	2.05	2.00	2.01	2.61	2.21	2.19	2.13	2.01
Mn	0.04	0.05	0.00	0.05	0.05	0.08	0.05	0.06	0.04
Zn	0.00	0.01	0.01	0.00	0.00	0.00	0.00	0.01	0.00
Ca	1.79	1.82	1.78	1.83	1.81	1.80	1.83	1.83	1.84
Na	0.30	0.33	0.34	0.33	0.14	0.18	0.15	0.18	0.21
K	0.04	0.04	0.04	0.04	0.00	0.00	0.00	0.01	0.01
Cl	0.01	0.01	0.01	0.01	0.05	0.00	0.00	0.00	0.00
F	0.00	0.00	0.00	0.00	0.00	0.00	0.00	0.00	0.00
O	23.00	23.00	23.00	23.00	23.00	23.00	23.00	23.00	23.00
CatTot	15.43	15.43	15.43	15.42	15.26	15.21	15.28	15.32	15.32
Total	38.43	38.43	38.43	38.42	38.26	38.21	38.28	38.32	38.32

B.5. Amphibole Compositional Analysis

Sample	5026	5026
Oxides		
SiO2	45.45	44.37
TiO2	0.59	0.73
Al2O3	8.59	9.44
Cr2O3	0.02	0.05
FeO	20.89	21.24
MgO	8.56	8.07
MnO	0.55	0.55
ZnO	0.10	0.00
CaO	11.37	11.06
Na2O	0.87	0.94
K2O	0.78	0.81
Cl	0.00	0.01
F	0.00	0.00
Total	97.77	97.27
Atom Proportions		
Si	7.21	7.09
Ti	0.07	0.09
Al	1.61	1.78
Cr	0.00	0.01
Fe	2.77	2.84
Mg	2.02	1.92
Mn	0.07	0.08
Zn	0.01	0.00
Ca	1.93	1.90
Na	0.27	0.29
K	0.16	0.17
Cl	0.00	0.00
F	0.00	0.00
O	24.00	24.00
CatTot	16.13	16.16
Total	40.13	40.16

Sample
Oxides
SiO2
TiO2
Al2O3
Cr2O3
FeO
MgO
MnO
ZnO
CaO
Na2O
K2O
Cl
F
Total
Atom Proportions
Si
Ti
Al
Cr
Fe
Mg
Mn
Zn
Ca
Na
K
Cl
F
O
CatTot
Total

B.6. Mineral Compositions Used for Quantitative Pressure and Temperature Estimation

Garnet

	Oxides				Molar Proportions				Activities			
Samples	FeO	MgO	MnO	CaO	Gr	Py	Alm	Sp	Gr	Py	Alm	Sp
0278b core adj Bt inc	31.92	5.23	0.69	1.77	0.051	0.211	0.722	0.016	0.000133	0.009394	0.376367	0.000004096
10a core	35.61	3.25	1.54	0.8	0.023	0.132	0.810	0.035	1.24E-05	0.002278	0.531265	4.41586E-05
10a rim	36.81	2.68	1.99	0.72	0.021	0.107	0.827	0.045	8.9E-06	0.001235	0.565393	9.17358E-05
10a core	35.86	3.23	1.48	0.71	0.021	0.131	0.814	0.034	9.06E-06	0.002227	0.540101	3.99647E-05
10a rim	36.36	2.81	1.88	0.74	0.022	0.113	0.822	0.043	9.96E-06	0.001447	0.556128	7.96489E-05
0287b grt core, adj bt inc.	32.41	5.04	0.74	1.6	0.046	0.203	0.734	0.017	9.73E-05	0.008365	0.395447	0.000004913
0278b core, iso bt	32.8	4.89	0.76	1.88	0.054	0.195	0.734	0.017	0.000157	0.007415	0.395447	0.000004913
0278b bt inc.	32.5	5.19	0.77	1.65	0.058	0.203	0.722	0.017	0.000195	0.008365	0.376367	0.000004913
0278b bt inc.	33.03	5.06	0.7	1.91	0.054	0.200	0.731	0.016	0.000157	0.008	0.390618	0.000004096
0278b grt rim, bt adj.	32.31	4.82	0.77	1.74	0.051	0.196	0.736	0.018	0.000133	0.00753	0.398688	0.000005832
0278b grt rim, iso bt	32.31	4.82	0.77	1.74	0.051	0.196	0.736	0.018	0.000133	0.00753	0.398688	0.000005832
5000 grt rim, adj pl, adj bt.	32.97	3.26	1.31	1.14	0.035	0.140	0.793	0.032	4.37E-05	0.002725	0.499055	3.24503E-05
5000 adj bt inc.	35.19	3.02	1.6	0.87	0.026	0.124	0.813	0.037	1.69E-05	0.001912	0.537009	5.2323E-05
5000 grt core, bt inc.	35.3	2.94	1.37	1.88	0.026	0.122	0.820	0.032	1.8E-05	0.001796	0.551347	3.34809E-05
5000 grt core, bt inc.	35.07	3.46	1.33	0.945	0.028	0.141	0.801	0.031	2.11E-05	0.002796	0.513378	2.91381E-05
5000 grt rim, bt adj.	35.47	3.09	1.435	0.823	0.024	0.127	0.816	0.033	1.43E-05	0.002036	0.542536	3.73334E-05
5000 grt core	35.3	2.94	1.37	1.88	0.026	0.122	0.820	0.032	1.8E-05	0.001796	0.551347	3.34809E-05
5000 grt core	35.07	3.46	1.33	0.945	0.028	0.141	0.801	0.031	2.11E-05	0.002796	0.513378	2.91381E-05
5000 grt rim	35.47	3.09	1.435	0.823	0.024	0.127	0.816	0.033	1.43E-05	0.002036	0.542536	3.73334E-05
5002	34.58	3.13	2.05	0.93	0.027	0.129	0.796	0.048	2.06E-05	0.002124	0.504795	0.000109318
5004a rim	34.97	3.06	1.704	0.977	0.029	0.126	0.806	0.040	2.4E-05	0.001981	0.523214	6.28667E-05
5011 grt core	34.22	3.74	0.93	1.75	0.049	0.164	0.762	0.025	0.000118	0.004385	0.443177	1.54735E-05
5011 grt core, bt inc.	33.22	4	1.08	1.67	0.051	0.151	0.776	0.021	0.000133	0.003474	0.467839	9.59254E-06
5023	34.31	3.94	1.39	1.05	0.030	0.159	0.778	0.032	2.81E-05	0.004037	0.471467	3.30231E-05
5068 grt rim	35.51	2.348	2.624	0.915	0.027	0.096	0.816	0.061	1.95E-05	0.000888	0.543122	0.000227671
5068 grt core	35	3.6	1.699	0.905	0.026	0.145	0.790	0.039	1.8E-05	0.003029	0.493545	5.86677E-05
5068 grt rim	35.2	3.47	1.726	0.881	0.025	0.140	0.795	0.039	1.66E-05	0.002732	0.502898	6.15554E-05
5088 core, bt inc.	32.9	3.97	2.17	1.8	0.052	0.159	0.740	0.049	0.000139	0.004024	0.404823	0.00012011
5088 grt rim	32.44	3.4	2.3	2.9	0.083	0.136	0.728	0.052	0.000579	0.002523	0.386424	0.000141694
5088 core, iso bt	32.9	3.97	2.17	1.8	0.052	0.159	0.740	0.049	0.000139	0.004024	0.404823	0.00012011
5088 grt rim, iso bt	32.44	3.4	2.3	2.9	0.083	0.136	0.728	0.052	0.000579	0.002523	0.386424	0.000141694
5100 grt core	33.25	3.12	2.27	1.7	0.050	0.129	0.768	0.053	0.000127	0.002129	0.453155	0.000148891
5100 grt rim	33.41	2.83	2.48	1.7	0.050	0.117	0.774	0.058	0.000128	0.001608	0.464273	0.000196564
5100 grt rim	33.41	2.83	2.48	1.7	0.050	0.117	0.774	0.058	0.000128	0.001608	0.464273	0.000196564
5131 grt core	34.52	3.14	2.447	0.933	0.027	0.128	0.788	0.057	2.03E-05	0.002082	0.490066	0.000181487
5131 grt rim	33.56	3.31	2.329	0.878	0.026	0.137	0.782	0.055	1.8E-05	0.002584	0.477561	0.000165805
7005b grt core	34.77	3.23	2.61	0.88	0.025	0.130	0.785	0.060	1.63E-05	0.002197	0.48394	0.000210919
7005b grt rim	34.74	3.14	2.41	0.83	0.024	0.128	0.792	0.056	1.44E-05	0.002082	0.497292	0.000173124
5000 grt adj plag.	35.840	2.850	1.660	0.900	0.026	0.116	0.819	0.038	1.85E-05	0.001561	0.54974	5.65516E-05

B.6. Mineral Compositions Used for Quantitative Pressure and Temperature Estimation

Biotite

	Oxides		Molar Proportions						
Samples	FeO	MgO	xMg	xFe	xTi	xAlVI	xK	xOH	xMn
0278b core adj Bt inc	13.98	14.55	0.55	0.297	0.026	0.073	0.947	0.9999	0.001
10a core	20.12	8.66	0.351	0.457	0.039	0.082	0.988	0.999	0.000
10a rim	20.12	8.66	0.351	0.457	0.039	0.082	0.988	0.999	0.000
10a core	20.12	8.66	0.351	0.457	0.039	0.082	0.988	0.999	0.000
10a rim	20.12	8.66	0.351	0.457	0.039	0.082	0.988	0.999	0.000
0287b grt core, adj bt inc.	15.47	13.19	0.503	0.331	0.040	0.067	0.970	0.999	0.001
0278b core, iso bt	18.46	11.12	0.437	0.407	0.037	0.063	0.972	0.999	0.000
0278b bt inc.	14.03	14.67	0.552	0.296	0.027	0.073	0.932	0.999	0.000
0278b bt inc.	13.98	14.55	0.552	0.296	0.027	0.073	0.932	0.999	0.000
0278b grt rim, bt adj.	17.97	10.79	0.420	0.393	0.038	0.079	0.978	0.999	0.000
0278b grt rim, iso bt	18.46	11.12	0.437	0.407	0.037	0.063	0.972	0.999	0.000
5000 grt rim, adj pl, adj bt.	20.38	8.71	0.347	0.455	0.009	0.116	0.973	0.999	0.002
5000 adj bt inc.	19.4	9.76	0.381	0.425	0.030	0.090	0.967	0.999	0.002
5000 grt core, bt inc.	18.63	9.54	0.367	0.402	0.044	0.099	0.960	0.999	0.000
5000 grt core, bt inc.	21.96	8.11	0.317	0.483	0.004	0.123	0.970	0.999	0.001
5000 grt rim, bt adj.	21.62	8.18	0.330	0.489	0.023	0.092	0.968	0.999	0.000
5000 grt core	21.42	8.07	0.316	0.470	0.037	0.097	0.966	0.999	0.001
5000 grt core	21.42	8.07	0.316	0.470	0.037	0.097	0.966	0.999	0.001
5000 grt rim	21.42	8.07	0.316	0.470	0.037	0.097	0.966	0.999	0.001
5002	18.87	9.3	0.370	0.427	0.037	0.087	0.979	0.999	0.001
5004a rim	18.53	8.88	0.359	0.421	0.037	0.095	0.973	0.999	0.000
5011 grt core	19.14	11.57	0.522	0.332	0.02	0.077	0.943	0.999	0.001
5011 grt core, bt inc.	15.74	13.88	0.439	0.407	0.028	0.073	0.940	0.999	0.000
5023	19.13	9.6	0.337	0.376	0.038	0.163	0.943	0.999	0.000
5068 grt rim	19.77	8.87	0.353	0.441	0.036	0.091	0.975	0.999	0.001
5068 grt core	19.77	8.87	0.353	0.441	0.036	0.091	0.975	0.999	0.001
5068 grt rim	19.87	9.37	0.351	0.418	0.032	0.123	0.975	0.999	0.000
5088 core, bt inc.	18.85	11.52	0.456	0.419	0.059	0.023	0.964	0.999	0.001
5088 grt rim	20.91	10.82	0.427	0.463	0.049	0.025	0.968	0.999	0.001
5088 core, iso bt	19.16	11.06	0.440	0.427	0.056	0.029	0.984	0.999	0.002
5088 grt rim, iso bt	19.16	11.06	0.440	0.427	0.056	0.029	0.984	0.999	0.002
5100 grt core	20.22	10.48	0.402	0.435	0.024	0.081	0.949	0.999	0.002
5100 grt rim	20.22	10.48	0.402	0.435	0.024	0.081	0.949	0.999	0.002
5100 grt rim	19.56	10.7	0.409	0.419	0.024	0.088	0.951	0.999	0.001
5131 grt core	19.09	8.05	0.292	0.388	0.038	0.174	0.972	0.999	0.003
5131 grt rim	19.09	8.05	0.292	0.388	0.038	0.174	0.972	0.999	0.003
7005b grt core	19.57	8.94	0.355	0.436	0.035	0.093	0.982	0.999	0.001
7005b grt rim	19.57	8.94	0.355	0.436	0.035	0.093	0.982	0.999	0.001
5000 grt adj plag.	20.51	9.1	0.350	0.442	0.017	0.113	0.976	0.999	0.001

Feldspar

	Activities/Molar Proportions		
Samples	An	Ab	Or
0278b core adj Bt inc	0.378	0.608	0.004
10a core	0.210	0.772	0.012
10a rim	0.210	0.772	0.012
10a core	0.210	0.772	0.012
10a rim	0.210	0.772	0.012
0287b grt core, adj bt inc.	0.374	0.614	0.002
0278b core, iso bt	0.378	0.608	0.004
0278b bt inc.	0.419	0.568	0.005
0278b bt inc.	0.419	0.568	0.005
0278b grt rim, bt adj.	0.381	0.607	0.003
0278b grt rim, iso bt	0.378	0.608	0.004
5000 grt rim, adj pl, adj bt.	0.228	0.759	0.004
5000 adj bt inc.	0.234	0.758	0.003
5000 grt core, bt inc.	0.226	0.702	0.066
5000 grt core, bt inc.	0.239	0.749	0.005
5000 grt rim, bt adj.	0.239	0.749	0.005
5000 grt core	0.232	0.752	0.011
5000 grt core	0.232	0.752	0.011
5000 grt rim	0.232	0.752	0.011
5002	0.265	0.718	0.008
5004a rim			
5011 grt core	0.318	0.675	0.000
5011 grt core, bt inc.	0.339	0.652	0.002
5023	0.251	0.734	0.006
5068 grt rim	0.267	0.707	0.019
5068 grt core	0.267	0.707	0.019
5068 grt rim	0.267	0.707	0.019
5088 core, bt inc.	0.410	0.574	0.011
5088 grt rim	0.410	0.574	0.011
5088 core, iso bt	0.410	0.574	0.011
5088 grt rim, iso bt	0.410	0.574	0.011
5100 grt core	0.285	0.698	0.004
5100 grt rim	0.285	0.698	0.004
5100 grt rim	0.289	0.701	0.002
5131 grt core	0.262	0.716	0.015
5131 grt rim	0.262	0.716	0.015
7005b grt core	0.231	0.756	0.010
7005b grt rim	0.231	0.756	0.010
5000 grt adj plag.	0.210	0.772	0.012

APPENDIX C: Location of the Samples Used

Appendix C: Location of Samples used.